Development of Pillared Clays for Water and Waste Water Treatment

A Thesis Submitted for the Degree of Doctor of Philosophy of the University of London.

by

May Kwan Syuen Chan



Department of Chemical Engineering
and Chemical Technology,
Imperial College of Science, Technology and Medicine,
London SW7 2BY

January 2000

Abstract

PILCs such as Al-PILC and Fe-PILC were prepared and modified specifically for their applications in water treatment. The physical structure and chemical properties of these PILCs were characterised using standard characterisation techniques. The cation exchange capacity of the clays for strontium, manganese and their adsorption capacity for organic compounds such as humic substances were studied. Parallel studies were also carried out on the PILCs and the raw clay (Montmorillonite).

The modified Fe-PILC, prepared using a simple preparation method, the 'short-cut' method, has a significantly higher capacity for strontium, manganese and humic substances than do the Al-PILC and raw Montmorillonite. The fact that the capacity of the Fe-PILC can be enhanced using a base ($NaHCO_3$) suggests that it has the potential to be a good water treatment agent. Preparing the modified Fe-PILC using the 'short-cut' method and also eliminating the washing process of the clay would significantly reduce the production cost of the clay. Furthermore environmental factors such as the regeneration of the clay are also considered. The results showed that the used clay, which had adsorbed organic compounds, could be recycled.

Table of Contents

Abstract 2

List of Figures 11

Acknowledgements 18

Dedication 19

Chapter 1 Introduction 20

1.1 Scope of the Thesis 20

1.2 General Description of Pillared Clays 20

1.2.1 History of Pillared Clays (PILCs) 23

1.2.2 General Applications of Pillared Clays (PILCs) 24

1.3 Removal of Heavy Metals by Cation Exchange 25

1.4 Removal of Organic Compounds by Adsorption 26

1.5 Data Interpretation 27

1.6 General Discussion of Water Treatment Processes 28

1.7 Research Aims 30

Chapter 2 Literature Survey 32

2.1 The Langmuir Adsorption Model 32

2.2 Raw Clay (Montmorillonite) as a Cation Exchanger 32

2.3 Pillaring Agents 35

2.4 Pillared Clays (PILCs) as Adsorbents and Cation Exchangers 37

2.4.1 Synthesis Of Aluminium Pillared Clay (Al-PILC) 40

2.4.2 Synthesis of Iron Pillared Clay (Fe-PILC) 43

2.4.3 Factors that Enhance the Cation Exchange and Adsorption Property Of Fe-PILC 46

2.4.3.1 Introduction 46

Chapter 3 Preliminary Characterisation and Techniques for Analysing PILCs 50

3.1 X-ray Diffraction (XRD) Analysis 50

3.2 Nitrogen Adsorption Analysis 51

3.3 Inductively Coupled Plasma Atomic Emission Spectrometry (ICP-AES) 53

3.4 Thermal Gravimetric Analysis (TGA) 53

3.5 Zeta Potential Analysis 54

3.6 Strontium Adsorption Isotherm 55

3.7 Atomic Absorption Spectrometry (A.A.S.) and Atomic Emission Spectrometry (A.E.S.) 56

3.8 Ultraviolet Spectrometry 57

Chapter 4 Experiments with Al-PILC 59

4.1 Introduction 59

4.2 Experimental Procedure of Synthesis of Al-PILC via the 'Short-cut' and Conventional Methods 59

4.3 Strontium Adsorption Analysis 62

4.4 Effect of Varying the Synthesis Parameters 63

4.4.1 Introduction 63

4.4.2 Experiment in Varying the Synthesis Parameters 64

4.4.2.1 Effect of Varying the Al/clay Ratio (R_A) 64

4.4.2.2 Effect of Varying OH/Al Ratio (R_{OA}) 65

4.4.2.3 Effect of Varying the Thermal Treatment Temperature 65

4.4.3 Results and Discussion of Preliminary Characterisations 65

4.4.3.1 Results and Discussion of XRD Analysis 66

4.4.3.2 Results and Discussion of Nitrogen Adsorption Analysis 68

4.4.3.3 Results and Discussion of ICP-AES Analysis 69

4.4.3.4 Results and Discussion of Strontium Adsorption Analysis 70

4.4.4 Conclusions 71

Chapter 5 Experiments with Fe-PILC 80

5.1 Introduction 80

5.2 Experiment in Synthesis of Fe-PILC via the 'Short-cut' Method 80

5.3 Strontium Adsorption Analysis 82

5.3.1 Introduction 82

5.3.2 Experimental Procedure of Contact Tests 82

5.4 Effect of Varying the Starting Material 83

5.4.1 Experiment in Varying the Starting Material 83

5.4.2 Results and Discussion of Preliminary Characterisations 83

5.4.2.1 Results and Discussion of XRD Analysis 84

5.4.2.2 Results and Discussion of Nitrogen Adsorption Analysis 85

5.4.2.3 Results and Discussion of Strontium Adsorption Analysis 85

5.4.3 Conclusions 86

5.5 Effect of Varying the Synthesis Ratios 92

5.5.1 Introduction 92

5.5.2 Experiment in Varying the Fe/clay Ratio (R_F) 93

5.5.3 Experiment in Varying the OH/Fe Ratio (R_{OF}) 93

5.5.4 Results and Discussions of Preliminary Characterisations 93

5.5.4.1 Results and Discussion of XRD Analysis 94

5.5.4.2 Results and Discussion of Nitrogen Adsorption Analysis 94
5.5.4.3 Results and Discussion of ICP-AES Analysis 95
5.5.4.4 Results and Discussion of Strontium Adsorption Analysis 95
5.5.5 Conclusions 96

5.6 Effect of Varying the Thermal Treatment Temperature 108
5.6.1 Introduction 108
5.6.2 Experiment in Varying the Thermal Treatment Temperature 108
5.6.3 Results and Discussion of Preliminary Characterisations 109
5.6.3.1 Results and Discussion of TG Analysis 109
5.6.3.2 Results and Discussion of XRD Analysis 110
5.6.3.3 Results and Discussion of Nitrogen Adsorption Analysis 110
5.6.3.4 Results and Discussion of Strontium Adsorption Analysis 111
5.6.4 Conclusions 111

5.7 Effect of Varying the Base Concentration 119
5.7.1 Introduction 119
5.7.2 Experiment in Varying the Base Concentration 119
5.7.3 Results and Discussion of Preliminary Characterisations 120
5.7.3.1 Results and Discussion of XRD Analysis 120
5.7.3.2 Results and Discussion of Nitrogen Adsorption Analysis 121

5.7.3.3 Results and Discussion of Strontium Adsorption Analysis 122
5.7.4 Conclusions 122

5.8 Effect of Eliminating the Washing Step 134
5.8.1 Introduction 134
5.8.2 Experiment in Eliminating the Washing Step 134
5.8.3 Experiment to Test for Leaching of Iron 135
5.8.4 Results and Discussion of Preliminary Characterisations 136
5.8.4.1 Results and Discussion of XRD Analysis 136
5.8.4.2 Results and Discussion of Nitrogen Adsorption Analysis 136
5.8.4.3 Results and Discussion of Strontium Adsorption Analysis 137
5.8.4.4 Results and Discussion of the Test for Leaching of Iron 137
5.8.5 Conclusions 138

5.9 Determination of Ion Exchange Property of PILCs via Zeta Potential Analysis 144
5.9.1 Introduction 144
5.9.2 Experimental Procedures 144
5.9.3 Results and Discussion of Zeta Potential Analysis 146

5.10 Determination of Particle Size 148
5.10.1 Introduction 148
5.10.2 Experimental Procedures 148

5.10.3 Results and Discussion of Particle Size Analysis 149

5.11 Summary of Results and Conclusions 151

Chapter 6 Removal of Contaminants from Water 153

6.1 Removal of Manganese from Water 153

6.1.1 Introduction 153

6.1.2 Adsorption Experiments 154

6.1.3 Results and Discussion of the Effect of Varying the Synthesis Ratios 154

6.1.3.1 A Comparison of the Capacity of the PILCs and Starting Clays for Manganese 155

6.1.3.2 Effect of Varying the Fe/clay Ratio (R_F) 155

6.1.3.3 Effect of Varying the OH/Fe Ratio (R_{OF}) 156

6.1.4 Results and Discussion of the Effect of Varying the Base Concentration 160

6.1.5 Results and Discussion of the Effect of Eliminating the Washing Step 163

6.1.6 Conclusions 163

6.2 Removal of Humic Substances from Water 165

6.2.1 Introduction 165

6.2.2 Adsorption Experiments 165

6.2.3 Results and Discussion of the Effect of Varying the Base Concentration 166

6.3 Regeneration Experiments for Fe-PILC 171

6.3.1 Introduction 171

6.3.2 Experimental Procedures 171

6.3.3 Results and Discussion of the Regeneration Experiments 172

6.4 Conclusions 174

Chapter 7 Summary of Results and Conclusions 175

7.1 Future Work 184

References 186

List of Figures

Fig. 1.1 Schematic diagrams that describe the mechanism of the formation of PILCs. 21

Fig. 1.2 The possible structures of pillared clays: (a) ordered structure and (b) disordered structure. 23

Fig. 2.1 The structure of Montmorillonite. 34

Fig. 2.2 Effect of pH on the d001 (basal) spacing (Å) of sodium Montmorillonite. 34

Fig. 3.1 The three basic adsorption isotherm types: type I, type II and type IV. 52

Fig. 3.2 The calibration curve of humic substances. 58

Fig. 4.1 XRD spectrum of (a) sodium Montmorillonite, Na Mont, (b) Al-PILC, AC-1. 75

Fig. 4.2 XRD spectrum of (a) raw Montmorillonite, Ca & Na Mont, (b) Al-PILC, AS-3. 76

Fig. 4.3 Nitrogen adsorption and desorption isotherms of sodium Montmorillonite, NM, and Al-PILC, AC-1, respectively. 77

Fig. 4.4 Nitrogen adsorption and desorption isotherms of raw Montmorillonite, RM, and Al-PILC, AS-3, respectively. 77

Fig. 4.5 Strontium adsorption isotherm of (a) sodium Montmorillonite and (b) Al-PILC, AC-1. 78

Fig. 4.6 Strontium adsorption isotherm of (a) raw Montmorillonite & (b) Al-PILC, AS-3. 79

Fig. 5.1 XRD spectrum of (a) raw Montmorillonite and (b) Fe-PILC, F-RM. 89

Fig. 5.2 The effect of varying the starting material on the (a) the BET surface area and (b) the micropore area of the Fe-PILC. 90

Fig. 5.3 The effect of varying the starting material on the C.E.C. of the PILCs. 91

Fig. 5.4 A graphic interpretation of R_{PI} index. 98

Fig. 5.5 The effect of varying the Fe/clay ratio (R_F) on the degree of pillaring in the clay. 103

Fig. 5.6 The effect of varying the OH/Fe ratio (R_{OF}) on the degree of pillaring in the clay. 103

Fig. 5.7 The effect of varying the Fe/clay ratio (R_F) on the BET surface area and micropore area of the clay. 104

Fig. 5.8 The effect of varying the OH/Fe ratio (R_{OF}) on the BET surface area and micropore area of the clay. 104

Fig. 5.9 The effect of varying the Fe/clay ratio (R_F) on the iron oxide content of the clay. 105

Fig. 5.10 The effect of varying the OH/Fe ratio (R_{OF}) on the iron oxide content of the clay. 105

Fig. 5.11 The effect of varying the Fe/clay ratio (R_F) on the C.E.C. of the clay. 106

Fig. 5.12 The effect of varying the OH/Fe ratio (R_{OF}) on the C.E.C. of the clay. 106

Fig. 5.13 The effect of varying the Fe/clay ratio (R_F) on the pH of the thermally-treated clay. 107

Fig. 5.14 The effect of varying the OH/Fe ratio (R_{OF}) on the pH of the thermally-treated clay. 107

Fig. 5.15 The TG graph of (a) raw Montmorillonite and (b) air dried Fe-PILC. 114

Fig. 5.16 The effect of varying the treatment temperature on the degree of pillaring in the clay. 116

Fig. 5.17 The effect of varying the treatment temperature on the BET surface area and micropore area of the clay ((a) washed and (b) unwashed Fe-PILC). 116

Fig. 5.18 The effect of varying the treatment temperature the C.E.C. of the clay. 117

Fig. 5.19 The Effect of varying the treatment temperature on the final pH of the thermally-treated clay. 118

Fig. 5.20 The effect of varying the base concentration on the degree of pillaring in the clay. 130

Fig. 5.21 The effect of varying the base concentration on the BET surface area and micropore area of the clay ((a) Batch A1 (b) Batch B1, (c) Batch C1 and (d) Batch D1. 131

Fig. 5.22 The effect of varying the base concentration of the clay on the C.E.C. of the clay. 133

Fig. 5.23 The effect of varying the base concentration of the clay on the pH of the thermally-treated clay. 133

Fig. 5.24 The effect of eliminating the washing step on the degree of pillaring in the clay ((a) samples prepared at different thermal treatment temperature & (b) samples prepared at different base concentration). 139

Fig. 5.25 The effect of eliminating the washing step on the BET surface area of the clay ((a) samples prepared by varying the treatment temperature and (b) samples prepared by varying the base concentration). 140

Fig. 5.26 The effect of eliminating the washing step on the micropore area of the clay ((a) samples prepared by varying the treatment temperature and (b) samples prepared by varying the base concentration). 141

Fig. 5.27 The effect of eliminating the washing step on the C.E.C. of the clay ((a) samples prepared by varying the treatment temperature and (b) samples prepared by varying the base concentration). 142

Fig. 5.28 The effect of eliminating the washing step on the pH of the thermally-treated clay ((a) samples prepared by varying the treatment temperature and (b) samples prepared by varying the base concentration). 143

Fig. 5.29 The variation of zeta potential value with a change in the pH of the clay (RM and NM are raw and sodium Montmorillonite) and metal oxide suspensions. 147

Fig. 6.1 A comparison of the capacity of the PILCs and the starting clays for manganese. 158

Fig. 6.2 The effect of varying the synthesis ratio (R_F) on the capacity of the clay for manganese. 159

Fig. 6.3 The effect of varying the synthesis ratio (R_{OF}) on the capacity of the clay for manganese. 159

Fig. 6.4 The effect of varying the base concentration on the capacity of the clay for manganese. 162

Fig. 6.5 A comparison of the capacity of the Fe-PILC prepared using the high base concentration and the starting clay for manganese. 162

Fig. 6.6 The effect of eliminating the washing step on the capacity of the clay prepared by varying the base concentration of the clay. 164

Fig. 6.7 The effect of varying the base concentration on the capacity of the clay for humic substances. 169

Fig. 6.8 The effect of varying the base concentration on the pH of the thermally-treated clay dispersed in distilled and tap water. 170

Fig. 6.9 A comparison of the capacity of the PILCs and starting clays for humic substances. 170

Fig. 6.10 The effect of regeneration on the capacity of the Fe-PILC for humic substances. 173

Fig. 7.1 Effect of pillaring on the C.E.C. of the clay (prepared by varying the thermal treatment temperature) for strontium. 180

Fig. 7.2 Effect of pillaring on the C.E.C. of the clay (prepared by varying the synthesis ratios) for strontium. 180

Fig. 7.3 Effect of pillaring on the capacity of the clay for strontium. 181

Fig. 7.4 Effect of pillaring on the capacity of the clay for manganese. 182

Fig. 7.5 Effect of pillaring on the capacity of the clay for humic substances. 182

Fig. 7.6 An illustration of variations in pH of the thermally-treated clay (prepared by varying the synthesis ratios) and the degree of pillaring in the clay. 183

Fig. 7.7 An illustration of variations in the base concentration of the clay and the degree of pillaring in the clay. 183

Acknowledgements

There are many people whom I wish to thank for their support in the writing of this thesis. In particular my supervisor, Dr. D.A. White, for his invaluable guidance, informative discussions and constant encouragement during my studies.

I am greatly indebted to the following people: Dr. R. Rautiu, Prof. R. Kandiyoti and Dr. P.G. Clay for their helpful advice; Pat Carry for her help in the operation of the AAS and performing the N_2 adsorption analysis; Dr. I. Aydin for performing the thermal treatment process; members of staff of the Department of Geology: Martin Gill for performing the XRD analysis, and Dr. H. Shaw for his help in the interpretation of the XRD results, and Gill Ragg for performing the ICP-AES analysis; members of staff of Birbeck College: Neil Cohen for performing the TGA and, Dr. M. Odlyha for her help in the interpretation of the results of TGA.

I would like to thank all my friends and colleagues, especially May Wibulswas and Guleda Engin for their support and friendship, which made my studying so enjoyable. I would like to thank my English tutor Mary Rendall especially for her time and effort in improving my English.

I would like to acknowledge the EPSRC for the award of a research studentship without which this work would not have been possible.

Finally I would like to thank my family, especially my eldest brother Victor, for his constant support.

Dedication

To Mum and Dad

Chapter 1 Introduction

1.1 Scope of the Thesis

This thesis will consider the development and use of pillared clays for applications in water purification. Pillared clays such as aluminium and iron pillared clays were made for this purpose by introducing pillaring agents between the layers of the natural clay Montmorillonite. Attempts were made to develop simple and cost-effective methods of producing pillared clays for the industrial water treatment process.

The structural characteristics of the pillared clays were analysed using X-ray diffraction, nitrogen adsorption and ICP-AES. The ability of the pillared clays to remove inorganic cations (strontium) heavy metals (manganese), and coloured organic pollutants (humic substances) from contaminated water will also be discussed.

1.2 General Description of Pillared Clays

Pillared clays are also known as pillared interlayer clays (PILCs). They are two dimensional porous structures which are composed of layers of clay sheets that are permanently separated from each other by pillars of metal oxide. The pore size of the clays may be controlled by the insertion of different types of metal oxide pillars into the layered structure. Hydrated metal oxides of Al, Fe, and Ti, and other metals, can be introduced into the layered structure of

a clay such as Montmorillonite. After thermal treatment the large cations between the silicate layers of the clay are converted into oxide pillars. An additional advantage of the synthesis process is the use of inexpensive inorganic reagents. The mechanism of the formation of PILCs may be described by the following steps (see **fig. 1.1**).

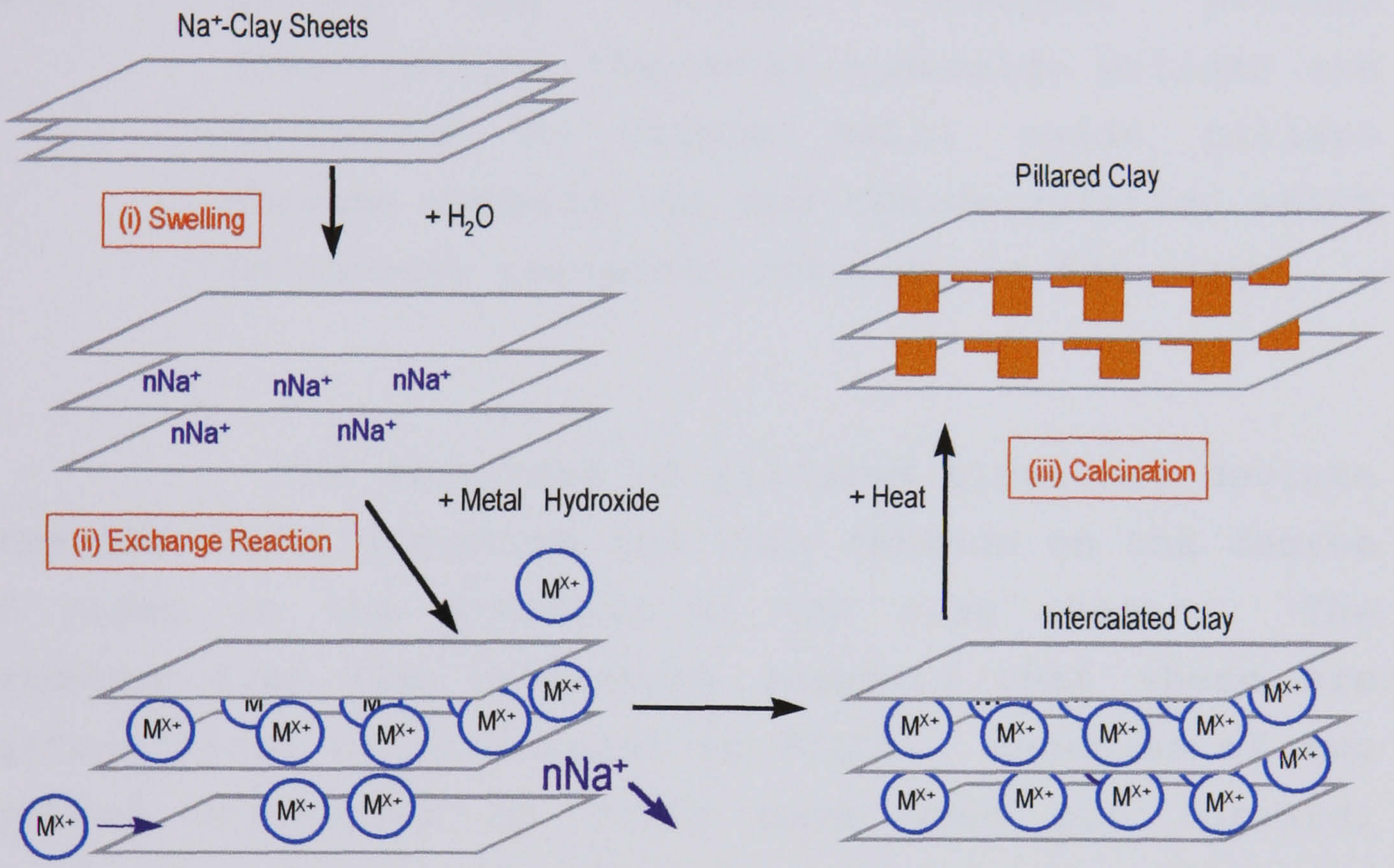


Fig. 1.1 Schematic diagrams that describe the mechanism of the formation of PILCs.

(i) When the clay is dispersed in water the interlayer spacing of the clay, the spaces between the silicate layers of the clay sheets, expands. This then enables the large and positively charged pillaring agents to enter the spaces.

(ii) The large pillaring agents, which are formed by the hydrolysis of a base metal and metal salt, exchange with the smaller exchangeable cations such as Ca^{2+} or Na^{+} in the clay. After a complete exchange process, the separation distance between the clay sheets further increases because of the presence of the larger pillaring agents.

(iii) During the thermal treatment process (calcination) the metal hydroxide pillars are converted to stable metal oxide pillars through dehydration and dehydroxylation which introduces permanent porosity to the clay.

The structure of pillared clays may deviate from the ideal structure and this depends on the degree of order in the stacking of the clay sheets. The evidence from the literature suggests that there are various kinds of structures in PILCs. Examples of two typical structures of PILCs have been put forward, namely the ordered and disordered structures. Pillared clays that have an ordered structure (see **fig. 1.2** (**a**)) consist of layered clay sheets that are arranged parallel to each other, separated by a narrow size distribution of metal oxide pillars which keep them permanently apart. In the clay that has a disordered structure, on the other hand, (see **fig. 1.2** (**b**)) the clay sheets are deformed. The deformation is the result of the clay having been pillared by a wide size distribution of metal oxide pillars.



Fig. 1.2 The possible structures of pillared clays:
(**a**) ordered structure and
(**b**) disordered structure.

1.2.1 History of Pillared Clays (PILCs)

Pillared clays were developed in the early 1970's due to a demand for a new catalyst for cracking crude oil. A material with a pore size larger than that of the maximum pore size of a synthetic zeolite was needed for the catalytic process.

The early pillared clays were prepared by exchanging natural cations in a Montmorillonite clay for organic compounds such as quaternary ammonium ones. These clays lacked thermal stability therefore they had little value for catalysis. In the late 1970's there was a major breakthrough in the development of pillared clays when inorganic hydroxyl cations replaced their organic counterparts and were successfully introduced into the layered structure of the clay. The final product was thermally more stable and chemically more resistant than that of clays pillared with organic reagents. By pillaring the clay with different metal

salts, PILCs with a wide range of surface areas and interlayer spacing values were produced. The pillared clay which has been studied most extensively is an aluminium pillared clay. This is because it is thermally very stable and therefore suitable for application in catalysis.

Researchers succeeded in preparing the early Al-PILC's with inorganic reagents. The clay was also stable at temperatures as high as 500 °C. Another pillared clay, Fe-PILC, was first prepared with organic compounds. Further improvement in the synthesis of Fe-PILC was achieved by preparing Fe-PILC with inorganic reagents such as ferric nitrate. The clay was calcined at 550 °C leading to the formation of a PILC with surface area as high as 244 m^2/g and interlayer spacing value of 20 Å but with an irregular structure.

1.2.2 General Applications of Pillared Clays (PILCs)

The physical structure and property (such as the porous structure and the active sites) of pillared clays give them selectivity, which makes them potentially good catalysts. The main drawback of using these clays for catalysis is that some of them are thermally unstable. Other applications of pillared clays which are being investigated include the clays functioning as adsorbents, as lubricants, in coating and controlled release systems, and in water treatment. Studies from the literature show that the role of pillared clays in water treatment may be important. There is reason to believe that the micropore and

active sites of metal oxides in the pillared clays may enhance the ability of the raw clays to remove certain pollutants from water. The driving force behind this field of research is that it appears that pillared clays can be used as cation exchangers and adsorbents for removal of pollutants from water.

1.3 Removal of Heavy Metals by Cation Exchange

The process in which a clay such as Montmorillonite is used to remove cationic contaminants from the water is often explained using an ion exchange model. Ion exchange is a reversible process and is a chemical reaction which is an equilibrium process between ions in the exchanger and ions in the solution. Ion exchange can only occur between ions of the same charge. An example of exchange reactions between Ca^{2+} and Na^{+} ions from the raw Montmorillonite and Sr^{2+} ions in solution can be expressed in the following reversible reaction equations (**equations 1.1** and **1.2**):

$$\mathbf{Ca^{2+}\text{-}clay} + \mathbf{Sr^{2+}\text{-}solution} \leftrightarrows \mathbf{Sr^{2+}\text{-}clay} + \mathbf{Ca^{2+}\text{-}solution} \quad (1.1)$$

$$\mathbf{2Na^{+}\text{-}clay} + \mathbf{Sr^{2+}\text{-}solution} \leftrightarrows \mathbf{Sr^{2+}\text{-}clay} + \mathbf{2Na^{+}\text{-}solution} \quad (1.2)$$

A general equation of the above exchange reactions can be written for ion $\mathbf{A^{m+}}$ and $\mathbf{B^{n+}}$ and the equation can be expressed as follows (**equation 1.3**):

$$nA^{m+}{}_R + mB^{n+} \leftrightarrows nA^{m+} + mB^{n+}{}_R \quad (1.3)$$

R represents an ion exchange medium.

1.4 Removal of Organic Compounds by Adsorption

For other adsorption media, such as silica gel, zeolite, or activated carbon, which have porous structures, the mechanism of sorption is by a number of processes, such as ion pair attraction, the effect of Van der Waals forces, ion exchange, or a combination of these. The removal of organic contaminants such as humic substances from water by adsorbents such as PILCs may be described using an ion exchange reaction and an adsorption model. A classic adsorption model known as the Langmuir isotherm is used to describe the equilibrium process. This model is based on the adsorption of a solute onto a homogenous surface and also based on the assumption that there are no interactions between sorption sites. The isotherm is expressed in the following equation (**equation 1.4**):

$$y = \frac{Ax}{1 + Bx} \quad (1.4)$$

x is the concentration of the species being adsorbed in the fluid phase (mg/L or meq/L (milli-equivalent/L)), and **y** is the concentration of the species on the adsorbent material (mg/g or meq/kg (milli-equivalent/kg)). **A** and **B** are Langmuir constants. To determine whether the equilibrium data can be correlated with the Langmuir model, the data is analysed using the linear form of the Langmuir

equation. The linear form of the Langmuir equation is expressed in the following format (**equation 1.5**):

$$\frac{x}{y} = \frac{B}{A}x + \frac{1}{A} \qquad (1.5)$$

In the above equation the monolayer capacity of the adsorbent can be determined from the inverse of the gradient.

1.5 Data Interpretation

The concentration of adsorbed species in the adsorbent can be determined from a mass balance equation:

$$y_c m = v(x_o - x_e) \qquad (1.6)$$

In this expression, y_c is the final concentration of species in adsorbent (mg/g or meq/kg of adsorbent), and x_o is the initial concentration of species (mg/L or meq/L). x_e is the final concentration of species (mg/L or meq/L), and m is the mass of adsorbent (g or kg). v is the volume of solution (L). The mass of the adsorbent, the volume of the solution, the initial and the final concentration of the species can be measured experimentally. The values of the final concentration, y_c, can be determined from the above mass balance equation. The data can then be correlated with the Langmuir isotherm by plotting x_e/y_c against x_e at a constant temperature. A linear relationship means the monolayer capacity of the adsorbent (clay or PILCs) can be determined from the inverse of the gradient.

1.6 General Discussion of Water Treatment Processes

(i) Removal of Inorganic Contaminants

Inorganic contaminants such as iron II and manganese II species in water are relatively harmless to human health compared to other heavy metals. However the oxidative products of Fe and Mn increase turbidity in the water, stain clothing during the washing process, and also add an unpleasant taste to water and beverages. Therefore their removal from the water is important.

The primary method (Faust and Ally, 1997) of removal of manganese and iron involves a series of treatment steps. These include oxidation of Mn^{2+} or Fe^{2+} and subsequent precipitation of the metals to their insoluble forms which is followed by sedimentation and filtration. For example in the removal of Mn^{2+} from water, Mn^{2+} is first oxidised into MnO_2 by using oxidants such as chlorine or chlorine dioxide. After that the oxidised product, manganese dioxide (MnO_2 (s)), is filtered through a bed of sand. This is followed by the addition of a chemical coagulant to speed up the final sedimentation process. The main problem with the above conventional method of removing MnO_2, which is formed after the oxidation step, is that the colloidal suspension is difficult to destabilise; and therefore additional treatment steps may be required.

Another process for the removal of manganese is the ion exchange process which is currently used industrially (Faust and Ally, 1997). A manganese-zeolite filter system is used, and the

zeolite acts as an oxidising contact medium, an adsorbent of soluble manganese and also as a filter medium. For large industrial use the filter is limited to the removal of 1 ppm of Mn or Fe. For most effective removal the pH value of the water should be kept at 7.5 or greater. This means care in controlling the pH is crucial for this removal process. Although the overall processes for manganese removal may be effective, they involve many steps which make the treatment procedures complex.

(ii) Removal of Organic Contaminants

Humic substances (Davies and Ghabbour, 1999) are one of the most abundant types of naturally occurring organic compounds which formed by the slow decay and transformation of animal and plant remains. These substances are made up of humic acids, fulvic acids and humins which give soil their brown or black colour. The organic acids are found in soil, groundwater, sewage and brown coals, and in live animals and plants as breakdown products or metabolic by-products. These organic acids consist of complex aliphatic-aromatic macromolecules with alcohol, amine, amide, carbonyl, carboxylic, phenol and quinole functional groups. They are anchored by binding to clays, minerals or metals. The selective binding abilities of humic substances make them useful in applications such as removal of toxic metals from water. Determining the exact chemical formula and the chemical or physical behaviour of these organic acids is still a challenge to researchers.

Humic acids can complex with heavy metals such as Fe^{3+} which makes it difficult for the heavy metal to be removed from the water using the conventional methods. These organic acids have to be removed by carbon adsorption (Eckenfelder, 1989) or chemical coagulation (Carberry, 1990). Hence several stages of water treatment process are essential for the removal of both humic acids and heavy metals. This makes the water treatment process more complex and expensive.

1.7 Research Aims

The overall aim of this research is to develop a PILC for use as a water treatment agent. The possible applications of these PILCs in the field of water treatment have received little attention. Hence it is the focus of this research to explore their potential applications.

Work published in the technical literature has shown that the PILCs, such as Al-PILC, prepared using the conventional method so as to meet the specifications for use in high temperature applications, have a low cation exchange capacity (C.E.C.). The low C.E.C. value of an Al-PILC is the result of high consumption of the natural exchange sites of the parent clay by aluminium metal oxide pillars. Therefore one main aim of this work is to improve the C.E.C. of the PILCs and to explore the possible methods of enhancing the capacity of the clays via the synthesis route. The studies will involve determining the effect of varying the different

synthesis parameters of PILCs (Al-PILC and Fe-PILC) on the C.E.C. of the clay.

Attempts will be made to analyse the structure of the PILC samples prepared by varying the synthesis parameters using the standard characterisation methods. The ion exchange properties of the PILCs and the parent clays will also be characterised using zeta potential analysis. The average particle size range of the PILCs and their parent clay will be determined using a particle size analyser. To determine the C.E.C. of the PILCs and the parent clays, strontium adsorption analysis will be used. This will involve carrying out a series of batch contact tests. The C.E.C. of the clay will be estimated using the Langmuir model (see **section 1.5**).

Attempts will also be made to modify and simplify the synthesis method for PILCs in order to investigate the possibilities of developing a simple method ('short-cut' method) of preparing the PILCs. The synthesis method can be simplified by preparing the PILCs from non-processed clay (raw Montmorillonite), and by eliminating the washing step.

In addition other batch contact tests will be carried out on the modified Fe-PILC to assess the ability of this clay to remove heavy metals (such as manganese) and organic compounds (such as humic substances) from water. The possibilities of regenerating the PILC (modified Fe-PILC) will also be considered.

Chapter 2 Literature Survey

2.1 The Langmuir Adsorption Model

The adsorption of metals from aqueous solutions onto clay has often been described by adsorption models such as the Langmuir model (Faut and Aly, 1987). This model gives a good description of the sorption process (Altin et al., 1998; Srivastava et al., 1989; Lo and Liljestrand, 1996) of heavy metals such as Pb onto clay or modified clays. Other adsorption processes (Faust and Aly, 1997) such as the adsorption of phenolic compounds on activated carbon have also been described by the above model. This is one of the classic adsorption isotherms for adsorption from water systems. The model is simple and has the ability to describe experimental results at low concentrations.

2.2 Raw Clay (Montmorillonite) as a Cation Exchanger

There are a number of clay minerals (Ohtsuka, 1997) that are possible hosts for pillared clays. Montmorillonite (Kooli et al., 1997; Michot and Pinnavaia, 1992; and Heylen and Vansant, 1996) has been the most extensively studied as a starting material for aluminium, iron, titanium, and many other pillared clays. Montmorillonite is the most suitable choice as a starting material because it is inexpensive and is readily available in nature. The clay is able to swell in water and at the same time it has a high cation

exchange capacity value. It also has a simple X-ray diffraction pattern which enables easy interpretation of data of PILCs.

Montmorillonite has two tetrahedral silica sheets, and sandwiched between them is an octahedral alumina sheet (see **fig. 2.1**). Its exchange capacity derives from the substitution of magnesium or iron for aluminium in the octahedral layer (Grimshaw and Harland, 1975). The exchange capacity of this particular clay is considered high compared to other clays. To retain the high cation exchange capacity, the clay should be pillared with the minimum required number of metal oxide pillars so as to 'prop open' the clay sheets, and at the same time to retain the majority of the natural exchange sites. The swelling ability of the clay is an important factor in pillaring the clay. It has been shown (Mohan and Fogler, 1997) that when the clay is dispersed in water to form a homogeneous suspension, the platelets of clay particles are able to move apart which leads to an increase in interlayer spacing. The spacing of the clay is also pH dependent and it decreases with an increase in pH (see **fig. 2.2**).

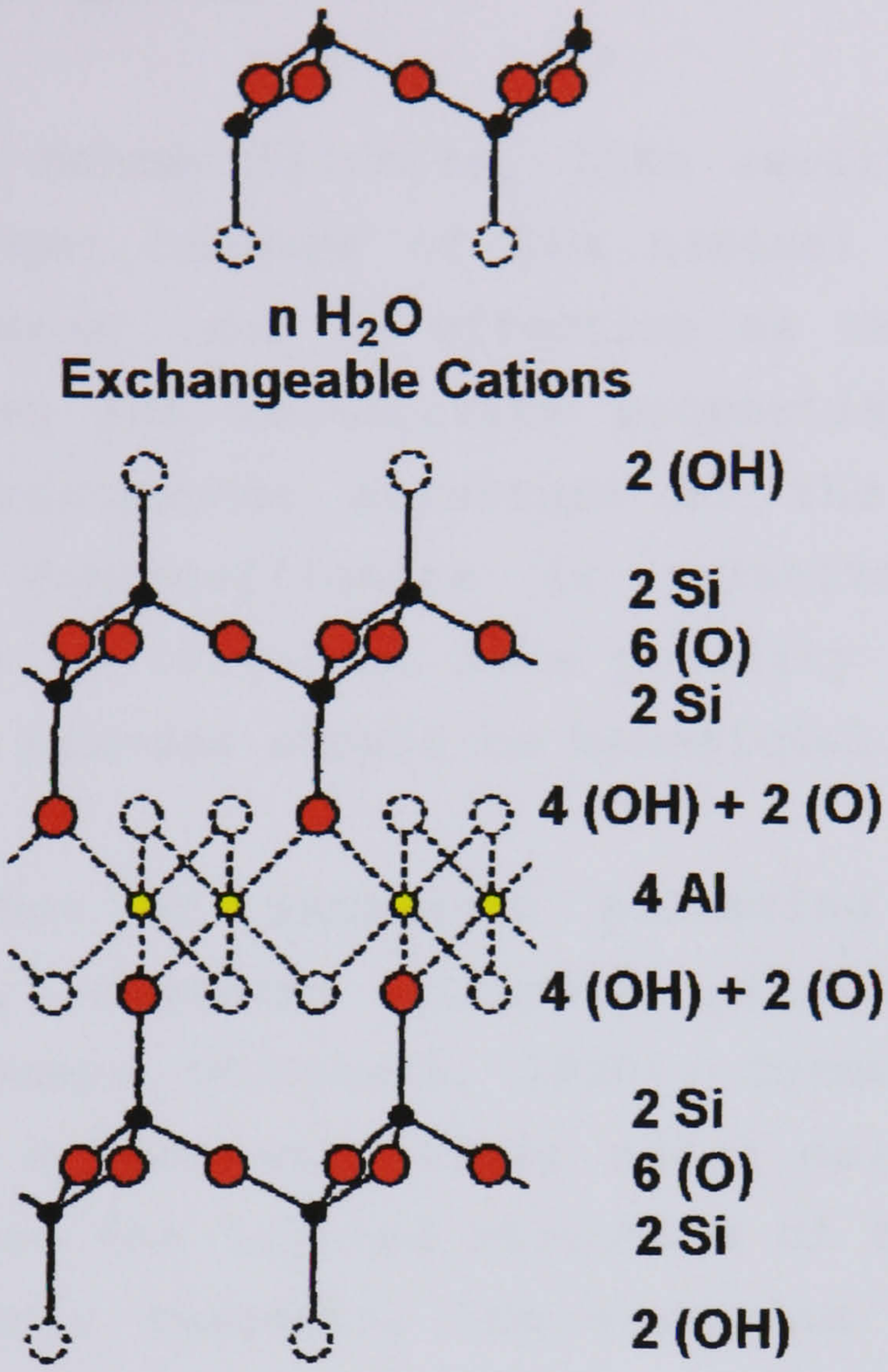


Fig. 2.1 The structure of Montmorillonite (Grim, 1968).

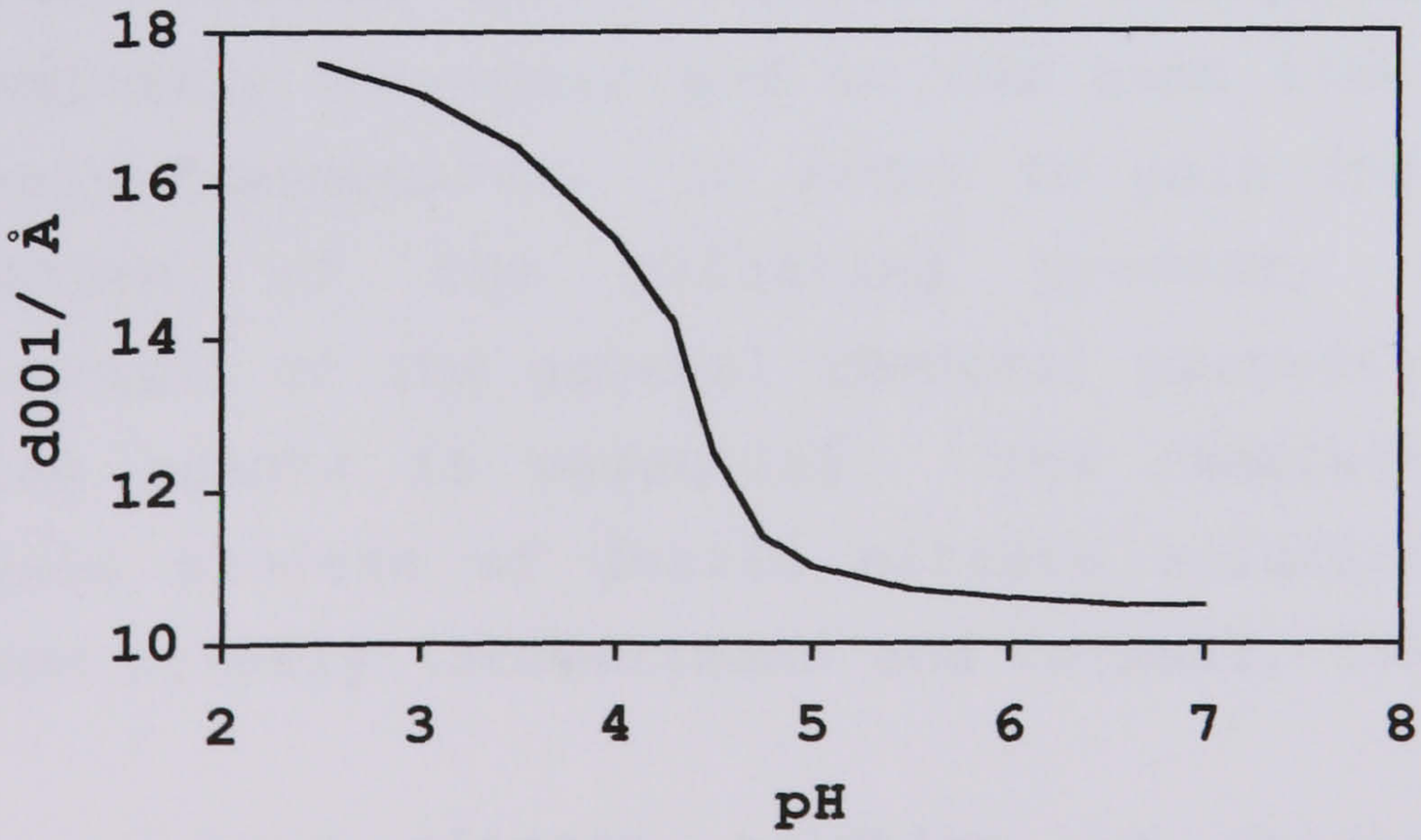


Fig. 2.2 Effect of pH on the d001 (basal) spacing (Å) of sodium Montmorillonite (Schnitzer and Khan, 1972).

2.3 Pillaring Agents

Raw Montmorillonite, like zeolite, is a good cation exchanger because of its natural exchange sites. It is, however, not as effective as zeolite in terms of adsorption and selectivity properties, which arise from the microporous structure of the mineral concerned. Raw Montmorillonite is relatively non-porous. Therefore to introduce more porosity into the clay the pillaring process should be beneficial.

A number of inorganic pillaring agents, namely, zirconium, chromium, silicate, aluminium and iron cationic polymers (Mitchell, 1990), formed during the hydrolysis of a base with their metal salts, have been introduced into the layered structure of the clay. Among these inorganic reagents, the aluminium and iron pillaring agents may be the most promising ones selected for the syntheses of pillared clays for water treatment. This is mainly because the aluminium, the iron salts and their hydrolysed forms are also used as coagulants in the conventional water treatment process (Jiang and Graham, 1997). These two inorganic reagents are chemically non-toxic and at the same time they are relatively inexpensive. In order to gain insight into the nature of the pillaring process, a better understanding of the general chemical properties of the pillaring agents is essential. The chemistry of the hydrolysis process of ferric nitrate solution will be described briefly (Schwertmann and Cornell, 1991).

Iron nitrate solution is acidic, bright yellow and a clear solution. The hydrolysis of the ferric solution involves the elimination of protons

from the six water molecules surrounding the ferric ion. Examples of hydrolysis reactions are:

$$
\begin{aligned}
Fe^{3+} + H_2O &\rightarrow FeOH^{2+} + H^+ \\
Fe^{3+} + 2H_2O &\rightarrow Fe(OH)_2^+ + 2H^+ \\
Fe^{3+} + 2H_2O &\rightarrow FeOOH + 3H^+ \\
2Fe^{3+} + 3H_2O &\rightarrow Fe_2O_3 + 6H^+
\end{aligned}
\qquad (2.1)
$$

The method of inducing the hydrolysis process of the aluminium or ferric solution may involve heat or the addition of an alkaline salt solution such as sodium hydroxide. If the process is base induced, then, at the early stages of the hydrolysis process, protons will be formed and, as a result, the pH of the system will fall. If the process is heat-induced, due to the temperature rise the pH of the system could also fall to a low value. This will inhibit further hydrolysis. The yield of the product would then be reduced because of incomplete hydrolysis of the salt solution. Therefore it is important to reduce the acidity of the solution by pH adjustment, such as addition of a base, which will raise the pH of the system and enhance the process.

Other physical aspects of these hydrolysed species such as the charge and molecular weight will also affect the pillaring process, and these effects will now be discussed. The pillaring reagents may have various charges (M^+, M^{2+}, M^{x+}), or even a negative charge, and a wide range of molecular weights. These factors will directly influence the pillaring process because the process itself is dependent on the degree

of ion exchange in the clay. If the majority of the pillaring agents have a high positive charge, they can exchange freely with the cations in the clay which leads to layer expansion in the clay structure. The pillaring agents are significantly larger than the natural exchangeable cations, so they will 'prop' open the clay sheets. After calcination the pillaring agents are converted to stable metal oxide pillars which are permanently attached to the clay sheets.

2.4 Pillared Clays (PILCs) as Adsorbents and Cation Exchangers

The development of pillared clays (PILCs) in the field of catalysis (Pinnavaia and Thorpe, 1995) has been rapid and extensive but their application in water treatment has received little attention. From recent literature reviews it can be concluded that the development of PILCs in the area of water treatment has been slow. A few PILCs, aluminium, zirconium, and chromium clays have been synthesised by the conventional methods and their performance in the removal of various contaminants from water has also been studied by a number of researchers (Mishael et al., 1999). These studies involve assessing the ion exchange and adsorption properties of pillared clays for inorganic or organic contaminants.

A study (Williams and Hudson, 1990) of the ion exchange properties of Zr-PILC and Al-PILC shows that pillaring of the clay increases the cation exchange capacity of the clay. The researchers suggest that the increase of the C.E.C. of PILCs is due to the presence of the metal oxide pillars. The behaviour of

the ion exchange properties of the pillared clays was studied and compared with that of the alumina and zirconium oxides for the uptake of Cs^+, Rb^+, and other ions. The results show that the exchange properties of the two pillared clays depend on the pH of the exchanging solution which also suggests that the ion exchange properties of the clays are very similar to those of hydrous metal oxides. The ion exchange properties of the clays were studied using pH titration. Although it was the analysis method that was frequently used to study the ion exchange properties of hydrous metal oxides it may not be as reliable as the following method. The more accurate method of analysis would involve batch contacting tests and directly measuring the equilibrium concentration of cations in the solution. This is a standard method of determining the C.E.C. of clays.

For the above reason, other more recent research work, using the standard method to determine the C.E.C. of various pillared clays, has led to other findings. Studies (Li and Scala, 1996) into the adsorption of Al-PILC show that the cation exchange capacity of the clay for heavy metal cations such as copper, Cu^{2+}, chromium, Cr^{2+}, and lead, Pb^{2+}, suffers a reduction of approximately 80%. The results of these studies demonstrate that the loss of C.E.C. is a direct consequence of pillaring the clay with a pillaring agent such as aluminium polymeric cations. This indicates the obvious major drawback of using Al-PILC for water treatment. However, research has also shown that the cation exchange capacity of Al-PILC may be partially restored by treating the clay with a base such as potassium carbonate or ammonia.

The effectiveness of Al-PILC and Zr-PILC to adsorb radioactive cobalt was compared with that of their parent clay, Montmorillonite and with an organoclay. In these experiments (Nava-Galve et al., 1996) the performance of Zr-PILC was much higher than any of the others. When the capacity of Zr-PILC for cobalt is compared to that of the parent clay, an increase of 18% is observed. Conversely, when the performance of Zr-PILC for cobalt is compared with that of Al-PILC, an increase of almost as much as 50% is observed. This indicates that cobalt retention in inorganic pillared clay depends very much on the type of pillar.

Other studies (Wibulswas et al., 1999) on the capability of pillared clays to remove organic compounds such as humic substances and organic toxicants like chlorinated phenols from water, has also been carried out. Other findings (Amin et al., 1996) show that Zr-PILC prepared with Montmorillonite is more effective than other PILCs which have been synthesised with starting materials such as kaolin and bentonite.

Michot and Pinnavaia (1991) show that Al-PILCs modified by addition of a nonionic surfactant, Tergital 15S-5, exhibit interesting adsorption properties with regard to chlorinated phenols. Their results show that the surfactant increases the affinity of S-Al-PILC for phenolic compounds by providing more adsorption sites, whereas the conventional pillared clay without the surfactant may have fewer of these adsorption sites. The disadvantage of using surfactant modified Al-PILC is the effect of possible leaching of surfactant into the water under specific chemical conditions such as a change of pH.

2.4.1 Synthesis of Aluminium Pillared Clay (Al-PILC)

Aluminium pillared clays have been extensively studied. The large volume of literature (Burch, 1988) on the method of synthesis and physical and chemical properties of Al-PILC show that the clay may be used as a catalyst and an adsorbent. The detailed information of the synthesis procedures available from the literature provides valuable guidelines for the development of PILCs for water treatment. The main reason that Al-PILC is a suitable choice for study is because it is thermally stable at temperatures of as high as 400 °C (Occelli and Tindwa, 1983). It is also chemically more stable than many of the other PILCs (Storaro et al., 1998) and less expensive.

The conventional method of synthesis of Al-PILC involves the use of inorganic reagents and the final product usually has a high surface area and porosity compared to its parent clay. For the purpose of water treatment, preparing Al-PILC from inorganic reagents can be viewed as cost effective as well. The main disadvantage of the conventional way of synthesising Al-PILC is that there are too many steps and, at the same time, the process is time consuming. In order to increase the ability of Al-PILC to act as a reagent for water treatment, the conventional method of synthesising Al-PILC needs to be assessed. The general steps in the conventional synthesis may be summarised below.

(i) Before pillaring, the clay is refined by conventional sedimentation techniques or dialysed or pre-exchanged (Diano et al., 1994) with a calcium or sodium salt solution.

(ii) The pillaring solution, which consists of a mixture of aluminium polyoxications, is prepared by a dropwise addition (Ge et al., 1994) of a base solution to an aluminium salt solution while it is being stirred vigorously at 50 °C. The solution is then aged (Gil et al., 1994) for 12 or 48 hours.

(iii) During the pillaring process (Peinemann and Helmy, 1994) the clay suspension is added dropwise into the pillaring solution while the solution is being stirred and heated to 80 °C for 2 to 3 hours.

(iv) At the final stage, the clay is washed, dried and calcined at a given temperature.

Below is a summary of the main disadvantages of the conventional method of synthesis of Al-PILC. For an industrial scale the process of synthesis would be expensive because of the many steps it entails, and it would also be time consuming. In order to prepare a competitive Al-PILC as a reagent for water treatment the conventional method of synthesising Al-PILC will need to be modified. A summary of the modifications on the synthesis is discussed below.

(1) A raw non-refined Montmorillonite clay in its calcium form will be used. There are several

advantages of using raw calcium Montmorillonite. These are listed below.

(a) Raw Montmorillonite is commonly found in nature.

(b) It can swell but it does not gel at high concentration. Therefore it may be possible to pillar the clay at a high clay concentration on an industrial scale.

(c) The swollen form of the clay should have interlayer spacing that is sufficient to receive aluminium and iron polyoxocations.

(d) The clay often has sheets that are regularly stacked which should favour the formation of a well-ordered Al-PILC.

(2) In the modified form of the method the clay is directly dispersed in the base solution and then quickly added to an aluminium salt solution. The number of steps is therefore reduced and the process is less time-consuming.

(3) The entire process takes place at room temperature which makes it less expensive.

By synthesising the Al-PILC using the above 'short-cut' method the overall production cost of the clay can be reduced.

The focus of this project is to utilise the properties of Al-PILC for effective water treatment

processes. The main objective is to assess the role of the clay for the uptake of pollutants from water. Therefore it is important to characterise the cation exchange capacity (C.E.C.) of the Al-PILC. Literature reviews (Oades, 1984) show that the C.E.C. of a hydroxly-Al-Montmorillonite is lower than that of a raw clay, whereas for ferric polycation treated clay the C.E.C. remains high. Because of this, studying the potential of iron pillared clays as water treatment reagents is even more important.

2.4.2 Synthesis of Iron Pillared Clay (Fe-PILC)

Many publications in the literature of PILCs focus on the synthesis of Al-PILC and Zr-PILC because these clays offer good thermal stability, which is crucial for catalysis applications. In contrast, very few publications consider Fe-PILC because it is thermal less stable than the other PILCs. However main advantages of Fe-PILC are that it is cheaper to prepare and it has a micropore size which can be as large as 20 Å. The larger pore size means that the clay may be able to remove the large pollutants from water. Most importantly, there is evidence from the literature (Oades, 1984) that the C.E.C. of a Montmorillonite clay after being treated with ferric polycations remains considerably higher than that of the clay which has been treated with aluminium polycations. It has been proposed that the higher charge and the shape of the aluminium polycations lead to the blockage of a larger number of negative exchange sites in the clay. These planar aluminium polycations are more effective than

ferric polycations in blocking and even neutralising the negative sites of the clay, whereas the spherical ferric polycations block a smaller number of negative sites. The advantages of Fe-PILC over Al-PILC can be summarised in the following points:

(i) Fe-PILC should have a higher C.E.C. than Al-PILC.

(ii) Fe-PILC will have a larger micropore size than Al-PILC. It will therefore adsorb larger molecules.

(iii) The production cost of Fe-PILC would be lower than that of an Al-PILC due to the cheaper cost of ferric salts used to make the pillaring agent.

(iv) Iron salts are less harmful to humans than aluminium salts which may cause Alzheimer's disease.

The main disadvantage of Fe-PILC compared to Al-PILC is that it is thermally unstable (Burch, 1988). The process being studied in this project is linked for use in water treatment at a low temperature. Therefore the material need not be thermally stable at a high temperature. The outline of the pillaring procedures is very similar to that of Al-PILC and the general steps are as follows:

(i) A ferric salt solution is partially hydrolysed with a base.

(ii) This is followed by the addition of a clay suspension to the pillaring solution.

(iii) The mixture is washed with distilled water to remove the excess salt.

(iv) Finally the raw pillared clay is heated. The final stage of the treatment gives rise to the formation of stable iron oxide pillars which prop open the clay sheets.

Conditions such as the acidity of the pillaring mixture may affect the structure of Fe-PILC more than that of Al-PILC. A ferric salt solution tends to hydrolyse and precipitate at a lower pH than an aluminium salt solution. Therefore by pillaring the clay with ferric polycations rather than aluminium polycations, a more acidic PILC results. The main problems of pillaring a clay with ferric polycations are structural. Fe-PILCs synthesised by conventional methods (Maes and Vansant, 1995) often lack order and crystallinity, leading to a low interlayer spacing. Few of the existing methods of synthesising Fe-PILC result in an ordered structure with high interlayer spacing.

Reviews from the literature show that the methods of synthesis of Fe-PILC may be categorised into two routes. Fe-PILC can be synthesised by conventional methods with inorganic or organic reagents. Using an organic pillaring agent such as $[Fe\{COOCH_3\}_7OH_2H_2O]^+NO_3^-$ (Mishra et al., 1996) would give additional advantages such as control over the structure of the Fe-PILC. The final product usually has higher interlayer spacing and greater crystallinity. The main disadvantage of this

method is that it would involve higher production costs because of the need to use organic reagents and to calcine the clay at a high temperature, as high as 400 °C, to remove the organic compound present in the clay. The complex steps involved also contribute to increased costs. By using inorganic reagents to pillar the clay, the production cost of Fe-PILCs is reduced. Fe-PILC have been synthesised from ferric percholate, chloride, nitrate solutions, and a base such as calcium carbonate (Rightor et al., 1991). The main disadvantages of this method are that it is time-consuming and complex.

2.4.3 Factors that Enhance the Cation Exchange and Adsorption Property of Fe-PILC

2.4.3.1 Introduction

Two main factors may directly affect the cation exchange capacities (C.E.C.) of Fe-PILC: the synthesis ratio of Fe/clay and the final pH of the synthesised clay. The final Fe-PILC has both natural and synthetic exchange sites. Therefore the clay should have unique exchange and adsorption properties. Unfortunately, studies (Sanchez and Montes, 1998) into the ion exchange properties of PILCs (such as Al-PILC) have shown that PILC has low C.E.C compared to the parent clay.

(i) Effect of Varying the Synthesis Ratios on the Cation Exchange Property of PILCs

Studies (Li and Scala, 1996) from the literature show that pillaring a sodium Montmorillonite with OH/Al ratio of 2.4 and Al/clay ratio in the range of 2.8 - 3.0 mmol/g resulted in an 85% reduction in the cation exchange capacity (C.E.C.) of the clay. Other studies (Gil and Montes, 1994) from the literature show that the C.E.C. of an Al-PILC decreases as the OH/Al molar ratio and the content of Al_2O_3 increases. Studies from other research (Oades, 1984) also suggest that the interaction of Al rather than Fe pillaring agents with the natural exchange sites of the clay may have resulted in the blocking of greater number of neighbouring sites of the clay.

(ii) Effect of Varying the Thermal Treatment Temperature on the Cation Exchange Property of PILCs

Studies (Corma, 1997) from the literature show that the temperature at which the PILCs are thermally treated often influences their final structure and physical properties. This synthesis parameter is also one of the most important factors in the preparation of ordered and porous (Hutson et al., 1999) PILCs. Structural collapse of the clay can result when treating the clay at an unnecessarily high temperature (above 400 °C), and this may lead to a reduction in natural exchange sites and adsorption sites in the PILCs. The formation of a stable metal oxide is also temperature dependent (Bandosz and Cheng

1997). Hence treating the raw PILC at an optimum temperature is important.

A PILC prepared for usage in low temperature applications, such as water treatment, may be treated at a lower temperature. Therefore the effect of thermal treatment on the structure, ion exchange and adsorption properties of PILCs is important and needs investigation.

(iii) Effect of Varying the Base Concentration on the Cation Exchange Property of PILCs

(a) The Capacity of the Clay for Humic Substances

The mechanisms of the main reactions (Schnitzer and Khan, 1972) that remove humic substances using clay include anion-exchange reactions or non-specific adsorption; ligand exchange reactions, and hydrogen bonding. Both the anion-exchange reaction, and the surface reaction depend on chemical factors such as the pH of a solution containing humic substances when it makes contact with the clay. Therefore the pH of the clay undoubtedly plays an important part in removal of humic substances from water. The other mechanism may depend on factors such as the nature of the binding of organic compounds to the surface of the clay; the molecular weight and the solubility of the organic acid in water; water speciation; the nature of the clay and the temperature. It is also known that clays with high aluminium or iron content are good adsorbents for humic compounds (Schnitzer and Khan, 1972, Tipping and Cooke, 1982, and Amal et al., 1992).

(b) The Capacity of the Clay for Heavy Metals

Studies (Eslinger and Pevear, 1988) of zeta potential analysis show that ferric oxide acts as an anion exchanger at a low pH but as a cation exchanger at a higher pH. At approximately pH 6 the iron III oxide has a point zero charge. This property of iron oxide may suggest that by increasing the pH in the synthesis of Fe-PILC, the C.E.C. of the clay may be enhanced. Adsorption of heavy metals such as Zn^{2+}, Cu^{2+}, Pb^{2+}, and Co^{2+} on an oxide surface also depends on the effect of a the variation of pH (Srivastava et al., 1998). The effect of the increase of pH results in a direct increase in the adsorption capacity of the oxide for the heavy metals. The above findings are also in agreement with the findings of Li and Scala (1996). These studies show that treating PILCs with bases such as ammonium hydroxide solution can lead to a 79% recovery of the original C.E.C. of PILCs.

Chapter 3 Preliminary Characterisation and Techniques for Analysing PILCs

3.1 X-ray Diffraction (XRD) Analysis

X-ray diffraction is used to obtain information about the structure, and degree of crystallinity of PILCs. The approach used to interpret diffraction data is based on Bragg's law which is expressed by the equation:

$$n\lambda = 2d \sin\theta \qquad (3.1)$$

here λ is the X-ray wavelength in this case 1.5406 Å (CuKα radiation); **n** the diffraction order with values, **n** = 1, 2, 3,....; θ is the Bragg angle, and **d** is the perpendicular distance between pairs of adjacent planes having the same Miller indices (Moore and Reynolds, 1997) and is usually equal to 1. The technique is used to monitor any expansion between silicate layers of Montmorillonite, resulting from the insertion of metal oxide in the clay structure. The distance between the silicate layers is the spacing of the crystallographic planes which lie parallel to the sheet structure of the clay. This is known as the basal spacing of the clay.

Clay samples were suspended in distilled water for 24 hours. A known amount of the suspensions was then pipetted on to ceramic tiles and oriented onto the tile surfaces by vacuum filtration. Finally all the samples were air dried at room temperature for 4 days. The samples were mounted on ceramic tiles and

scanned as oriented powder at low angle X-ray (1.6° - 20°) 2θ by PW1710 equipment with Cu Kα radiation. All the samples were scanned at stepsize of 2° and the time per step was 3 seconds. For more details of the analysis refer to studies of the technique in the literature (Velde, 1992).

3.2 Nitrogen Adsorption Analysis

This is a standard procedure to determine the surface area of finely divided and highly porous materials. By determining the nitrogen adsorption and desorption isotherm of the porous materials, information such as their BET surface area, pore size and microporosity can be obtained. Nitrogen adsorption is measured gravimetrically. There are three main types of isotherm (Sing, 1989), type I, II and IV, (see **fig. 3.1**) and they describe the amount of nitrogen molecules adsorbed by the materials at different relative pressure and at constant temperature. Type I represents a microporous solid with a small pore, and has a limited uptake of the nitrogen gas related to accessible micropore volume. Type II represents a non-porous or macroprous solid. Type IV represents a mesoporous solid and its isotherm has a hysteresis loop which is a feature of capillary condensation of nitrogen gas.

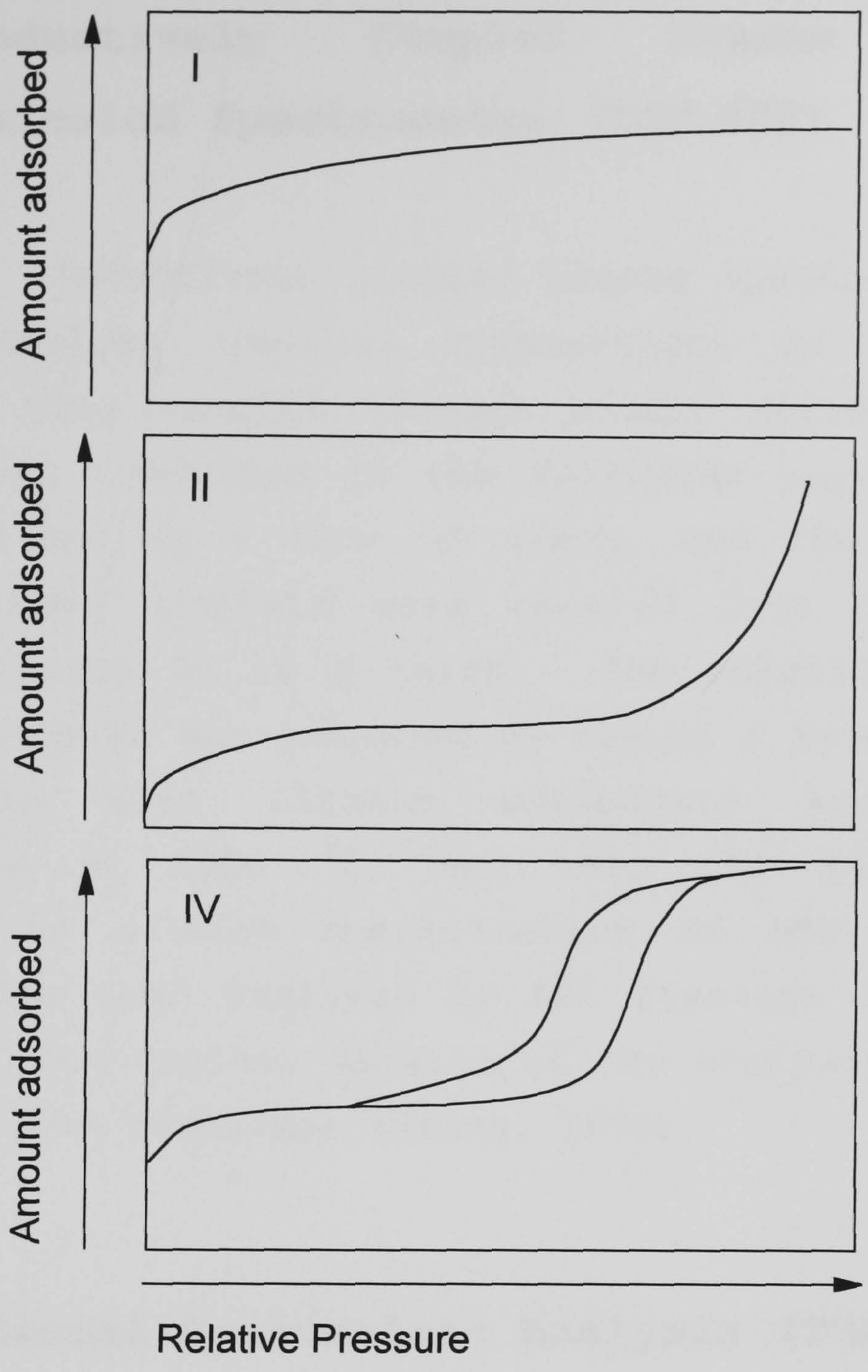


Fig. 3.1 The three basic adsorption isotherm types: type I, type II and type IV.

Approximately 0.1 - 0.2 g of the samples, previously dried in an oven at 110 °C, was degassed at 110 °C at a constant pressure for 3 or 4 hours and the isotherms were recorded at 77 K (liquid nitrogen). The nitrogen adsorption and desorption isotherms of the samples were recorded on an ASAP 2000 Micromeritics apparatus.

3.3 Inductively Coupled Plasma Atomic Emission Spectrometry (ICP-AES)

Inductively coupled plasma spectrometry was used to analyse chemical compositions in percentage weight of clay samples through atomic emission. The analysis was conducted in the following way. Samples were nebulized by a flow of argon, and the resulting finely-divided droplets were carried into the plasma source referred to as a torch. The solution form of the clay samples was prepared by fusing a known mass of the sample with lithium metaborate and lithium tetraborate at 1000 °C, and then the solids were dissolved in a high concentration of HNO_3 solution. Samples were then analysed by ARL Fissions 3580B, ICP Analyser. For further details of the analysis refer to studies of the technique (Skoog, 1996).

3.4 Thermal Gravimetric Analysis (TGA)

Thermal gravimetric analysis (Velde, 1992) is a standard technique which is used to study the thermal stability of materials. This method of analysis was also used in this study to determine a suitable temperature range at which the starting material would be stable. The information obtained from TGA indicates the possible temperature range at which the raw pillared clay may be treated. Hence thermally treating the raw pillared clay within the measured temperature range should avoid damaging the basic clay structure of raw Montmorillonite. The instrument measured the amount of weight loss in the

sample while the sample was heated at a regular rate with constant temperature monitoring.

10 mg of the clay sample was weighed into a crucible (5 mm in diameter and made of aluminium oxide) of the differential scanning calorimeter (Shimadzu, TGA-50) and then heated by raising the temperature from 25 °C to a maximum of 800 °C in a flowing oxygen atmosphere at a rate of 2 or 10 °C per minute. The results are illustrated on a plot of the amount of weight loss in the sample versus the temperature at which the sample was treated. It has often been found that the weight loss was due to the loss of water in the clay. The different types of water which can be removed from the clay during thermal treatment may be categorised into adsorbed water, bound water, and crystalline water.

3.5 Zeta Potential Analysis

This is a rapid method of determining the sign of charges on colloidal particles and also their electropheretic mobility, and hence their apparent zeta potential. The zeta potential measurements of the particles were obtained using a standard Zetamaster (Malvern with Zetasizer 4, P.S.C.). The instrument has a cross beam laser anemometer for electropheresis measurements, and a parallel beam along the axis of a cell for particle sizing. The light scattering effect resulting from the motion of the particles in an electric field is correlated electronically and this results in a zeta potential measurement.

In this study, zeta potential analysis (Hunter, 1988) is used to characterise the ion exchange properties of PILCs by determining the net charge on the surface of clay particles. To measure the zeta potential, a sample of the clay is suspended in potassium nitrate solution at a given pH. The total net charge of the smectite clay is derived mostly from the permanent charge, which is negative. Hence zeta potential value would remain negative, but may change at extremely low pH. Rautiu et al. (1994) show that for a cation exchange process, which involves cations from the exchanger exchanging stoichiometrically with the counter ions from the solution, the net electrical charge within the cation exchanger is unaltered. Therefore for PILCs to act as a cation exchanger, the zeta potential of the clays should be a constant and negative value over a wide range of pH.

3.6 Strontium Adsorption Isotherm

The strontium adsorption isotherm (Wilson, 1987) is one of the standard methods of determining the cation exchange capacity (C.E.C.) of clay minerals. It is also used in this study to characterise the cation exchange properties of PILCs and Montmorillonite clays. This standard method is well established and well known in the field of clay mineralogy. The reasons for this choice are that strontium ions do not naturally occur as an exchangeable cation in clay minerals and they will also remain as stable divalent ions (Sr^{2+}) in a wide range of solution pH. In this study a series of adsorption experiments were conducted using strontium as an index ion. In each case, a constant amount of clay sample was contacted with a constant volume, but

with different concentrations of strontium chloride solution under the given experimental conditions. The concentrations of strontium in the solution were determined using atomic emission spectrometry. A strontium adsorption isotherm was constructed for each clay sample from the mass balance equation (see **chapter 1, equation 1.6**).

3.7 Atomic Absorption Spectrometry (A.A.S.) and Atomic Emission Spectrometry (A.E.S.)

Atomic absorption (A.A.S.) and emission (A.E.S.) spectrometry (Skoog, 1996) are rapid, versatile analysis techniques to determine whether metals are present in water. The main advantage of using these techniques for this study is that the water samples can be introduced directly into the instrument, and often only a minimum of pre-treatment is necessary. In this study A.A.S. was used to determine the concentration of iron III or manganese in solution whereas A.E.S. was used to determine the concentration of strontium in solution.

The analysis was carried out using the Perkin-Elmer spectrometer with an air-acetylene flame. The instrument was calibrated with a series of standard solutions. The sample solutions were nebulized and carried into the flame by a flow of gaseous oxidant or fuel. The emission and absorption spectra were generated in the resulting hot, gaseous medium and the data obtained was directly converted from absorbance value to concentration values in parts-per-million

(ppm) by the instrument. The typical values of the sensitivity and the detection limit of the instrument for iron III, manganese and strontium are given in the table below (see **table 3.1**). A solution of lanthanum chloride was added to the samples and standards to enhance strontium atomisation.

Table 3.1 The sensitivity and detection limit of A.A.S. and A.E.S..

Sample Type	Wavelength (λ) /nm	Sensitivity /ppm	Detection Limit /ppm	Analysis Technique
Fe	248.3	0.10	0.005	A.A.S.
Mn	279.5	0.05	0.001	A.A.S.
Sr	460.7	0.11	0.001	A.E.S.

Fe is iron III. **Mn** is manganese. **Sr** is strontium.

A.A.S. is Atomic Absorption Spectrometry.

A.E.S. is Atomic Emission Spectrometry.

3.8 Ultraviolet Spectrometry

Ultraviolet spectrometry (Skoog, 1996) was used to determine the concentration of coloured organic compounds such as humic substances in water. The concentration of humic substances in water was calculated from the measured absorbance value of an unknown concentration of the sample solution using a linear calibration curve.

To determine the humic substances concentration in water the spectrometer was set at 400 nm, which is at the maximum absorption line for humic substances. A calibration curve was constructed from

the adsorption spectrum of humic substances measured at 400 nm. A linear calibration curve was produced from the standard solution of humic substances (5, 10, 20, 40 and 50 ppm). By plotting the absorbance values of the standards, against the concentration of the standards a linear calibration curve was obtained (see **fig. 3.2**).

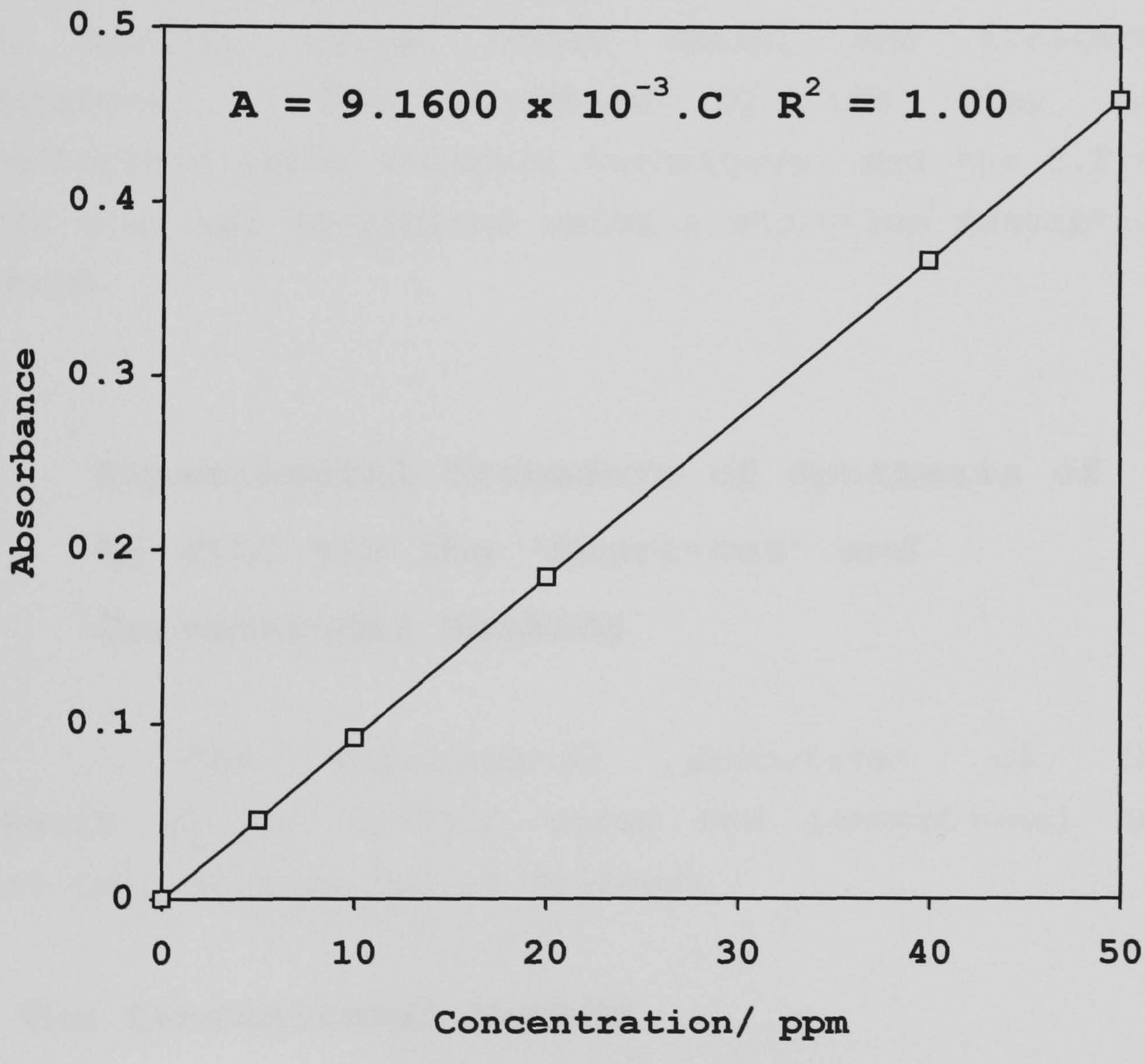


Fig. 3.2 The calibration curve of humic substances. **A** is the absorbance and **C** is the concentration. $\mathbf{R^2}$ is the square of correlation coefficient.

Chapter 4 Experiments with Al-PILC

4.1 Introduction

The focus in this chapter will be on Al-PILC. The effect of simplifying the method of Al-PILC preparation on structure and cation exchange capacity is discussed. The methods of enhancing the C.E.C. of the clay are also discussed. These methods include varying the synthesis parameters, such as the starting clay, Al/clay ratio, OH/Al ratio, and treatment temperature. The structure of the clay was characterised using standard techniques, and the C.E.C. of the clay was determined using a strontium adsorption isotherm.

4.2 Experimental Procedure of Synthesis of Al-PILC via the 'Short-cut' and Conventional Methods

The experimental procedures of the synthesis of the Al-PILC using the conventional and 'short-cut' methods are as follows:

(i) The Conventional Method

This method consists of 3 major steps as described in the following section:

(a) Conversion of Raw Montmorillonite to Sodium Montmorillonite

50 g of raw Montmorillonite was contacted with 2 litres of sodium chloride solution (1 M) three times. After this the clay was washed with distilled water to remove the excess ions in the clay. When the conductance of the clay suspension was less than 20 µS, the clay was separated from suspension using a centrifuge (MSE, Centaur 2) at 3500 r.p.m. for 30 minutes. The clay slurry was then dried at 90 °C in a hot-box for 18 hours and stored in an air-tight sample bottle.

(b) Preparing the Pillaring Solution

300 ml of NaOH(aq) solution (0.2 molar) was added to 125 ml of $AlCl_3$(aq) (0.2 molar) solution in a three litre beaker at a rate of one drop per second while the reaction mixture was stirred vigorously with a magnetic stirrer (this stirrer was covered with PTFE and it was 10 mm in diameter and 40 mm in length). The reaction temperature was kept at 80 °C throughout the addition.

(c) The Pillaring Process

10 g of sodium Montmorillonite was dispersed in 400 ml of distilled water and heated to 50 °C for an hour. The clay suspension was then added to 425 ml of the prepared pillaring solution, at a rate of 150 ml per minute while the reaction mixture was stirred vigorously. The reaction temperature was kept at 70 °C throughout this process, and the mixture was stirred for a further 2 hours. After that the clay was

cooled and the mixture was stirred for a further 16 hours at room temperature. Subsequently the clay was separated from the suspension using a centrifuge at 3500 r.p.m. for 1 hour and then dried in a hot-box at 120 °C for 18 hours. Finally the clay was ground to a fine powder using a pestle and mortar.

(ii) The 'Short-cut' Method

With this method the number of steps were reduced to one major step because aluminium chloride solution was added directly to the clay suspension in the sodium hydroxide solution. Additional advantages were that the reaction took place at room temperature, and the addition time was reduced. The process is as follows:

(a) The Pillaring Process

20 g of raw Montmorillonite was suspended in 1000 ml of NaOH (aq) solution (see **table 4.1**) and the mixture was stirred vigorously for 10 minutes. After 10 minutes a 1000 ml of $AlCl_3$ solution (see **table 4.1**) was added quickly to the alkaline clay suspension while it was stirred vigorously. The reaction mixture was stirred for a further 3 hours. The clay was then separated from suspension using a centrifuge at 3500 r.p.m. for 1 hour and washed with distilled water until the conductance was less than 20 µS. The clay was then dried at 120 °C in a hot-box for 18 hours. Finally the clay was ground to a fine powder using a pestle and mortar.

4.3 Strontium Adsorption Analysis

To determine the cation exchange capacity (C.E.C.) of the Al-PILC samples (AC-1 and AC-2 prepared using the conventional method, and AS-1, AS-2, and AS-3 prepared using the 'short-cut' method) a known amount of the clay was contacted with a known volume and different ranges of concentrations of strontium chloride solutions. For detailed descriptions of the samples see **table 4.1.** For comparison, the same experimental procedures were also repeated with the raw Montmorillonite, and sodium Montmorillonite. The concentrations of strontium remaining in solution were determined using atomic emission spectrometry. The experimental procedures are described below.

0.1 g of the clay sample was contacted with 50 ml of a known concentration of strontium chloride solution in an air-tight polyethylene bottle. The contacting solution was prepared by diluting a stock solution of strontium chloride (prepared from $SrCl_2.6H_2O$, AnalaR, BDH, 99-103%) in double-purified water. The contacting sample was shaken for 18 hours on a shaker with the temperature set at 16 °C to allow the process to reach equilibrium. A series of blank strontium solutions were also set up under the same experimental conditions. The sample solution for analysis containing 1% lanthanum chloride solution was prepared by adding 0.2 M of $LaCl_3$ (prepared from $LaCl_3.7H_2O$ AnalaR, BDH, 99% in 0.5 molar HCl Convol, BDH) to 5 ml of the clear solution collected from each sample. The Lanthanum chloride solution was added to each sample to enhance strontium atomisation. A linear calibration curve was produced using standard solutions of strontium chloride (prepared from $SrCl_2.6H_2O$ BDH,

spectrosol for A.A.S., 99%) at a wavelength of 460.7 nm, and at the energy level of 66 eV.

4.4 Effect of Varying the Synthesis Parameters

4.4.1 Introduction

The aim of this study is to determine the methods of enhancing the exchange capacity of Al-PILC. Studies from the literature show that altering the chemical composition of Al-PILC (Al/clay and OH/Al ratios) leads to an increase in the clay capacity. Therefore this study will consider the effect of varying the Al/clay and OH/Al ratios on the exchange capacity of Al-PILC.

The definitions of the two synthesis ratios are given below. The Al/clay ratio is represented by the symbol R_A, which is the number of millimoles of Al^{3+} per gram of clay added during the synthesis. The OH/Al ratio is represented by the symbol R_{OA}, which is the number of moles of hydroxide ion divided by the number of moles of Al^{3+} in the pillaring solution. The investigation is based on the following premise:- Lowering the Al/clay ratio may result in a lower aluminium oxide content in the Al-PILC. Therefore introducing a minimum required amount of aluminium oxide pillars between the silicate layers of the clay it would not only 'prop open' the clay sheet but it should also reduce the consumption of natural exchange sites by the metal oxide pillars. The effect of lowering R_{OA} was also investigated because, as shown in

the literature review, lowering the R_{OA} value would enhance the exchange capacity of Al-PILC. The thermal treatment temperature of the synthesis of Al-PILC was also investigated. An attempt was made to determine the effect of varying the thermal treatment temperature of Al-PILC on the exchange capacity. To confirm whether the clay had a pillared structure samples of Al-PILC were characterised using standard characterisation techniques (see **chapter 3**). A strontium adsorption isotherm was constructed for each clay sample from the experimental data obtained from a series of batch contact tests.

4.4.2 Experiment in Varying the Synthesis Parameters

The outline of the experiments in varying the synthesis ratios and the treatment temperature can be seen in the following sections.

4.4.2.1 Effect of Varying the Al/clay Ratio (R_A)

For the purpose of this study all the samples were prepared using the 'short-cut' method. Two samples were prepared with the same R_{OA} (2.4) but different R_A (1.25 and 2.5 mmol/g).

4.4.2.2 Effect of Varying the OH/Al Ratio (R_{OA})

To study the effect of lowering the R_{OA} on the exchange capacity of Al-PILC, two samples of Al-PILC were prepared with the same R_A (1.25 mmol/g) but different R_{OA} (2 and 2.4). The Al-PILC samples were prepared using the 'short-cut' method.

4.4.2.3 Effect of Varying the Thermal Treatment Temperature

To investigate the effect of lowering the thermal treatment temperature on the exchange capacity of Al-PILC samples, the samples were thermally treated at two different temperatures. One sample of Al-PILC was thermally treated in a hot-box (Gallenkamp) at 120 °C whereas the other was treated at 200 °C in a furnace (electric, carbolite furnace made by Sheffield Ltd.) for 18 hours.

4.4.3 Results and Discussion of Preliminary Characterisations

The results of XRD, nitrogen adsorption, ICP-AES and strontium adsorption analysis are discussed, and general conclusions drawn from the overall results are presented in the following sections.

4.4.3.1 Results and Discussion of XRD Analysis

The results of XRD analysis of the Fe-PILC samples are as follows:

(i) Comparing the 'Short-cut' Method with the Conventional Method

The XRD spectra of the starting materials are used as reference spectra. The spectra of the sodium clay, raw clay and Al-PILC (AC-1 and AS-3) are shown as representative spectra (see **fig. 4.1** and **4.2**) for the following discussion.

The XRD spectra of samples of Al-PILC (AC-1) prepared using the conventional method, show a shift of the first order peak from a higher 2θ angle (see **fig. 4.1** (**a**)) to a lower one (see **fig. 4.1** (**b**)). The results indicate that there were layers of expansion in the clay, and the expansion started from 12.6 Å to approximately 19 Å (see **table 4.2**). Silicate layers can be pillared with two stacked rings of aluminium hydroxide, $2[Al_6(OH)_{12}(H_2O)_{12}]^{6+}$. The overall thickness of the rings is approximately equal to two sheets of gibbsite, $Al(OH)_3$, (9.4 Å) in addition to that of the Montmorillonite layer (approximately 9.6 Å), giving a total of 19 Å.

The XRD spectra of samples prepared using the 'short-cut' method also show a shift of the first order peak from a higher X-ray angle to a lower X-ray angle (see **table 4.2** and **fig. 4.2**). A comparison of the spacing of the Al-PILC samples prepared using the conventional method with that of Al-PILC prepared using

the 'short-cut' method shows that there is a decrease in the expansion in the latter samples. This decrease of spacing in these samples may result from the formation of reduced size aluminium oxide pillars between the layers of the clay structure.

(ii) Effect of Varying the Synthesis Ratios and Thermal Treatment Temperature

The results (see **table 4.2**) of XRD analysis show that even after lowering the R_A, from 2.5 (AS-3) to 1.25 mmol/g (AS-2) (see **table 4.1** for sample descriptions), there was no significant change in the spacing of Al-PILC. The results (see **table 4.2**) of the analysis also show that the spacing of an Al-PILC sample remained relatively unchanged (15.3 Å) after the R_{OA} was lowered from 2.4 (AS-2) to 2 (AS-1). These results suggest that varying the R_{OA} in the given range did not affect the process of formation of the pillared structure.

The results of the analysis also indicate that raising the thermal treatment temperature of the Al-PILC from 120 (AC-1) to 200 °C (AC-2) did not change the spacing. They further suggest that there was no noticeable change to the structure of Al-PILC, even after the treatment temperature had been raised. This indicates that a stable Al-PILC structure can be formed at both low and high temperatures.

4.4.3.2 Results and Discussion of Nitrogen Adsorption Analysis

The results of the nitrogen analysis of the Al-PILC samples are as follows:

(i) Comparing the 'Short-cut' Method with the Conventional Method

The nitrogen isotherms of the starting materials, sodium and raw Montmorillonite, are a combination of type II and IV (see the representative isotherm in **fig. 4.3** and **4.4**). The BET surface area, micropore area and micropore volume values of these clays are low, which indicates that the materials are not very porous. Nevertheless, the average pore sizes (see **table 4.3**) of the samples suggest that the structures consist mainly of mesopores and macropores.

The Al-PILC samples, AC-1 and AC-2, prepared using the conventional method have a combination of type I and IV nitrogen isotherms (see **fig. 4.3**). The BET surface areas, micropore areas and micropore volumes of the Al-PILC samples are higher than those of the starting material. The small average pore sizes of the samples suggest that the samples contain mainly micropores. These results indicate that after pillaring, a large number of micropores are generated leading to an increase in the porosity of the clay.

The results of nitrogen adsorption analysis also show that the Al-PILC samples, prepared using the 'short-cut' method, also have a combination of type I

and IV nitrogen isotherms (see **fig. 4.4**). These results also suggest that the samples have porous structures, which consist mainly of micropores and mesopores. The BET surface area, micropore area and micropore volume of these Al-PILC samples are lower than those prepared using the conventional method but are significantly higher than those of the starting material. The above results suggest that by using the 'short-cut' method, an Al-PILC can be prepared from a non-processed clay. The Al-PILCs prepared using this method will be less microporous than those prepared using the conventional method.

(ii) Effect of Varying the Synthesis Ratios and the Thermal Treatment Temperature

The effect of increasing the thermal treatment temperature from 120 °C (AC-1) to 200 °C (AC-2) led to a substantial decrease in the BET surface area, micropore area, and micropore volume. These reductions may have resulted from the formation of a more compact structure. The results (see **table 4.3**) may be attributed to the temperature rise.

4.4.3.3 Results and Discussion of ICP-AES Analysis

The results (see **table 4.4**) of ICP-AES show that the %weight of Na_2O is significantly higher than that of CaO in the raw Montmorillonite. These results suggest that the clay consisted of a mixture of calcium and sodium exchangeable cations. They further suggest

that the clay had mainly sodium exchangeable cations. The results of the analysis show significant decreases in %weight of CaO and Na_2O in the Al-PILC samples when compared with those of the starting clay. These decreases can be explained by the replacement of calcium and sodium exchange sites with aluminium oxide pillars.

Evidence of an Al-PILC can be seen by comparing the (%wt Al_2O_3)/(%wt SiO_2) ratio of the raw clay and the Al-PILC. A noticeable increase of Al_2O_3 content in all the Al-PILC samples was observed (see **table 4.4**). These results further suggest that aluminium oxide had been successfully incorporated into the clay structure.

4.4.3.4 Results and Discussion of Strontium Adsorption Analysis

Comparing the cation exchange capacity (C.E.C.) (see **table 4.5, fig. 4.5** and **4.6**) of the starting materials with that of sample, AC-1, (prepared using the conventional method) and AS-3, (prepared using the 'short-cut' method) for strontium it is apparent that there are significant reductions in the C.E.C. of the Al-PILC samples. A reduction of approximately 80% or more in the C.E.C. of the Al-PILC samples was observed. These results may suggest that a large quantity of the natural exchange sites in the parent clays was either consumed or blocked by the aluminium oxide pillars in the clays. The effects of varying the synthesis parameters are discussed below and they are also summarised in **table 4.5**.

The results of strontium adsorption analysis show that when R_{OA} was increased from 2 (AS-1) to 2.4 (AS-2), an increase in the C.E.C. of the Al-PILC samples was observed. These results suggest that increasing the R_{OA} within the given range (2 to 2.4) enhances the C.E.C. of the Al-PILC. The results gathered from ICP-AES (see **table 4.4**) of the Al-PILC prepared using the 'short-cut' method, also appear to support this. These results seem to show that increasing the R_{OA} from 2 (AS-1) to 2.4 (AS-2) did not lead to an increase in aluminium oxide content of the clay. The results of varying the other parameters such as the R_A and the thermal treatment temperature are discussed below.

Comparing the samples AS-2 and AS-3 (which were prepared from the same R_{OA} (2.4) but different R_A (AS-3, 2.5 mmol/g and AS-2, 1.25 mmol/g), the results show there is a substantial increase (approximately 59%) in the C.E.C.. The effects of lowering the thermal treatment temperature from 200 °C (AC-2) to 120 °C (AC-1) on the C.E.C. of the Al-PILC samples are also shown in **table 4.5**. These results suggest that the C.E.C. of the Al-PILC may be increased by lowering the thermal treatment temperature in the given range.

4.4.4 Conclusions

General conclusions can be drawn from the results of preliminary characterisations. The results of XRD analysis, nitrogen adsorption analysis and ICP-AES confirmed the structure and chemical composition of the Al-PILC. These results also demonstrate that an Al-PILC can be prepared from non-refined clay using the

'short-cut' method which would lower the production cost of an Al-PILC. However, introducing aluminium oxide into the sodium or raw Montmorillonite leads to a decrease of approximately 80% or more in the cation exchange capacity (C.E.C.) of the clay. The large reduction in the C.E.C. of the clay will render the Al-PILC unsuitable to be used as a cation exchanger in water treatment processes. The methods of enhancing the C.E.C. of the Al-PILC, which involved varying the synthesis parameters, did not appear to lead to any significant increase in the C.E.C.. Therefore, further and more extensive investigations on PILCs experiments will focus on Fe-PILC instead of Al-PILC.

Table 4.1 A summary of the synthesis conditions.

S.N.	**Method**	**Temp /°C**	**R_{OA} /Ratio**	**R_A /mmol.g^{-1}**	**[NaOH] /Molar**	**[$AlCl_3$] /Molar**
AC-1	C	120	2.4	2.50	0.20	0.20
AC-2	C	200	2.4	2.50	0.20	0.20
AS-1	S-C	120	2.0	1.25	0.05	0.025
AS-2	S-C	120	2.4	1.25	0.06	0.025
AS-3	S-C	120	2.4	2.50	0.12	0.05

Method: **C** represents the conventional method and **S-C** represents the 'short-cut' method. **S.N.** represents sample name. **R_A** is the Al/clay ratio. **R_{OA}** is the OH/Al ratio.

Table 4.2 A summary of results of XRD analysis.

Sample Type	X-ray angle /°2θ	α1 d001 /Å	%Relative Peak Intensity
RM	5.9^{Ca}, 7.1^{Na}	14.9^{Ca}, 12.5^{Na}	100^{Ca}, 52^{Na}
NM	7.0	12.6	100
CM	5.8	15.1	100
AC-1	4.6	19.2	100
AC-2	4.6	19.1	100
AS-1	5.8	15.1	100
AS-2	5.8	15.3	99
AS-3	5.9	14.9	100

RM represents raw Montmorillonite. **NM** and ^{Na} represent sodium Montmorillonite. **CM** and ^{Ca} represent calcium Montmorillonite. **d001** is the basal spacing of the clay.

Table 4.3 A summary of results of nitrogen adsorption analysis.

Sample Name	BET Surface Area /$m^2.g^{-1}$	Micropore Area /$m^2.g^{-1}$	Micropore Volume /$cc.g^{-1}$	Average Pore Diameter /Å
RM	25.1	0.95	0.000186	145.5
NM	25.6	4.4	0.0019	136.6
AC-1	188.6	121.9	0.149	23.2
AC-2	128.6	82.1	0.039	26.6
AS-1	107.1	60.5	0.029	35.8
AS-2	110.7	68.8	0.031	33.4
AS-3	110.4	72.0	0.034	32.5

RM represents raw Montmorillonite. **NM** represents sodium Montmorillonite. **AC** represents Al-PILC prepared using the conventional method. **AS** represents Al-PILC prepared using the 'short-cut' method.

Table 4.4 A summary of results of ICP-AES analysis.

The chemical composition of the samples in percentage weight (%wt).								
Sample Name	**SiO_2**	**Al_2O_3**	**Fe_2O_3**	**MgO**	**CaO**	**Na_2O**	**K_2O**	**$\frac{Al_2O_3}{SiO_2}$ /Ratio**
RM	63.7	19.8	3.7	2.4	1.1	2.3	0.6	0.31
AS-1	55.0	26.4	3.2	2.0	0.2	0.5	0.6	0.48
AS-2	57.6	24.3	3.3	2.1	0.3	0.6	0.6	0.42
AS-3*	54.5	25.6	3.2	2.0	0.2	0.5	0.5	0.47

* The conventional Al-PILC (AC-1 and AC-2) should have these compositions (see synthesis **table 4.1**). $\frac{Al_2O_3}{SiO_2}$ is the alumina and silica ratio.

Table 4.5 A summary of results of batch contact tests.

Sample Name	**Cation Exchange Capacity /meq.kg^{-1}**	**R^2**
RM	664.3	0.998
NM	741.1	0.993
AC-1	83.9	0.998
AC-2	0	-
AS-1	0	-
AS-2	102.3	0.992
AS-3	41.5	0.983

R^2 is the square of correlation coefficient. The cation exchange capacity is in milli-equivalent per kg. **RM** represents raw Montmorillonite. **NM** represents sodium Montmorillonite. **AC** represents Al-PILC prepared using the conventional method. **AS** represents Al-PILC prepared using the 'short-cut' method.

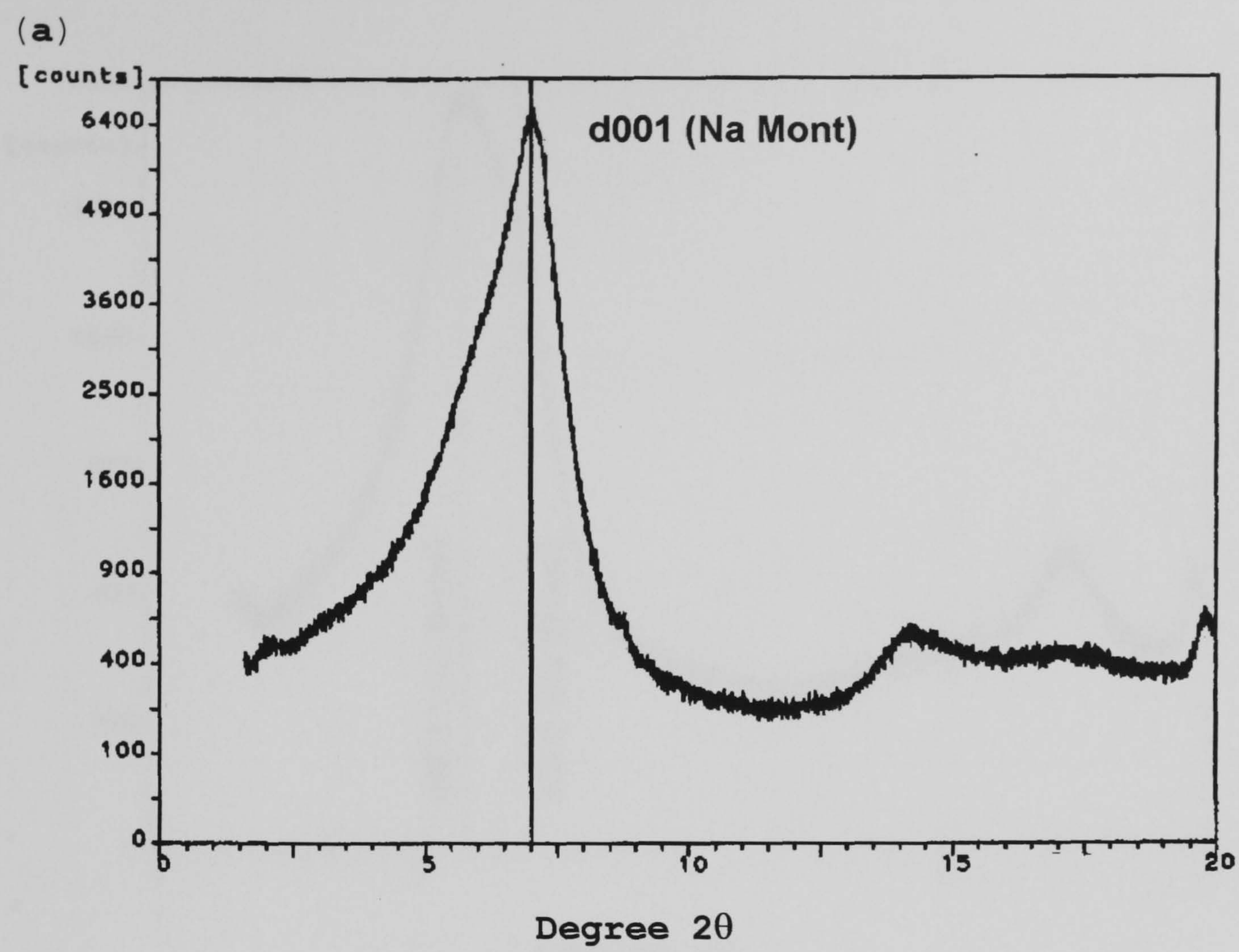
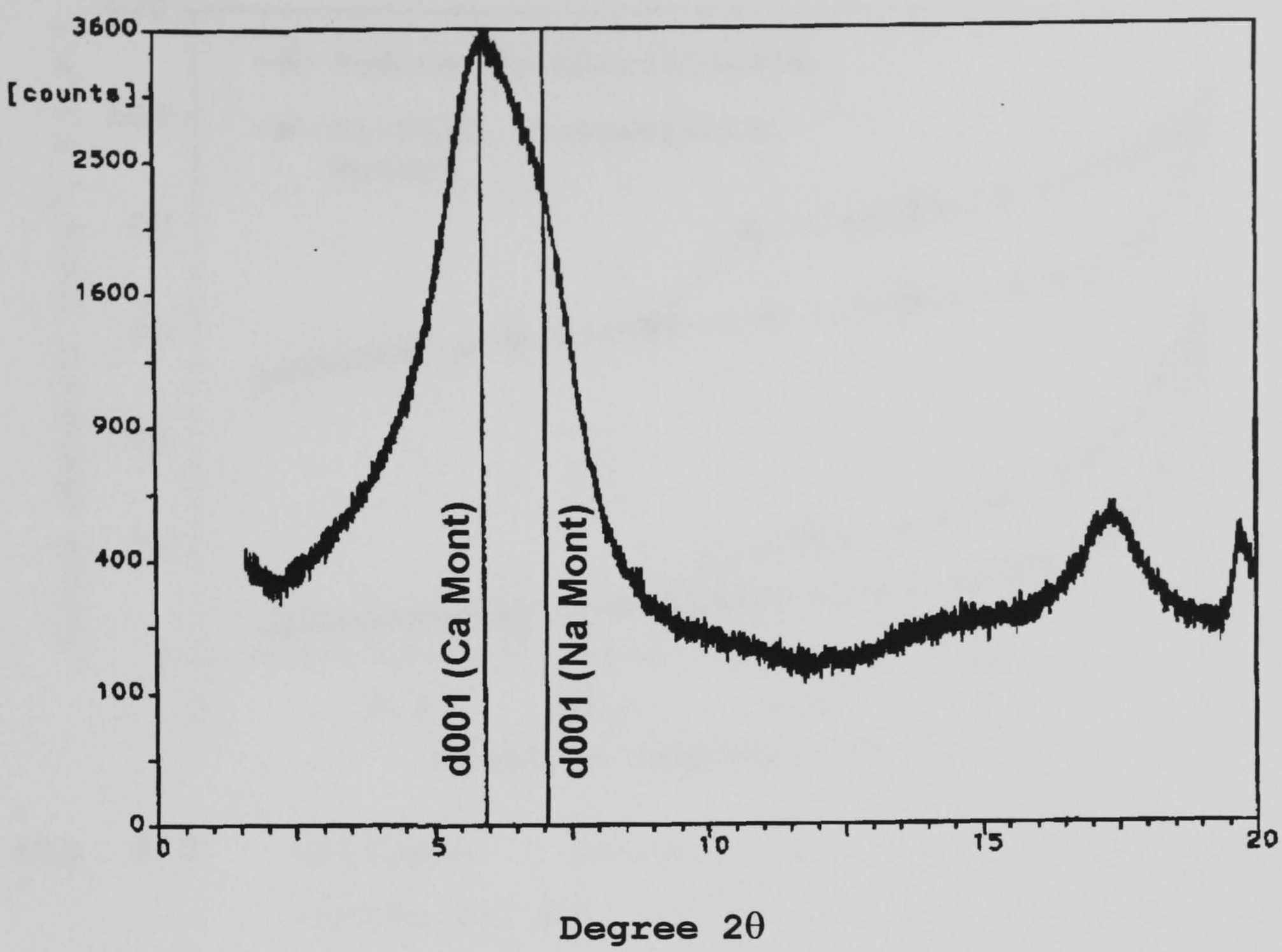


Fig. 4.1 XRD spectrum of (**a**) sodium Montmorillonite, **Na Mont**, (**b**) **Al-PILC, AC-1** (see **table 4.1**).

(a)



(b)

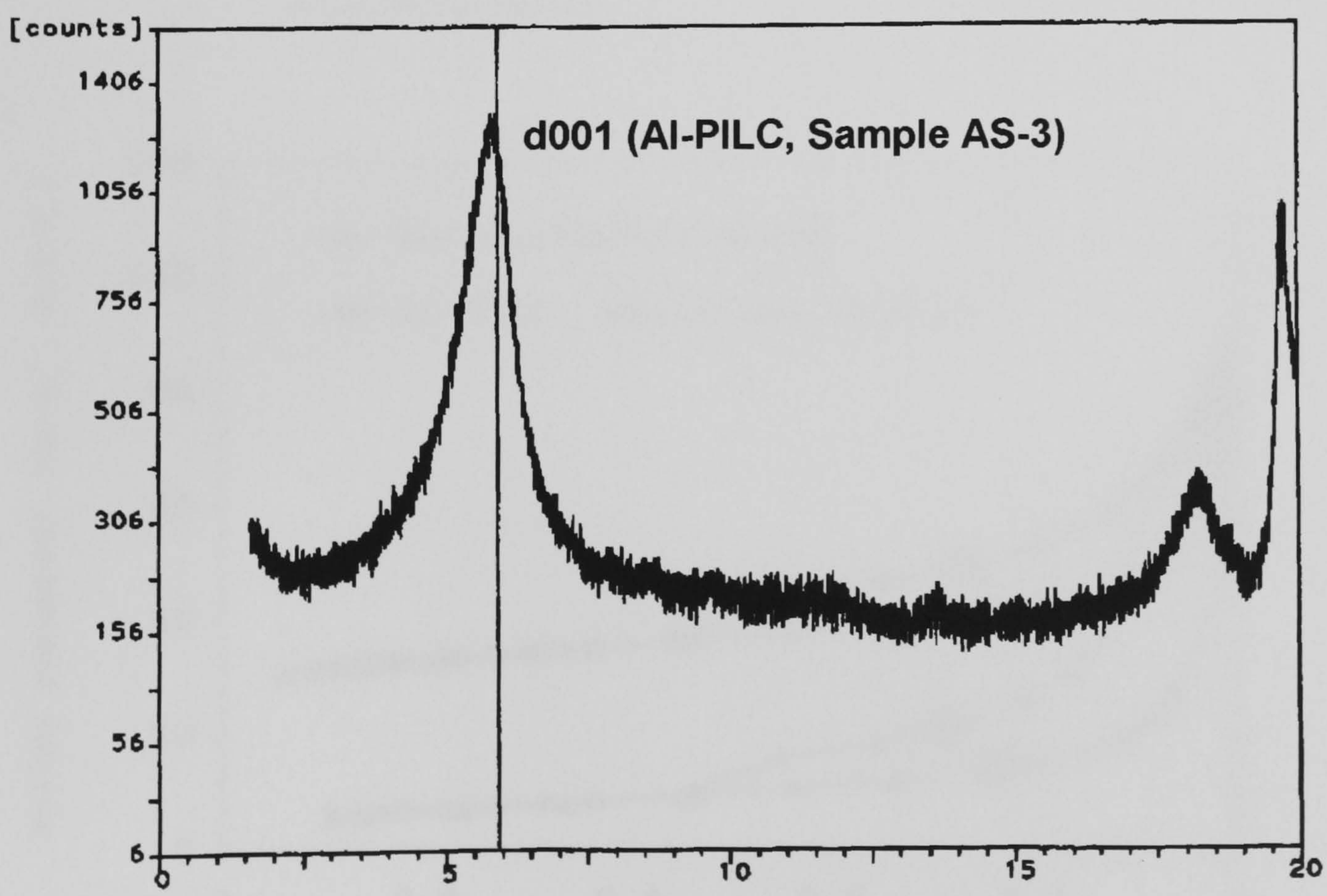


Fig. 4.2 XRD spectrum of (**a**) raw Montmorillonite, **Ca & Na Mont**, (**b**) **Al-PILC, AS-3** (see **table 4.1**).

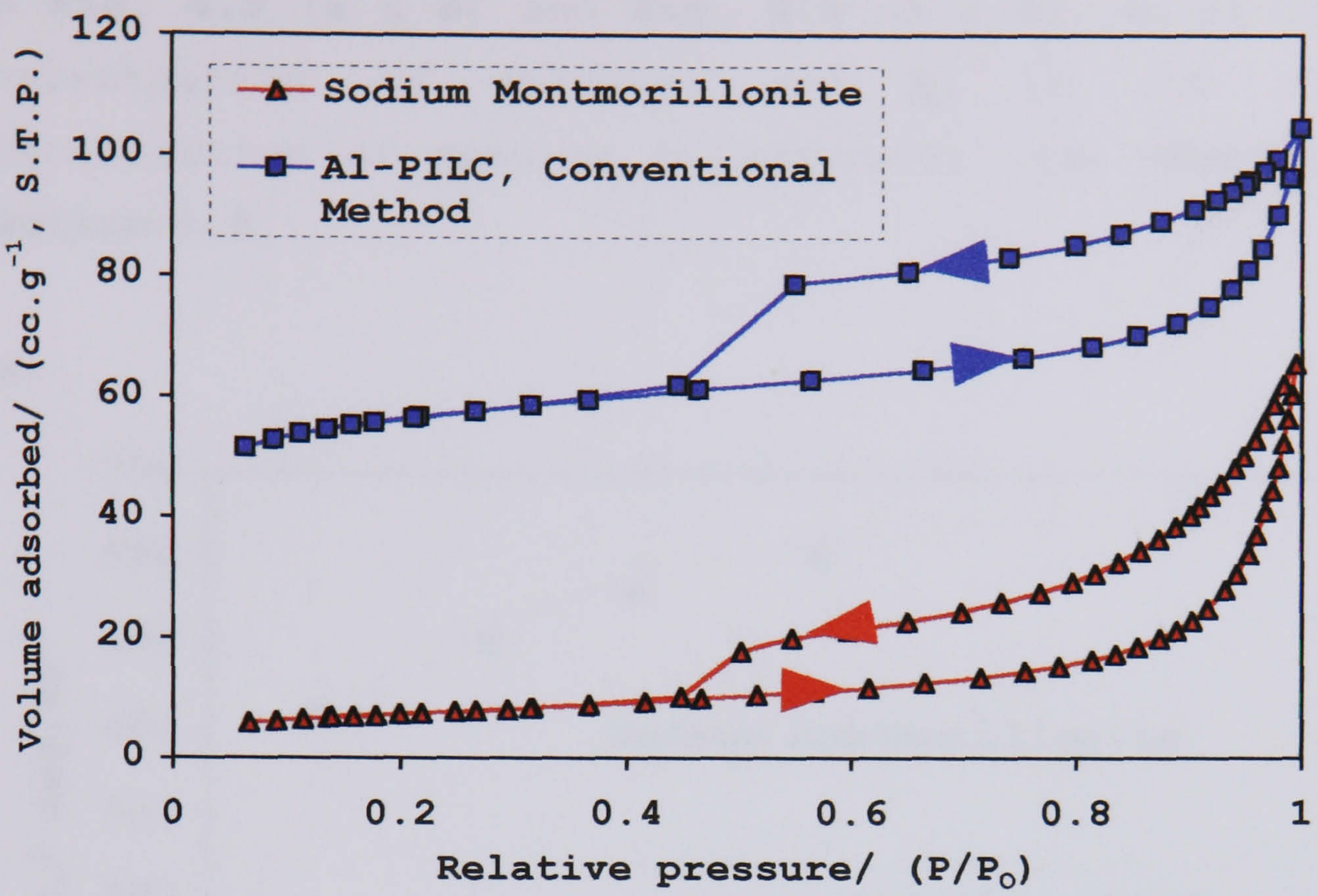


Fig. 4.3 Nitrogen adsorption and desorption isotherms of sodium Montmorillonite, NM, and Al-PILC, AC-1 (see **table 4.1**) respectively.

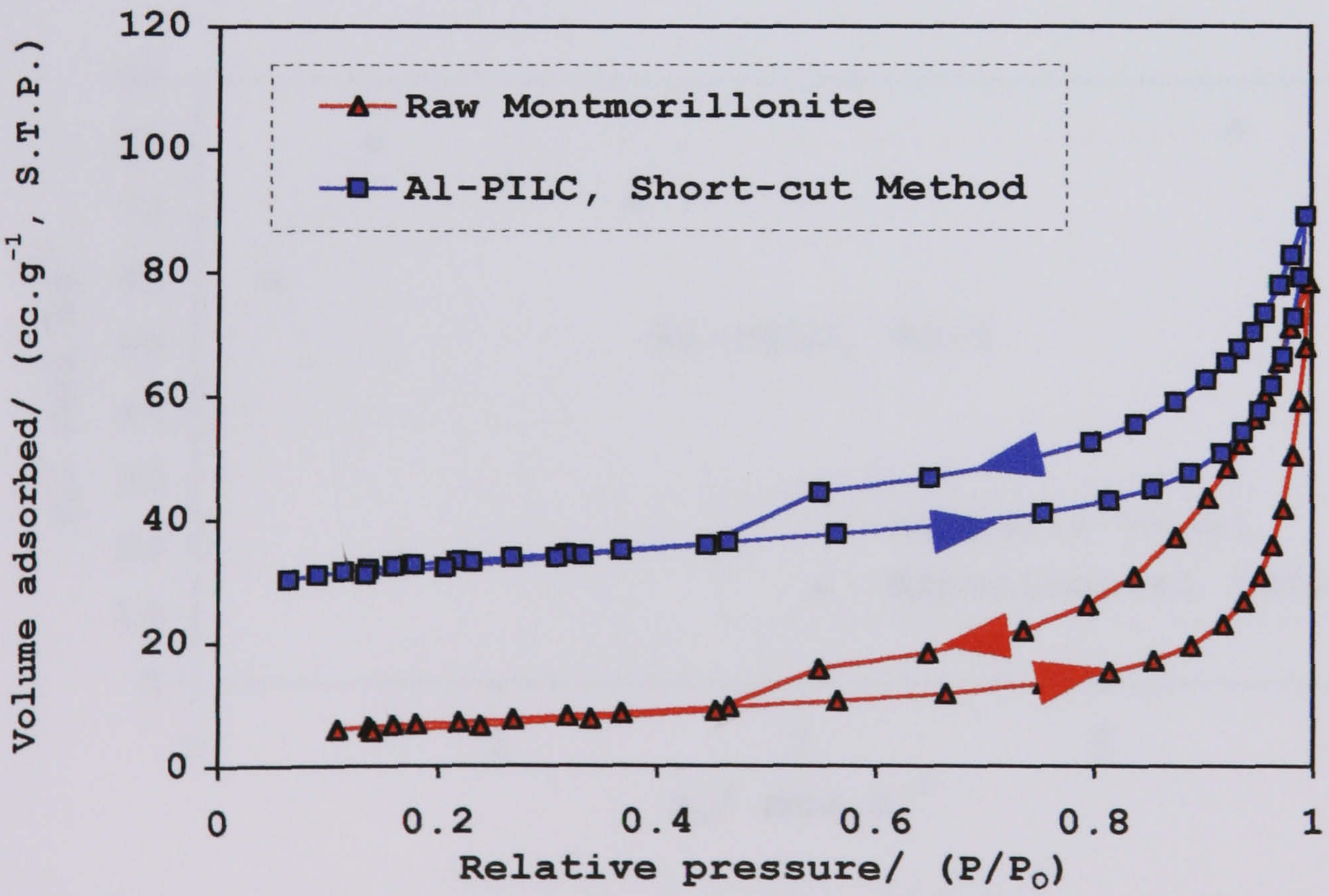
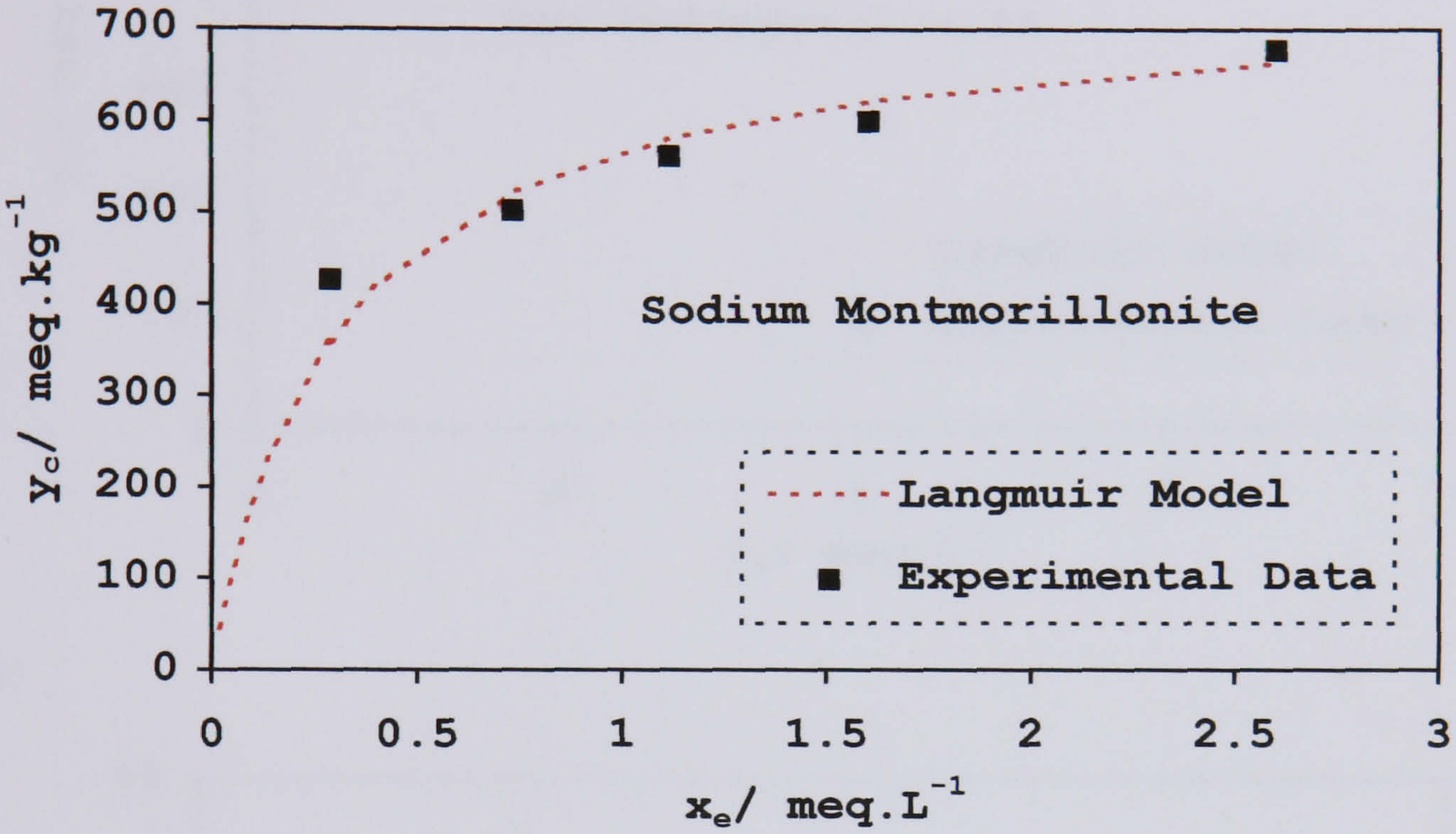


Fig. 4.4 Nitrogen adsorption and desorption isotherms of raw Montmorillonite, RM, and Al-PILC, AS-3 (see **table 4.1**) respectively.

In **fig. 4.5** (**a** & **b**) and **fig. 4.6** (**a** & **b**), x_e is final concentration in solution and y_c is the final concentration of species in adsorbent (see **chapter 1, section 1.5**).

(**a**)



(**b**)

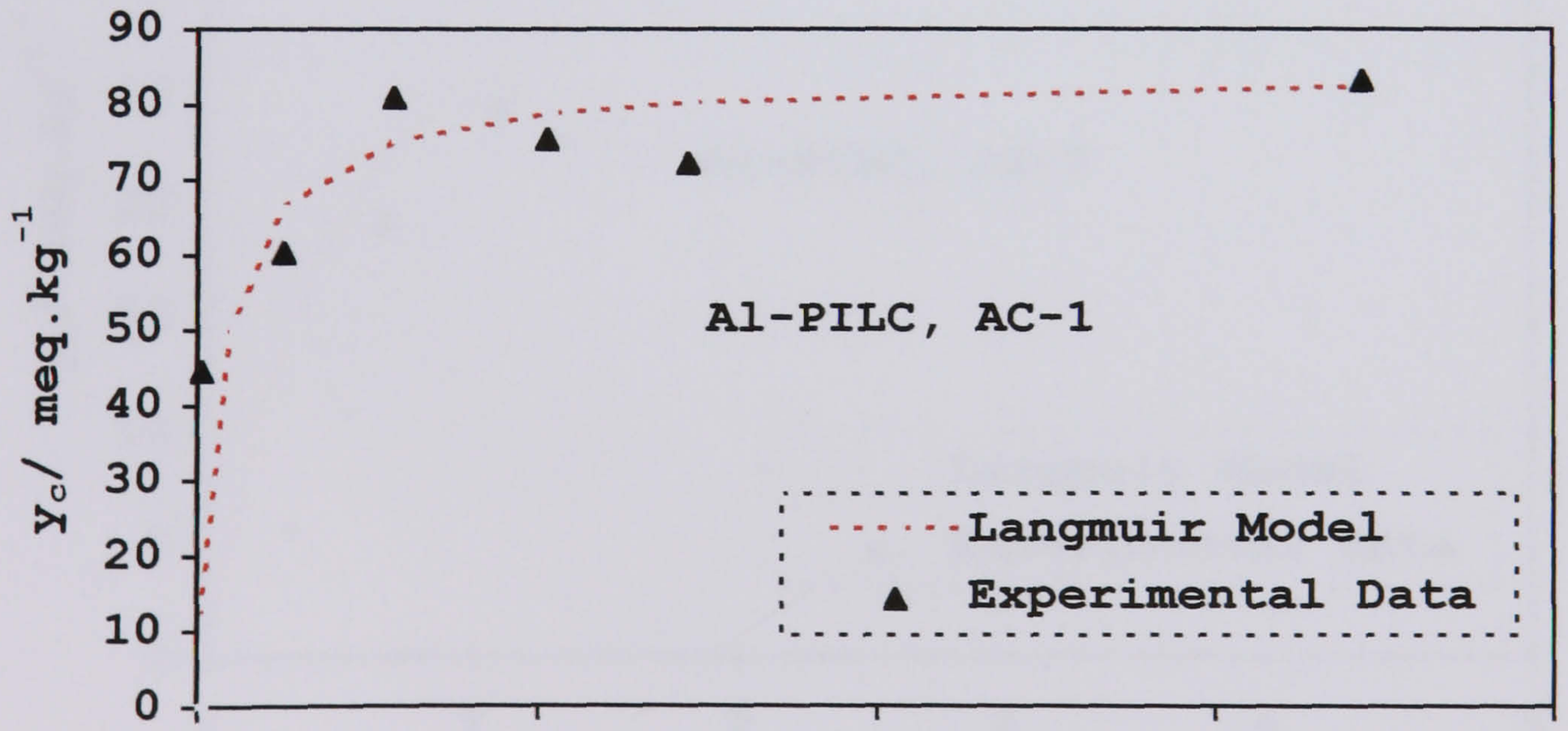
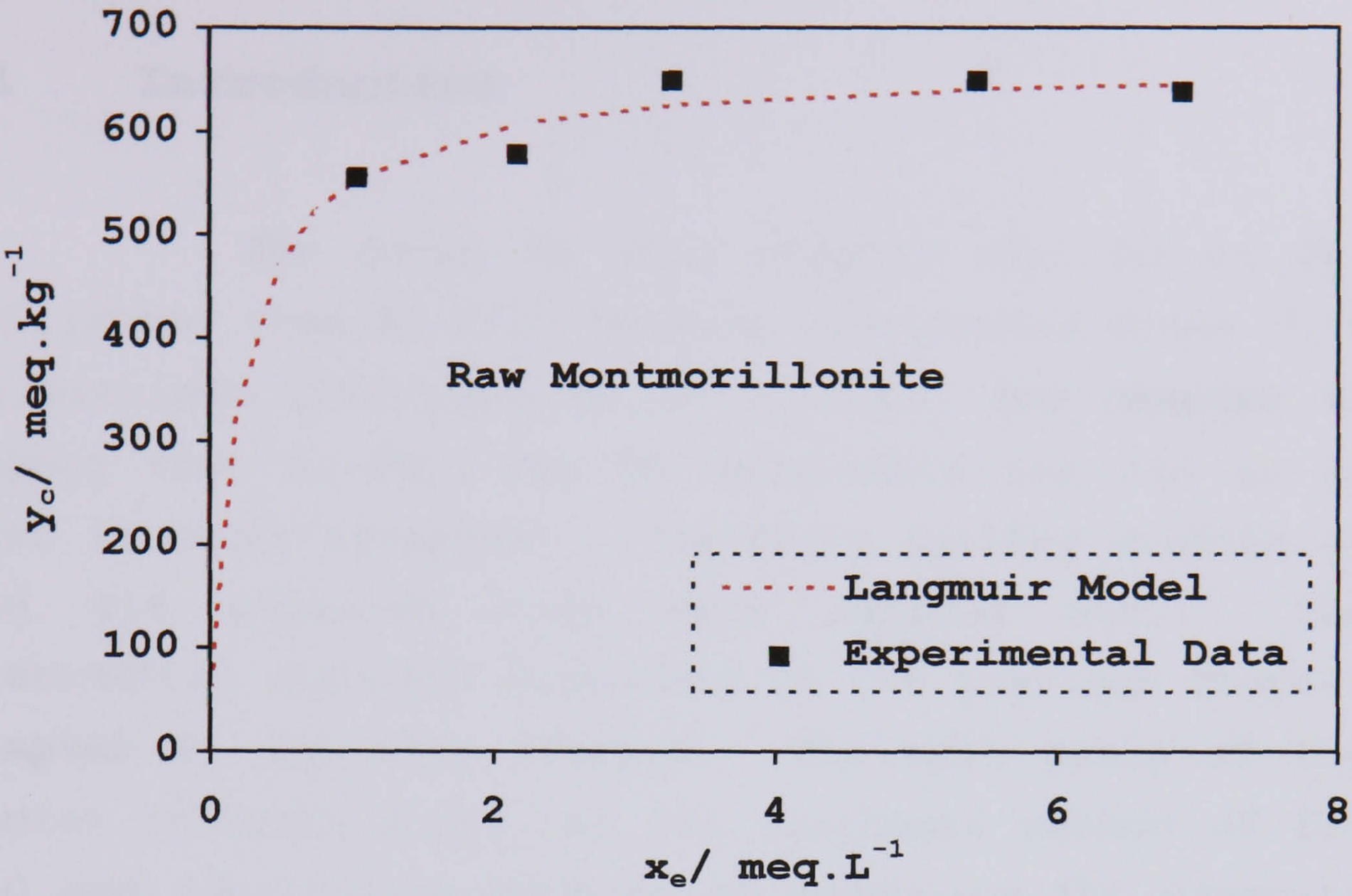


Fig. 4.5 Strontium adsorption isotherm of (**a**) **sodium Montmorillonite** and (**b**) **Al-PILC, AC-1** (see **table 4.1**).

(a)



(b)

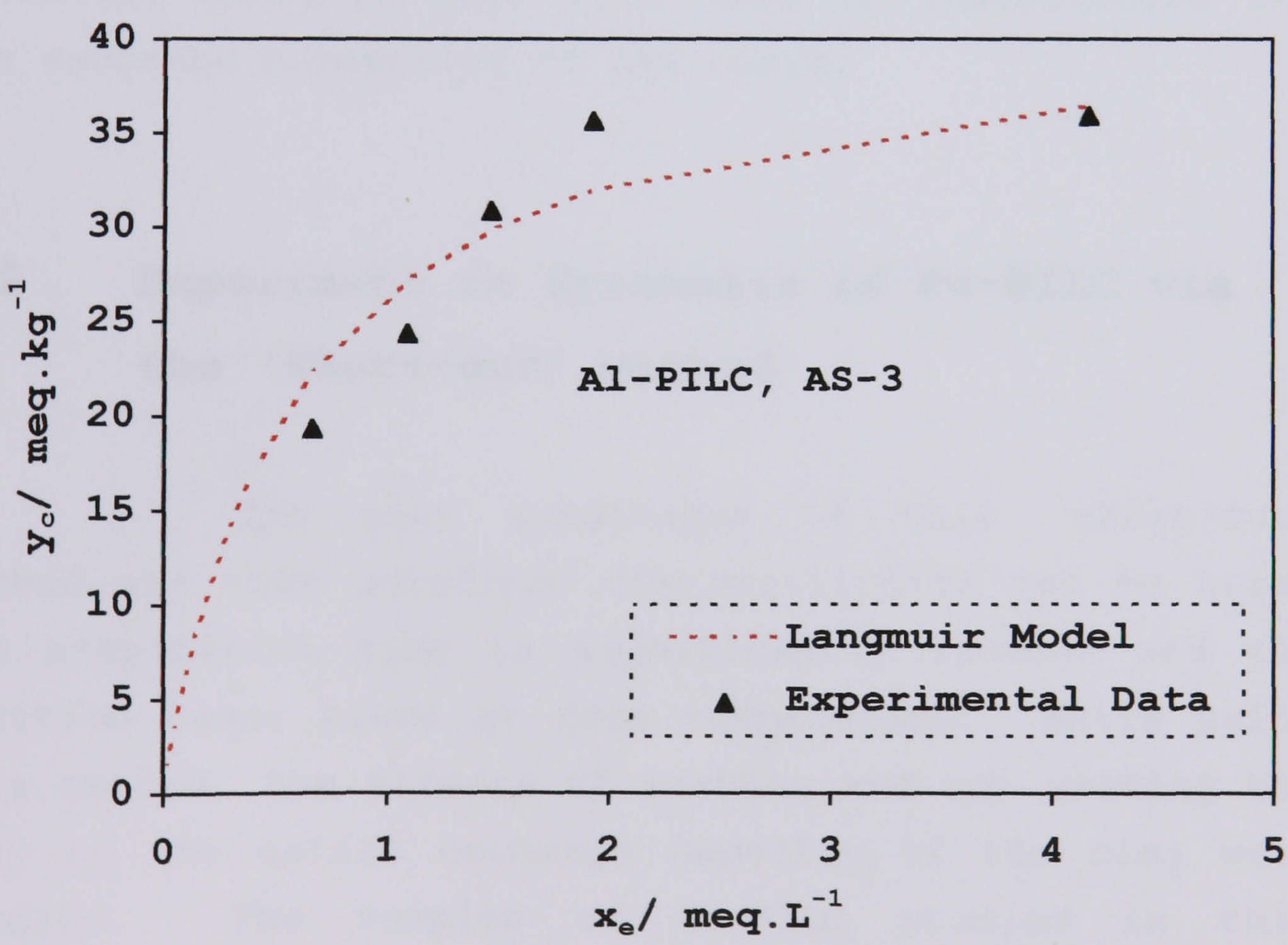


Fig. 4.6 Strontium adsorption isotherm of (**a**) **raw Montmorillonite** and (**b**) **Al-PILC, AS-3** (see **table 4.1**).

Chapter 5 Experiments with Fe-PILC

5.1 Introduction

The focus in this chapter will be on Fe-PILC rather than Al-PILC because conclusions drawn from the previous investigation on Al-PILC (see **chapter 4**) suggest that Al-PILC may be unsuitable for use as an agent in water treatment. Therefore further studies on iron III pillared clay were carried out. The experimental approach discussed in the previous chapter (**chapter 4**) was also adopted. The main goals of the studies included modifying the synthesis method of Fe-PILC and identifying methods of enhancing the capacity of Fe-PILC. Other analysis techniques such as zeta potential analysis were also used to characterise the ion exchange properties of the clays.

5.2 Experiment in Synthesis of Fe-PILC via the 'Short-cut' Method

The main advantages of this 'short-cut' method are that unrefined Montmorillonite can be used; the preparation time is significantly reduced and the reaction takes place at room temperature. While using this method, the effects of washing and not washing the clay on the cation exchange capacity of the clay were studied. The samples of Fe-PILC studied in this section were synthesised using the following steps:

(a) Preparing the Pillaring Solution

100 ml of a known concentration of NaOH solution (prepared by dissolving a known mass of NaOH pellets, BDH, Analar, 99% in distilled water) was quickly added to 100 ml of a known concentration of $Fe(NO_3)_3$ solution (prepared by dissolving a known mass of $Fe(NO_3)_3.9H_2O$ in distilled water) while the solution was stirred vigorously with a magnetic stirrer. The time taken for the addition was up to half a minute and the cloudy orange solution was stirred for a further 5 minutes.

(b) The Pillaring Process

A clay suspension consisting of 4 g of raw Montmorillonite (Volclay Ltd., Cyprus), labelled as the calcium form, was dispersed in 200 ml of distilled water for a minimum of 3 hours and quickly added to the fresh pillaring solution while it was stirred vigorously for 2 hours. The addition time was half a minute and, following this, the pH value of the mixture was recorded. After the 2 hours, the clay was separated from suspension using a centrifuge at 3500 r.p.m. for 5 minutes. The clay was washed with distilled water until the conductance was less than 20 µS, or it was left unwashed. The clay was then either dried in a hot-box for 18 hours or air-dried at room temperature for 48 hours. The clay was then ground to a fine powder with a pestle and mortar. The particles with a diameter of 100 µm or less were collected using a sieve. Finally the clay was heated in a temperature programmable tube furnace at a given range of temperatures.

5.3 Strontium Adsorption Analysis

5.3.1 Introduction

The aim of this study was to investigate the effect of pillaring on the cation exchange capacity of Fe-PILC. The influence of various synthesis factors (such as Fe/clay ratio, and OH/Fe ratio; thermal treatment temperature, pH adjustment on the raw pillared clay and washing or not washing the clay) on the clay capacity was assessed. The clay capacity was characterised by strontium adsorption isotherms. An isotherm was constructed for each sample from experimental data obtained from a series of batch tests, which involved contacting the clay samples with a known range of strontium chloride concentrations. The data was analysed using a mass balance equation (see **chapter 1, equation 1.6**) and the capacity of the clay samples was estimated using the Langmuir model (see **chapter 1, equation 1.5**).

5.3.2 Experimental Procedure of Contact Tests

To determine the cation exchange capacity of samples of Fe-PILC (for description of the samples see later sections) the samples were contacted with a known range of strontium chloride concentrations. Before A.E.S., the solution was diluted by a known dilution factor with double-purified water and a known volume of 0.2 molar Lanthanum chloride stock solution. For details of experimental procedures and sample preparation for A.E.S. analysis see **chapter 4, section 4.3.**

5.4 Effect of Varying the Starting Material

To investigate the possibility of synthesising Fe-PILC with alternative starting material such as raw Montmorillonite, samples of Fe-PILC were prepared with three different starting materials, namely sodium, calcium and raw Montmorillonite. The outline of the experimental procedure is described in the following section.

5.4.1 Experiment in Varying the Starting Material

The clays were synthesised under the same experimental conditions and with the same synthesis ratio of 1.25 mmol/g of Fe/clay and 2 of OH/Fe. For the summary of the description of the samples see **table 5.1.** These clays were dried in a hot-box (Gallenkamp) before being thermally treated at 200 °C in a furnace (Electric, Carbolite Furnace, Sheffield).

5.4.2 Results and Discussion of Preliminary Characterisations

The results of XRD, nitrogen adsorption, and strontium adsorption analysis are discussed, and general conclusions drawn from the overall results are presented in the following sections.

5.4.2.1 Results and Discussion of XRD Analysis

A summary of results of XRD analysis is shown in **table 5.2.** The XRD spectrum of the raw Montmorillonite, RM, (see **fig. 5.1** (**a**)) is used as a reference spectrum for the Fe-PILC sample F-RM. The spectra of RM and F-RM (see **fig. 5.1**) are used as representative spectra for the following discussion. The results of XRD analysis of the other clay samples are summarised in **table 5.2.** The XRD spectrum of the Fe-PILC sample, F-RM shows that the d001 peak consists of overlapping peaks which can be resolved (see **fig. 5.1** (**b**) and **table 5.2**). The results indicate that there were layers of expansion in the clays, whereas the other peak of F-RM may result from structural distortion in the pillared clay samples. The variations of the spacing value suggest that the structure of the clay was supported by different sizes of iron oxide pillars.

The XRD spectrum of the Fe-PILC and that of the Al-PILC are different. The XRD spectrum of the Fe-PILC samples shows double d001 peaks, whereas that of the Al-PILC samples shows only a single peak. The spacing values of the Fe-PILC suggests that the degree of layers of expansion in the Fe-PILC samples was generally much higher than that of the Al-PILC samples. Reduction in the peak intensity was also observed in the spectrum of the Fe-PILC which indicates that the structure consists of irregularly stacked clay sheets.

5.4.2.2 Results and Discussion of Nitrogen Adsorption Analysis

The results (see **fig. 5.2** (**a**) and (**b**)) of nitrogen adsorption analysis show that the BET surface area, micropore area and micropore volume of the Fe-PILC samples are significantly higher than those of the starting materials. These results are also similar to those of the Al-PILC as expected (see **chapter 4, table 4.3**). Introducing iron oxide into the clay structure leads to an increase in porosity or microporosity of the clays. The high porosity of the clay samples, F-NM and F-RM may also have resulted from an increase in the number of mesopores in the clays, hence the observed high average pore size (see **table 5.3**).

5.4.2.3 Results and Discussion of Strontium Adsorption Analysis

The results (see **table 5.4, fig. 5.3**) show that a general decrease in the C.E.C. of the Fe-PILC samples is observed when compared with that of their starting materials. In this case the reduction in the C.E.C. of the Fe-PILC samples resulted from the consumption of natural sites of the raw clay by iron oxide pillars. This reduction in the C.E.C. of the Fe-PILC sample (F-RM) (see **fig. 5.3**) is much less than that of the Al-PILC, which implies that the former is a better cation exchanger than the latter.

5.4.3 Conclusions

The results of XRD analysis give confirmation of the structure of the Fe-PILC. These results demonstrate that the pillared structure of the Fe-PILC is different from that of the Al-PILC. The structure of the Fe-PILC sample consists of distorted layers of clay sheet. Hence overlapping d001 peaks were observed in its XRD spectrum. The results of nitrogen adsorption analysis also support the results of XRD analysis by showing the various distinctive characteristics of PILCs in the clay samples. These characteristics include high surface area, micropore area and volume in comparison with those of the raw Montmorillonite. The results of the contact tests show that the Fe-PILC samples prepared with different starting materials have similar C.E.C. values. The C.E.C. of the Fe-PILC is significantly higher than that of the Al-PILC.

The above results confirm that it is possible to prepare an Fe-PILC using the simple method, the 'short-cut' method, and different starting materials. Most importantly the results demonstrate that an Fe-PILC can be prepared with a non-processed and an inexpensive starting material such as raw Montmorillonite. Further experiments on Fe-PILC will focus on the clay samples which were prepared using the 'short-cut' method and raw Montmorillonite.

Table 5.1 A summary of sample descriptions.

Sample Name	Starting Montmorillonite	R_F /mmol.g^{-1}	R_{OF} /Ratio
F-RM	Raw	1.25	2.0
F-NM	Sodium	1.25	2.0
F-CM	Calcium	1.25	2.0

R_{OF} is the OH/Fe ratio. **R_F** is the Fe/clay ratio. **F** represents iron pillared clay (Fe-PILC).

Definitions of Synthesis Ratios

The definitions of Fe/clay ratio and OH/Fe ratio are given below. The Fe/clay ratio is represented by the symbol **R_F** and the OH/Fe ratio is represented by the symbol **R_{OF}**. **R_F** is the number of millimoles of Fe^{3+} per gram of clay. **R_{OF}** is the number of moles of hydroxide ion divided by the number of moles of Fe^{3+}.

Table 5.2 A summary of results of XRD analysis.

Sample Name	Starting Material	X-ray Angle /°2θ		α1 d001 /Å		%Relative Peak Intensity	
		LA	HA	LA	HA	LA	HA
RM	-	5.9^{Ca}	7.1^{Na}	14.9^{Ca}	12.5^{Na}	100^{Ca}	52Na
NM	-	-	7.0	-	12.6	-	100
CM	-	5.8	-	15.1	-	100	-
F-RM	RM	3.4	7.1	25.7	12.5	90	100
F-NM	NM	3.9	5.9	22.6	14.9	41	100
F-CM	CM	3.7	6.8	24.1	12.9	82	100

RM represents raw Monmorillonite. **NM** and ^{Na} represent sodium Montmorillonite. **CM** and ^{Ca} represent calcium Montmorillonite. **LA** represents low X-ray angle and **HA** represents high X-ray angle. **F** represents iron pillared clay. **d001** is the basal spacing of the clay.

In **tables 5.3** & **5.4**, **RM**, **NM** & **CM** represent raw, sodium, calcium Montmorillonite. **F** represents a sample of an Fe-PILC. **AS** represents Al-PILC prepared using the 'short-cut' method. $\mathbf{R^2}$ represents the square of correlation coefficient. **C.E.C.** is the cation exchange capacity (in milli-equivalent per kg).

Table 5.3 A summary of results of nitrogen adsorption analysis.

Sample Name	**BET Surface Area /$m^2.g^{-1}$**	**Micropore Area /$m^2.g^{-1}$**	**Micropore Volume /$cc.g^{-1}$**	**Average Pore Diameter /Å**
RM	25.1	0.95	0.000186	145.5
NM	25.6	4.4	0.0019	136.6
CM	27.2	0	0	149.4
F-RM	86.1	18.4	0.00811	54.6
F-NM	102.0	23.1	0.0103	49.8
F-CM	58.2	9.9	0.00429	77.0

Table 5.4 A summary of results of batch contact tests.

Sample Name	**C.E.C. /$meq.kg^{-1}$**	**R^2**
RM	664.3	0.998
NM	741.1	0.993
CM	522.2	0.997
F-RM	411.5	1.000
F-NM	422.7	0.994
F-CM	349.1	0.994
AS-3	41.5	0.983

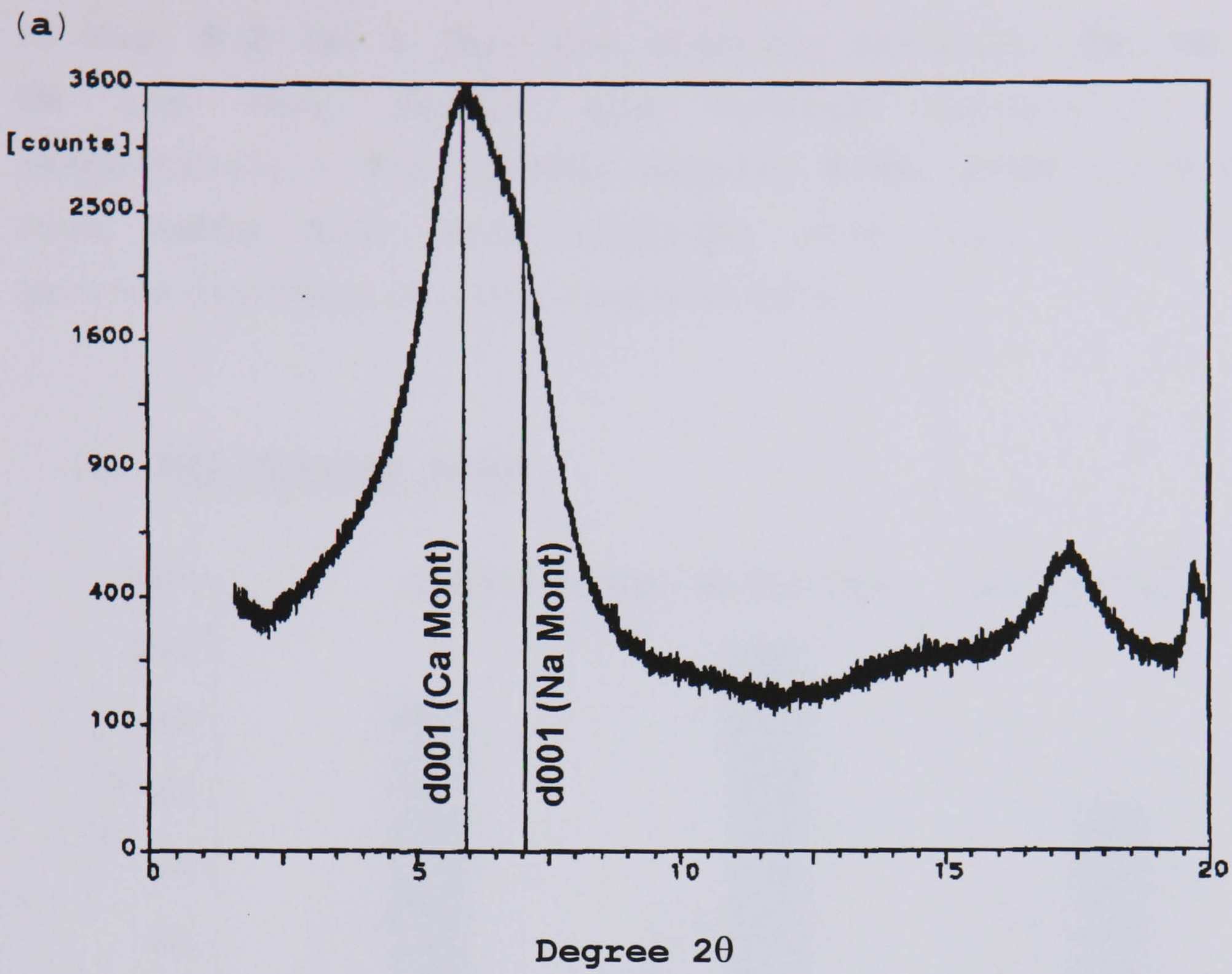
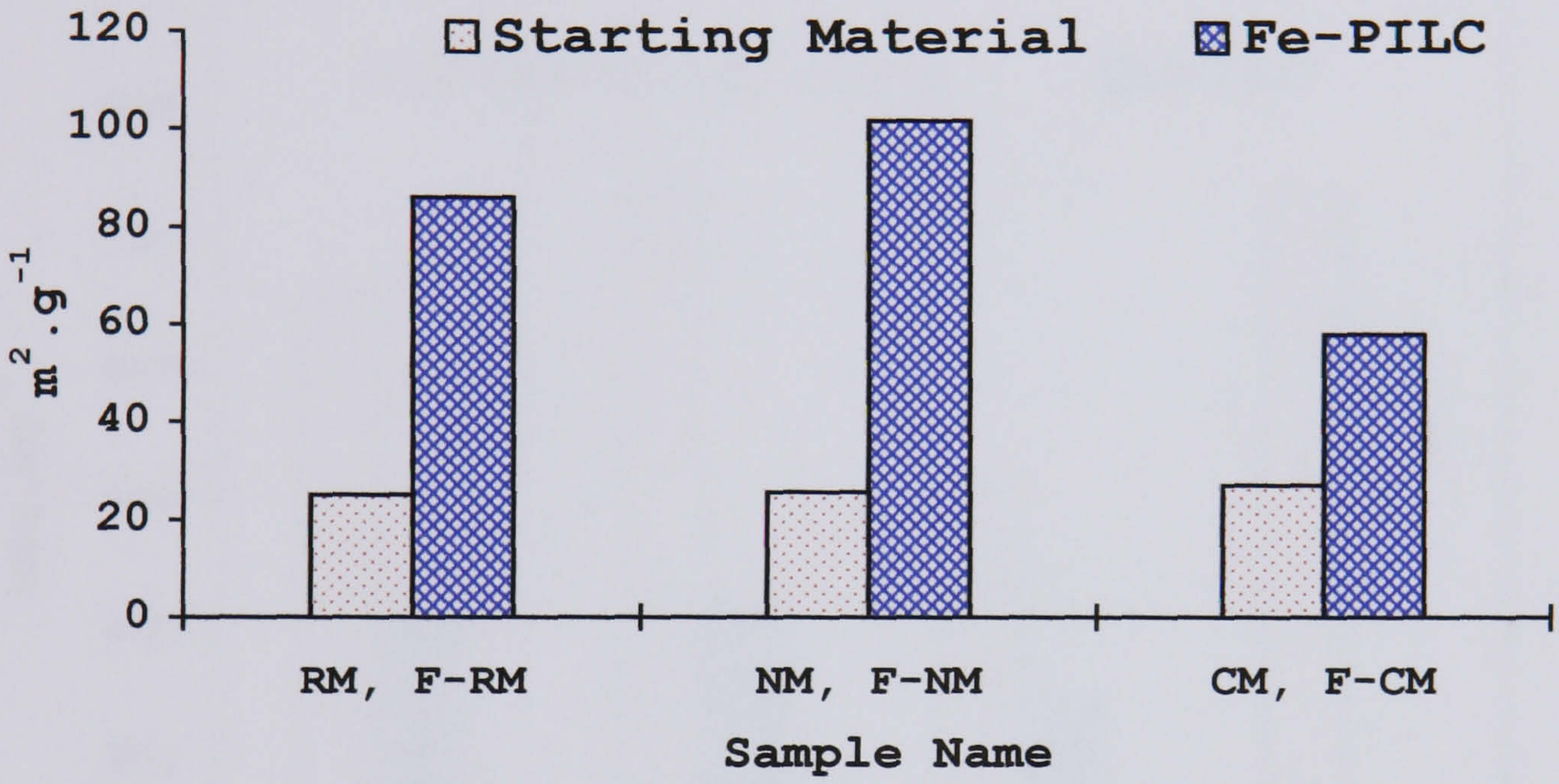


Fig. 5.1 XRD spectrum of (**a**) raw Montmorillonite, **Ca & Na Mont**, and (**b**) Fe-PILC, F-RM (see **table 5.1**).

In **fig. 5.2** (**a**) & (**b**), the starting material, **RM**, **NM** & **CM** are raw, sodium and calcium Montmorillonite respectively. The Fe-PILC samples **F-RM**, **F-NM** and **F-CM** (see **table 5.1**) were prepared with raw, sodium & calcium Montmorillonite respectively.

(a) **BET Surface Area:**



(b) **Micropore Area:**

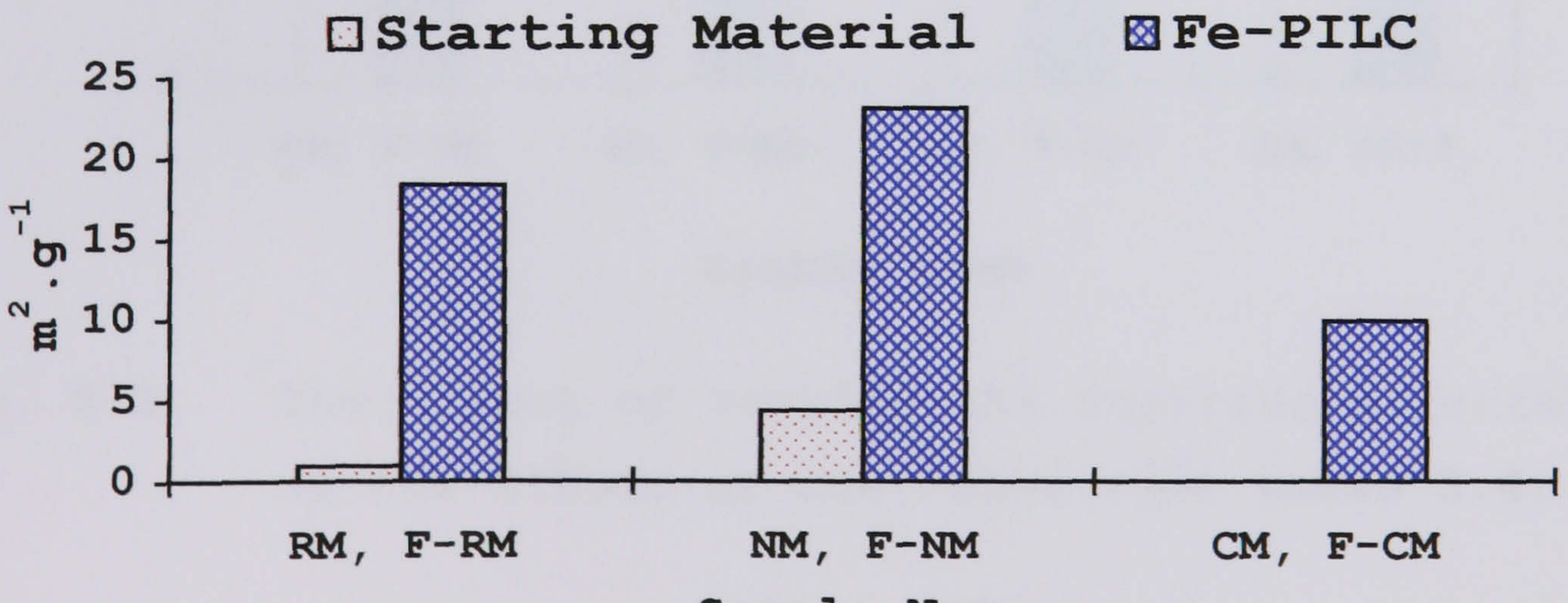


Fig. 5.2 The effect of varying the starting material on the (**a**) the BET surface area and (**b**) the micropore area of the Fe-PILC (see **table 5.3**).

In **fig. 5.3**, the starting material, **RM**, **NM** & **CM** are raw, sodium and calcium Montmorillonite respectively. The Fe-PILC samples **F-RM**, **F-NM** and **F-CM** (see **table 5.1**) were prepared with raw, sodium & calcium Montmorillonite respectively. The Al-PILC, **AS-3** (see **table 4.1**), was prepared with sodium Montmorillonite.

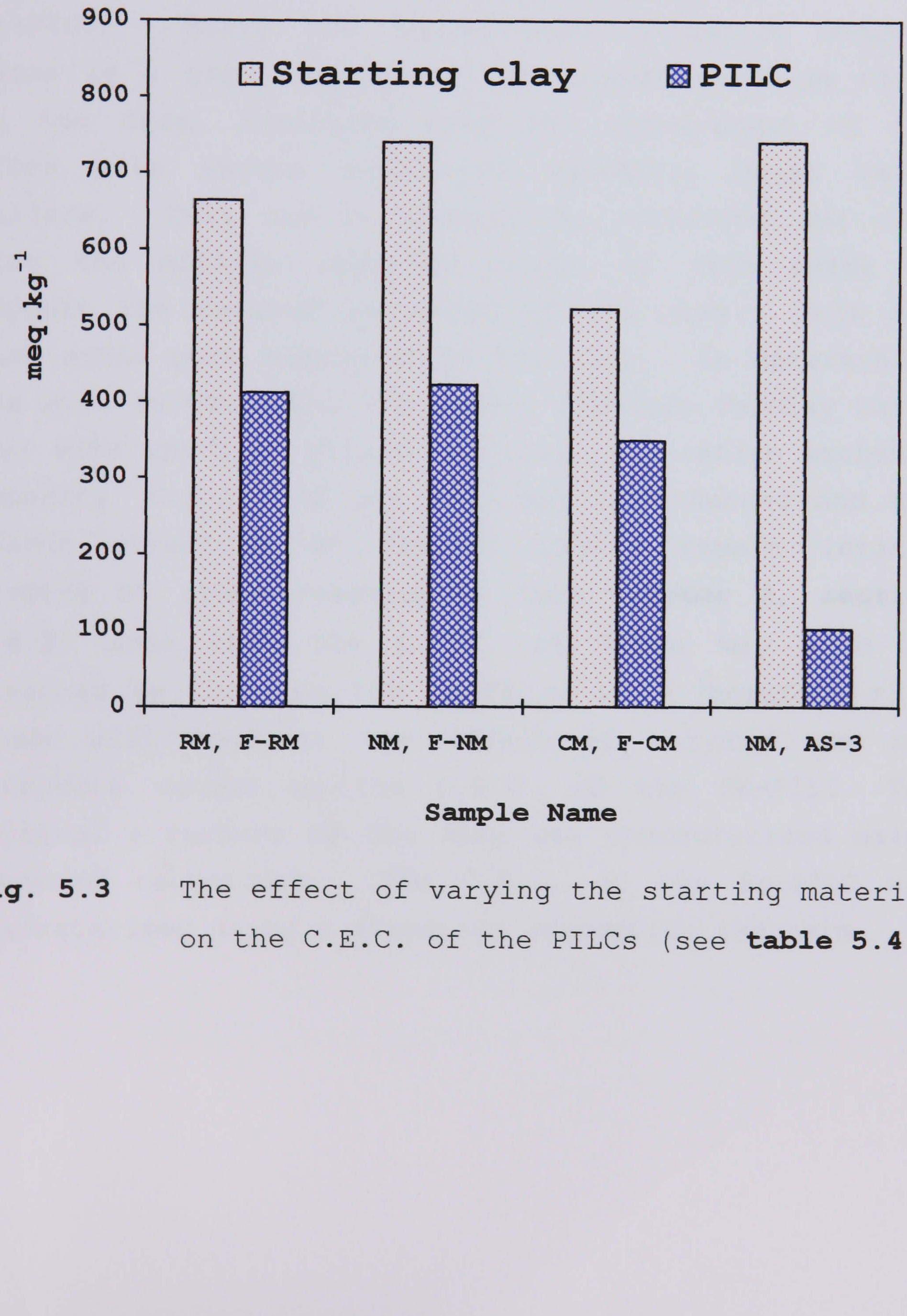


Fig. 5.3 The effect of varying the starting material on the C.E.C. of the PILCs (see **table 5.4**).

5.5 Effect of Varying the Synthesis Ratios

5.5.1 Introduction

The relationship between the physical structure and ion exchange properties of Fe-PILC was studied by investigating the effect of altering the chemical composition (Fe/clay and OH/Fe ratios) of the Fe-PILC. Using the conventional pillaring method, there is a high consumption of natural exchange sites in the clay, resulting from the replacement of the sites with excess amount of synthetic metal oxide pillars. This can be reduced by pillaring the clay with the minimum required amount of iron oxide to support the layered structure of the clay. This may also avoid pore blockages in the clay. In determining the most suitable and the lowest possible Fe/clay ratio (R_F) with which to pillar the clay, the cation exchange capacity (C.E.C.) of the clay may be enhanced and the porous structure of Fe-PILC should remain intact. Studies by other researchers (see **chapter 2, section 2.4.3**) show that the C.E.C. of PILCs may also be enhanced by lowering the OH/Fe ratio. Therefore this study will consider the effect of varying the two synthesis ratios on the C.E.C. of the Fe-PILC. The physical structure of the clay was characterised using standard techniques. The C.E.C. of the Fe-PILC was characterised using a strontium adsorption isotherm.

5.5.2 Experiment in Varying the Fe/clay Ratio (R_F)

To investigate the effect of changing R_F of the clay, a series of Fe-PILC samples were synthesised under the same conditions. The OH/Fe synthesis ratio was kept constant and the R_F value was varied from 0.5-5 mmol/g. These samples were finally heated at 200 °C. For details of the synthesis procedures see **section 5.2**. The outline of the experimental and synthesis conditions is given in **table 5.5**.

5.5.3 Experiment in Varying OH/Fe Ratio (R_{OF})

The possibility of enhancing the cation exchange capacity of the clay by lowering R_{OF} was examined. Samples of the Fe-PILC were synthesised under the same experimental conditions by keeping R_F the same but varying R_{OF} (see **table 5.6**).

5.5.4 Results and Discussion of Preliminary Characterisations

The results of XRD, nitrogen adsorption, ICP-AES and strontium adsorption analysis are discussed, and general conclusions drawn from the overall results are presented in the following sections.

5.5.4.1 Results and Discussion of XRD Analysis

The results of X-ray diffraction analysis of samples of Fe-PILC synthesised with the same OH/Fe synthesis ratio, (R_{OF}) 2, but with various Fe/clay (R_F) synthesis ratios, are presented graphically. R_{PI} describes the degree of pillaring in the Fe-PILC and a graphic interpretation of R_{PI} is shown in **fig. 5.4**. The results of the effect of varying the Fe/clay ratio (R_F) on the degree of pillaring are summarised in **table 5.7**. The results presented on a graph (see **fig. 5.5**) appear to indicate that to synthesise a Fe-PILC with a high degree of pillaring the suitable range of R_F values is between 1.25 and 1.3 mmol/g. The results of the effect of changing OH/Fe ratio (R_{OF}) on the degree of pillaring are summarised in **table 5.8** and presented on a graph. The results presented on a graph (see **fig. 5.6**) show that the optimum R_{OF} for the synthesis of Fe-PILC ranges from 1-2.

5.5.4.2 Results and Discussion of Nitrogen Adsorption Analysis

The general trend of the results of nitrogen adsorption analysis shows that there is a small and steady rise in BET surface area with an increase in R_F (see **fig. 5.7**) or R_{OF} (see **fig. 5.8**). In contrast, the results of micropore analysis show that changing R_F or R_{OF} did not have a significant effect on the micropore area. These results imply that increases in the BET surface area are likely to be mainly due to an increase in the mesoporosity of the clay. More

significant increases in the BET surface area are observed by increasing R_F rather than by increasing R_{OF}.

5.5.4.3 Results and Discussion of ICP-AES Analysis

In general, the results of ICP-AES analysis of all the Fe-PILC samples when compared to those of the raw Montmorillonite, show increases in the iron oxide content of the clay samples. These increases are also accompanied by significant decreases in calcium and sodium in the clay (see **tables 5.11** and **5.12**). The increase in iron oxide content of the clay suggests that iron oxide has been successfully incorporated into the clay structure, whereas the decreases in calcium and sodium in the clay may be interpreted as consumption of these natural exchange sites by the iron oxide pillars. The results (see **fig. 5.9** and **5.10**) suggest that the capacity of the raw clay in assimilating iron oxide reached a limiting value. Although increasing the R_{OF} value resulted in an increase of iron oxide content in the clay, it can also lead to problems such as precipitation of iron hydroxide on the surface of the clay.

5.5.4.4 Results and Discussion of Strontium Adsorption Analysis

The results of strontium adsorption analysis are summarised in tables (see **tables 5.13** and **5.14**) and on graphs (see **fig. 5.11** and **5.12**). The graph in **fig. 5.11** shows a decrease in the C.E.C. with

an increase in the R_F value. This is explained by factors such as an increase of percentage weight of iron oxide in the Fe-PILC, hence higher consumption of natural exchange sites of the raw clay. An additional factor, such as an increase in acidity of the clay by contacting the clay with a higher concentration of iron III nitrate solution, could be the cause of the observed decrease in the C.E.C. of the samples (see **fig. 5.13** for the pH of the clay). In general the C.E.C. values of the clay appear to vary according to the change in R_{PI} values which describe the degree of pillaring in the clay (see **fig. 5.5**). In the case of samples with lower C.E.C. values, on the other hand, the thermal treatment of the samples resulted in the formation of a compact clay structure.

The results (see **fig. 5.12**) of the analysis of clay samples prepared by altering the R_{OF} value also show that the C.E.C. values of the samples appear to vary according to the change in pH (see **fig. 5.14**).

5.5.5 Conclusions

The results of XRD analysis clearly show evidence of a pillared structure in the Fe-PILC samples prepared from a specific range of R_F or R_{OF} values. An Fe-PILC prepared from a certain range of R_F and R_{OF} values (see **fig. 5.5** and **5.6**) can have the highest possible degree of pillaring. It can also be concluded that the structural information on the pillared clay obtained from nitrogen adsorption analysis can be used to support the findings of the XRD analysis. The evidence obtained from ICP-AES analysis of the chemical

composition of the Fe-PILC confirmed that it would be possible to control the iron oxide content of the Fe-PILC by lowering the R_F or R_{OF} values. However it would not be advisable to regulate the iron oxide content of the clay by adjusting the R_{OF} value because of the problem of precipitation of iron hydroxide on the surface of the clay.

From the results of strontium adsorption analysis, it can be concluded that the reduction in the C.E.C. of the clay was the result of consumption of natural exchange sites by the synthetic iron oxide. Preparing an Fe-PILC using the lower R_F and R_{OF} range can result in an increase in the C.E.C. of the clay.

Table 5.5 The synthesis conditions for varying Fe/clay ratio (R_F).

Sample Name	R_F /mmol.g^{-1}	R_{OF} /Ratio	[NaOH] /Molar	[$Fe(NO_3)_3$] /Molar
F-F1	0.5	2.0	0.04	0.02
F-F2	1.0	2.0	0.08	0.04
F-F3	1.25	2.0	0.10	0.05
F-F4	1.30	2.0	0.104	0.052
F-F5	1.40	2.0	0.112	0.056
F-F6	1.50	2.0	0.120	0.060
F-F7	1.60	2.0	0.128	0.064
F-F8	1.70	2.0	0.136	0.068
F-F9	1.80	2.0	0.144	0.072
F-F10	2.0	2.0	0.16	0.080
F-F11	3.0	2.0	0.24	0.120
F-F12	4.0	2.0	0.32	0.160
F-F13	5.0	2.0	0.40	0.200

R_{OF} is the OH/Fe ratio.

Table 5.6 The synthesis conditions for varying OH/Fe synthesis ratio (R_{OF}).

Sample Name	R_{OF} /Ratio	R_F /mmol.g^{-1}	[NaOH] /Molar	[$Fe(NO_3)_3$] /Molar
F-O1	0.5	1.25	0.025	0.05
F-O2	1.0	1.25	0.050	0.05
F-O3	2.0	1.25	0.100	0.05
F-O4	2.5	1.25	0.125	0.05
F-O5	3.0	1.25	0.150	0.05
F-O6	4.0	1.25	0.20	0.05

R_F is the Fe/clay ratio.

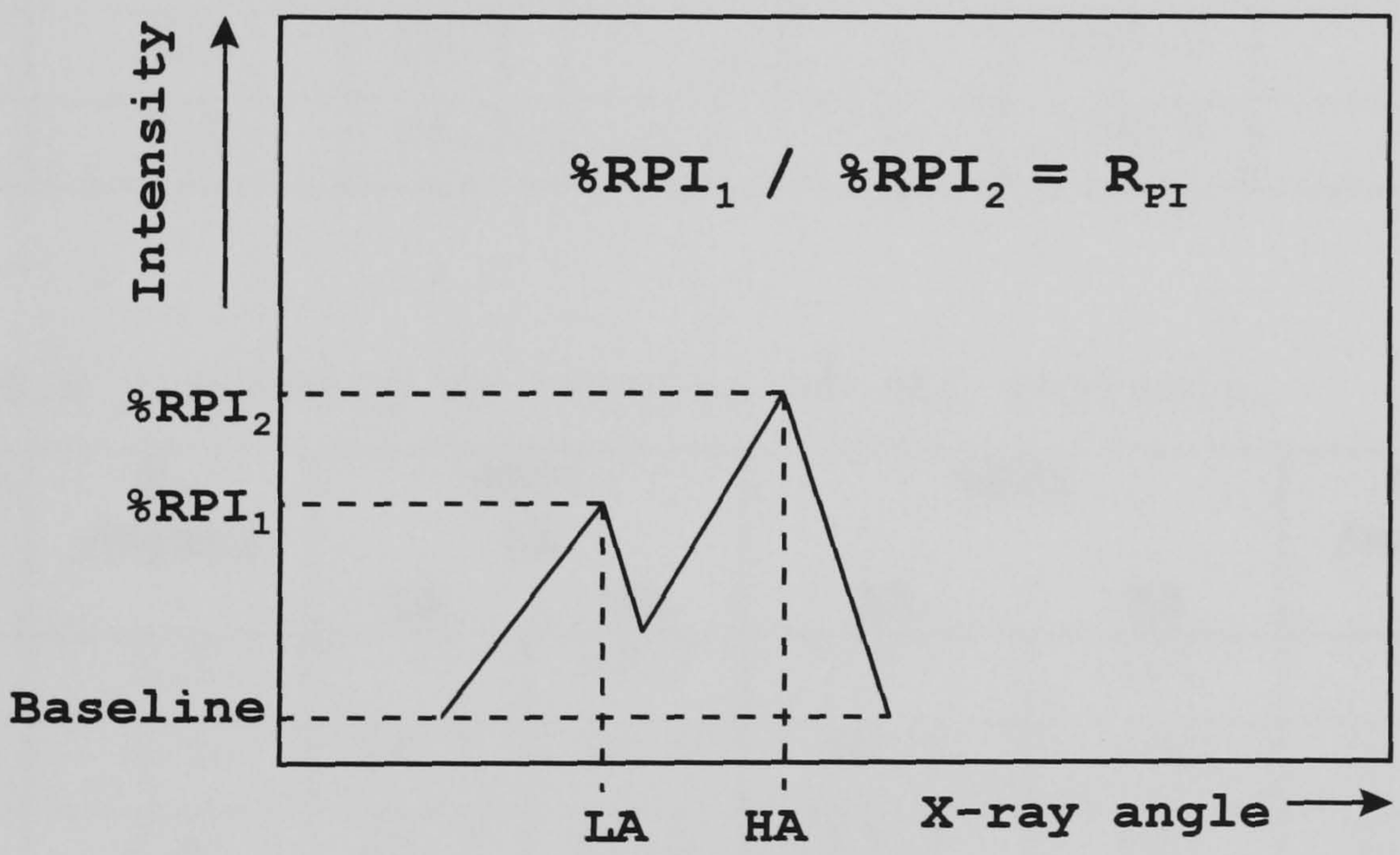


Fig. 5.4 A graphic interpretation of R_{PI} index, the estimated relative peak intensity ratio, (**%RPI** of **LA**)/(**%RPI** of **HA**). **LA** and **HA** represent the low and high X-ray angles, and **%RPI** is the estimated relative peak intensity in %.

Table 5.7 A summary of results of XRD analysis.

Sample Name	R_F /mmol.g^{-1}	d001 /Å		%RPI		R_{PI} /Ratio
		LA	HA	LA	HA	
F-F1	0.5	14.4	-	0	100.0	0
F-F2	1.0	12.4	-	0	100.0	0
F-F3	1.25	25.7	12.5	65.3	100.0	0.653
F-F4	1.30	26.4	12.8	94.8	100.0	0.948
F-F5	1.40	24.4	12.5	40.5	100.0	0.405
F-F6	1.50	23.5	12.8	36.3	100.0	0.363
F-F7	1.60	23.8	12.6	56.6	100.0	0.566
F-F8	1.70	23.6	12.4	46.3	100.0	0.463
F-F9	1.80	23.9	12.7	52.9	100.0	0.529
F-F10	2.0	14.4	-	0	100.0	0
F-F11	3.0	12.1	-	0	100.0	0
F-F12	4.0	12.2	-	0	100.0	0
F-F13	5.0	14.5	-	0	100.0	0

Table 5.8 A summary of results of XRD analysis.

Sample Name	R_{OF} /Ratio	d001 /Å		%RPI		R_{PI} /Ratio
		LA	HA	LA	HA	
F-O1	0.5	-	14.7	0	100	0
F-O2	1.0	24.5	12.6	98.1	100	0.981
F-O3	2.0	25.7	12.5	65.3	100	0.653
F-O4	2.5	24.2	15.1	51.6	99.4	0.516
F-O5	3.0	23.2	15.2	57.1	100	0.571
F-O6	4.0	22.6	15.0	50.2	100	0.502

The definitions of symbols in the **tables 5.7** and **5.8** are as follows: R_F is the Fe/clay ratio. **LA** and **HA** represent the low and high X-ray angles. **%RPI** is the estimated relative peak intensity in %. R_{PI} is the estimated relative peak intensity ratio, (**%RPI** of **LA**)/(**%RPI** of **HA**) (see **fig. 5.4**). R_{OF} is the OH/Fe ratio.

Table 5.9 A summary of results of nitrogen adsorption analysis.

Sample Name	R_F /mmol.g^{-1}	BET Surface Area /m^2.g^{-1}	Micro. Area /m^2.g^{-1}	Micro. Volume /cc.g^{-1}	Average Pore Diameter /Å
F-F1	0.5	48.1	11.5	0.00514	72.5
F-F2	1.0	71.4	7.84	0.00304	62.8
F-F3	1.25	82.2	9.01	0.00348	57.6
F-F4	1.30	87.5	13.3	0.00557	52.5
F-F5	1.40	92.3	14.7	0.00624	55.3
F-F6	1.50	93.6	16.0	0.00690	54.8
F-F7	1.60	96.2	12.6	0.00512	52.8
F-F8	1.70	97.6	10.1	0.00384	52.5
F-F9	1.80	98.2	8.65	0.00313	52.6
F-F10	2.0	109.5	13.9	0.00563	48.3
F-F11	3.0	111.4	4.00	0.000633	48.6
F-F12	4.0	133.9	13.3	0.00495	39.8
F-F13	5.0	157.6	13.3	0.00466	36.0

Micro. represents micropore. R_F is Fe/clay ratio.

Table 5.10 A summary of results of nitrogen adsorption analysis.

Sample Name	R_{OF} /mmol.g^{-1}	BET Surface Area /m^2.g^{-1}	Micro. Area /m^2.g^{-1}	Micro. Volume /cc.g^{-1}	Average Pore Diameter /Å
F-O1	0.5	51.9	13.1	0.00589	81.8
F-O2	1.0	66.1	15.9	0.00713	68.8
F-O3	2.0	82.2	9.0	0.00348	57.6
F-O4	2.5	77.1	11.5	0.00481	59.3
F-O5	3.0	81.8	6.5	0.00223	61.3
F-O6	4.0	85.6	4.6	0.00122	57.3

Micro. represents micropore. R_{OF} is OH/Fe ratio.

In **tables 5.11** and **5.12**, the definitions of $\mathbf{R_{FS}}$ is the %wt ratio of Fe_2O_3 and SiO_2. ^{RM} is the $\mathbf{R_{FS}}$ of the starting clay, raw Montmorillonite.

Table 5.11 A summary of results of ICP-AES analysis.

The chemical composition of the samples in percentage weight (%wt).							
R_F /mmol.g^{-1}	SiO_2	Al_2O_3	Fe_2O_3	CaO	Na_2O	K_2O	R_{FS}
0.0	63.7	19.8	3.7	1.1	2.3	0.6	0.06^{RM}
0.5	58.2	19.0	7.8	1.1	0.9	0.2	0.13
1.0	57.3	18.4	11.7	0.7	0.4	0.3	0.20
1.25	56.8	17.8	12.8	0.5	0.3	0.2	0.23
1.3	56.4	17.9	13.5	0.4	0.2	<0.1	0.24
1.4	54.7	17.6	14.2	0.3	0.1	<0.1	0.26
1.5	55.3	17.4	14.4	0.5	0.3	0.2	0.26
1.6	53.8	17.2	14.9	0.4	0.3	0.2	0.28
1.7	53.8	17.4	15.2	0.3	0.3	0.1	0.28
1.8	55.4	17.5	15.7	0.4	0.3	0.1	0.28
2.0	55.1	17.4	17.3	0.3	0.2	0.2	0.32
3.0	51.9	17.3	17.6	0.3	0.2	0.2	0.34
4.0	53.1	16.8	19.2	0.2	0.3	0.3	0.36

Table 5.12 A summary of results of ICP-AES analysis.

The chemical composition of the samples in percentage weight (%wt).							
R_{OF} /Ratio	SiO_2	Al_2O_3	Fe_2O_3	CaO	Na_2O	K_2O	R_{FS}
0.0	63.7	19.8	3.7	1.1	2.3	0.6	0.06^{RM}
0.5	59.2	18.8	8.8	0.3	0.3	0.3	0.15
1.0	58.5	18.7	10.3	0.3	0.3	0.2	0.18
2.0	56.8	17.8	12.8	0.5	0.3	0.2	0.23
2.5	55.6	17.7	13.4	0.8	0.9	0.2	0.24
3.0	52.2	16.5	18.0	1.0	1.5	0.2	0.34
4.0	49.7	20.1	20.1	1.4	1.8	0.3	0.41

Table 5.13 A summary of results of batch contact tests.

Sample Name	R_F /mmol.g^{-1}	C.E.C. /meq.kg^{-1}	R^2
F-F1	0.5	785.2	0.990
F-F2	1.0	655.4	0.967
F-F3	1.25	411.5	1.000
F-F4	1.30	813.3	0.981
F-F5	1.40	656.1	0.995
F-F6	1.50	319.0	0.994
F-F7	1.60	548.4	0.982
F-F8	1.70	390.1	0.997
F-F9	1.80	522.0	0.999
F-F10	2.0	534.5	0.973
F-F11	3.0	320.3	0.997
F-F12	4.0	253.1	1.000
F-F13	5.0	-	-

R_F is the Fe/clay ratio. R^2 is the square of correlation coefficient. **C.E.C.** is the cation exchange capacity (in milli-equivalent per kg).

Table 5.14 A summary of results of batch contact tests.

Sample Name	R_{OF} /Ratio	C.E.C. /meq.kg^{-1}	R^2
F-O1	0.5	-	-
F-O2	1.0	254.1	0.997
F-O3	2.0	411.5	1.000
F-O4	2.5	802.1	0.989
F-O5	3.0	479.3	0.994
F-O6	4.0	-	-

R_{OF} is the OH/Fe ratio. R^2 is the square of correlation coefficient. **C.E.C.** is the cation exchange capacity (in milli-equivalent per kg).

For the definition of the estimated relative peak intensity ratio, R_{PI}, in **fig. 5.5** and **fig. 5.6** (see **fig. 5.4**).

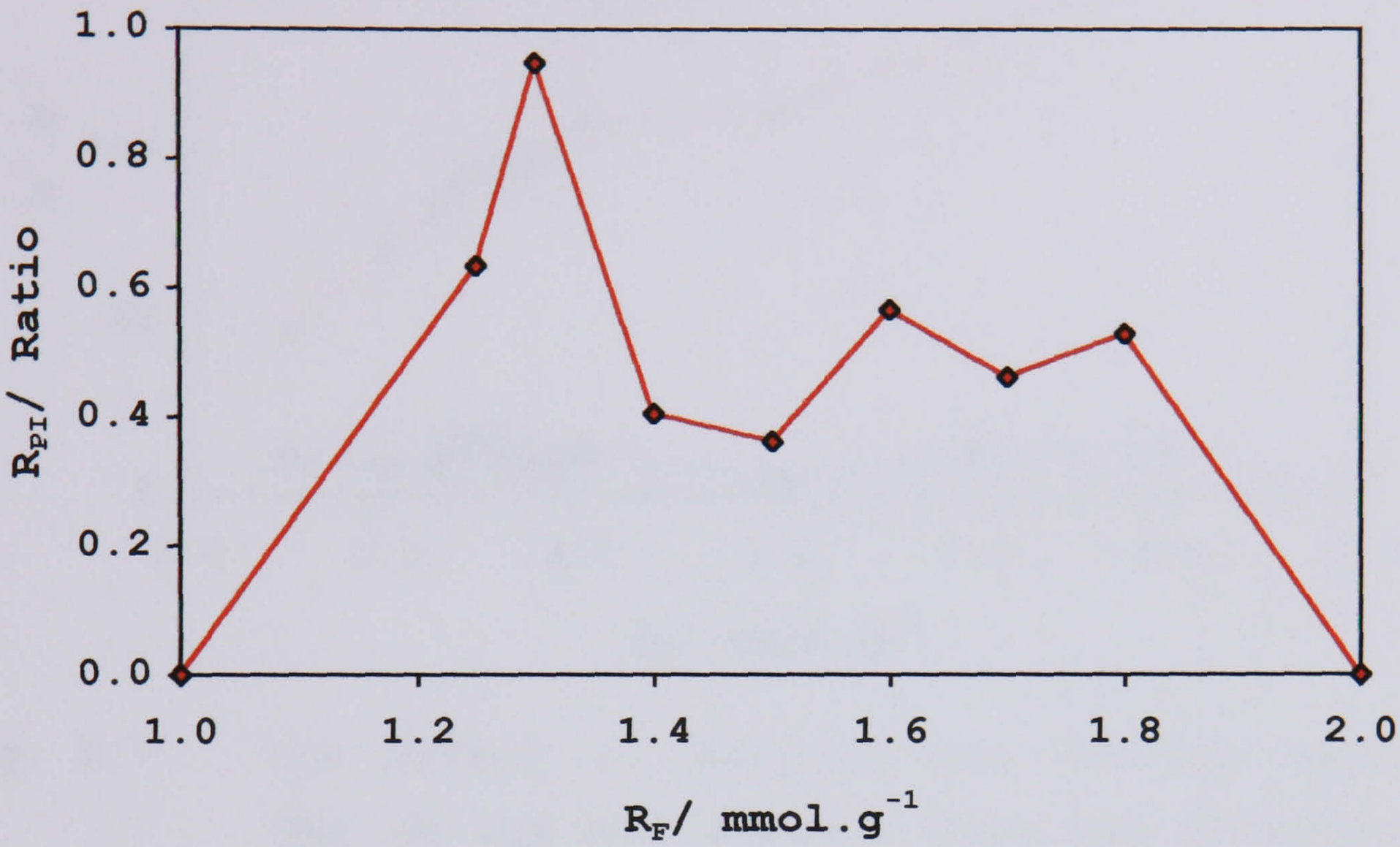


Fig. 5.5 The effect of varying the Fe/clay ratio (R_F) on the degree of pillaring in the clay (see **table 5.7**).

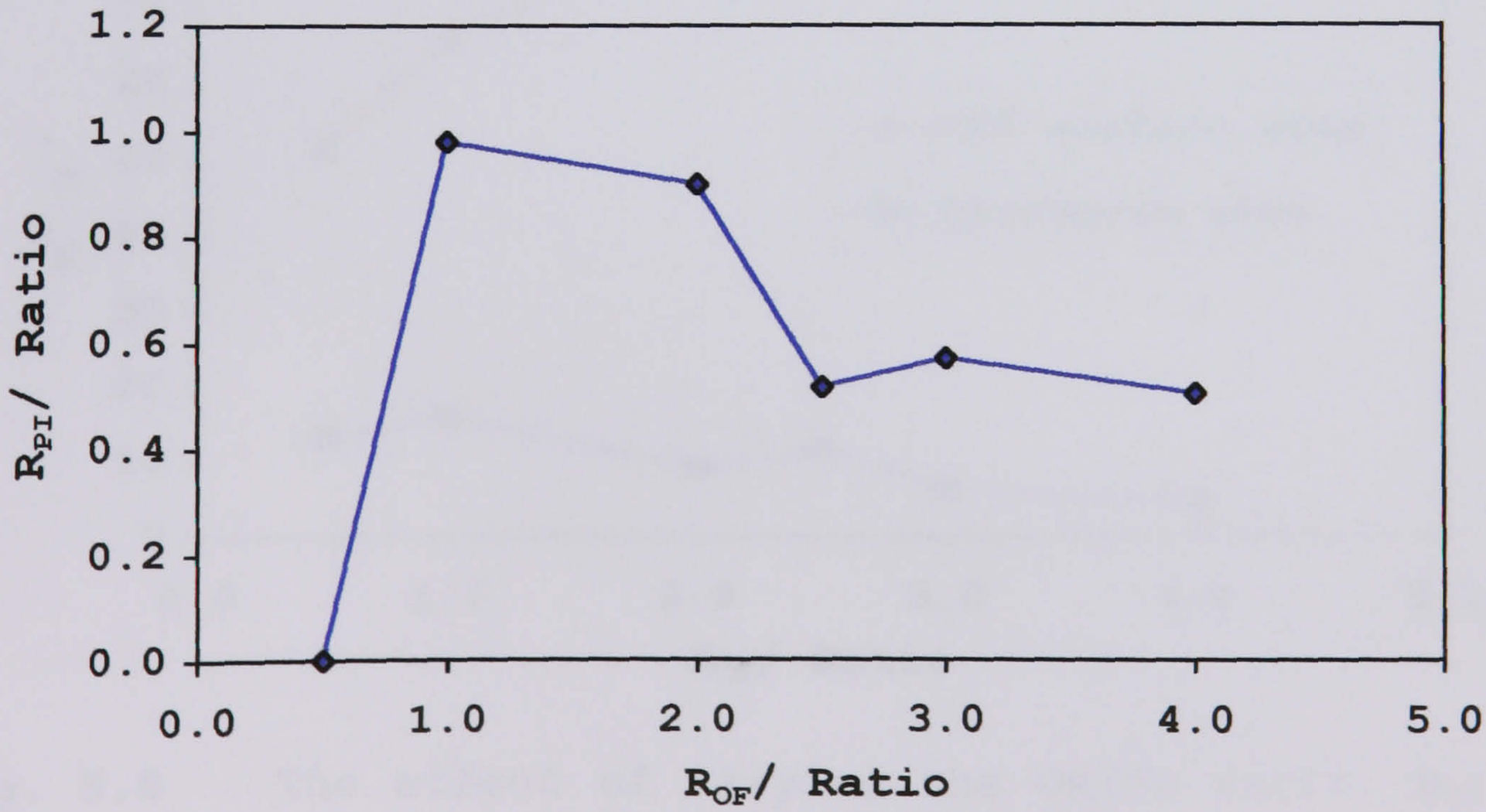


Fig. 5.6 The effect of varying the OH/Fe ratio (R_{OF}) on the degree of pillaring in the clay (see **table 5.8**).

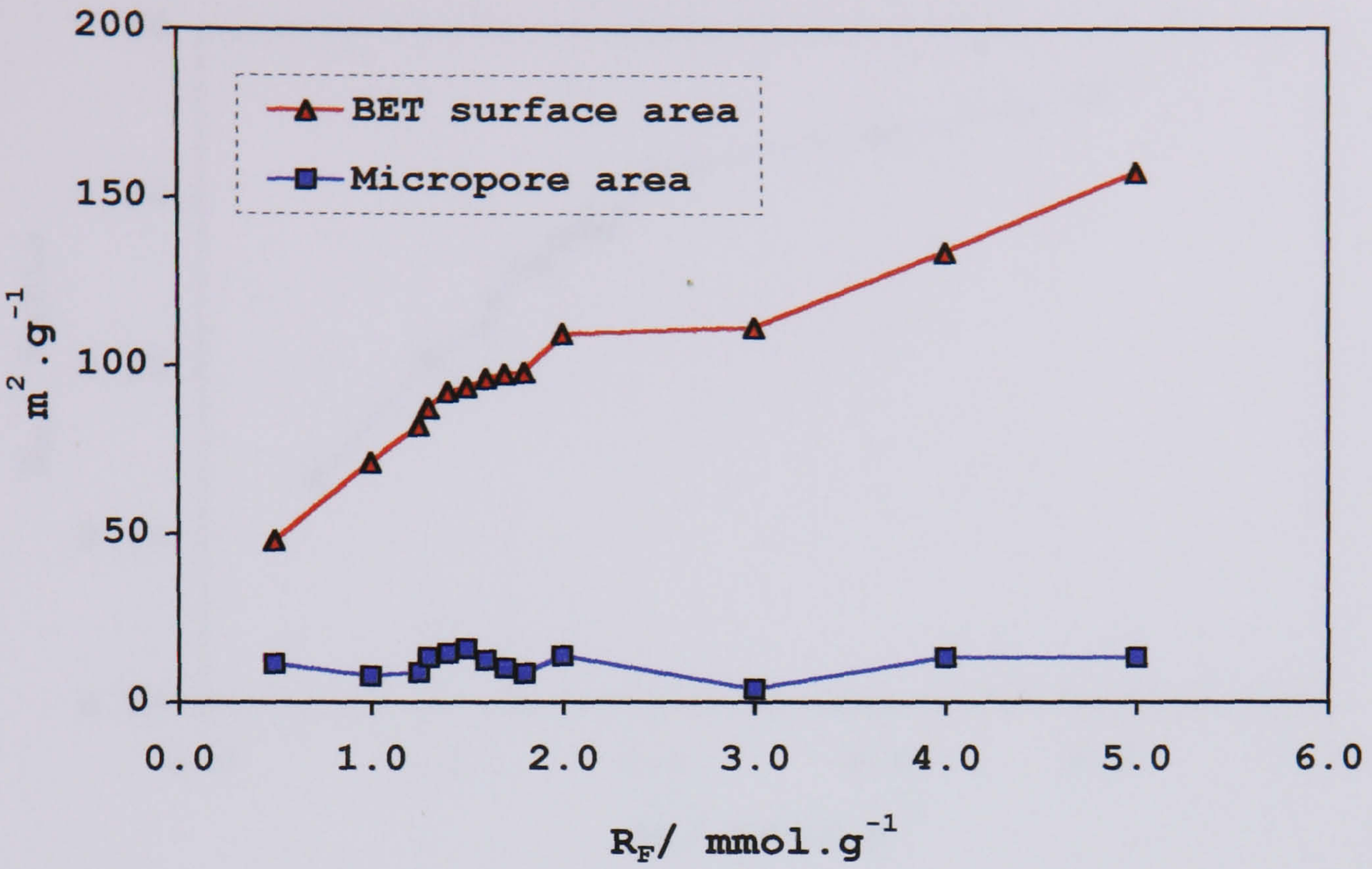


Fig. 5.7 The effect of varying the Fe/clay ratio (R_F) on the BET surface area and micropore area of the clay (see **table 5.9**).

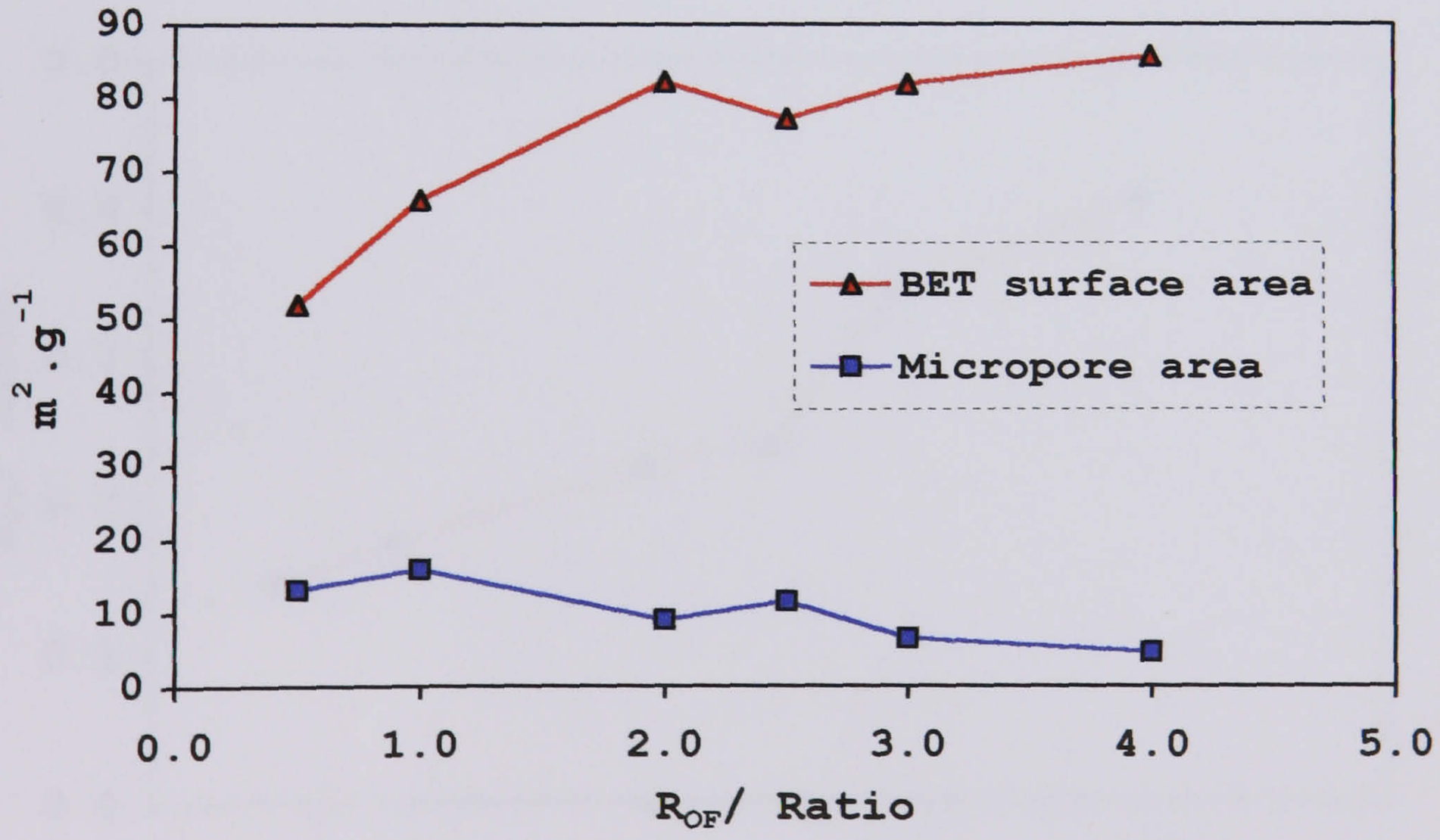


Fig. 5.8 The effect of varying the OH/Fe ratio (R_{OF}) on the BET surface area and micropore area of the clay (see **table 5.10**).

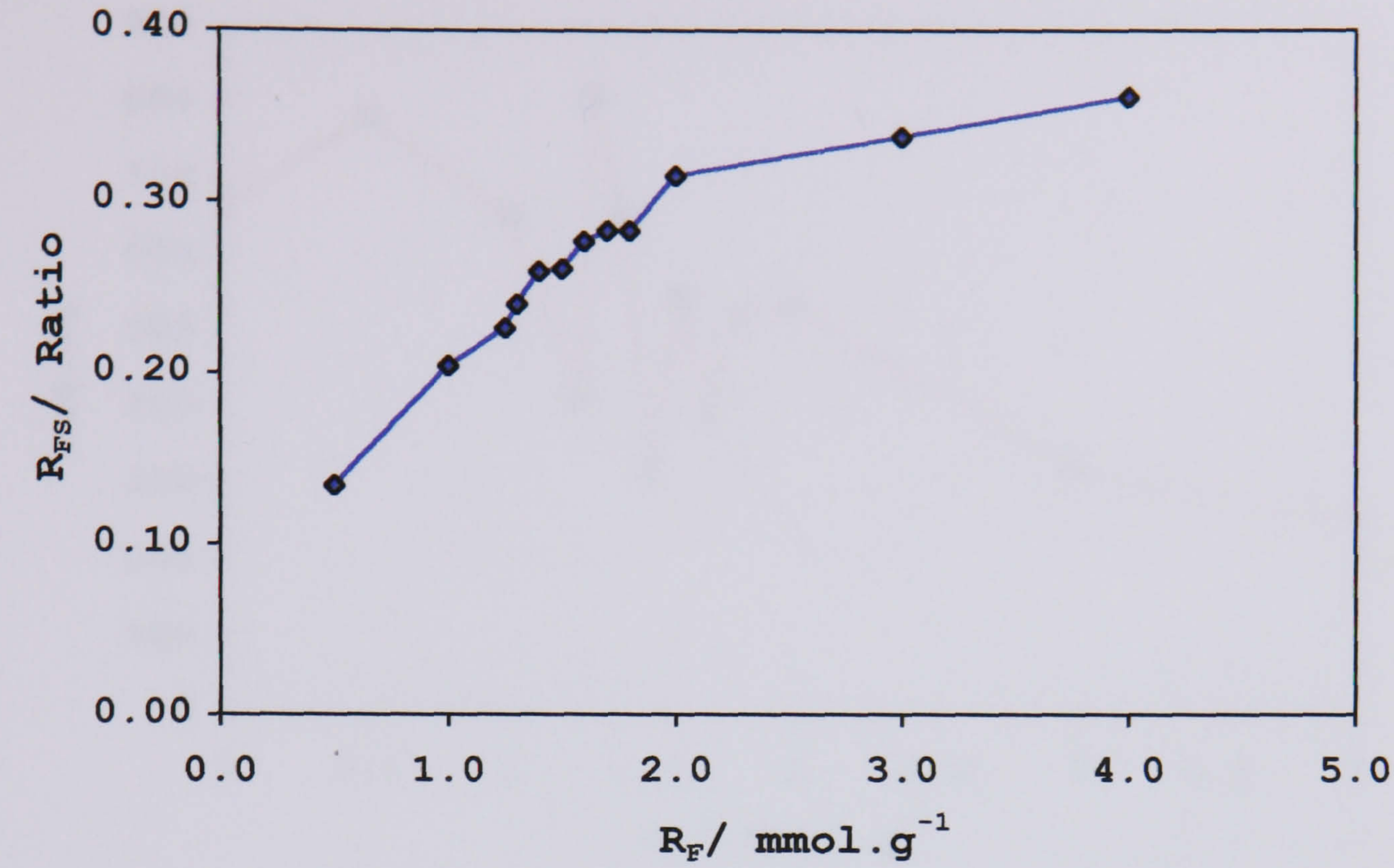


Fig. 5.9 The effect of varying the Fe/clay ratio (R_F) on the iron oxide content of the clay (see **table 5.11**).

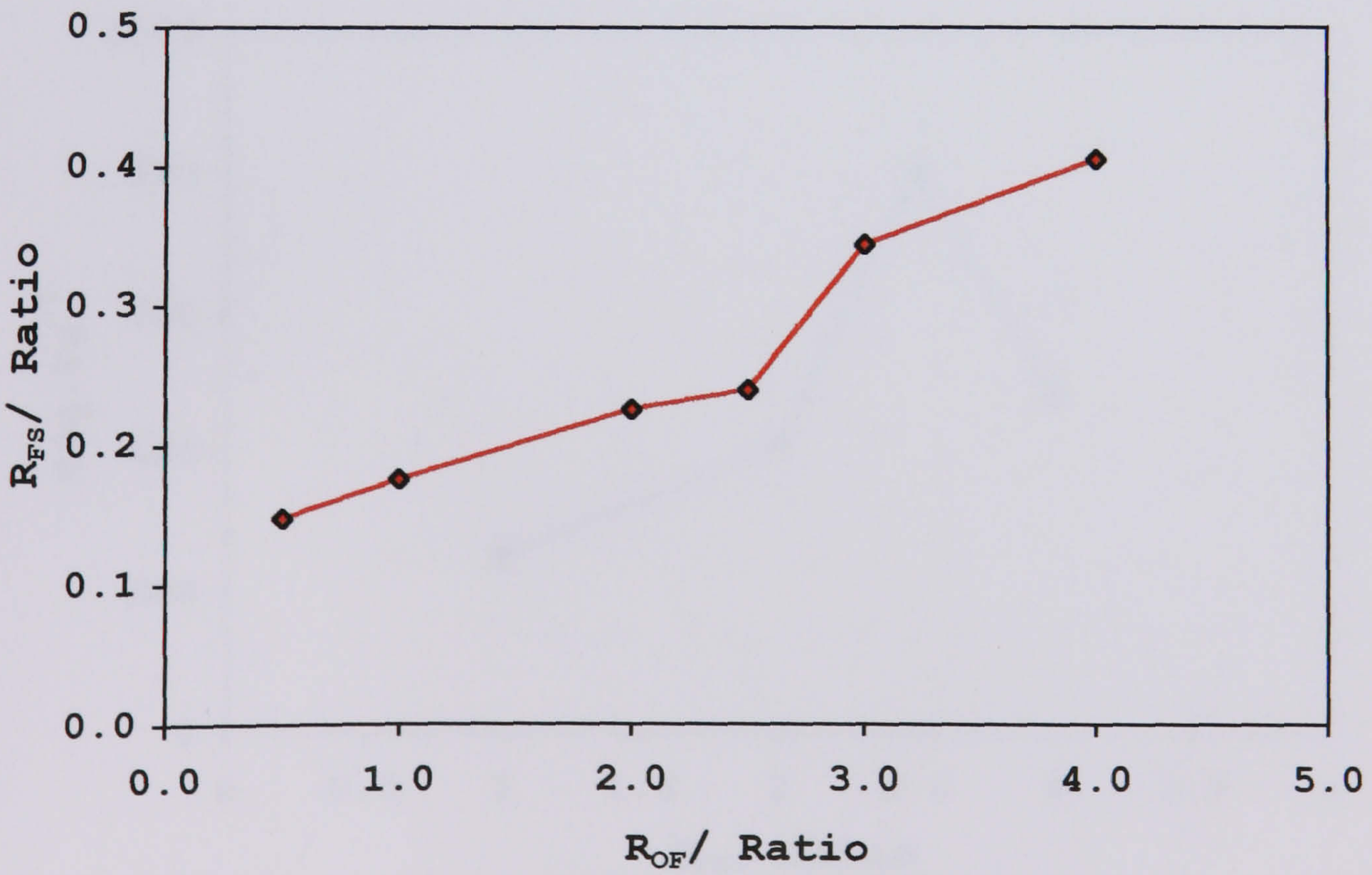


Fig. 5.10 The effect of varying the OH/Fe ratio (R_{OF}) on the iron oxide content of the clay (see **table 5.12**).

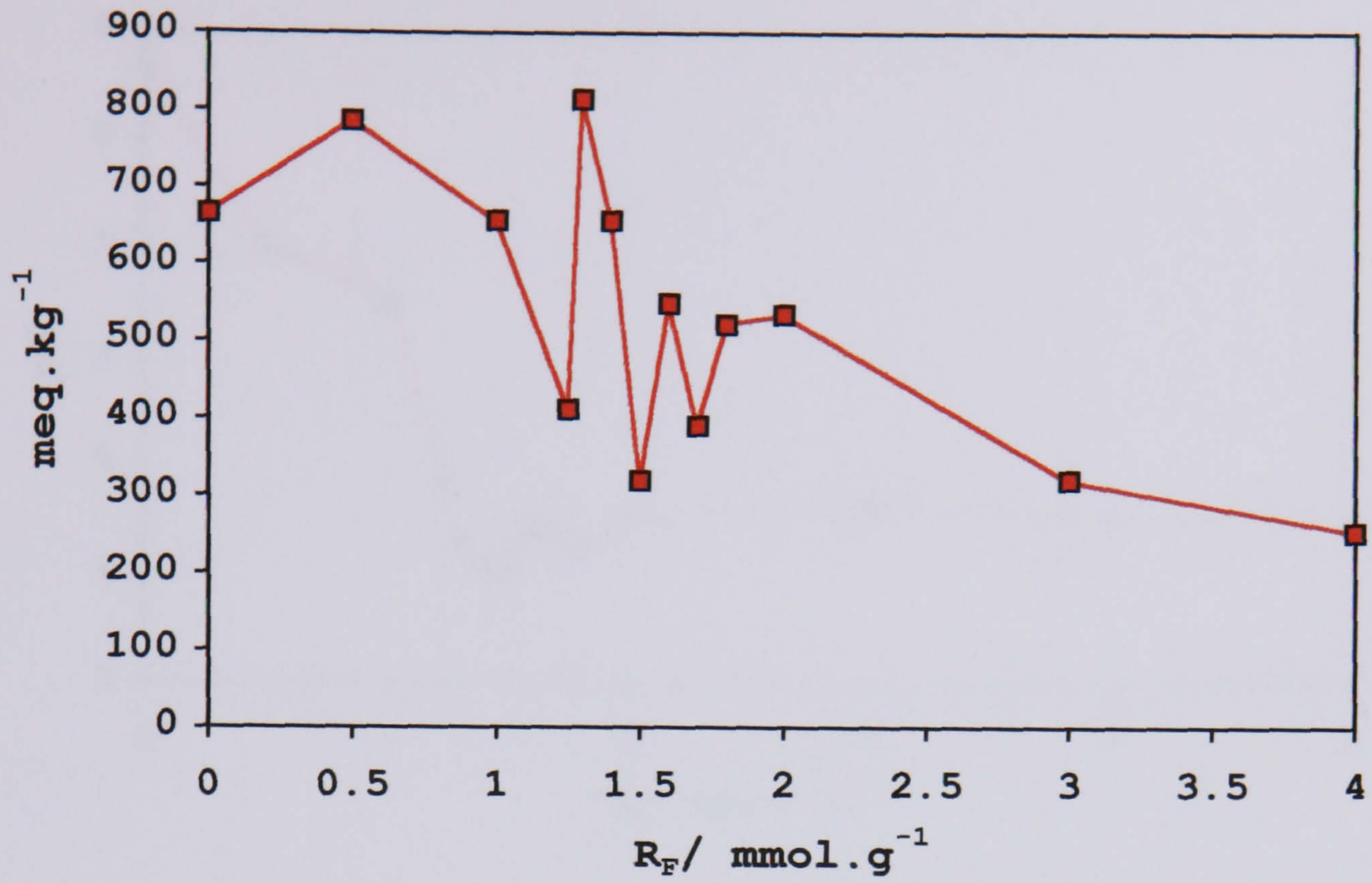


Fig. 5.11 The effect of varying the Fe/clay ratio (R_F) on the C.E.C. of the clay (see **table 5.13**).

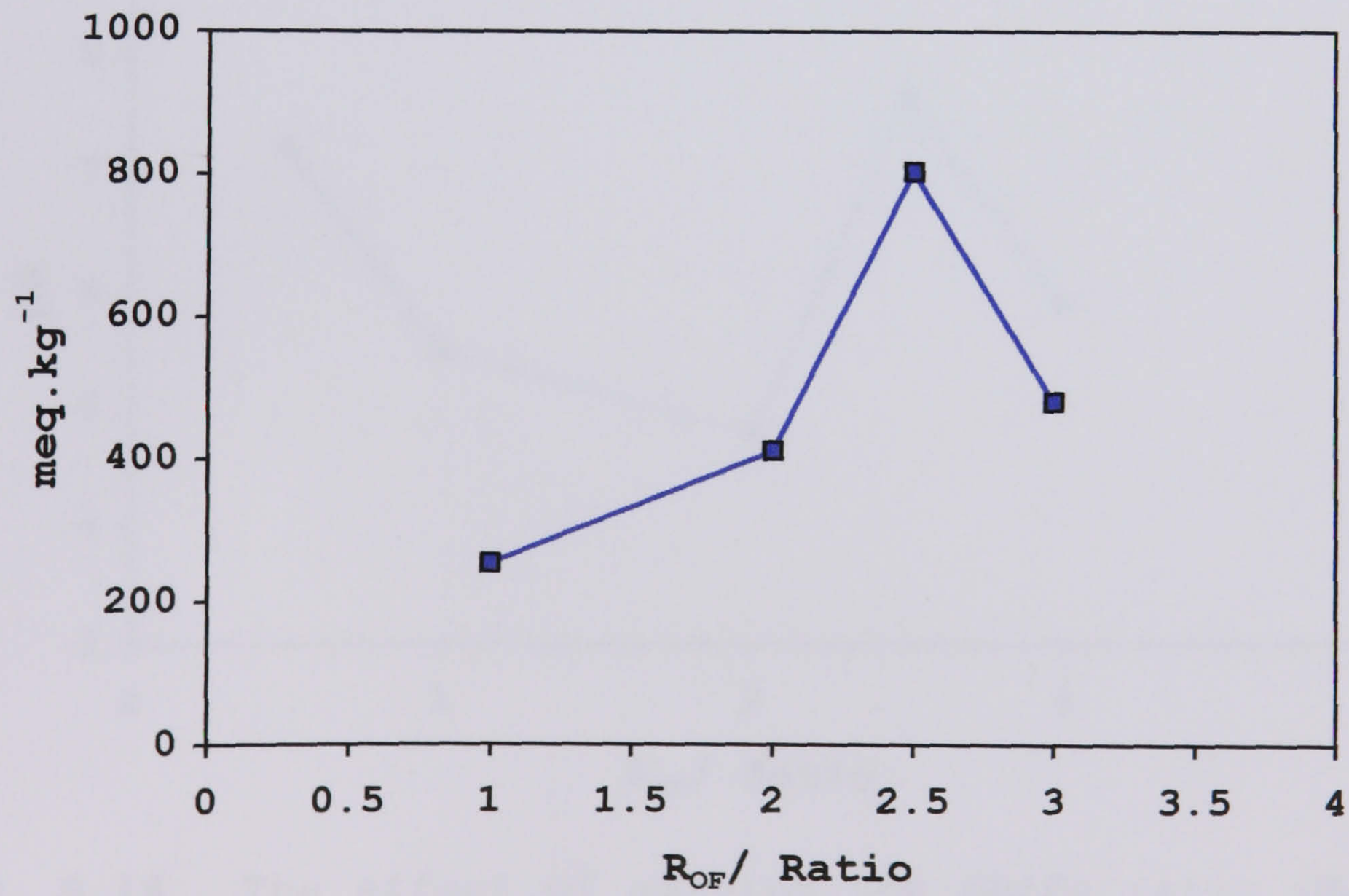


Fig. 5.12 The effect of varying the OH/Fe ratio (R_{OF}) on the C.E.C. of the clay (see **table 5.14**).

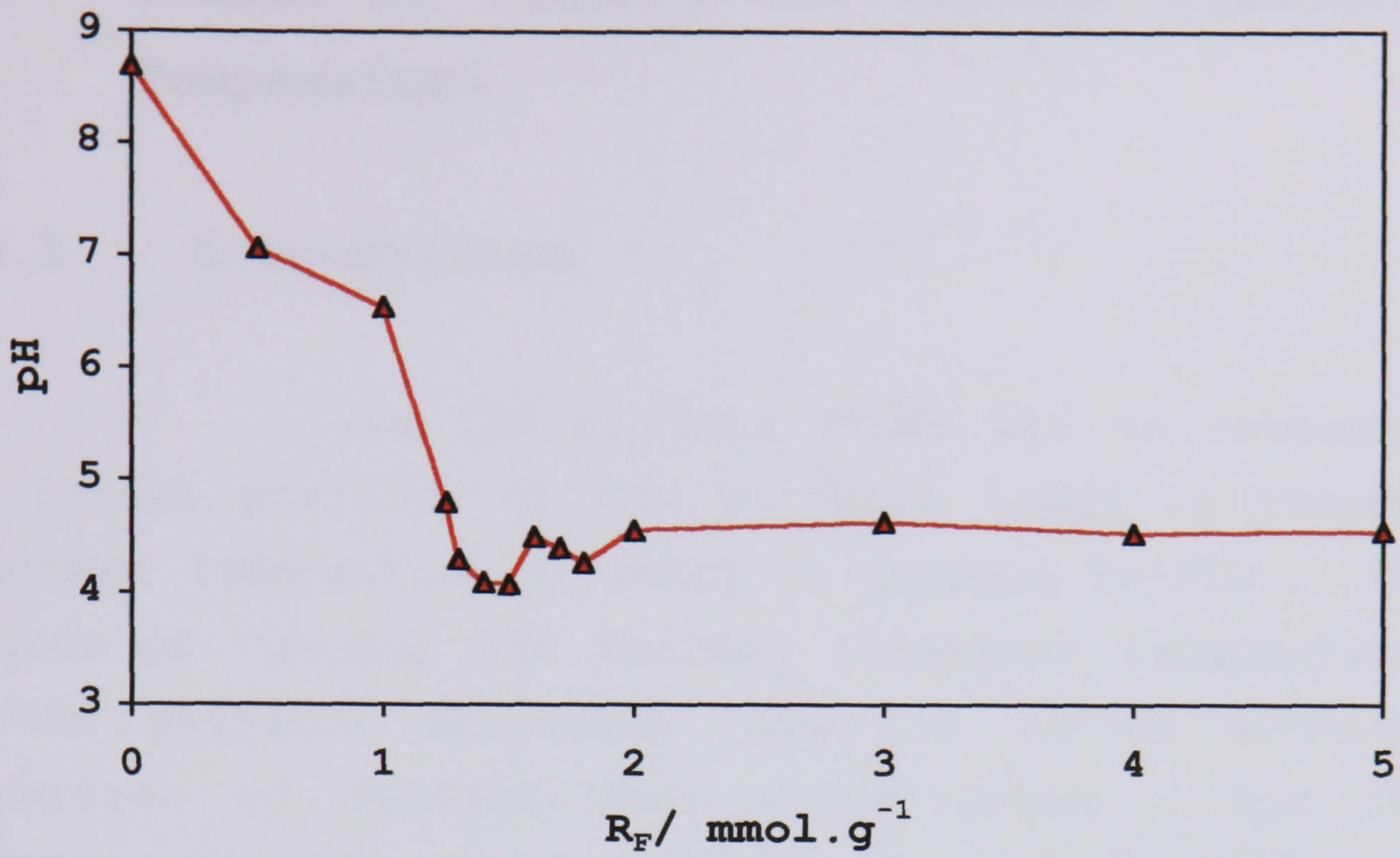


Fig. 5.13 The effect of varying the Fe/clay ratio (R_F) on the pH of the thermally-treated clay (see **table 5.5**).

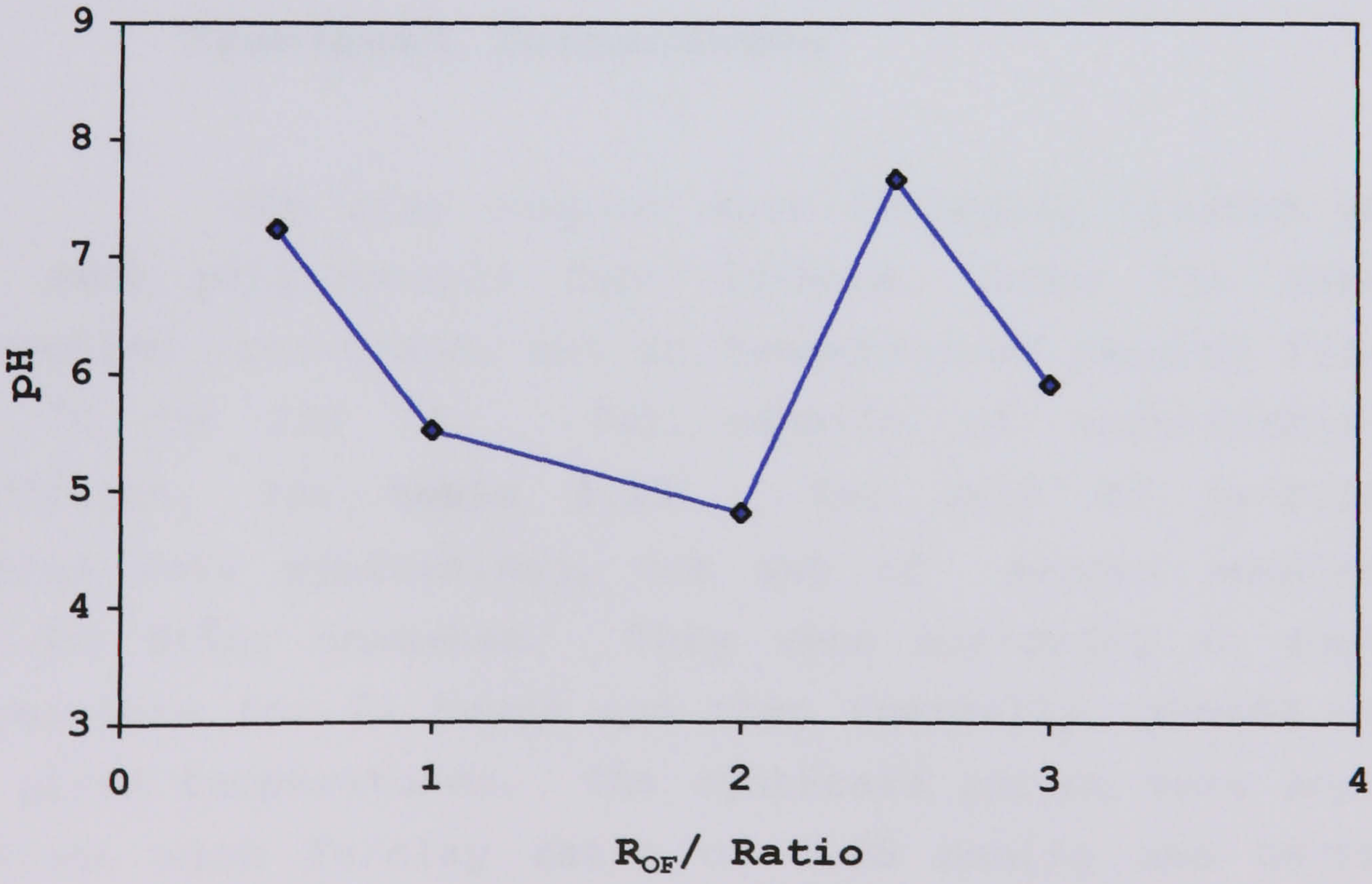


Fig. 5.14 The effect of varying the OH/Fe ratio (R_{OF}) on the pH of the thermally-treated clay (see **table 5.6**).

5.6 Effect of Varying the Thermal Treatment Temperature

5.6.1 Introduction

The aim of this study was to determine the lowest possible or the suitable range of thermal treatment temperature at which to prepare Fe-PILC. The effects of varying the thermal treatment temperatures on the physical structure, and the cation exchange properties of Fe-PILC were investigated. For the purpose of this study, each set of Fe-PILC was synthesised using the same synthesis ratios, while the thermal treatment temperature was varied.

5.6.2 Experiment in Varying the Thermal Treatment Temperature

The clay samples were thermally treated in the same programmable tube furnace, under the same controlled conditions, but at temperatures ranging from 100 °C to 250 °C. For details of experimental conditions, see **table 5.15**. Two sets of Fe-PILC samples were synthesised, one set of washed samples and the other unwashed. They were air-dried at room temperature for 24 hours and then thermally treated at the given temperatures. The synthesis ratios were kept constant with Fe/clay ratio of 1.25 mmol/g and OH/Fe ratio of 2. For details of synthesis procedures, see **section 5.2**. The structures and ion exchange properties of the clays were characterised using standard techniques.

5.6.3 Results and Discussion of Preliminary Characterisations

The results of TG, XRD, nitrogen adsorption, and strontium adsorption analysis are discussed, and general conclusions drawn from the overall results are presented in the following sections.

5.6.3.1 Results and Discussion of TG Analysis

The TG graphs of a raw Montmorillonite and an air-dried Fe-PILC sample, F-RM (see **table 5.1**), are shown in **fig. 5.15** (**a**) and (**b**) respectively. For the raw clay, the results (see **fig. 5.15** (**a**)) show that the amount of weight loss from the sample is divided into two stages. This is probably due to the removal of water from the clay. The raw clay appears to be thermally stable up to 500 °C. Above 500 °C, crystalline water is removed from the clay and the removal of this type of water would lead to structural changes. For Fe-PILC, the results (see **fig. 5.15** (**b**)) show that the amount of weight loss (water loss) from the Fe-PILC sample is divided into three different stages. The weight loss at stage one and two is unlikely to cause structural damage in the PILC, but that at stage three might alter the structure.

The overall result suggests that the most suitable range of thermal treatment temperature for treating the raw Fe-PILC is between 159.7 °C and 479.4 °C. For temperatures between 19.6 °C and 159.7 °C, the

water eliminated from the Fe-PILC sample should activate the phrase transformation of the pillaring agent from that of iron hydroxide pillars to that of more stable iron oxide pillars. Treating the clay below 479.4 °C may avoid structural collapse of the clay. These results show that it may be important to heat the raw Fe-PILC sample under controlled heating conditions because the water loss in the clay occurs at several stages.

5.6.3.2 Results and Discussion of XRD Analysis

The general trend of the results (see **fig. 5.16**) of the clay samples indicates that the most suitable temperature to heat the Fe-PILC appears to be 200 °C. Above 200 °C a decrease in the degree of pillaring in the clay is observed.

5.6.3.3 Results and Discussion of Nitrogen Adsorption Analysis

The results (see **table 5.17**) of the Fe-PILC samples, F-T (1W to 4W), are similar to those of sample F-RM (see **table 5.3**) which suggests that the clay samples were pillared. The results (see **fig. 5.17 (a)** and **table 5.17**) show that there is no significant variation in the structure of the washed Fe-PILC. In contrast, the results of the analysis of the unwashed Fe-PILC samples (see **fig. 5.17 (b)** and **table 5.17**) show that the porosity or thermal stability of the clay samples increases by treating the clay at 200 °C.

5.6.3.4 Results and Discussion of Strontium Adsorption Analysis

These results (see **table 5.18, fig. 5.18**) seem to imply that the most suitable treatment temperature for treating the raw Fe-PILC is 200 °C. The observed increase in the C.E.C. of the Fe-PILC was probably due to the formation of an open structure between the layers of the clay, whereas the decrease in the C.E.C. of the sample prepared at 250 °C was probably due to the formation of a compact clay structure, which led to a lack of availability of exchange sites for the strontium cations. The observed rise in the C.E.C. of the clay may also be partly due to the increase in pH (see **fig. 5.19**) of the thermally-treated clay.

5.6.4 Conclusions

The overall result of thermal gravimetric analysis shows that it can be used to monitor the thermal stability of the starting clay and raw PILC. The information obtained from this analysis can be used to select the suitable temperature range for treating the raw PILC. The conclusions drawn from the results of the two analyses, XRD and nitrogen adsorption analysis, suggest that the low thermal stability of the Fe-PILC was probably the result of varying the thermal treatment temperature. The general conclusion drawn from the strontium adsorption analysis is that preparing an Fe-PILC at an optimum thermal treatment temperature can lead to only a slight enhancement in the C.E.C. of the clay.

Table 5.15 A summary of thermal treatment conditions of the Fe-PILC.

Sample Name	Treatment Temp. /°C	Washed
F-T1W	100	Yes
F-T2W	150	Yes
F-T3W	200	Yes
F-T4W	250	Yes
F-T5NW	100	No
F-T6NW	150	No
F-T7NW	200	No
F-T8NW	250	No

W and **NW** represent the washed and unwashed samples, respectively.

Table 5.16 A summary of results of XRD analysis.

Sample Name	Treatment Temp. /°C	d001 /Å		%RPI		R_{PI} /Ratio
		LA	HA	LA	HA	
F-T1W	100	23.8	13.0	34.2	100	0.342
F-T2W	150	23.4	12.5	22.3	100	0.223
F-T3W	200	23.4	12.4	37.0	100	0.370
F-T4W	250	24.1	12.2	30.2	100	0.302
F-T5NW	100	22.8	12.7	49.9	100	0.499
F-T6NW	150	26.0	12.3	59.0	100	0.59
F-T7NW	200	23.7	12.4	69.8	100	0.698
F-T8NW	250	22.8	11.8	45.3	100	0.453

LA and **HA** represent the low and high X-ray angles respectively. **%RPI** is the estimated relative peak intensity in %. $\mathbf{R_{PI}}$ is the estimated relative peak intensity ratio (**%RPI of LA**)/(**%RPI of HA**) (see **fig. 5.4**). **W** represents the washed sample. **NW** represents the unwashed sample.

Table 5.17 A summary of results of nitrogen adsorption analysis.

Sample Name	**Treatment Temp. /°C**	**BET Surface Area /$m^2.g^{-1}$**	**Micro. Area /$m^2.g^{-1}$**	**Micro. Volume /$cc.g^{-1}$**	**Average Pore Diameter /Å**
F-T1W	100	65.6	22.4	0.0103	43.5
F-T2W	150	74.3	23.8	0.0110	64.3
F-T3W	200	71.4	17.7	0.00796	60.6
F-T4W	250	69.1	19.8	0.00906	59.4
F-T5NW	100	12.1	-	-	79.3
F-T6NW	150	9.5	53.9	0.0224	107.1
F-T7NW	200	35.0	6.5	0.00281	57.7
F-T8NW	250	31.7	2.7	0.000892	74.9

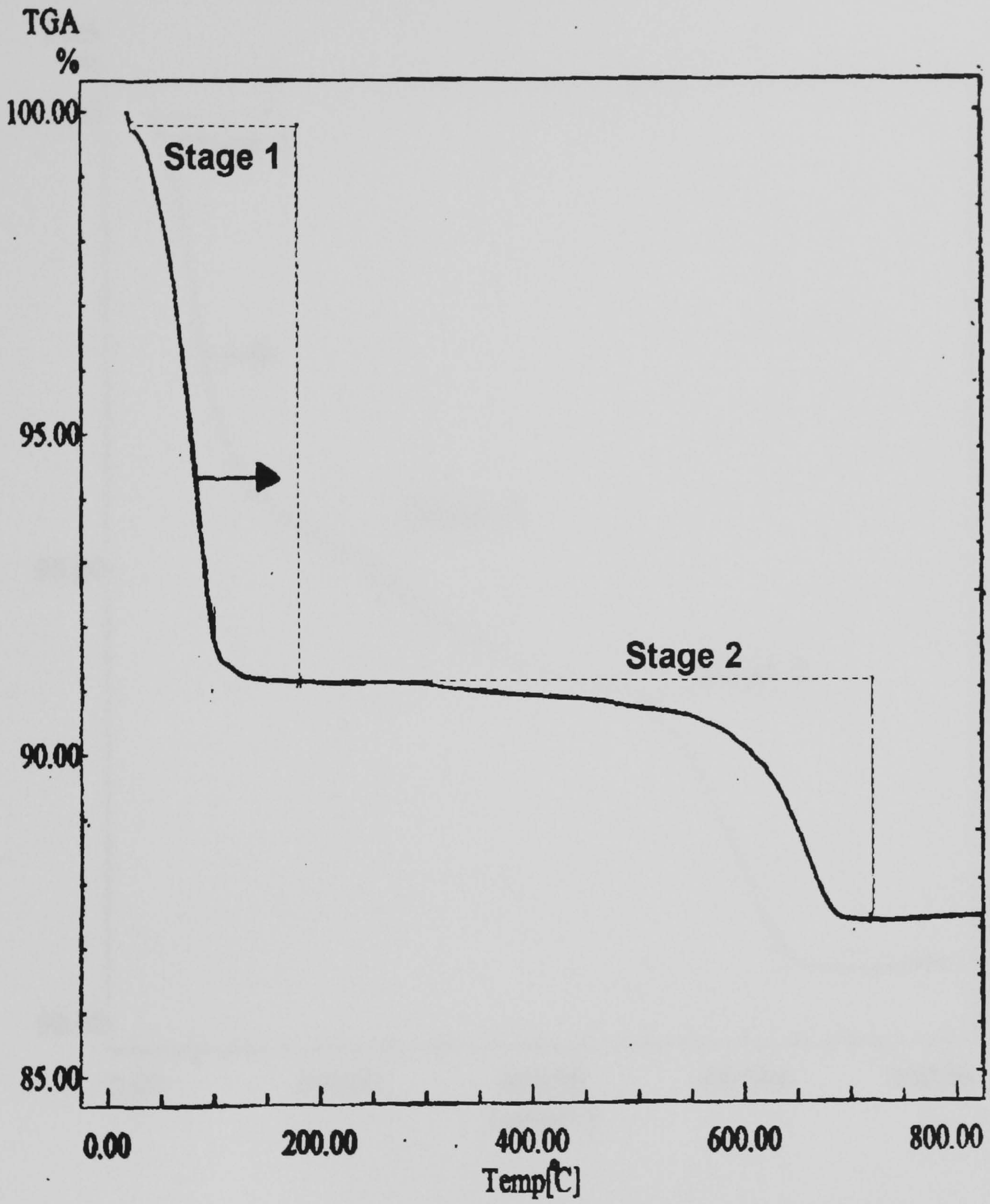
Micro. Represents micropore. **W** represents the washed sample. **NW** represents the unwashed sample.

Table 5.18 A summary of results of batch contact tests.

Sample Name	**Treatment Temp. /°C**	**C.E.C. /$meq.kg^{-1}$**	**R^2**
F-T1W	100	386.0	0.994
F-T2W	150	310.6	0.997
F-T3W	200	365.4	0.995
F-T4W	250	304.8	0.965
F-T5NW	100	423.1	0.999
F-T6NW	150	527.8	0.990
F-T7NW	200	592.8	0.991
F-T8NW	250	440.0	0.998

R^2 is the square of correlation coefficient. **C.E.C.** is the cation exchange capacity (in milli-equivalent per kg). **W** represents the washed sample. **NW** represents the unwashed sample.

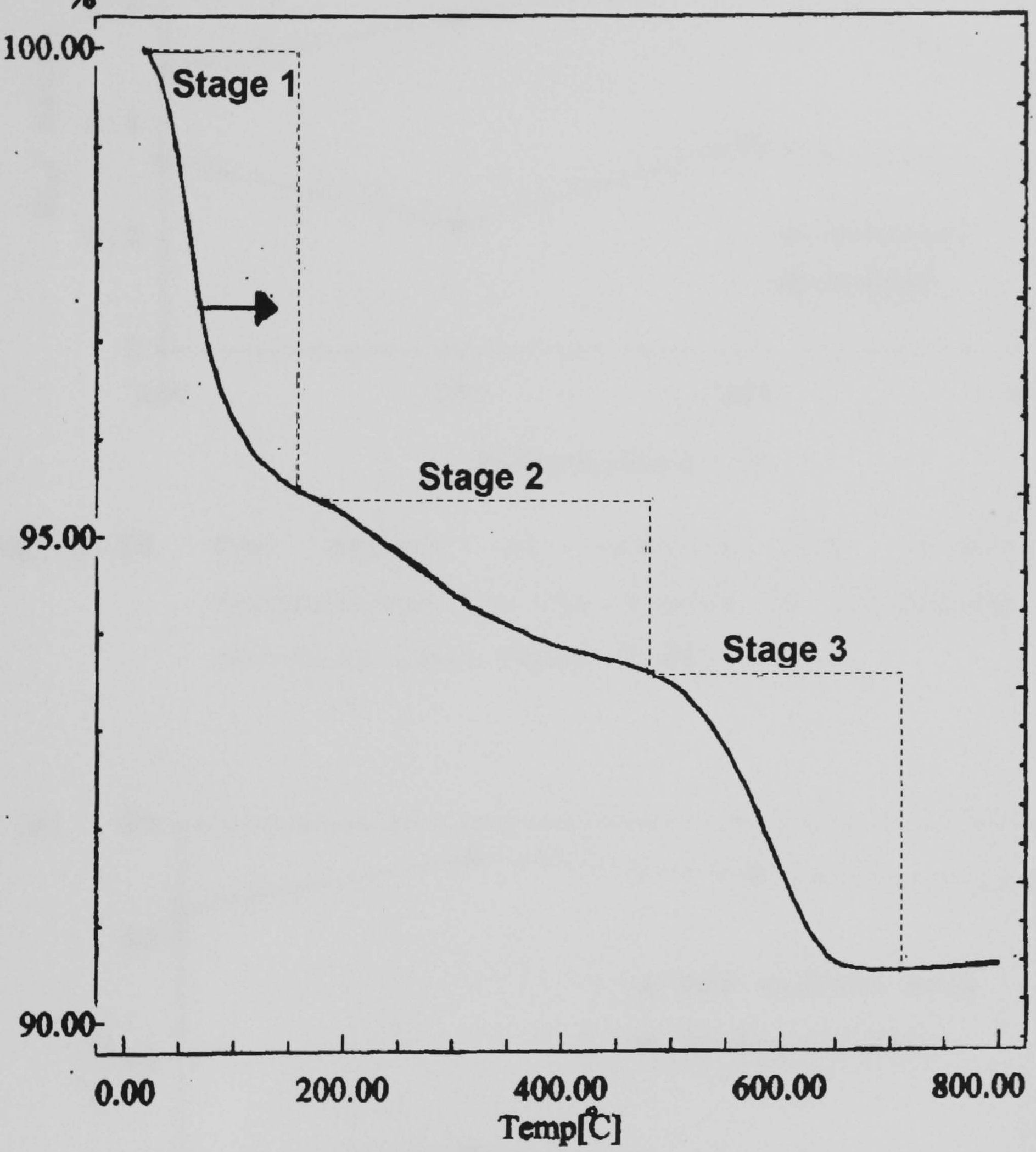
(a)



Stage	Start Temp./°C	End Temp./°C	Weight Loss
1	227.5	178.67	-1.26 mg (-8.6%)
2	180.97	718.81	-0.55 mg (-3.8%)

Fig. 5.15 (**a**) The TG graph of the raw Montmorillonite.

(b)



Stage	Start Temp./°C	End Temp./°C	Weight Loss
1	19.59	159.73	-0.54 mg (-4.5%)
2	181.24	479.45	-0.21 mg (-1.8%)
3	484.97	710.25	-0.36 mg (-3.0%)

Fig. 5.15 (**b**) The TG graph of the air dried Fe-PILC, F-RM, (see **table 5.1**).

For the definition of the estimated relative peak intensity ratio, R_{PI}, in **fig. 5.16**, see **fig. 5.4.**

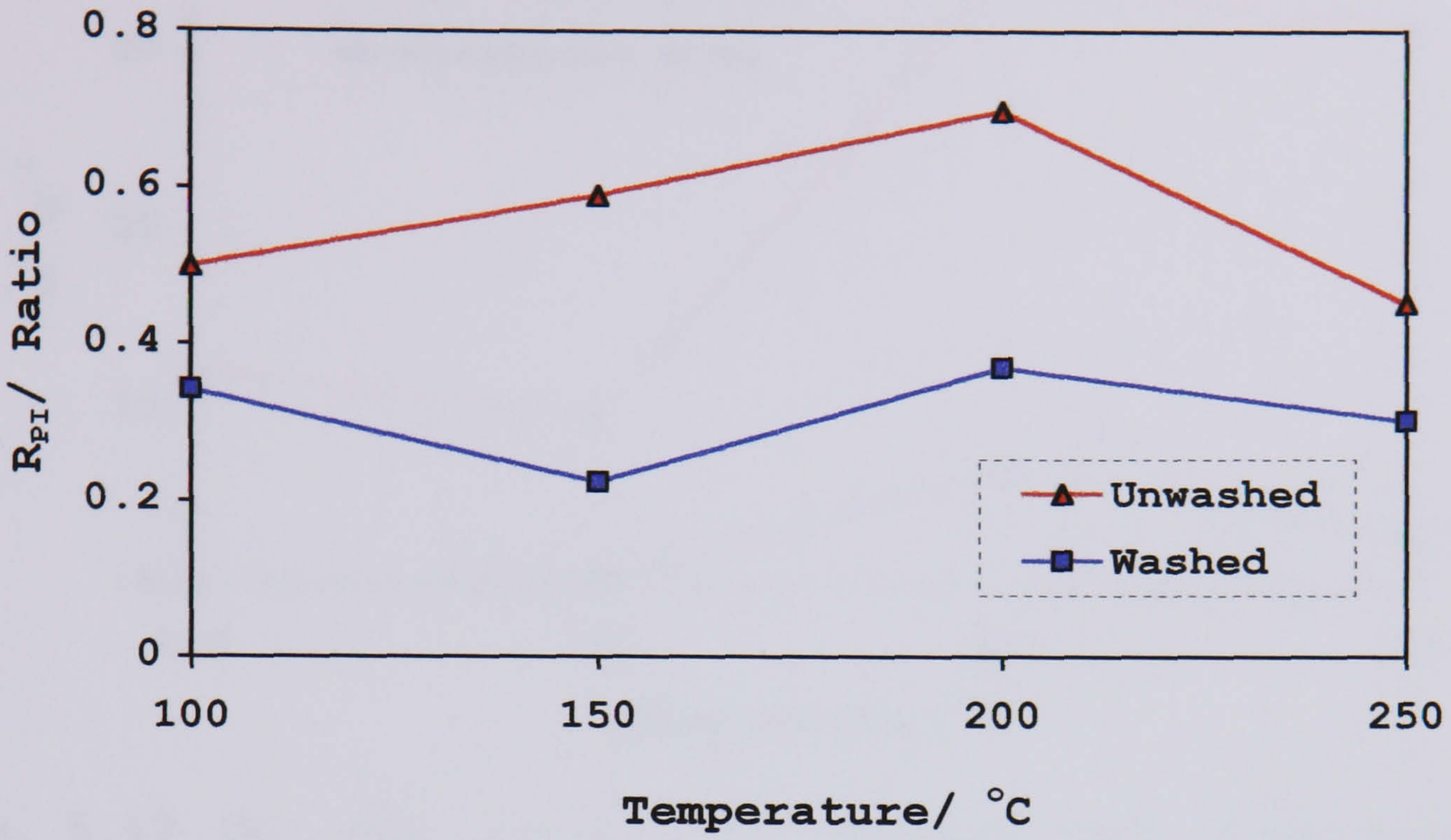


Fig. 5.16 The effect of varying the treatment temperature on the degree of pillaring in the clay (see **table 5.16**).

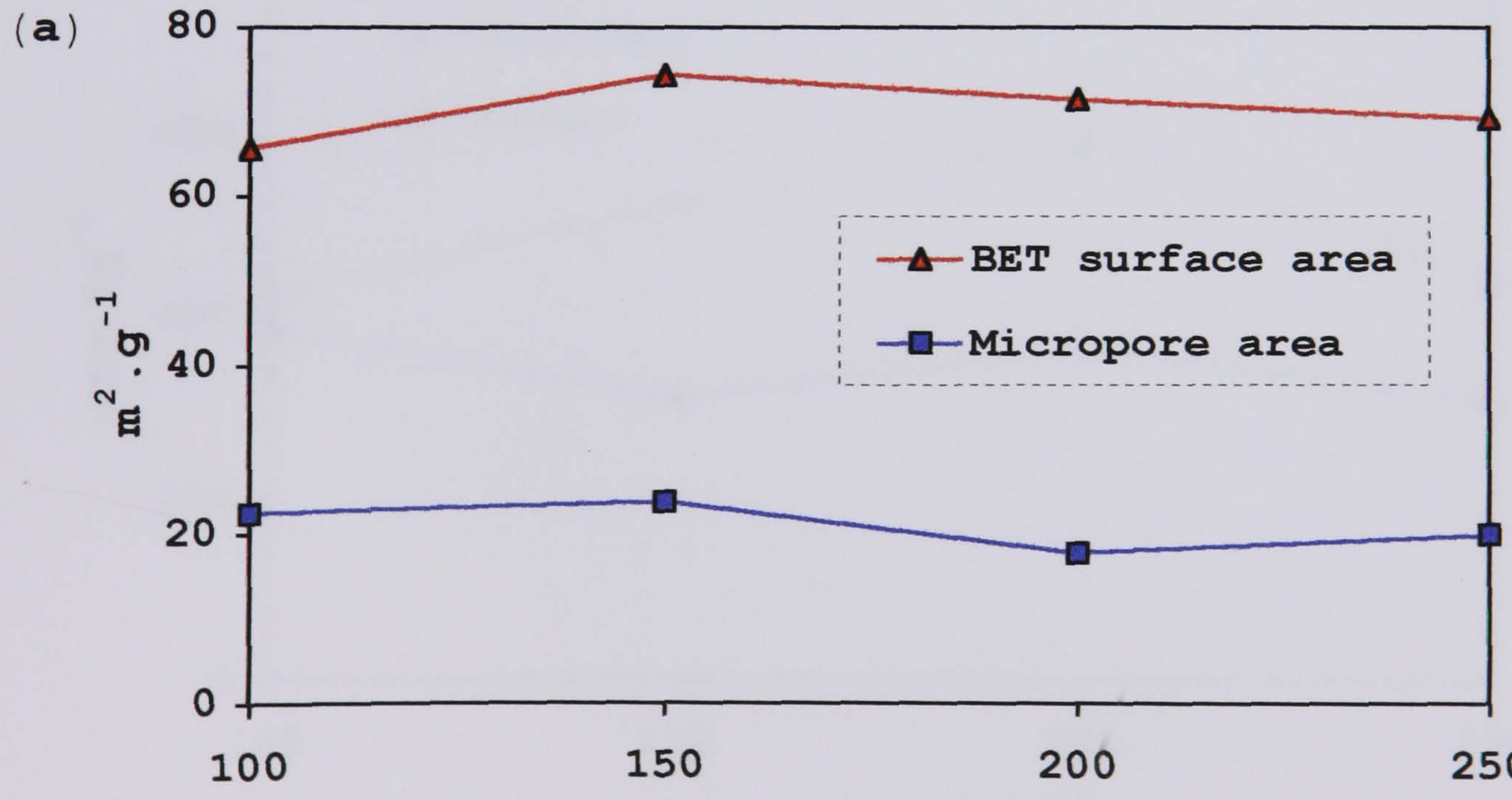


Fig. 5.17 (**a**) The effect of varying the treatment temperature on the BET surface area and micropore area of the washed clay (see **table 5.17**).

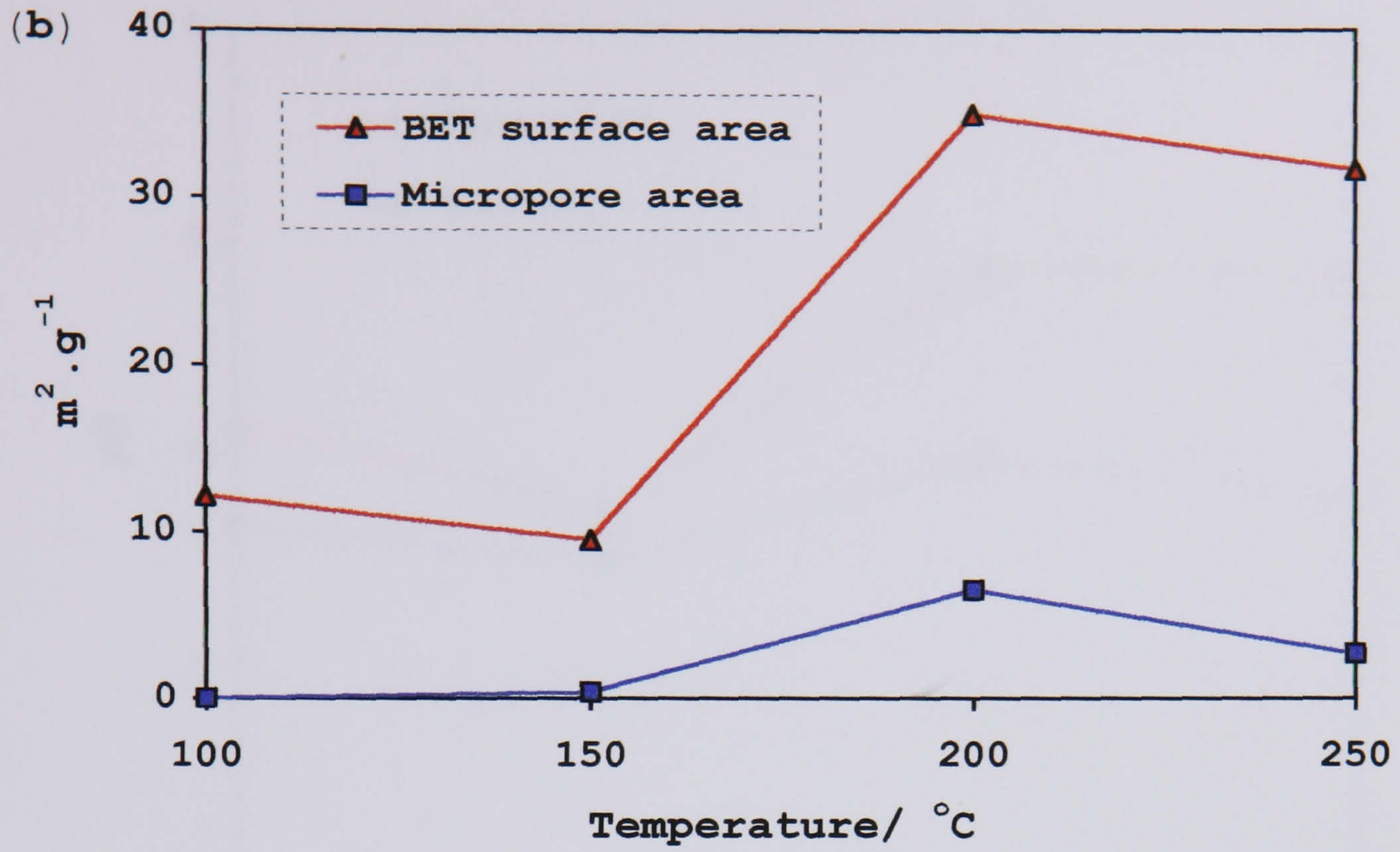


Fig. 5.17 (**b**) The effect of varying the treatment temperature on the BET surface area and micropore area of the unwashed clay (see **table 5.17**).

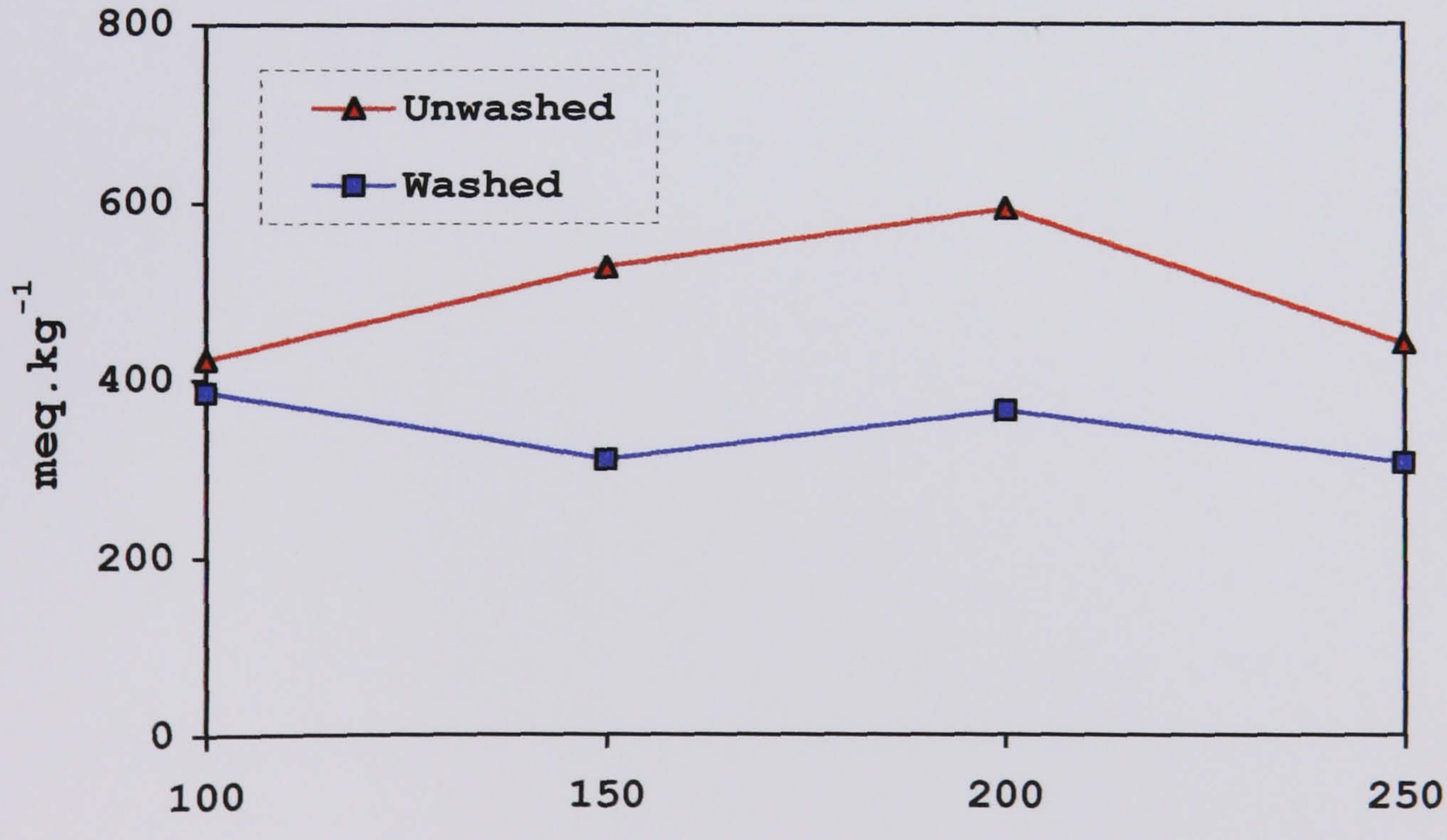


Fig. 5.18 The effect of varying the treatment temperature on the C.E.C. of the clay (see **table 5.18**).

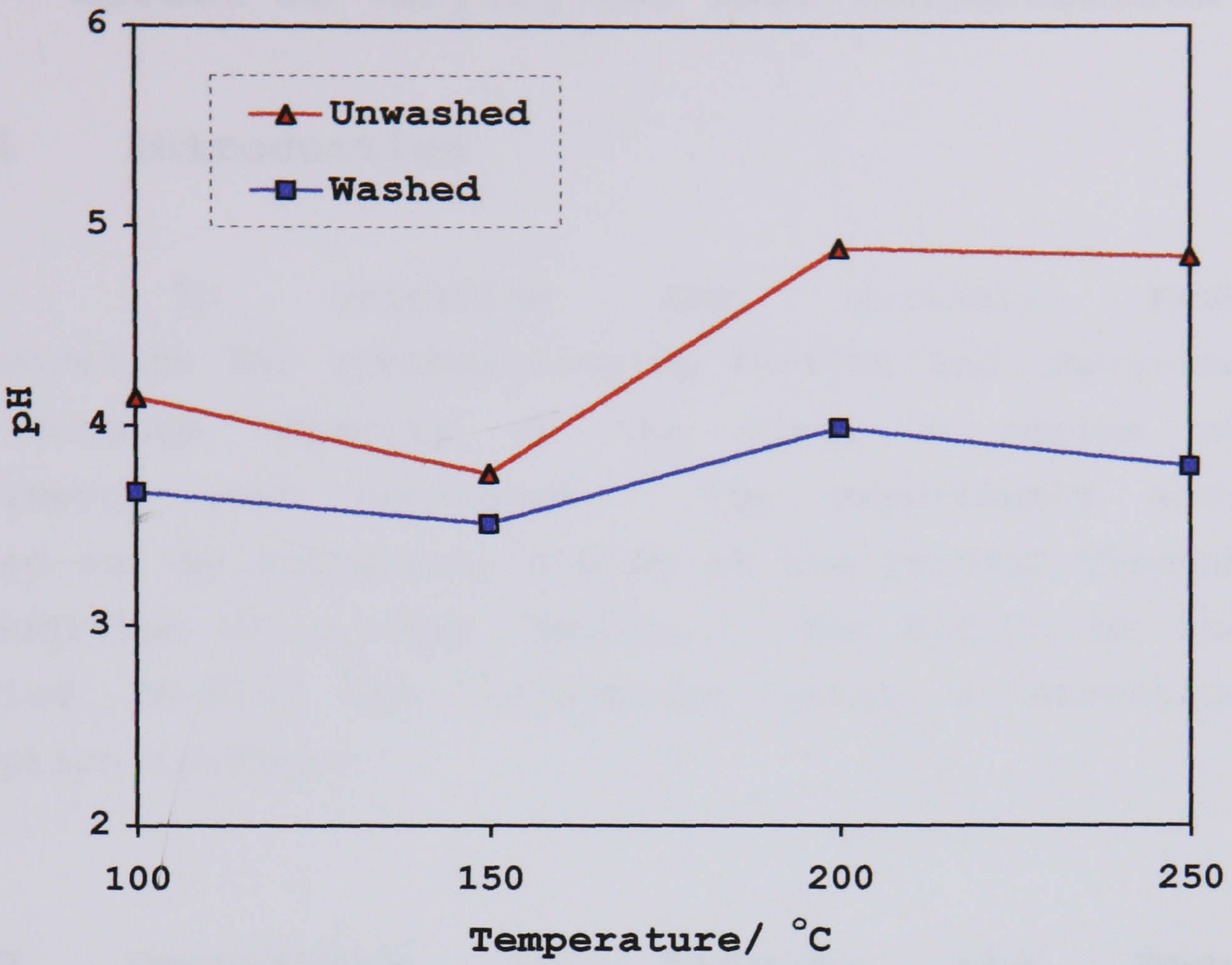


Fig. 5.19 The Effect of varying the treatment temperature on the pH of the thermally-treated clay (see **table 5.15**).

5.7 Effect of Varying the Base Concentration

5.7.1 Introduction

To determine the suitable base concentration for synthesising an Fe-PILC and improving the exchange capacity of the clay, a series of experiments were conducted. The experiments were carried out by increasing the pH of the Fe-PILC through the addition of a base ($NaHCO_3$). The C.E.C. of the modified Fe-PILC was determined using a strontium adsorption isotherm.

5.7.2 Experiment in Varying the Base Concentration

For the purpose of this study, samples of Fe-PILC were synthesised using the modified synthesis method of Fe-PILC (see **section 5.2**). For each set of experiments the parameters in the synthesis were kept constant, except after the raw clay suspension was contacted with the pillaring solution for 2 hours and a solution of $NaHCO_3$ was then added to the mixture. 50 ml of the solution of $NaHCO_3$ with concentrations ranging from 0.003 to 1 molar was used to adjust the pH of the mixture. $NaHCO_3$ was used instead of NaOH because experiments performed previously using NaOH had shown that NaOH caused rapid precipitation of iron hydroxide onto the clay and as a result the pillaring was unsuccessful. In addition, $NaHCO_3$ is not as expensive as NaOH. During the reaction, bubbles of CO_2 gas were observed. This indicates that the excess amount of acid of the clay was being neutralised by the base,

thus lowering the pH of the final product. The outline of the synthesis and experimental conditions is summarised in tables (see **tables 5.19, 5.20** and **5.21**).

5.7.3 Results and Discussion of Preliminary Characterisations

The results of XRD, nitrogen adsorption, strontium adsorption and tests for leaching of iron are discussed and general conclusions drawn from the overall results are presented in the following sections.

5.7.3.1 Results and Discussion of XRD Analysis

The overall trend of the results (see **tables 5.22, 5.23** and **5.24, fig. 5.20**) of the samples, prepared with the same synthesis ratios but increasing the base concentration, shows a general decrease in the degree of pillaring in the clay. In contrast the results of samples, (batch D1: F-B16NW, 18 and 19, see **fig. 5.20**) which were prepared from a different set of synthesis ratios show that it would be possible to increase the R_{PI} of the Fe-PILC by preparing the clay using the optimum synthesis ratios and at the same time keeping the base concentration high. This effect may be due to pillaring the clay with different types of polymeric ferric ions which may have formed by varying the synthesis ratios.

5.7.3.2 Results and Discussion of Nitrogen Adsorption Analysis

The results (see **table 5.25, fig. 5.21 (a)**) of the Fe-PILC samples (batch A1: F-B1 to F-B7) dried at 50 °C are also similar to those of sample F-RM (see **table 5.3**). These results suggest that varying the base concentration of the clay led to a slight change in the porous structure of the Fe-PILC samples.

The results of samples (batch B1, C1 and D1) that were prepared from the raw, washed Fe-PILC and the raw, unwashed Fe-PILC are shown in **fig. 5.21 (b)**, **(c)** and **(d)**. The results (see **fig. 5.21 (b)**, **(c)** and **(d)**, and **tables 5.26** and **5.27**) suggest that a moderate increase in the base concentration in the Fe-PILC led to a rise in the BET and micropore areas. However a high level of increase in the base of the clay resulted in a decrease in the BET and micropore area. The overall results of XRD analysis also support this by showing a lower degree of pillaring in the Fe-PILC samples with a higher base concentration of the clay (see **fig. 5.20**). These results also suggest possible structural contractions in the porous structure of the clay which may have occurred during the degassing process of the nitrogen analysis.

5.7.3.3 Results and Discussion of Strontium Adsorption Analysis

The results obtained from batch tests are summarised in **tables 5.28, 5.29** and **5.30**. The results (see **fig. 5.22**) show a general rising trend in the cation exchange capacity (C.E.C.) of the Fe-PILC with an increase in the base concentration. An increase in the base concentration of the Fe-PILC resulted in a rise of OH^- concentration and pH of the clay (see **fig. 5.23**). Hence there was a decrease in the number of protons, which were in competition with the other cations for cationic adsorption sites. This resulted in an enhancement of the C.E.C. of the clay.

When the C.E.C. values of each set of the Fe-PILC were compared with those of the starting material, raw Montmorillonite (664.3 meq/kg), general increases in the C.E.C. values of certain sets of the samples were observed (see **fig. 5.22**). The overall results show that the Fe-PILC sample F–B15NW of batch C1 prepared from the raw, unwashed Fe-PILC and with a base concentration of 0.0556 molar, has the highest C.E.C. (1267.9 meq/kg).

5.7.4 Conclusions

The general conclusion drawn from the results of XRD and nitrogen adsorption analysis is that the effect of increasing the base concentration of the washed or unwashed Fe-PILC can lead to the formation of a thermally less stable structured clay. Although the results suggest that the modified Fe-PILC samples were

thermally less stable than the non-modified Fe-PILC, it did not appear to hinder the ability of the modified Fe-PILC to act as a cation exchanger. This is seen from the results of the contact tests. From the results of strontium adsorption analysis, it can also be concluded that the C.E.C. of the Fe-PILC can be enhanced by increasing the base concentration of the clay in the given range. The results also show that the modified Fe-PILC can possess a C.E.C. that is higher than that of the raw Montmorillonite.

Table 5.19 The synthesis conditions for varying the base concentration (of the washed clay samples prepared with R_F of 1.25 mmol/g and R_{OF} of 2).

Sample Name	50 ml of $NaHCO_3$ /Molar	NaOH /Molar	$Fe(NO_3)_3$ /Molar
F-B1	0.00	0.10	0.05
F-B2	0.003	0.10	0.05
F-B3	0.060	0.10	0.05
F-B4	0.130	0.10	0.05
F-B5	0.250	0.10	0.05
F-B6	0.500	0.10	0.05
F-B7	1.000	0.10	0.05

The above samples were dried at 50 °C before thermal treatment.

Table 5.20 The synthesis conditions for varying the base concentration (of the samples prepared with $\mathbf{R_F}$ of 1.25 mmol/g and $\mathbf{R_{OF}}$ of 2).

Sample Name	Concentration of 50 ml of $[NaHCO_3]$ /Molar	Washed	NaOH /Molar	$Fe(NO_3)_3$ /Molar
F-B8	0.000	yes	0.10	0.05
F-B9	0.130	yes	0.10	0.05
F-B10	0.250	yes	0.10	0.05
F-B11	0.500	yes	0.10	0.05
F-B12NW	0.000	no	0.10	0.05
F-B13NW	0.130	no	0.10	0.05
F-B14NW	0.250	no	0.10	0.05
F-B15NW	0.500	no	0.10	0.05

The above samples were air-dried 25 °C before thermal treatment. **NW** represents the unwashed sample.

Table 5.21 The synthesis conditions for varying the base concentration (of the unwashed samples prepared with $\mathbf{R_F}$ of 1.3 mmol/g and $\mathbf{R_{OF}}$ of 1).

Sample Name	Concentration of 50 ml of $[NaHCO_3]$ /Molar	Washed	NaOH /Molar	$Fe(NO_3)_3$ /Molar
F-B16NW	0.000	no	0.052	0.052
F-B17NW	0.130	no	0.052	0.052
F-B18NW	0.250	no	0.052	0.052
F-B19NW	0.500	no	0.052	0.052

The above samples were air-dried at 25 °C before thermal treatment. **NW** represents the unwashed sample.

In **tables 5.22** and **5.23**, $^{conc.}$ is the concentration of $NaHCO_3$ in the pillaring mixture. **LA** and **HA** represent the low and high X-ray angles. **%RPI** is the estimated relative peak intensity in %. R_{PI} is the estimated relative peak intensity ratio, (**%RPI** of **LA**)/(**%RPI** of **HA**) (see **fig. 5.4**). **NW** represents the unwashed sample.

Table 5.22 A summary of results of XRD analysis.

Sample Name	$NaHCO_3{}^{conc.}$ /Molar	d001 /Å		%RPI		R_{PI} /Ratio
		LA	HA	LA	HA	
F-B1	0.00	25.7	12.4	90.1	100	0.901
F-B2	0.00333	23.9	15.6	53.0	100	0.530
F-B3	0.00667	24.4	15.5	73.3	100	0.733
F-B4	0.0144	24.4	15.3	61.0	100	0.610
F-B5	0.0278	26.3	13.8	77.6	100	0.776
F-B6	0.0556	25.2	15.4	63.1	100	0.631
F-B7	0.111	-	15.9	0	100	0

Table 5.23 A summary of results of XRD analysis.

Sample Name	$NaHCO_3{}^{conc.}$ /Molar	d001 /Å		%RPI		R_{PI} /Ratio
		LA	HA	LA	HA	
F-B8	0.00	23.4	12.4	37.0	100	0.370
F-B9	0.0144	-	15.2	0	100	0
F-B10	0.0278	22.1	11.6	1.4	100	0.014
F-B11	0.0556	21.9	11.5	0.9	100	0.009
F-B12NW	0.00	23.7	12.4	69.8	100	0.698
F-B13NW	0.0144	24.7	14.0	43.6	100	0.436
F-B14NW	0.0278	24.1	12.8	29.4	100	0.294
F-B15NW	0.0556	24.0	12.5	36.2	100	0.362

Table 5.24 A summary of results of XRD analysis.

Sample Name	$NaHCO_3$ conc. /Molar	d001 /Å		%RPI		R_{PI} /Ratio
		LA	HA	LA	HA	
F-B16NW	0.00	23.5	12.1	25.0	100	0.250
F-B17NW	0.0144	-	-	-	-	-
F-B18NW	0.0278	21.7	11.9	34.4	100	0.340
F-B19NW	0.0556	25.8	11.8	51.8	100	0.518

LA and **HA** represent the low and high X-ray angles. conc. is the concentration of $NaHCO_3$ in the pillaring mixture. **%RPI** is the estimated relative peak intensity in %. R_{PI} is the estimated relative peak intensity ratio (**%RPI** of **LA**)/(**%RPI** of **HA**) (see **fig. 5.4**). **NW** represents the unwashed sample.

Table 5.25 A summary of results of nitrogen adsorption analysis.

Sample Name	$NaHCO_3$ conc. /Molar	BET Surface Area /$m^2.g^{-1}$	Micr. Area /$m^2.g^{-1}$	Micro. Volume /$cc.g^{-1}$	Average Pore Diameter /Å
F-B1	0.00	82.2	9.0	0.00348	57.6
F-B2	0.00333	84.9	19.0	0.00843	57.7
F-B3	0.00667	77.2	11.1	0.00457	59.8
F-B4	0.0144	77.9	9.3	0.00371	57.3
F-B5	0.0278	66.5	6.4	0.00239	64.3
F-B6	0.0556	71.6	1.0	-	62.1
F-B7	0.111	77.9	3.5	56.3	56.3

Micro. represents micropore. conc. is the concentration of $NaHCO_3$ in the pillaring mixture.

Table 5.26 A summary of results of nitrogen adsorption analysis.

Sample Name	$NaHCO_3^{conc.}$ /Molar	BET Surface Area /$m^2.g^{-1}$	Micro. Area /$m^2.g^{-1}$	Micro. Volume /$cc.g^{-1}$	Average Pore Diameter /Å
F-B8	0.00	71.4	17.7	0.00796	60.6
F-B9	0.0144	80.0	11.1	0.00461	54.9
F-B10	0.0278	55.1	2.1	0.000385	58.6
F-B11	0.0556	43.3	-	-	72.6
F-B12NW	0.00	35.0	6.49	0.00281	57.7
F-B13NW	0.0144	74.3	23.8	0.0110	64.3
F-B14NW	0.0278	20.7	2.73	0.00109	112.1
F-B15NW	0.0556	8.2	0.428	0.000068	143.0

Micro. represents micropore. **NW** represents the unwashed sample. $^{conc.}$ is the concentration of $NaHCO_3$ in the pillaring mixture.

Table 5.27 A summary of results of nitrogen adsorption analysis.

Sample Name	$NaHCO_3^{conc.}$ /Molar	BET Surface Area /$m^2.g^{-1}$	Micro. Area /$m^2.g^{-1}$	Micro. Volume /$cc.g^{-1}$	Average Pore Diameter /Å
F-B16NW	0.00	21.2	-	-	72.9
F-B17NW	0.0144	31.3	6.2	0.00268	70.5
F-B18NW	0.0278	43.8	3.8	0.00138	68.2
F-B19NW	0.0556	19.9	4.0	0.00174	103.8

Micro. represents micropore. **NW** represents the unwashed sample. $^{conc.}$ is the concentration of $NaHCO_3$ in the pillaring mixture.

Table 5.28 A summary of results of batch contact tests.

Sample Name	$NaHCO_3$ conc. /Molar	C.E.C. /meq.kg^{-1}	R^2
F-B1	0.00	411.5	0.998
F-B2	0.00333	458.8	0.983
F-B3	0.00667	459.3	0.971
F-B4	0.0144	529.7	0.990
F-B5	0.0278	525.1	0.999
F-B6	0.0556	651.5	0.999
F-B7	0.111	-	-

R^2 is the square of correlation coefficient. **C.E.C.** is the cation exchange capacity (milli-equivalent per kg). **conc.** is the concentration of $NaHCO_3$ in the pillaring mixture.

Table 5.29 A summary of results of batch contact tests.

Sample Name	$NaHCO_3$ conc. /Molar	C.E.C. /meq.kg^{-1}	R^2
F-B8	0.00	365.4	0.995
F-B9	0.0144	733.7	0.996
F-B10	0.0278	783.9	0.999
F-B11	0.0556	-	-
F-B12NW	0.00	592.8	0.991
F-B13NW	0.0144	748.1	0.993
F-B14NW	0.0278	835.1	0.995
F-B15NW	0.0556	1267.9	0.982

NW represents the unwashed sample. **conc.** is the concentration of $NaHCO_3$ in the pillaring mixture. **R^2** is the square of correlation coefficient. **C.E.C.** is the cation exchange capacity (milli-equivalent per kg).

Table 5.30 A summary of results of batch contact tests.

Sample Name	$NaHCO_3$ conc. /Molar	C.E.C. /meq.kg^{-1}	R^2
F-B16NW	0.00	394.2	0.980
F-B17NW	0.0144	528.6	0.998
F-B18NW	0.0278	696.1	0.984
F-B19NW	0.0556	890.6	0.994

NW represents the unwashed sample. R^2 is the square of correlation coefficient. **C.E.C.** is the cation exchange capacity (in milli-equivalent per kg). Conc. is the concentration of $NaHCO_3$ in the pillaring mixture.

In **fig. 5.20, batch A1** contains samples F-B1 to 7 (see **table 5.19**); **batch B1** contains samples F-B8 to 11 (see **table 5.20**); **batch C1** contains samples F-B12NW to 15 (see **table 5.20**) and **batch D1** contains samples F-B16NW to 19 (see **table 5.21**). **Batch A1, B1, C1** were prepared with the same Fe/clay (1.25 mmol/g) & OH/Fe (2) ratios whereas **batch D1** was prepared with a different set of Fe/clay (1.30 mmol/g) and OH/Fe (1) ratios.

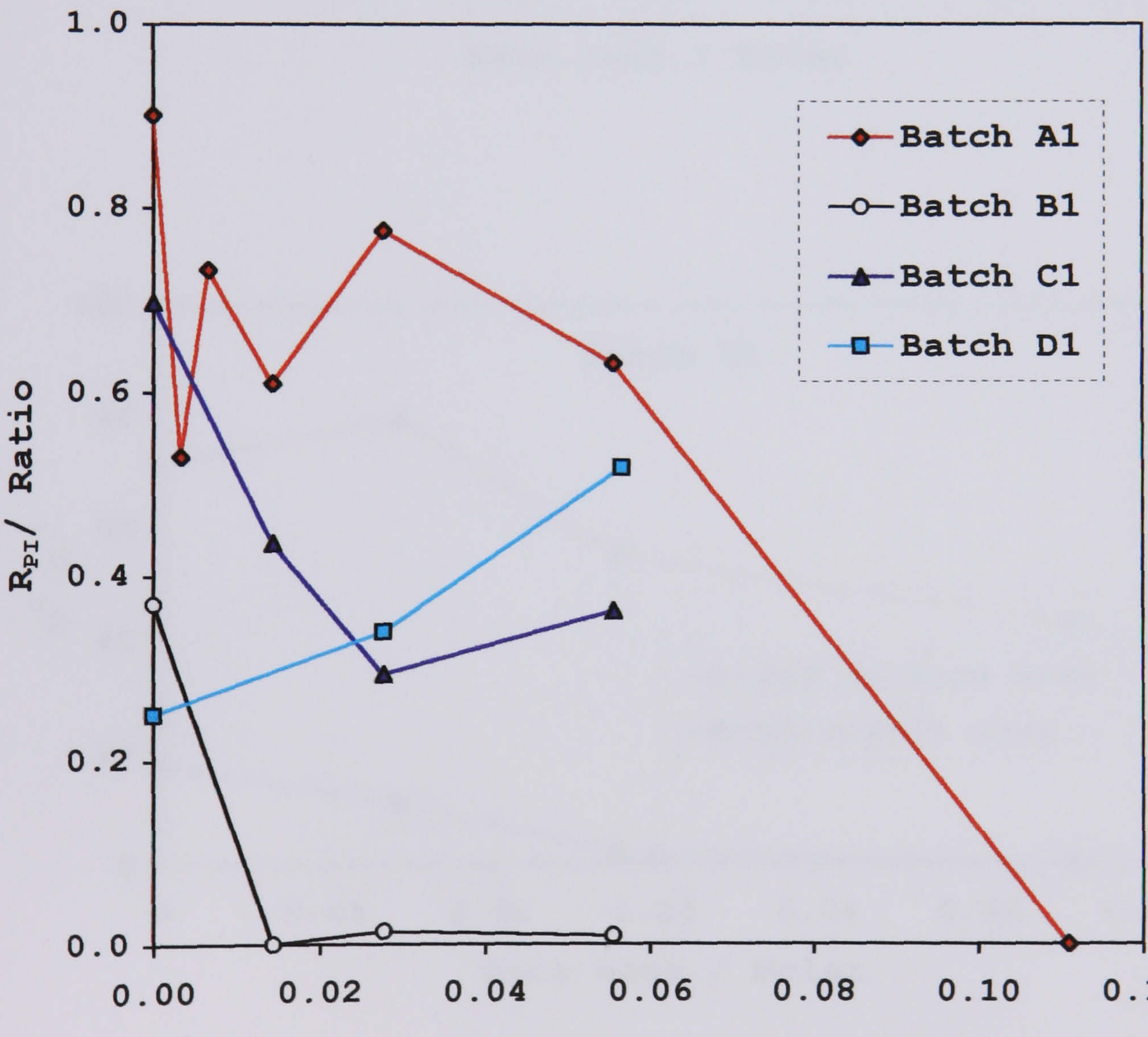
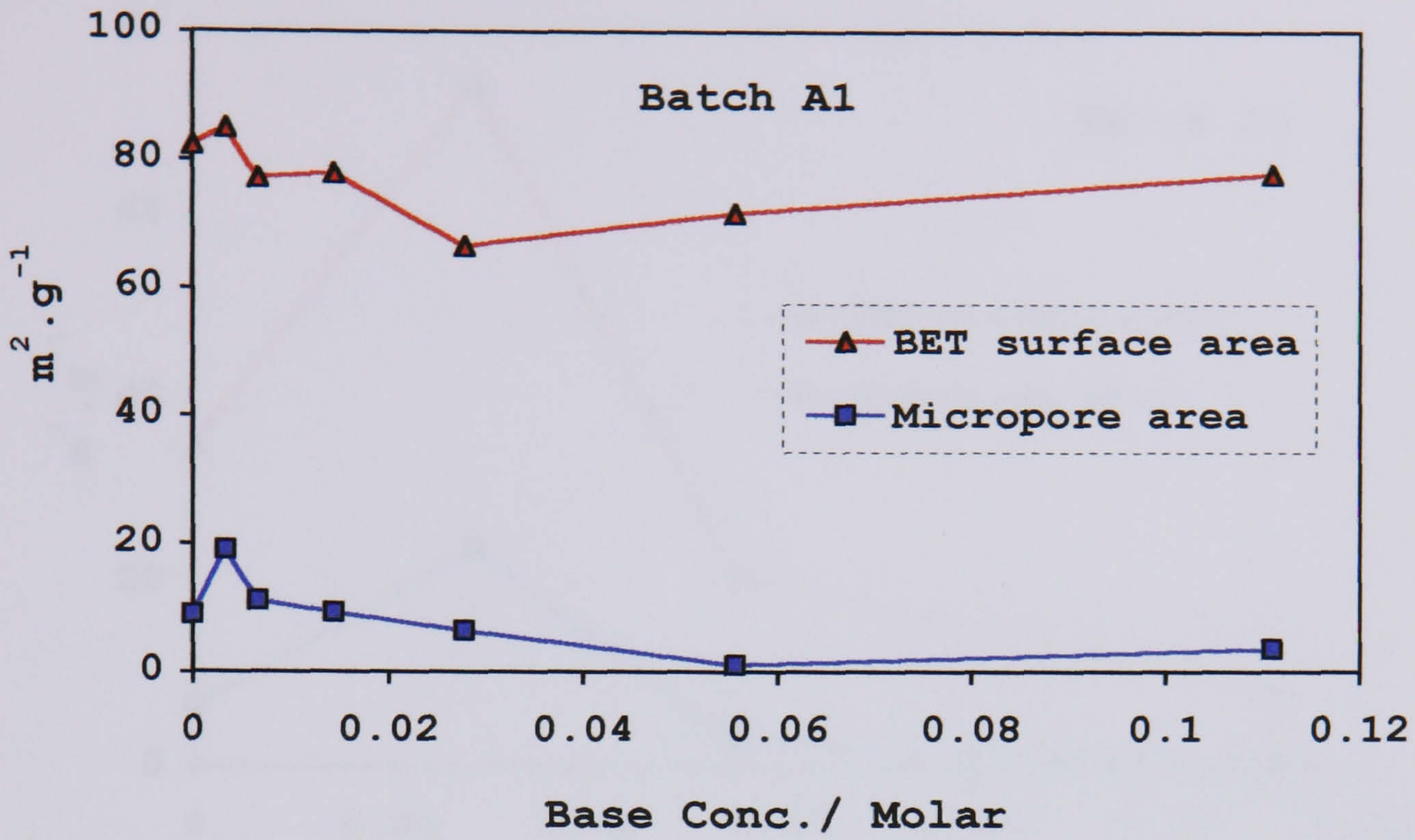


Fig. 5.20 The effect of varying the base concentration on the degree of pillaring in the clay.

(a)



(b)

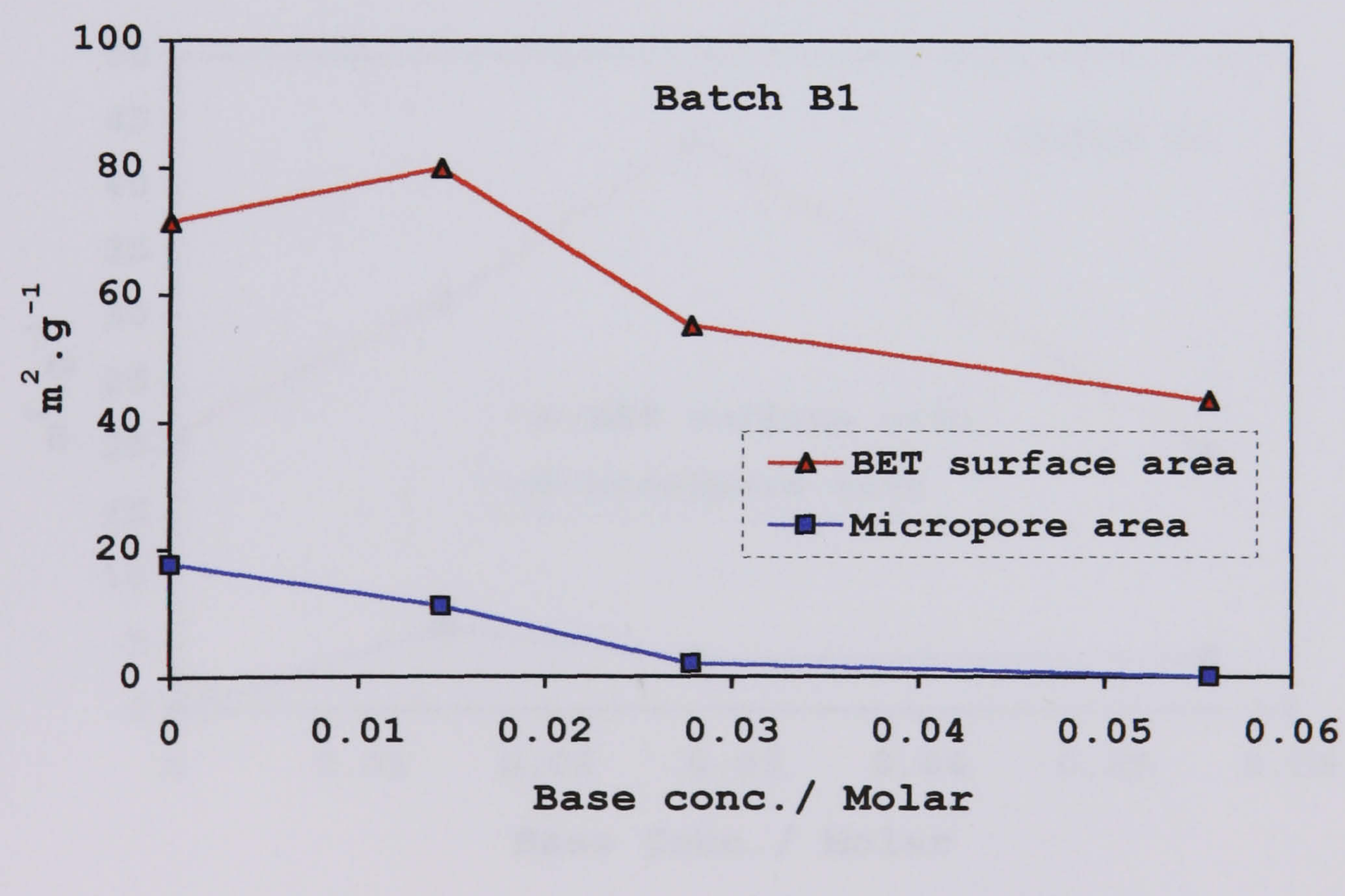
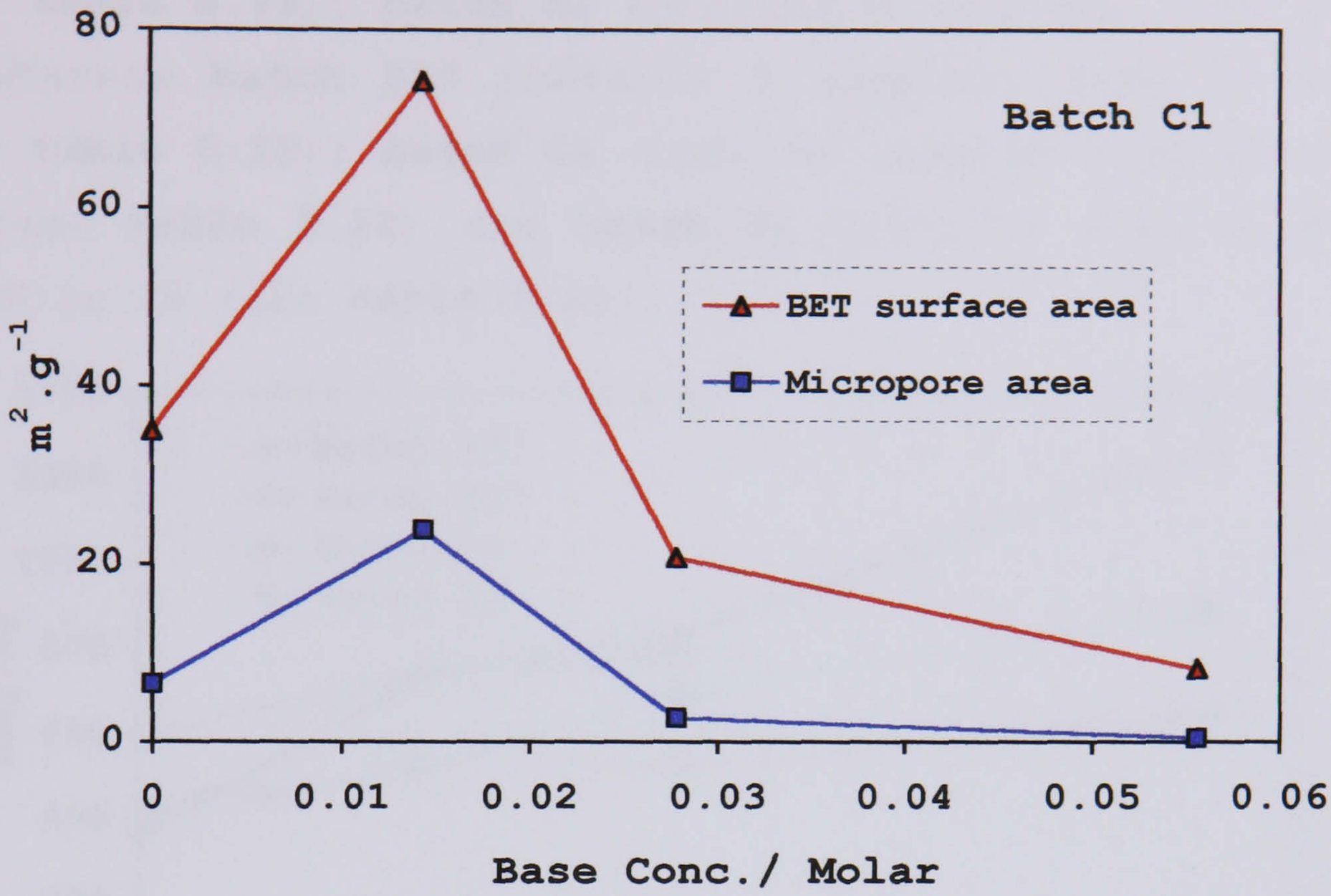


Fig. 5.21 The effect of varying the base concentration on the BET surface area and micropore area of the clay ((**a**) **batch A1** dried at 50 °C and (**b**) **batch B1** air-dried at 25 °C before the thermal treatment).

(C)



(d)

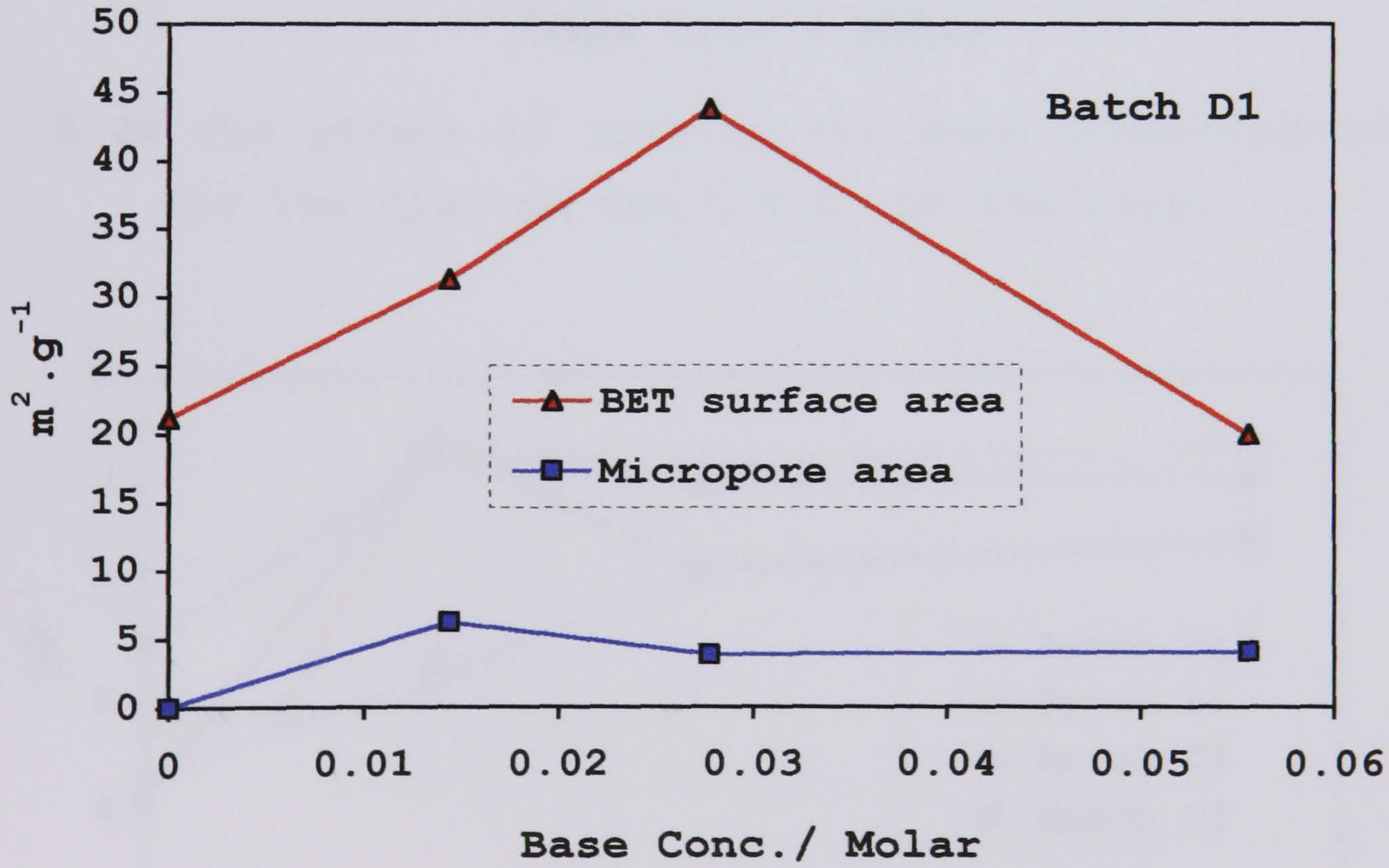


Fig. 5.21 The effect of varying the base concentration on the BET surface area and micropore area of the unwashed samples ((**c**) **batch C1** and (**d**) **batch D1** dried at 25 °C before thermal treatment).

In **fig. 5.22** & **5.23, A1"** contains samples F-B1 to 6 (see **table 5.19**); **batch B1** contains 4 samples, F-B8 to 11 whereas **batch B1"** contains 3 samples, F-B8 to 10 (see **table 5.20**); **batch C1** contains samples F-B12NW to 15 (see **table 5.20**) and **batch D1** contains samples F-B16NW to 19 (see **table 5.21**).

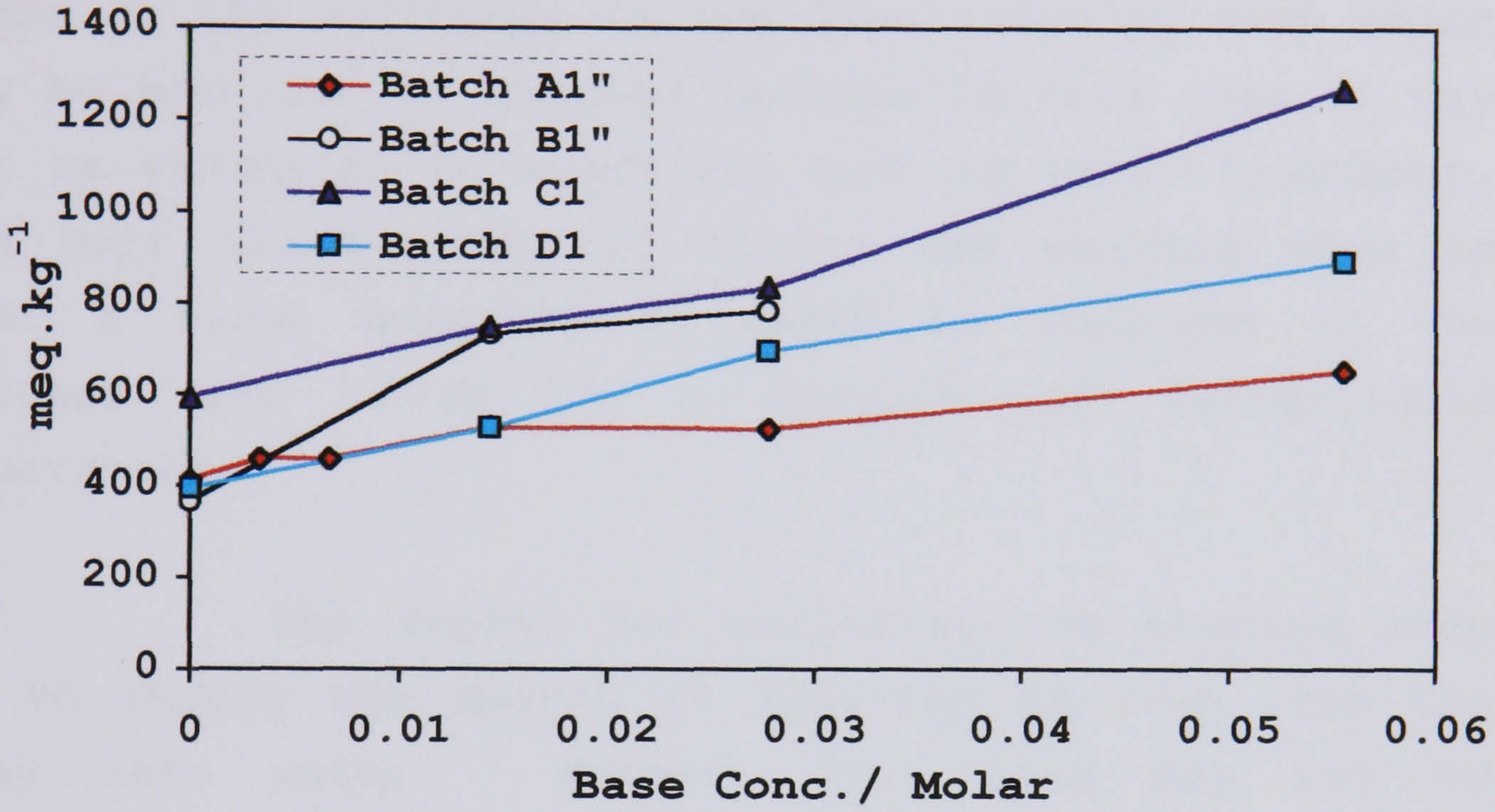


Fig. 5.22 The effect of varying the base concentration of the clay on the C.E.C. of the clay.

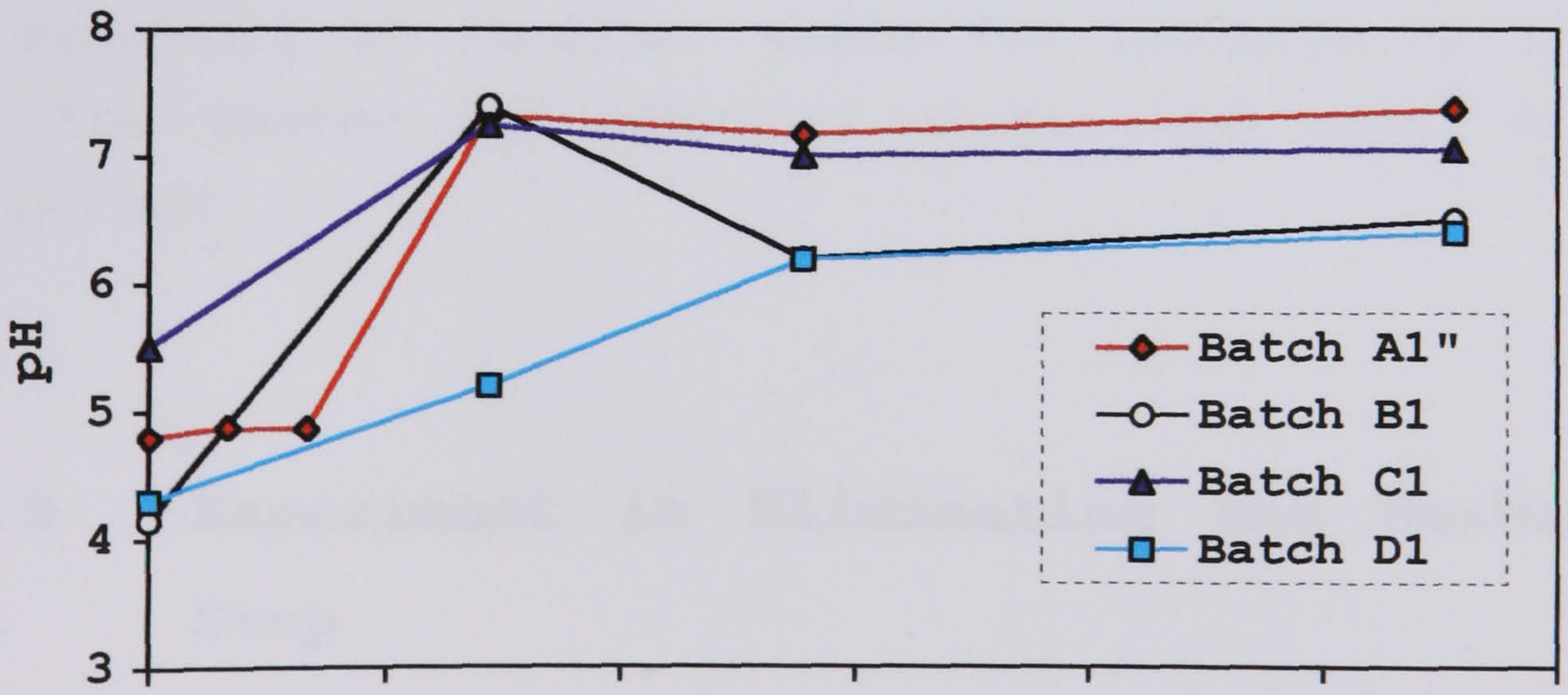


Fig. 5.23 The effect of varying the base concentration of the clay on the pH of the thermally-treated clay.

5.8 Effect of Eliminating the Washing Step

5.8.1 Introduction

This work has concentrated on reducing the complexity of the pillaring process. One of the many steps in the synthesis is the final washing step which may be modified or omitted because in this case it may not be essential to a process such as water treatment. The main disadvantage of having the washing step is that a large quantity of water is employed in the process and there is a problem of solid-liquid separation.

The reason for including the washing step is to reduce the amount of leaching of iron from the clay into water. However this step may not be necessary because this leaching may be lessened by the thermal treatment. The treatment may convert most of the iron hydroxide into the stable iron oxide. In order to justify the omission of the washing step in the synthesis of Fe-PILC, tests for leaching of iron from the washed and unwashed clays into water were carried out.

5.8.2 Experiment in Eliminating the Washing Step

To investigate the possibility of eliminating the washing step in the synthesis of Fe-PILC, two sets of Fe-PILC samples were prepared under identical synthesis conditions (see **section 5.2**) and

with the same synthesis ratios. The synthesis ratios for all the samples were 1.25 mmol/g of Fe/clay (R_F), and 2 of OH/Fe (R_{OF}). The samples were air-dried at room temperature for 24 hours and then thermally treated in a programmable tube furnace. One set of clay samples was washed and the other set was not washed. The effects of washing and not washing Fe-PILC on the structure and the physical properties of the clay were also characterised using X-ray diffraction analysis, nitrogen adsorption analysis and the strontium adsorption isotherm.

5.8.3 Experiment to Test for Leaching of Iron

The various Fe-PILC samples were also tested for the possibility of leaching of iron into the water. These tests were conducted on the solutions which had been contacted with the Fe-PILC samples during the batch tests. The iron concentration in the solutions was measured in parts-per-million (ppm) using atomic absorption spectrometry (A.A.S.).

The Fe-PILC samples, F-B1 (see **table 5.19** for sample descriptions) prepared from raw, washed Fe-PILC, and F-B12NW (see **table 5.20** for sample description), prepared from raw, unwashed Fe-PILC were tested for leaching of iron. The measurements were taken from the sample solutions with the instrument set at a wavelength of 248.3 nm.

5.8.4 Results and Discussion of Preliminary Characterisations

The results of XRD, nitrogen adsorption, strontium adsorption analysis and the test for leaching of Iron are discussed, and general conclusions drawn from the overall results are presented in the following sections.

5.8.4.1 Results and Discussion of XRD Analysis

In general, the results (see **fig. 5.24** (**a**) and (**b**)) show that the R_{PI} values of the samples prepared by eliminating the washing step are higher than those prepared without eliminating the step.

5.8.4.2 Results and Discussion of Nitrogen Adsorption Analysis

The results (see **fig. 5.25** and **5.26**) show that, in general, the washed samples have a higher BET surface area and micropore area than those of the unwashed samples. These results, together with those of the XRD analysis discussed in an earlier section, suggest that the pillared structure of the raw, unwashed Fe-PILC samples was thermally less stable than the washed samples. The structure of the unwashed Fe-PILC may have collapsed during the degassing process of nitrogen adsorption analysis.

5.8.4.3 Results and Discussion of Strontium Adsorption Analysis

The results (see **fig. 5.27**) suggest that an Fe-PILC prepared by eliminating the washing step resulted in an increase in the C.E.C.. The most likely cause of this increase was that the overall pH values of the thermally-treated unwashed samples were higher than those of the washed ones (see **fig. 5.28**). Washing the raw Fe-PILC resulted in a dilution in the base concentration of the clay. Hence the raw, unwashed samples had a higher base concentration and pH value.

5.8.4.4 Results and Discussion of the Test for Leaching of Iron

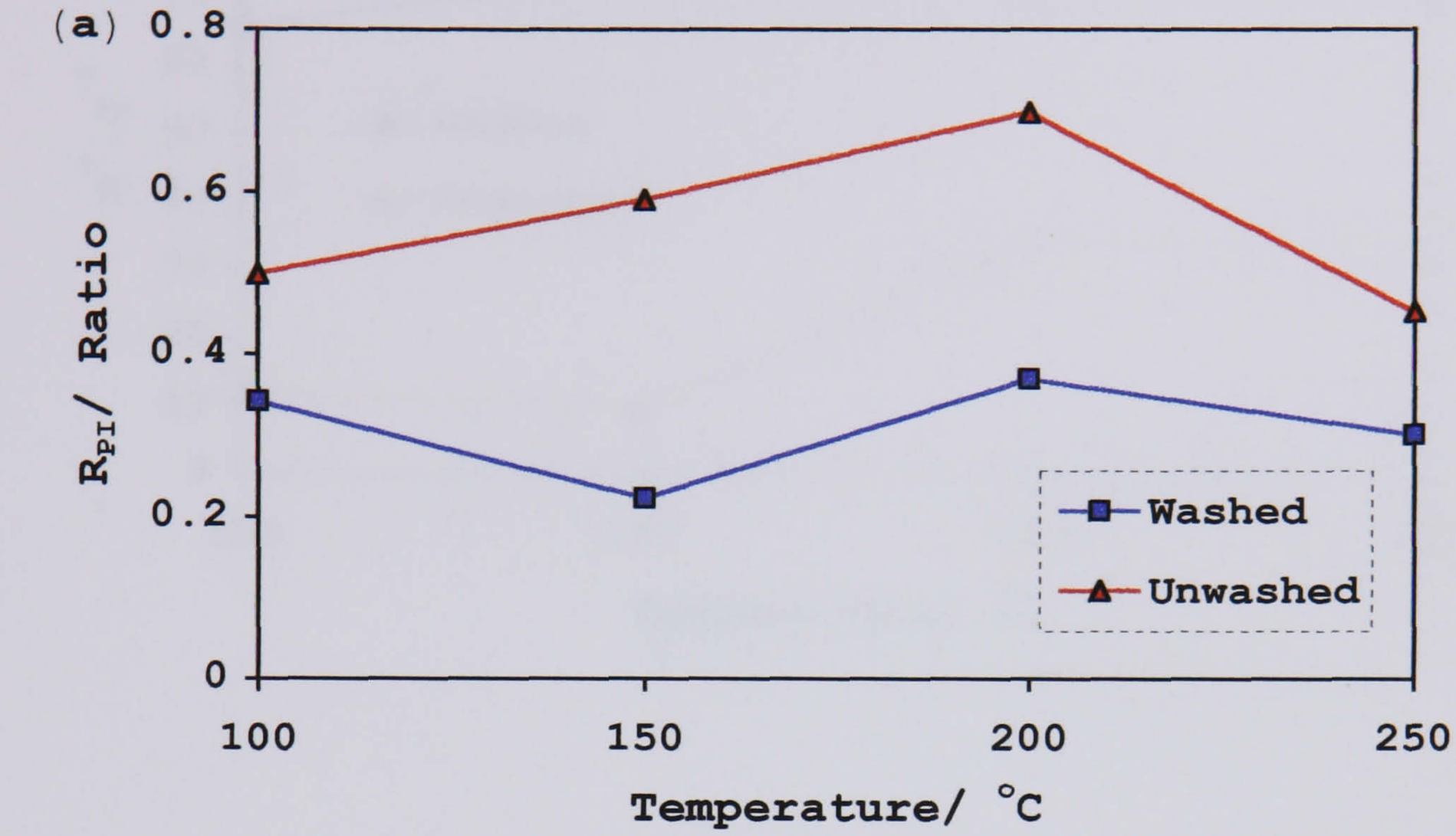
Fe-PILC samples, F-B1 and F-B12NW prepared from both the raw washed and unwashed Fe-PILC, were tested for the leaching of iron from the clay into the contacted strontium chloride solution during the batch test. The iron concentration in solution measured using atomic absorption spectrometry analysis (A.A.S.) shows zero concentration of iron in the solution contacted with the washed sample. These results show that there was no leaching of iron from the washed clay sample into the water, whereas for the measurements taken from solution contacted with the unwashed clay sample, a trace of iron was detected in the solution using A.A.S. analysis. The concentration of iron in solution was only 0.09 ppm and thus negligible.

5.8.5 Conclusions

Conclusive evidence from XRD analysis shows that an Fe-PILC can be prepared by eliminating the washing process from the synthesis procedures of the Fe-PILC. The results of both analyses (XRD and nitrogen adsorption) appear to suggest that eliminating the washing step resulted in a reduction in the thermal stability of the pillared structure of the clay. More importantly, eliminating the washing process resulted in an increase in the C.E.C. of the Fe-PILC.

The results of the test for iron leaching from the unwashed clay into water are encouraging because these results indicate that leaching of iron from the unwashed clay into water can be minimised by thermal treatment process.

For the definition of the estimated relative peak intensity, R_{PI}, in **fig. 5.24** (**a**) & (**b**) see **fig. 5.4.**



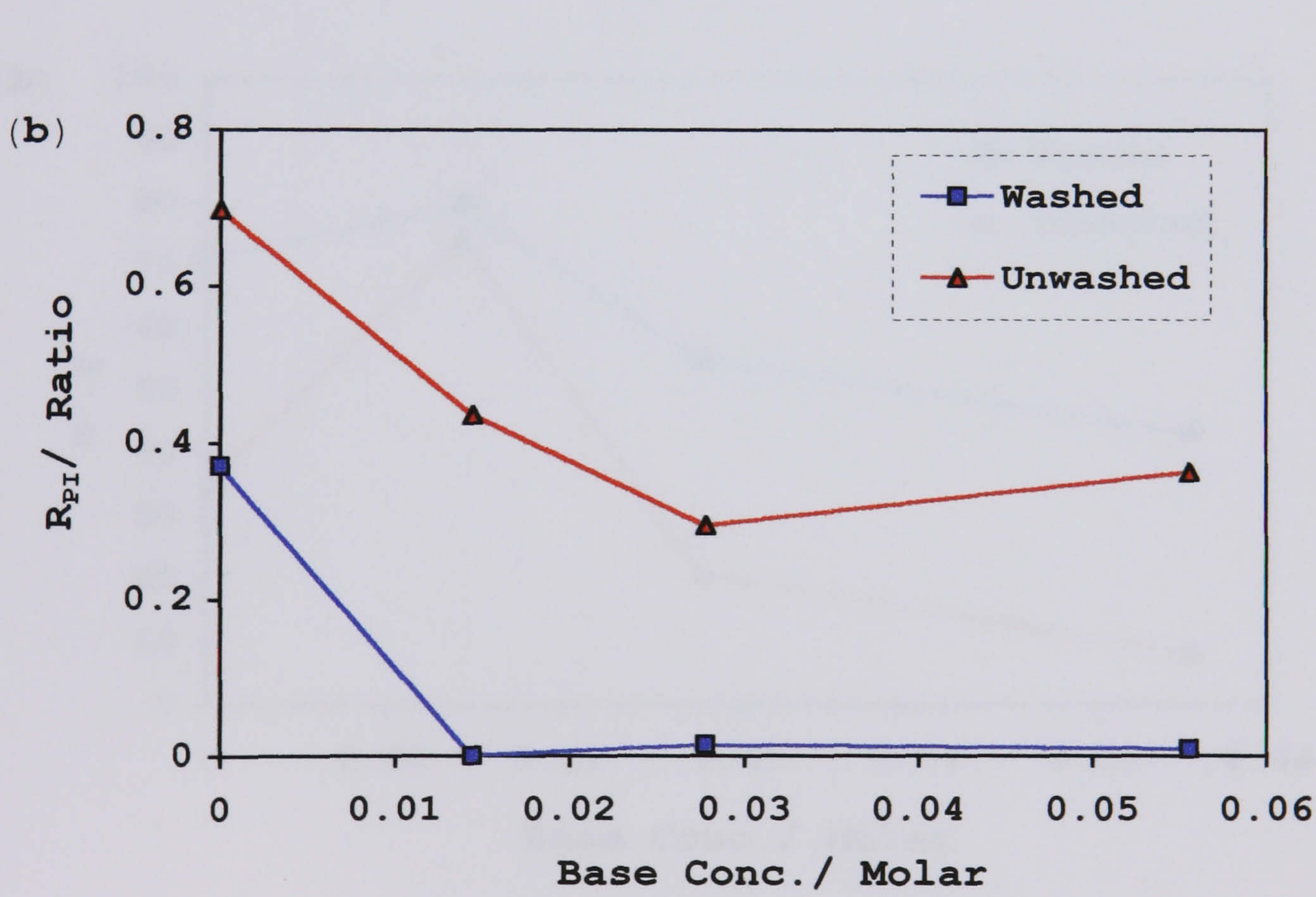
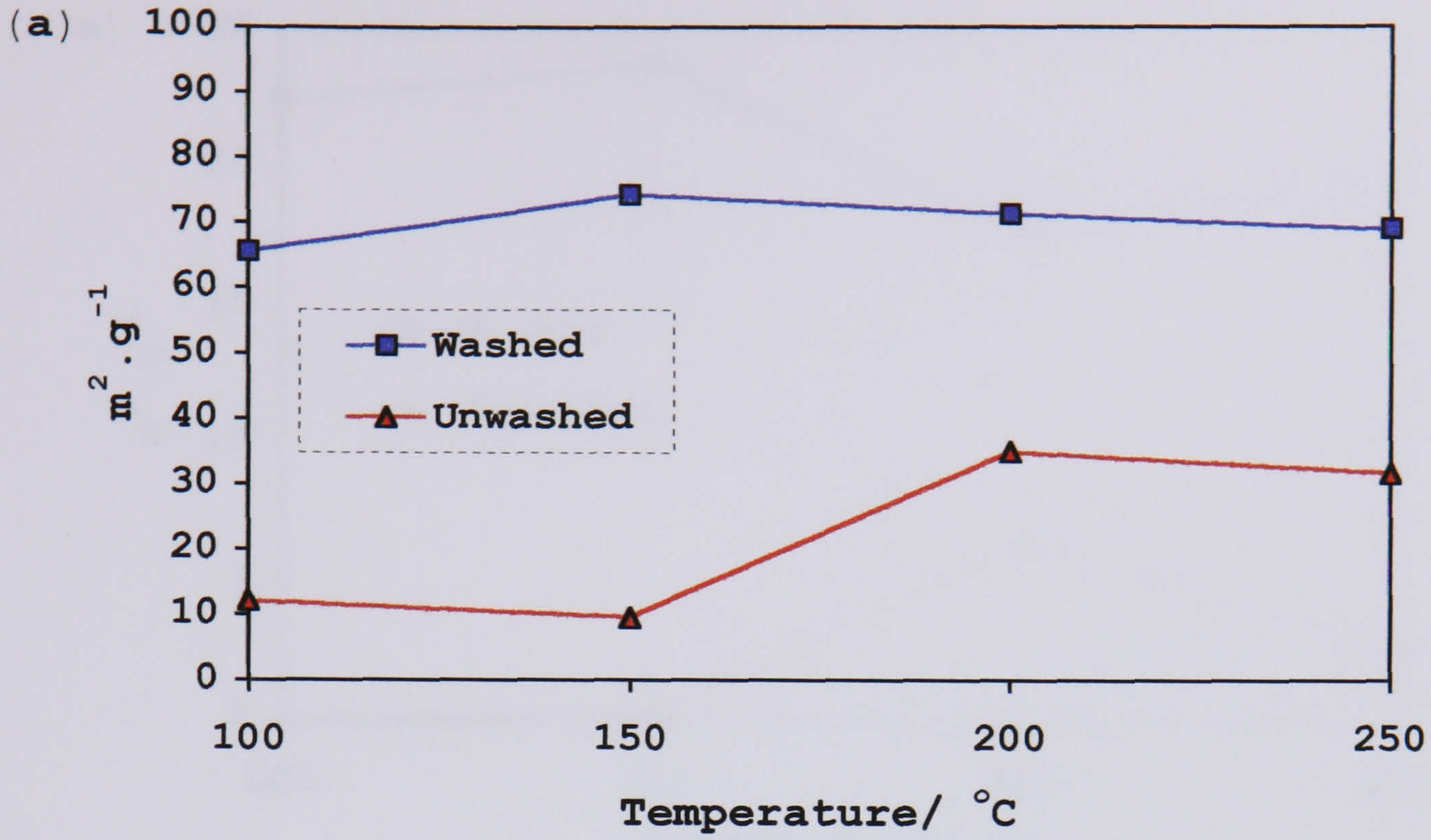


Fig. 5.24 The effect of eliminating the washing step on the degree of pillaring in the clay ((**a**) samples prepared at different thermal treatment temperature (see **table 5.16**) and (**b**) samples prepared at different base concentration (see **table 5.23**)).



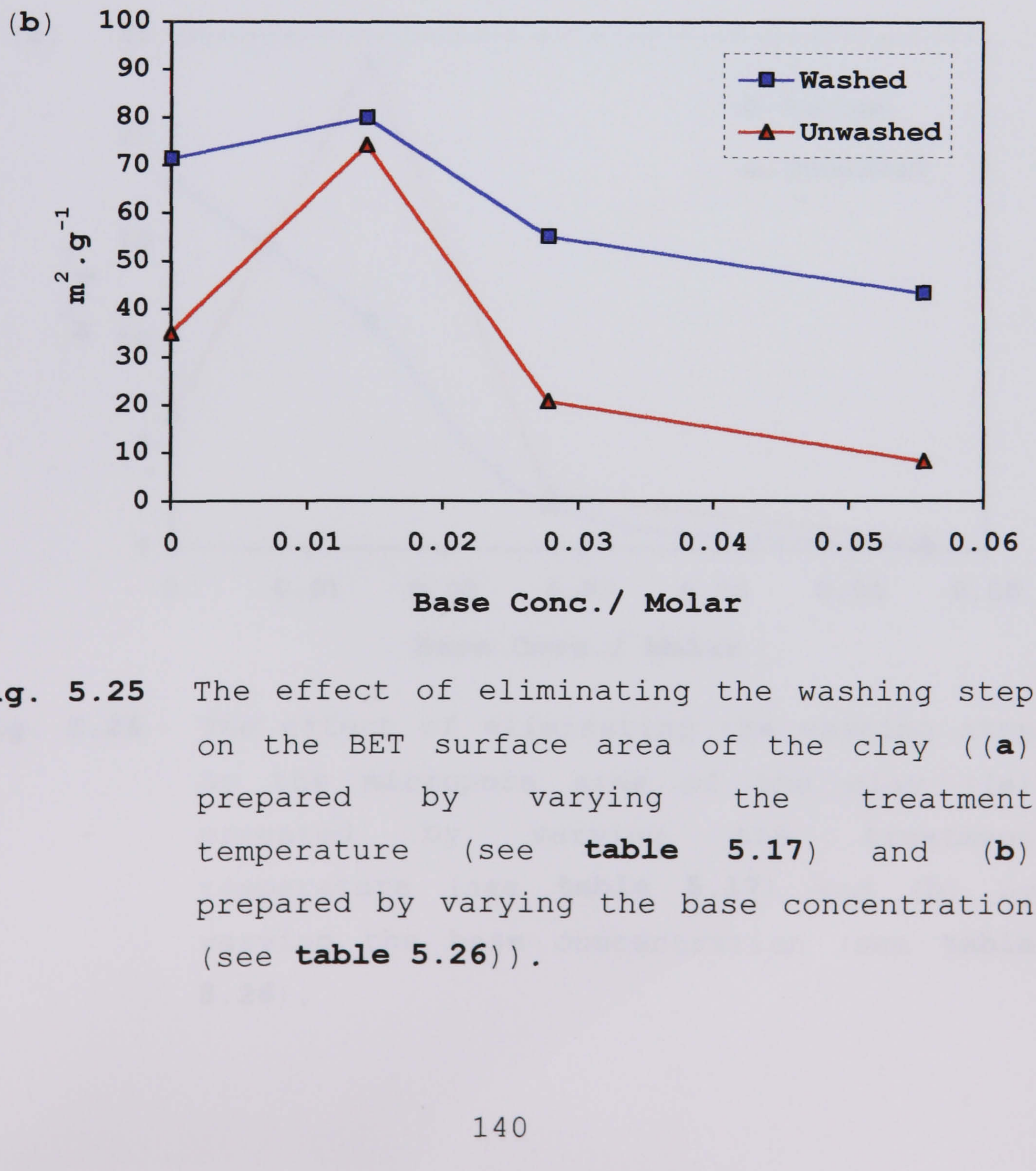
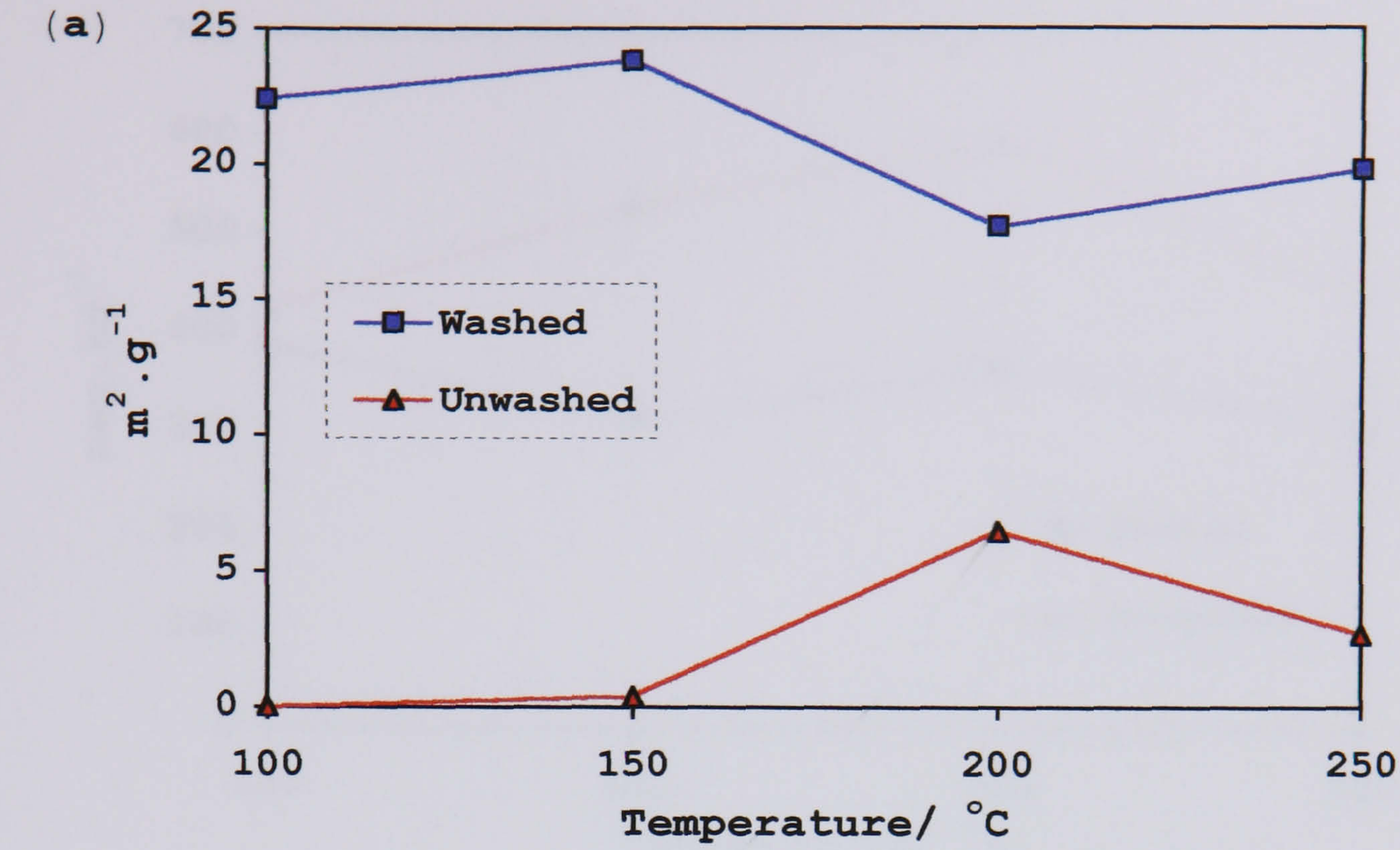


Fig. 5.25 The effect of eliminating the washing step on the BET surface area of the clay ((**a**) prepared by varying the treatment temperature (see **table 5.17**) and (**b**) prepared by varying the base concentration (see **table 5.26**)).



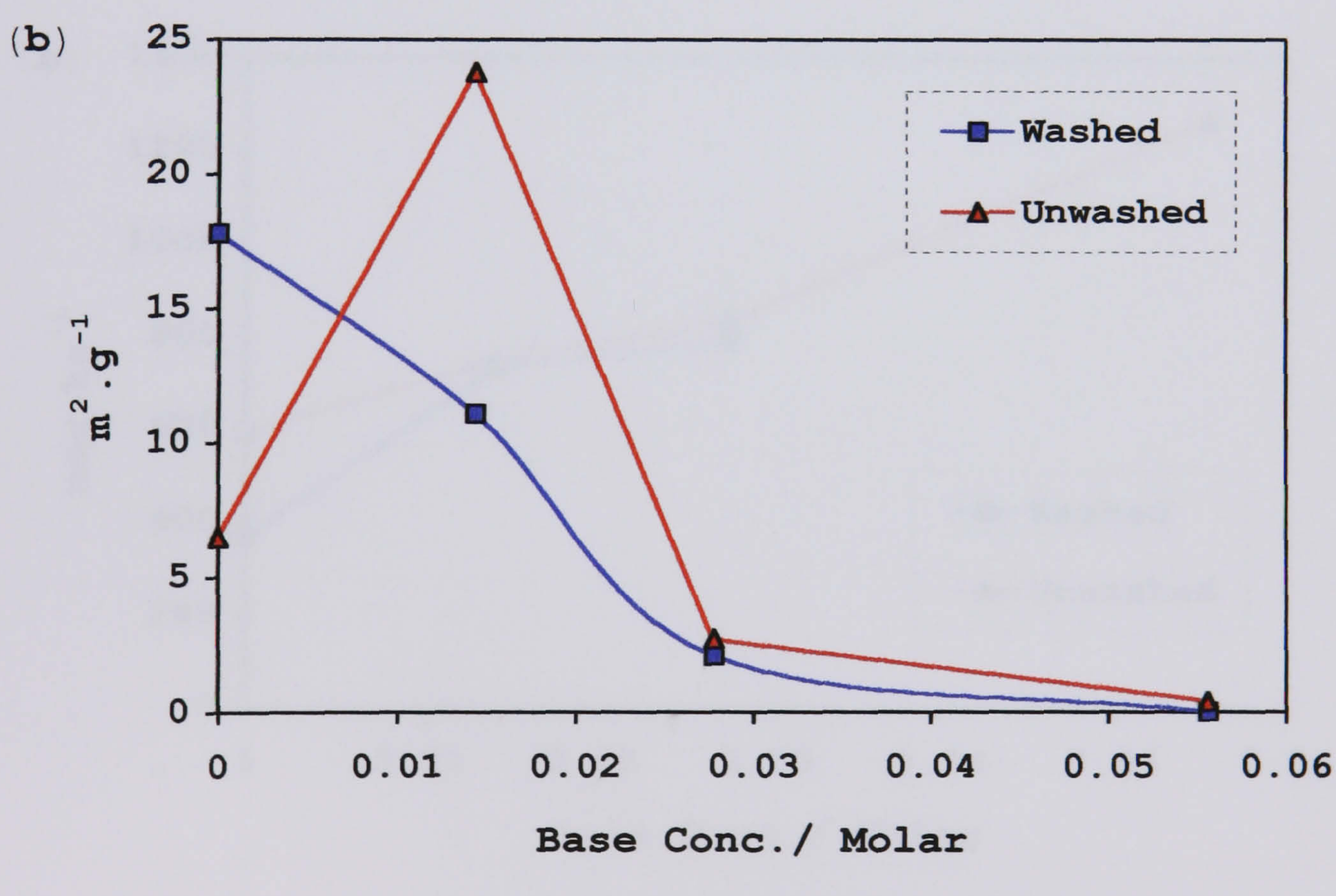
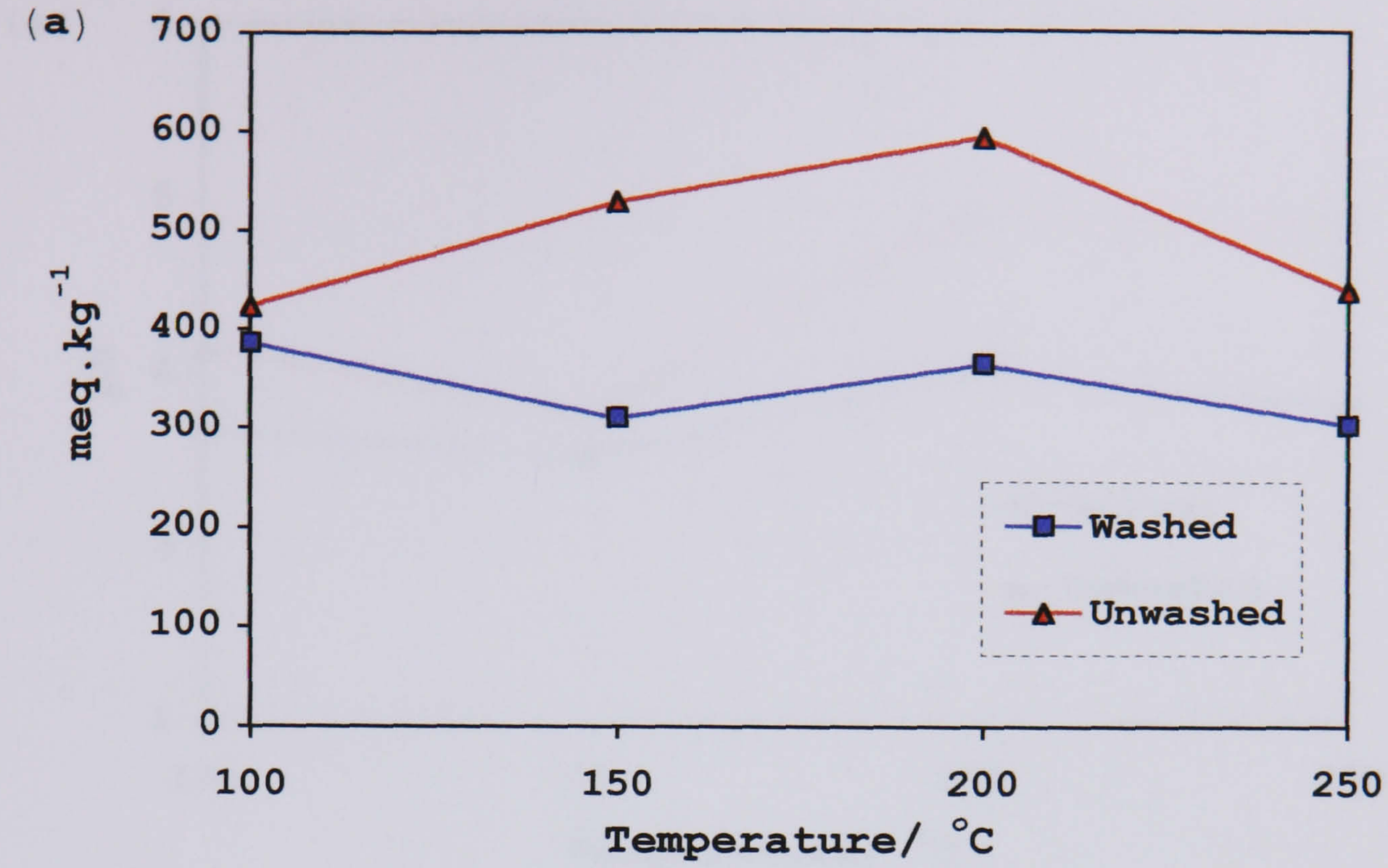


Fig. 5.26 The effect of eliminating the washing step on the micropore area of the clay ((**a**) prepared by varying the treatment temperature (see **table 5.17**) and (**b**) by varying the base concentration (see **table 5.26**).



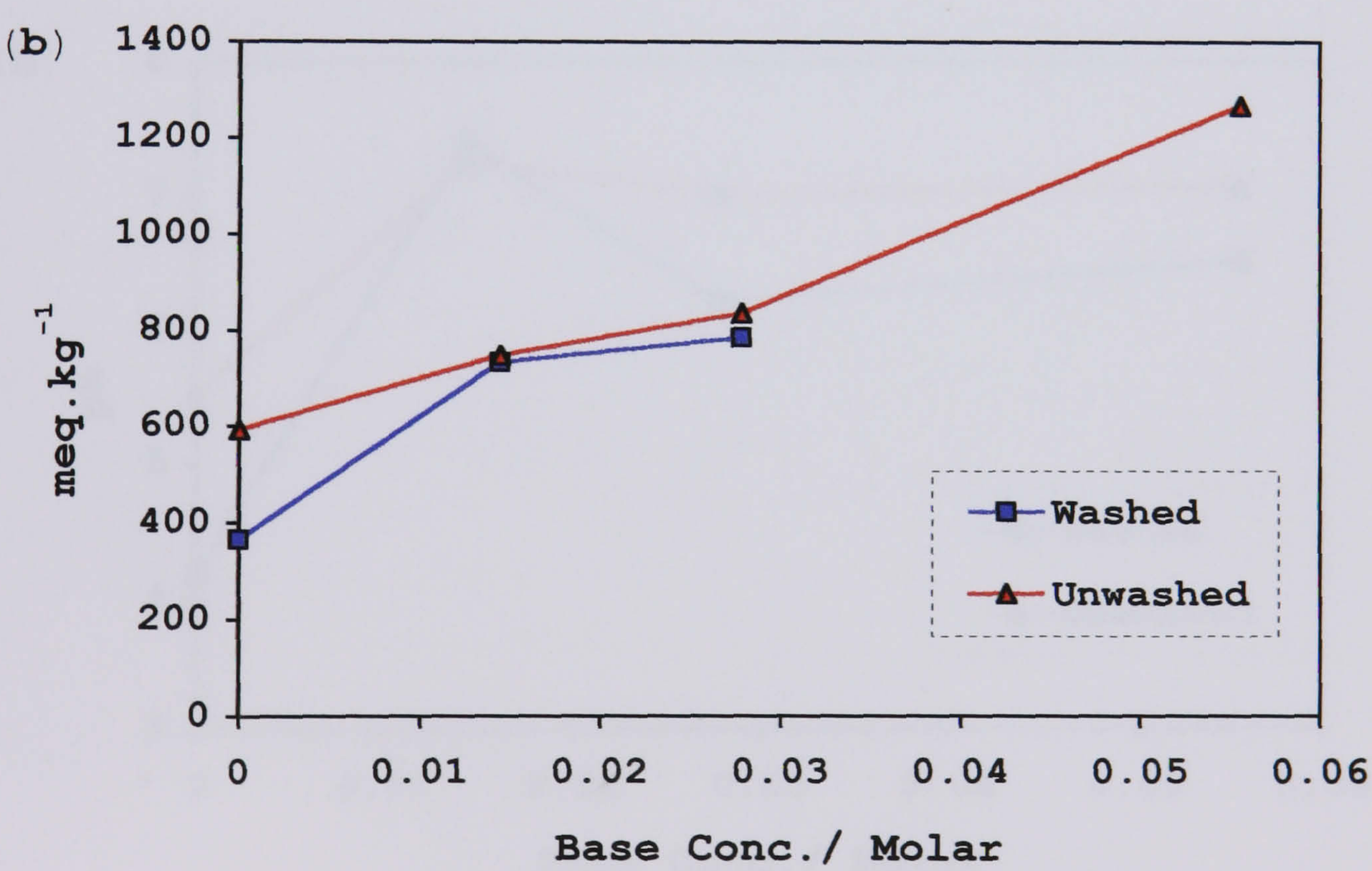
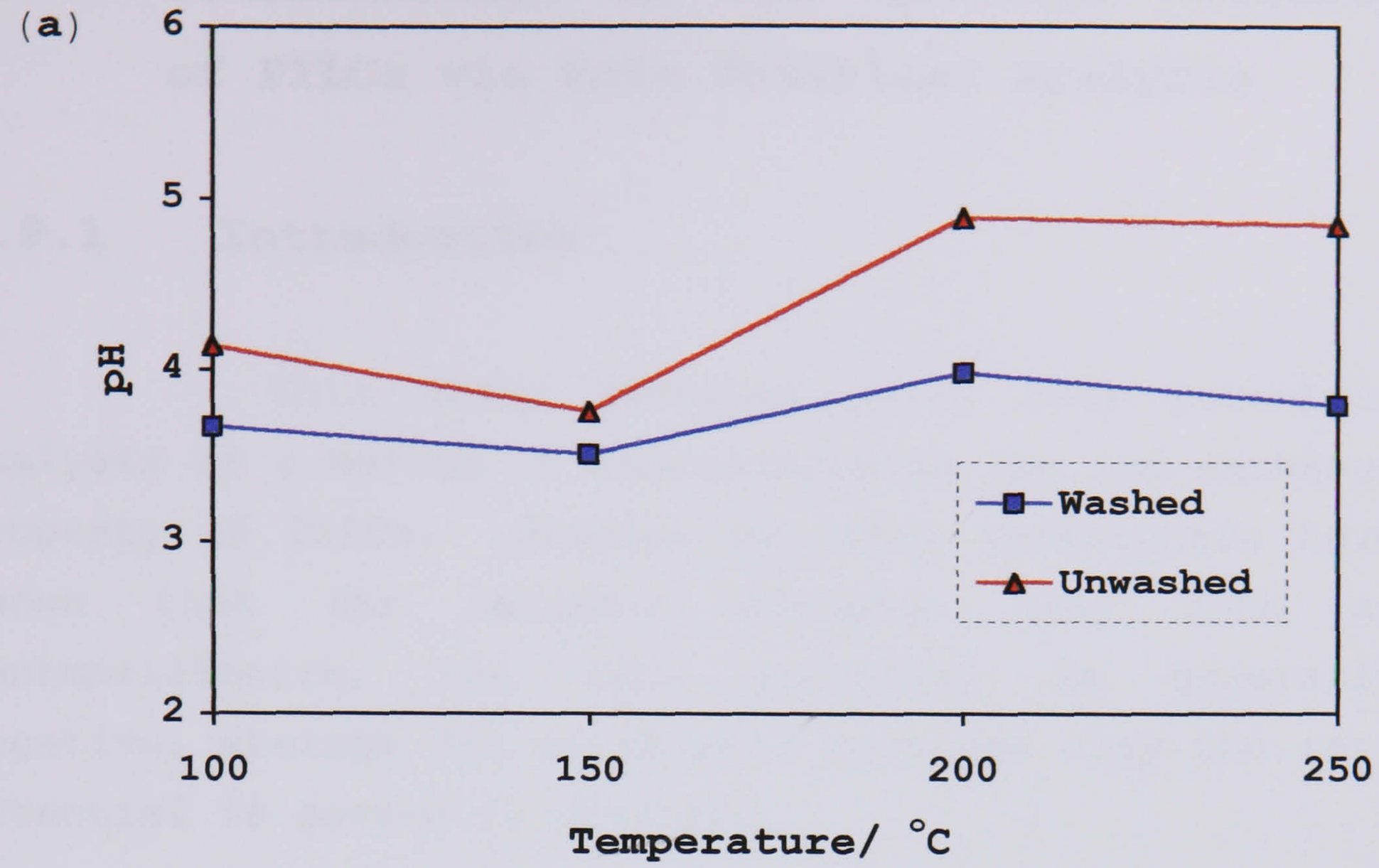


Fig. 5.27 The effect of eliminating the washing step on the C.E.C. of the clay ((**a**) prepared by varying the treatment temperature (see **table 5.18**) and (**b**) by varying the base concentration (see **table 5.29**)).



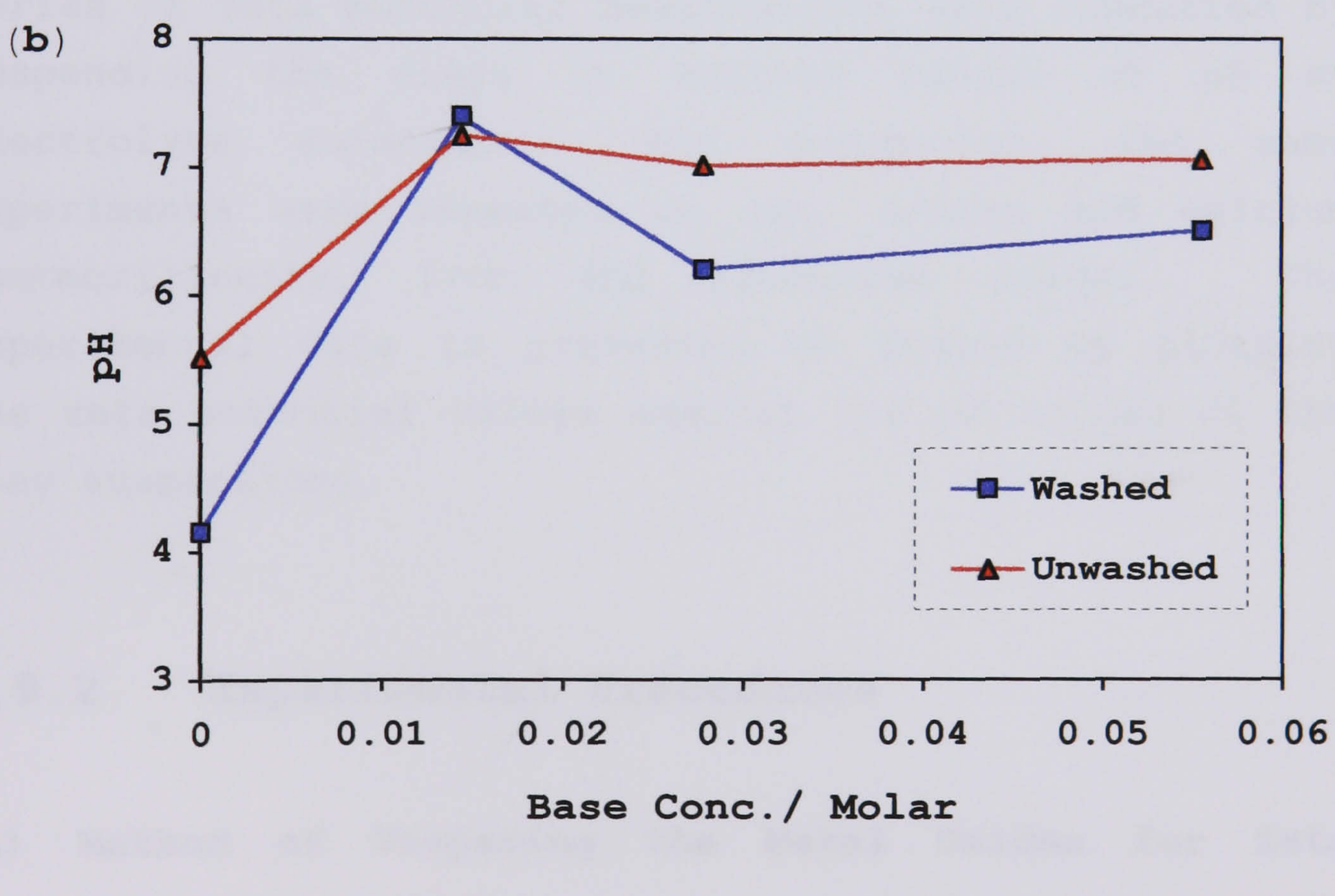


Fig. 5.28 The effect of eliminating the washing step on the pH of the thermally-treated clay ((**a**) prepared by varying the treatment temperature (see **table 5.15**) (**b**) prepared by varying the base concentration (see **table 5.29**)).

5.9 Determination of Ion Exchange Property of PILCs via Zeta Potential Analysis

5.9.1 Introduction

This study involves using zeta potential analysis as a method of characterising the ion exchange property of PILCs. Studies by other researchers have shown that for cationic exchange clay such as Montmorillonite, the zeta potential is generally negative, whereas for an anionic exchange clay the zeta potential is generally positive.

To demonstrate that PILCs such as Al-PILC and Fe-PILC would behave as a cation exchanger, a series of zeta potential measurements were conducted by suspending the clays in various ranges of pH of electrolyte solution. For comparison, the same experiments were repeated on raw, sodium and calcium Montmorillonite, iron and aluminium oxides. The experimental data is presented on graphs by plotting the zeta potential values against the pH values of the clay suspensions.

5.9.2 Experimental Procedures

(a) Method of Preparing the Metal Oxides for Zeta Potential Analysis

The aluminium and iron III oxides were prepared by the experimental procedures given below. The iron oxide sample was prepared by quickly adding 600 ml of NaOH solution (0.2 molar) to 240 ml $Fe(NO_3)_3$

solution while the solution was stirred vigorously with a magnetic stirrer. The aluminium oxide sample was prepared using the same quantities of reagents but aluminium chloride was used instead of ferric nitrate. In both cases, the pH of the suspensions was adjusted with 0.2 M NaOH solution. The precipitates obtained were separated from solution using a centrifuge at 3500 r.p.m. for 10 minutes and washed with distilled water to remove the excess salts. Finally the samples were dried in a hot-box at 120 °C for 18 hours.

(b) Analysis Procedures

(1) The clay suspensions were prepared by adding a 0.1 g of clay to potassium nitrate solution (0.01 molar) in a 250 ml volumetric flask. The mixture was shaken vigorously to give a homogeneous clay suspension.

(2) 50 ml of the clay suspension was transferred into a 50 ml centrifuge tube (Falcon, blue max 150, polypropylene, conical tube). The sample was then placed in an ultrasonic bath for 20 minutes to produce a homogeneous clay suspension.

(3) After that the pH of each set of samples was adjusted with a few drops of HNO_3 solution (0.1 or 0.01 molar) or KOH solution (0.1 and 0.01 molar) and shaken vigorously. The pH levels were measured just before zeta potential analysis with a pH meter (Corning, 240).

(4) Immediately after the pH was measured the zeta potential measurements were also taken from the samples.

(5) After 1 hour the pH and the zeta potential of the same samples were measured again to ensure that the measurements did not vary with time.

5.9.3 Results and Discussion of Zeta Potential Analysis

The results (see **fig. 5.29**) show that the zeta potential values of all the clays (RM, NM, Al-PILC and Fe-PILC) remained negative and almost constant. This behaviour of the clay is expected because the total net charge of a smectite clay is derived mostly from the permanent negatively charged structure of the clay.

The results of zeta potential analysis of the oxides are expected to vary according to the change of pH because of surface reactions. The iron oxide sample has a point zero charge (p.z.c.), 0 mV, at a lower pH value (5.8) than that of the alumina (7.2). These results suggest that below the pH values of p.z.c. the oxides will act as an anion exchanger but above these pH values they will act as a cation exchanger. When the oxide particles are in the solution at the p.z.c., and the pH is lowered, H_3O^+ will bond to the surface hydroxyls more than OH^- and a positively charged surface will result and vice versa. In comparing the zeta potential values of the aluminium and iron oxide it is apparent that the iron oxide

sample can act as a better cation exchanger than alumina in the given pH range.

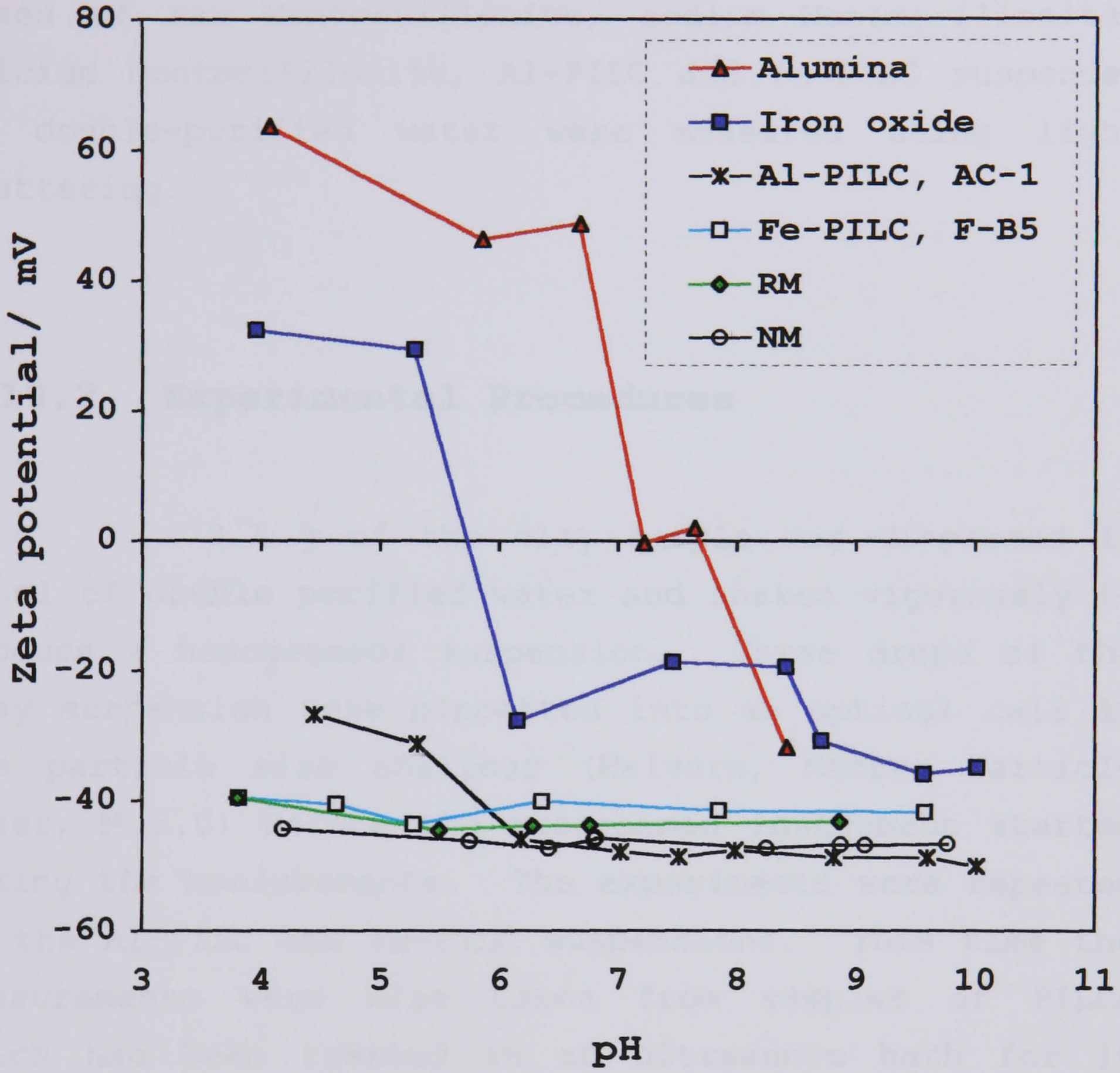


Fig. 5.29 The variation of zeta potential value with a change in the pH of the clay (**RM** and **NM** are raw and sodium Montmorillonite respectively) and metal oxide suspensions. For the description of the samples of Al-PILC & Fe-PILC see **chapter 4, table 4.1** and **chapter 5, table 5.19** respectively.

5.10 Determination of Particle Size

5.10.1 Introduction

The distribution of average particle sizes of raw Montmorillonite, sodium Montmorillonite, calcium Montmorillonite, Al-PILC and Fe-PILC suspended in double-purified water were measured using light scattering.

5.10.2 Experimental Procedures

0.1 g of the clay sample was dispersed in 10 ml of double purified water and shaken vigorously to produce a homogeneous suspension. Three drops of the clay suspension were pippetted into an optical cell in the particle size analyser (Malvern, Master Particle Sizer, M 3.0) before the programmed instrument started taking the measurements. The experiments were repeated on the Al-PILC and Fe-PILC suspensions. This time the measurements were also taken from samples of PILCs which had been treated in an ultrasonic bath for 10 minutes. In each case, the average particle size distribution was measured and a summary of the results is presented in **table 5.31**.

5.10.3 Results and Discussion of Particle Size Analysis

The results (see **table 5.31**) of the analysis give indications of the particle size of the clay samples that were dispersed in water. In comparing the particle size range of the starting materials with that of the pillared clay samples (without ultrasound treatment), it can be seen that the pillared clays have a wider range. The average particle size of the pillared clays is also larger than those of the starting clays, whereas the particle size of pillared clays measured after the ultrasound treatment on the samples is similar to their starting clays (RM and NM). These results indicate that the pillared clay samples consisted mainly of agglomerated particles. These large particles appear to remain as agglomerated particles when dispersed in water even with the aid of vigorous magnetic stirring, but they only broke up into smaller particles after the ultrasound treatment.

For water treatment the larger particle size of pillared clay would be an advantage because it would enable processing to be carried out more easily. After the treatment process the clay could be easily separated from suspension and collected for recycling or discharge. In contrast, it would be more difficult to separate the starting material, raw Montmorillonite, from suspension because of its smaller particle size.

In **table 5.31**, **Mont** represents Montmorillonite, and **U.T.** represents ultrasonic treatment. For the description of the samples, AC-2 and F-B14NW, see **chapter 4**, **table 4.1** and **chapter 5 table 5.20**, respectively.

Table 5.31 A summary of results of particle size analysis.

Sample Name	Sample Type	U.T.	Particle Size Range /μm	Average Particle Size /μm
RM	Raw Mont	None	23.7 - 1.5	5.5
NM	Sodium Mont	None	17.7 - <1.2	3.6
CM	Calcium Mont	None	54.9 - 1.9	9.9
F-B14NW	Fe-PILC	None	>118.4 - <1.9	67.0
AC-2	Al-PILC	None	>118.4 - <1.9	65.9
F-B14NW	Fe-PILC	Yes	16.7 - <1.9	4.2
AC-2	Al-PILC	Yes	16.7 - <1.9	4.4

5.11 Summary of Results and Conclusions

The following conclusions drawn from the extensive studies on the Fe-PILC are listed below:

(1) This research shows that a cheap Fe-PILC can be produced with a non-refined clay (raw Montmorillonite) using the modified synthesis method. This preparation method of the Fe-PILC requires only a limited number of synthesis steps and is also less time-consuming. The synthesis procedures have been made even more simple by eliminating the washing step of an Fe-PILC. This would be an advantage in the production of an Fe-PILC in term of cutting the costs. Although the Fe-PILC prepared using this method would be thermally less stable when the clay is in its dehydrated form, it would not hinder the clay's application in water treatment, which is a low temperature process.

(2) The changes in the structure and chemical composition in an Fe-PILC due to variations in the synthesis parameters and conditions could be monitored using the various characterisation methods. These methods include XRD, nitrogen adsorption, TG, and ICP-AES analysis. XRD analysis would be the most crucial analysis technique in providing the structural confirmation of pillared structure in the clay. Results of nitrogen adsorption analysis on the other hand, could only be used as supporting evidence for the results of XRD analysis.

(3) The experimental work shows that many Fe-PILCs have an exchange capacity which is significantly higher than that of the raw Montmorillonite. The results also show that it is possible to improve the C.E.C. of the Fe-PILC by varying the chemical composition of the clay. Enhancing the C.E.C. of the Fe-PILC through the addition of a base in the clay results in a substantial increase in the C.E.C..

(4) The conclusions drawn from the investigations into the ion exchange properties of the Fe-PILC using zeta potential analysis confirmed that Fe-PILC would act as a cation exchanger in a water treatment process.

The above findings clearly indicate that the modified Fe-PILC with improved C.E.C. would have a greater advantage over the Al-PILC in water treatment.

Chapter 6 Removal of Contaminants from Water

Conclusions drawn from the results of strontium adsorption analysis on the Fe-PILC, in **chapter 5**, have shown that modifying the chemical composition of the clay can lead to an enhancement of the cation exchange capacity. Therefore the focus of this chapter will be on assessing the ability of the clay to remove heavy metals (manganese) and organic contaminants (humic substances) from water. The possibility of regenerating the used clay will also be discussed.

6.1 Removal of Manganese from Water

6.1.1 Introduction

The aim of this study was to investigate the effect of varying the synthesis factors and conditions on the efficiency of Fe-PILC to remove heavy metals such as manganese from water. Manganese was selected for this study because it is a common constituent of drinking water and has a chemistry similar to heavy metals such as Zn^{2+} or Cd^{2+}. The additional problem caused by having manganese ions in the water is that they are fairly difficult to remove from water, and the overall treatment process often requires two steps. The complexity of the treatment process may be reduced using the PILC. This was investigated in the study. In order to investigate the ability of the clay to remove manganese from water, a series of batch contact tests were carried out by

contacting the clay with a range of concentrations of manganese solution. The capacity of specific samples of the Fe-PILC for manganese was determined by the tests and estimated using Langmuir adsorption model.

6.1.2 Adsorption Experiments

0.1 g of clay sample was contacted with 50 ml of known concentration (measured in parts-per-million, ppm) of manganese chloride solution while it was shaken vigorously on a shaker. The manganese solutions were prepared by diluting a 1000 ppm stock solution of manganese prepared by dissolving $MnCl_2.4H_2O$, AnalaR BDH, 99% in double-purified water. A linear calibration curve was constructed by calibrating the instrument with a set of manganese standard solutions. Measurements from each sample solution were taken with the wavelength set at 279.5 nm, the energy level at 58 eV, and the lamp current at 14 A.

6.1.3 Results and Discussion of the Effect of Varying the Synthesis Ratios

The capacities of the Al-PILC, Fe-PILC and their starting clays for manganese are compared and the results are discussed in the next section. This is followed by a discussion of varying the synthesis ratios on the capacity of the Fe-PILC for manganese.

6.1.3.1 A Comparison of the Capacity of the PILCs and Starting Clays for Manganese

The results (see **table 6.1, fig. 6.1**) show that the Al-PILC did not adsorb manganese whereas the Fe-PILC did. However the results (see **fig. 6.1**) also show a reduction in the capacity of the Fe-PILC (F-F3) when compared with all of the starting materials. Comparing the pH of the thermally-treated Fe-PILC (pH 4) with that of the raw clay (pH of 8.69) suggests that the increase in acidity of the Fe-PILC may have resulted in the decrease in capacity of the Fe-PILC. The high capacity of the alkaline raw clay may be explained by precipitation of manganese onto the clay surface as well as sorption in the clay because the manganese cations are unstable at high pH.

6.1.3.2 Effect of Varying the Fe/clay Ratio (R_F)

The results (see **table 6.2, fig. 6.2**) are in agreement with the results of strontium adsorption analysis in **chapter 5, fig. 5.11.** The results (see **fig. 6.2**) show that increases in the R_F resulted in decreases in the capacity of the clay for manganese. The increase in R_F also resulted in a decrease in pH of the Fe-PILC (see **chapter 5, fig. 5.13**). The rise in pH of the clay resulted in a reduction in the number of protons which competed with the manganese ions for the available exchange sites of the clay and vice versa.

6.1.3.3 Effect of Varying the OH/Fe Ratio (R_{OF})

The results (see **table 6.3**, **fig. 6.3**) show that a rise in the capacity of the clay for manganese is accompanied by a rise in pH (see **chapter 5**, **fig. 5.14**). The increase in capacity of the samples prepared at the higher base concentration may also be the result of some precipitation of manganese on the surface of the clay samples.

Table 6.1 A summary of results of batch contact tests.

Sample Name	Sample Type	Capacity /meq.kg^{-1}	R^2
RM	Raw Montmorillonite	809.4	0.997
NM	Sodium Montmorillonite	580.8	0.991
CM	Calcium Montmorillonite	640.2	0.998
AC-1	Al-PILC (conventional)	0	-
AS-3	Al-PILC ('short-cut')	0	-
F-F3	Fe-PILC ('short-cut')	357.2	0.991

R^2 is the square of correlation coefficient. The capacity is in milli-equivalent per kg. For description of the samples, **AC-1**, **AS-3** and **F-F3** see **chapter 4**, **table 4.1** for those of the former two and see **chapter 5**, **table 5.5** for that of the latter one.

Table 6.2 A summary of results of batch contact tests.

Sample Name	R_F /mmol.g^{-1}	Capacity /meq.kg^{-1}	R^2
F-F1	0.5	554.5	0.996
F-F2	1.0	-	-
F-F3	1.25	357.2	0.991
F-F4	1.30	289.6	0.994
F-F5	1.40	394.3	0.992
F-F6	1.50	435.2	0.999
F-F7	1.60	361.8	0.993
F-F8	1.70	366.3	0.985
F-F9	1.80	334.1	0.991
F-F10	2.0	296.0	0.988
F-F11	3.0	-	-
F-F12	4.0	504.5	0.985
F-F13	5.0	394.0	0.976

R^2 is the square of correlation coefficient. The capacity is in milli-equivalent per kg. **R_F** is the Fe/clay ratio. For description of the samples see **chapter 5, table 5.5.**

Table 6.3 A summary of results of batch contact tests.

Sample Name	R_{OF} /Ratio	Capacity /meq.kg^{-1}	R^2
F-O1	0.5	753.3	0.995
F-O2	1.0	505.6	0.981
F-O3	2.0	357.2	0.991
F-O4	2.5	501.9	0.990
F-O5	3.0	618.3	0.991

R_{OF} is the OH/Fe ratio. For the description of the samples see **chapter 5, table 5.6.**

In **fig. 6.1**, **RM**, **NM** and **CM** are raw, sodium and calcium Montmorillonite clays respectively. The samples of Al-PILC **AC-1** & **AS-3** (see **chapter 4**, **table 4.1**) were prepared using the conventional and the 'short-cut' method respectively. For the description of the Fe-PILC sample, F-F3, see **chapter 5**, **table 5.5**.

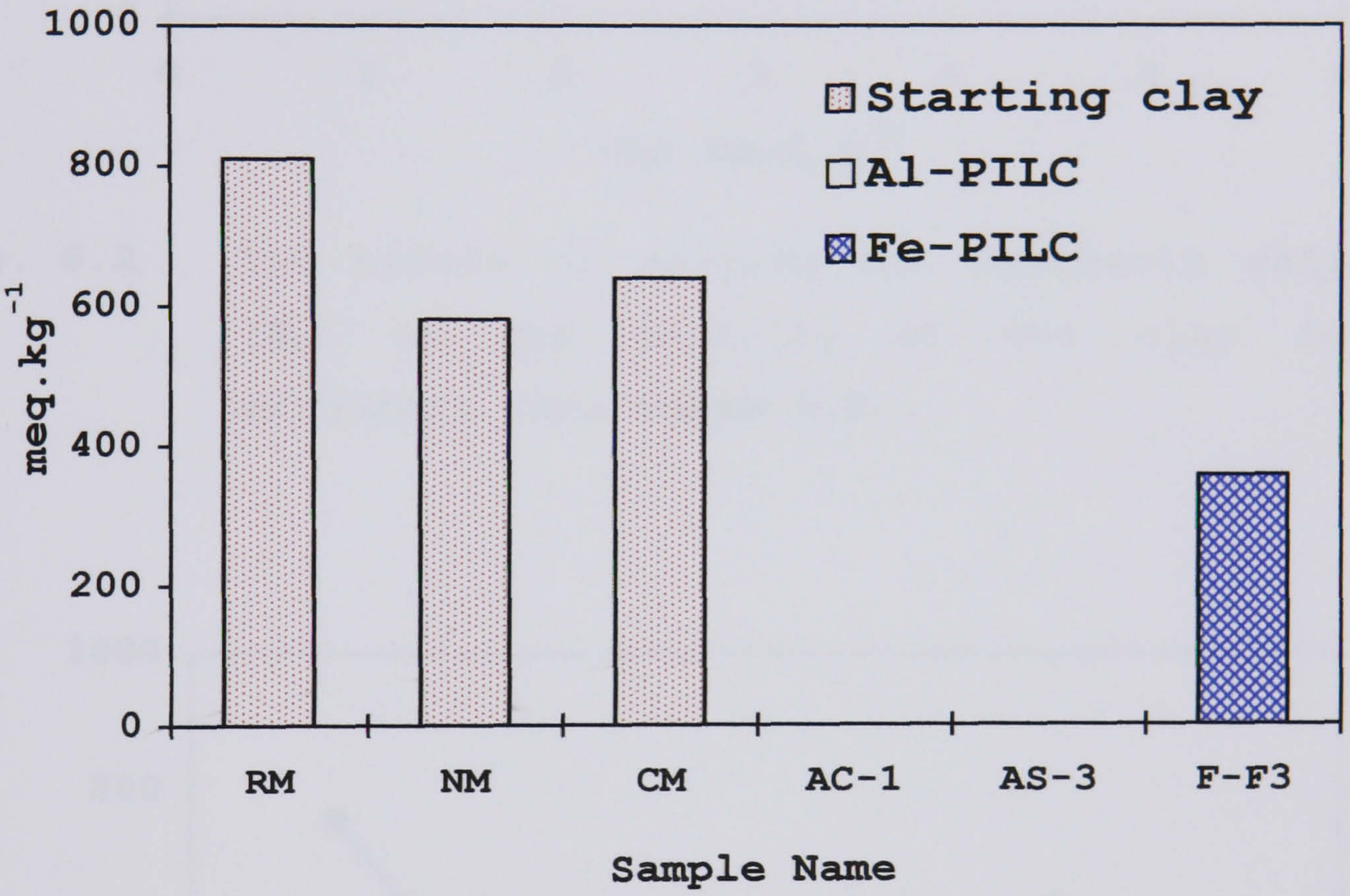


Fig. 6.1 A comparison of the capacity of the PILCs and the starting clays for manganese (see **table 6.1**).

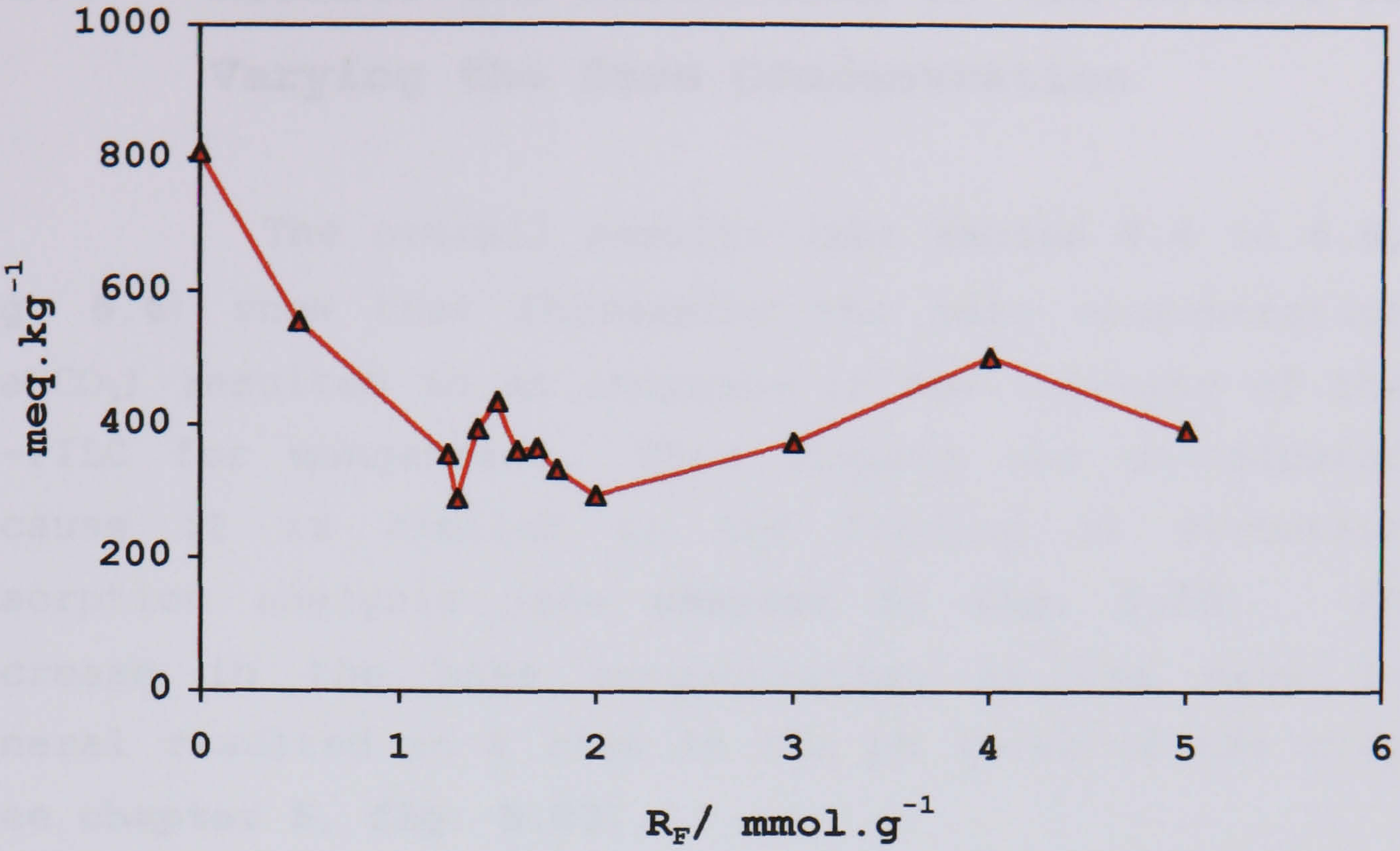


Fig. 6.2 The effect of varying the synthesis ratio (R_F) on the capacity of the clay for manganese (see **table 6.2**).

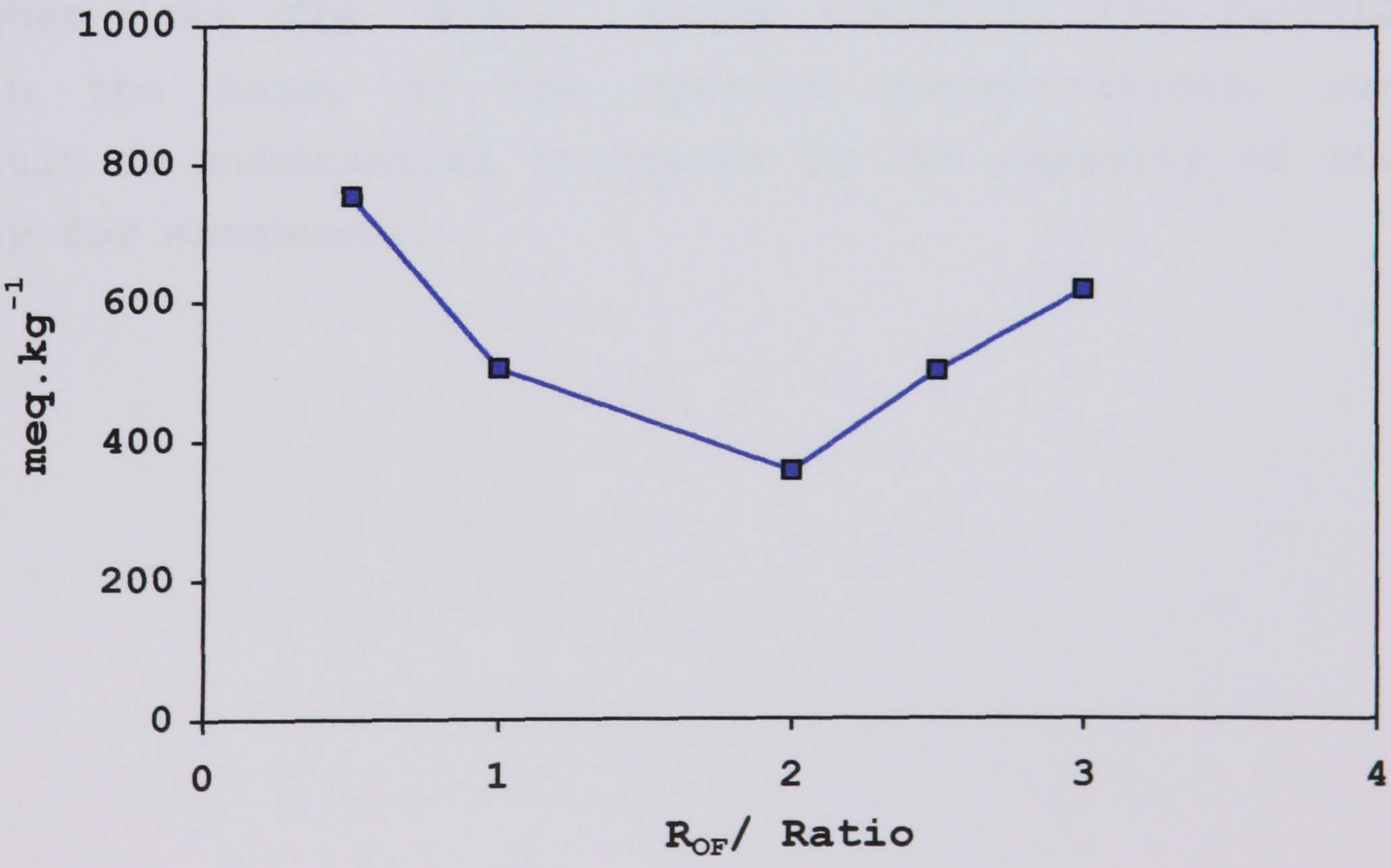


Fig. 6.3 The effect of varying the synthesis ratio (R_{OF}) on the capacity of the clay for manganese (see **table 6.3**).

6.1.4 Results and Discussion of the Effect of Varying the Base Concentration

The overall results (see **tables 6.4** to **6.6, fig. 6.4**) show that increasing the base concentration ($NaHCO_3$) resulted in an increase in the capacity of the Fe-PILC for manganese. This finding was anticipated because it is similar to the finding of strontium adsorption analysis (see **chapter 5, fig. 5.22**). An increase in the base concentration of the clay in general resulted in a rise in the pH level of the clay (see **chapter 5, fig. 5.23**).

When comparing the capacities of Fe-PILC samples (F-B13NW, 15 and 19 prepared with high base concentrations) with those of the starting materials (raw, sodium, and calcium Montmorillonite) it is apparent that those of the former are significantly higher (see **fig. 6.5**). Hence modifying the Fe-PILC with the base, at the optimum concentrations, can result in substantial increases in the capacity of the clay for manganese.

The definitions of the symbols in the following tables are as follows: **R^2** is the square of correlation coefficient. The capacity is in milli-equivalent per kg. **conc.** is the concentration of $NaHCO_3$ in the pillaring mixture. **NW** represents the unwashed sample.

Table 6.4 A summary of results of batch contact tests.

Sample Name	$NaHCO_3^{conc.}$ /Molar	Capacity /meq.kg^{-1}	R^2
F-B1	0.00	357.2	0.991
F-B2	0.00333	528.9	0.975
F-B3	0.00667	488.4	0.979
F-B4	0.0144	570.4	0.996
F-B5	0.0278	951.6	0.999
F-B6	0.0556	716.3	0.993
F-B7	0.111	-	-

Table 6.5 A summary of results of batch contact tests.

Sample Name	$NaHCO_3^{conc.}$ /Molar	Capacity /meq.kg^{-1}	R^2
F-B8	0.00	536.7	0.991
F-B9	0.0144	617.1	1.000
F-B10	0.0278	766.1	0.987
F-B11	0.0556	637.9	0.999
F-B12NW	0.00	521.3	0.990
F-B13NW	0.0144	700.6	1.000
F-B14NW	0.0278	859.0	0.991
F-B15NW	0.0556	1233.0	0.994

Table 6.6 A summary of results of batch contact tests.

Sample Name	$NaHCO_3^{conc.}$/ Molar	Capacity/ meq.kg^{-1}	R^2
F-B16NW	0.00	329.4	1.000
F-B17NW	0.0144	417.4	0.999
F-B18NW	0.0278	722.6	0.994
F-B19NW	0.0556	1584.5	0.996

In **fig. 6.4, batch A2** contains samples F-B1 to 6 (see **table 5.19**); **batch B2** contains samples F-B8 to 11 (see **table 5.20**); **batch C2** contains samples F-B12NW to 15 (see **table 5.20**) & **batch D2** contains samples F-B16NW to 19 (see **table 5.21**). In **fig. 6.5, RM, NM** & **CM** are raw, sodium & calcium Montmorillonite respectively. For the description of the samples of Fe-PILC in **fig. 6.4** see **tables 5.19, 5.20** & **5.21.**

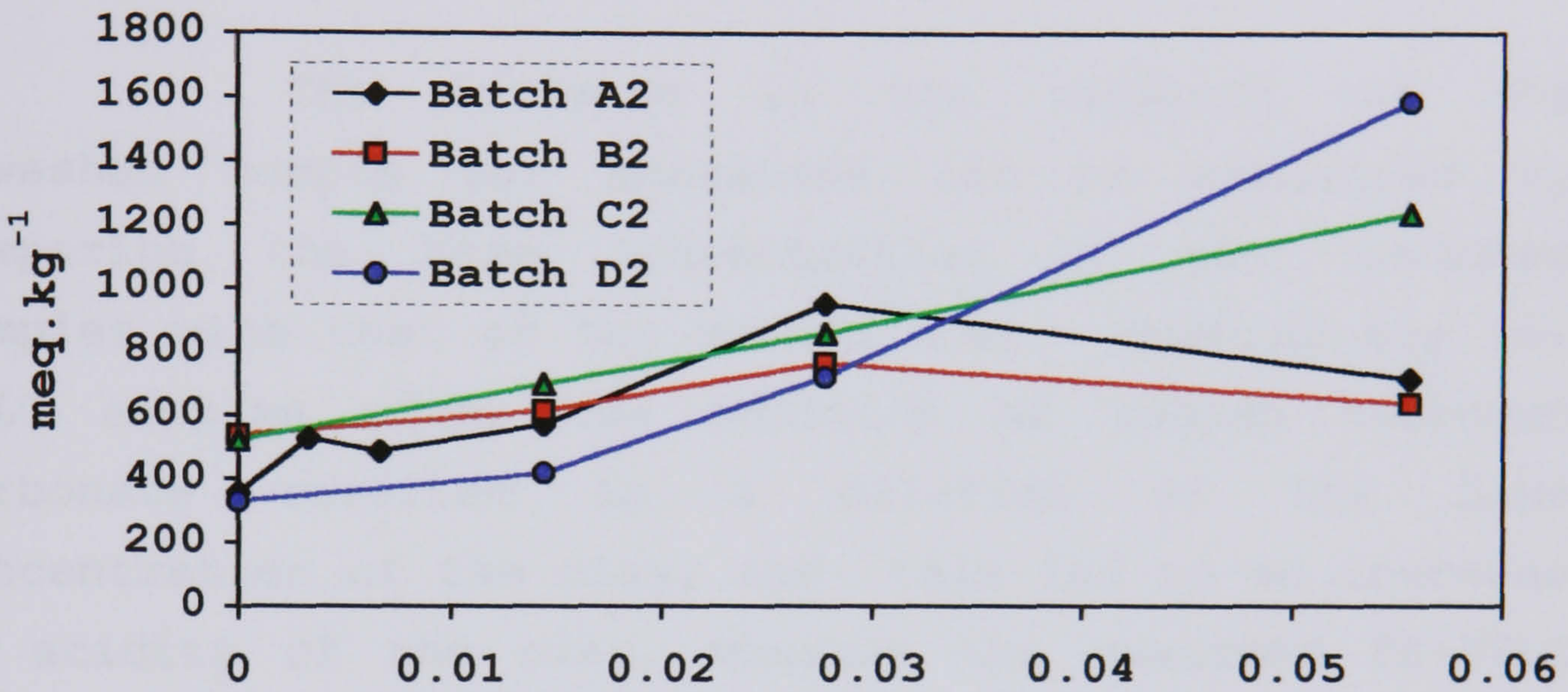


Fig. 6.4 The effect of varying the base concentration on the capacity of the clay for manganese (see **tables 6.4** to **6.6**).

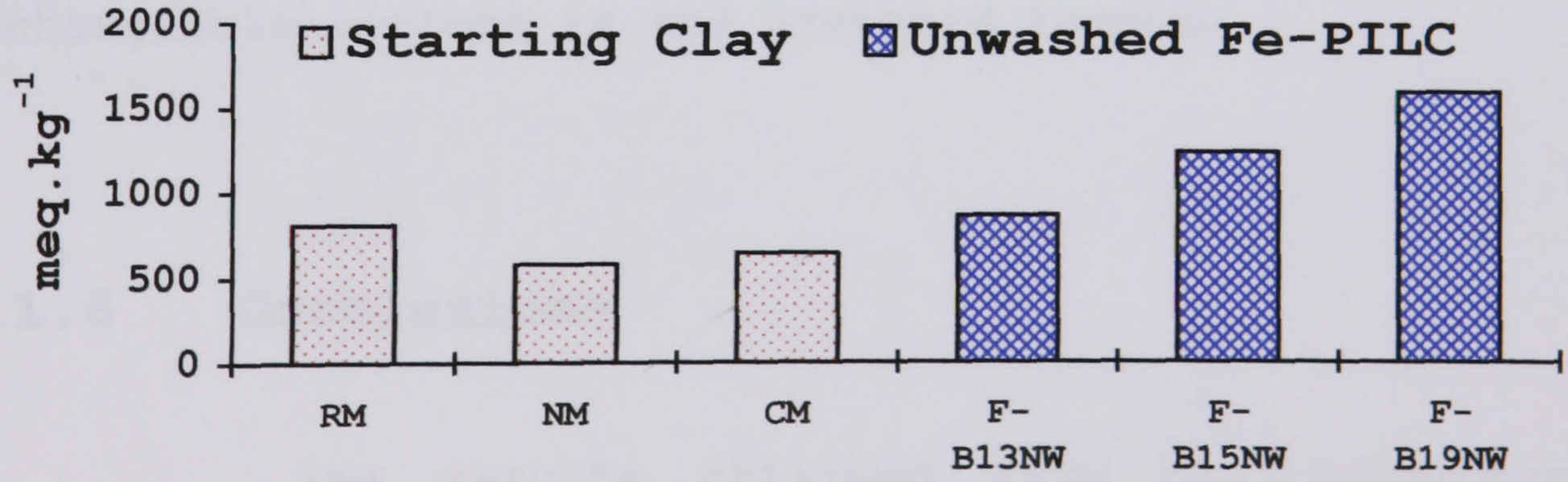


Fig. 6.5 A comparison of the capacity of the Fe-PILC prepared using the high base concentration and the starting clay for manganese (see **tables 6.1, 6.5** and **6.6**).

6.1.5 Results and Discussion of the Effect of Eliminating the Washing Step

The results (see **fig. 6.6**) suggest that eliminating the washing step resulted in an increase in the capacity of the clay for manganese. The results (see **chapter 5, fig. 5.27**) of the strontium adsorption analysis are also in agreement with the above finding.

The increase in the capacity of the unwashed sample for manganese can be explained by comparing the base concentration of the unwashed samples with that of the washed ones. Washing the Fe-PILC samples after the addition of sodium hydrogen carbonate resulted in a dilution in the base concentration of the clay, and this led to an increase in acidity of the clay, whereas the unwashed Fe-PILC became more basic resulting from the larger number of OH^- ions in the clay. The OH^- ions neutralised the protons in the clay, thus reducing the amount of protons in the clay that would have competed with the manganese cations. The rise in C.E.C. of the clay may partly result from an increase in number of Na^+ exchangeable cations in the unwashed samples.

6.1.6 Conclusions

The results obtained from the manganese contact tests are in agreement with those from the strontium adsorption analysis. This finding further suggests that the strontium adsorption analysis is a good method of assessing the overall abilities of the clay to remove inorganic cations. Furthermore the

results demonstrate that the Fe-PILC can adsorb manganese whereas the Al-PILC cannot. However these results also show that the capacity of the Fe-PILC for manganese is lower than that of the starting clays. The reduction in the capacity of the Fe-PILC can be lessened by preparing the clay using the optimum synthesis ratios and by eliminating the washing step. More importantly the results show that a modified Fe-PILC with a capacity that is significantly larger than that of the starting clays can be prepared by increasing the base concentration of the clay. The general conclusions drawn from the findings indicate that the modified Fe-PILC would be likely to act more effectively as a water treatment agent in removing heavy metals from water than the raw Montmorillonite.

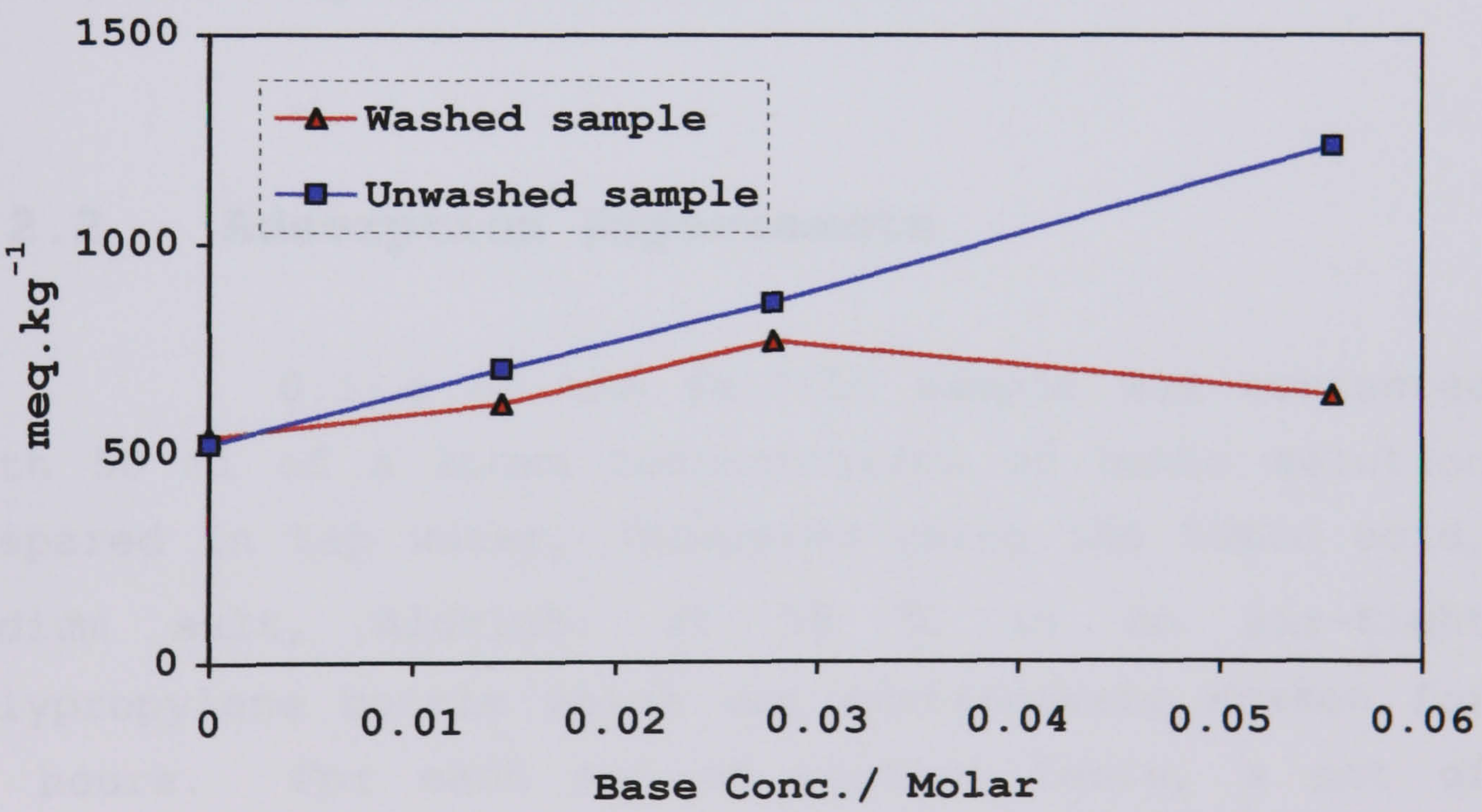


Fig. 6.6 The effect of eliminating the washing step on the capacity of the clay (prepared by varying the base concentration of the clay) (see **chapter 5, table 5.29**). The washed samples include F-B8 to 11 (see **table 5.20**) & the unwashed samples include F-B12NW to 15 (see **table 5.20**).

6.2 Removal of Humic Substances from Water

6.2.1 Introduction

The aim of this study was to investigate the effect of pH adjustment during the synthesis of Fe-PILC on the clay efficiency in removing organic contaminants such as humic substances from buffered water (tap water). Humic substances were selected for this study because they exist in nature as coloured contaminants and are easy to analyse. The Fe-PILC samples prepared by adding sodium hydrogen carbonate were contacted with humic substances in tap water. For a summary of descriptions and the results of structural characterisations of the samples see **chapter 4** (**section 4.4.3**) and **chapter 5** (**section 5.7.3**).

6.2.2 Adsorption Experiments

0.1 g of the Fe-PILC sample was contacted with 50 ml of a known concentration of humic solution prepared in tap water, (prepared using the humic acid, sodium salt, Aldrich) at 16 °C in an air-tight polypropylene bottle which was continuously shaken for 18 hours. For each set of contact tests, a set of blank solutions of humic substances was also set up under the same conditions. The concentrations of humic substances remaining in the tap water were determined using ultraviolet spectrometry (U.V. Spectrophotometry CECIL CE 1021, 1000 series). The samples with high concentrations were diluted with tap water before the analysis.

6.2.3 Results and Discussion of the Effect of Varying the Base Concentration

In general, the results (see **fig. 6.7**) show an overall increase in the capacity of the Fe-PILC for humic substances with an increase in the base concentration of the clay. The observed trend of increase in the capacity of the Fe-PILC for humic substances can be explained by the effect of pH variation on the ability of the clay to adsorb humic substances. The solubility of humic substances decreases with a decrease in pH and it becomes insoluble at pH < 2 (Amal et al., 1992). At approximately pH 8, the pH level at which the contact tests were carried out, the humic substances should remain soluble in the naturally buffered tap water.

The results (see **fig. 6.8**) of the pH measurements that were taken from the thermally-treated Fe-PILC samples dispersed in both distilled and tap water also support the above finding. The pH level of the distilled water contacted with the Fe-PILC samples indicates an apparent variation of acidity of the Fe-PILC, whereas the pH of the tap water contacted with the Fe-PILC shows only a slight increase in pH because of the effect of buffering in tap water.

The capacity of the Fe-PILC samples increases by factors of 6, 7 or 12 compared with the raw Montmorillonite. Compared to the Al-PILC sample AC-1 the capacity of the Fe-PILC samples is increased by factors of 2, 3 or 5. The results (see **fig. 6.9**) suggest that modifying the Fe-PILC with the base resulted in the large increase in capacity of the clay for humic substances.

Table 6.7 A summary of results of batch contact tests.

Sample Name	$NaHCO_3^{conc.}$ /Molar	Capacity /mg.g^{-1}	R^2
F-B1	0.00	5.9	0.998
F-B2	0.00333	6.9	0.974
F-B3	0.00667	6.9	0.983
F-B4	0.0144	13.3	0.979
F-B5	0.0278	22.5	0.984
F-B6	0.0556	16.5	0.998
F-B7	0.111	26.3	0.984

R^2 is the square of correlation coefficient. **conc.** is the concentration of the base of the clay suspension. For the description of the samples see **chapter 5, table 5.19.**

Table 6.8 A summary of results of batch contact tests.

Sample Name	$NaHCO_3^{conc.}$ /Molar	Capacity /mg.g^{-1}	R^2
F-B8	0.00	3.8	0.987
F-B9	0.0144	11.9	0.990
F-B10	0.0278	15.0	0.996
F-B11	0.0556	15.0	0.973
F-B12NW	0.00	15.5	0.982
F-B13NW	0.0144	14.7	0.975
F-B14NW	0.0278	22.0	0.972
F-B15NW	0.0556	-	-

R^2 is the square of correlation coefficient. **conc.** is the concentration of the base of the clay suspension. **NW** represents the unwashed sample. **R^2** is the square of correlation coefficient. For the description of the samples see **chapter 5, table 5.20.**

Table 6.9 A summary of results of batch contact tests.

Sample Name	$NaHCO_3^{conc.}$ /Molar	Capacity /mg.g^{-1}	R^2
F-B16NW	0.00	6.7	0.983
F-B17NW	0.0144	11.0	0.977
F-B18NW	0.0278	26.3	0.992
F-B19NW	0.0556	43.2	0.999

R^2 is the square of correlation coefficient. **conc.** The concentration of the base of the clay suspension. **NW** represents the unwashed sample. For the description of samples see **chapter 5, table 5.21.**

Table 6.10 A summary of results of batch contact tests.

Sample Name	Sample Type	Capacity /mg.g^{-1}	R^2
RM	Raw Montmorillonite	3.6	0.974
CM	Calcium Montmorillonite	2.9	0.984
AC-1	Al-PILC	8.3	0.997

R^2 is the square of correlation coefficient. For the description of the Al-PILC sample see **chapter 4, table 4.1.**

In **fig. 6.7, batch A2** contains samples F-B1 to 7 (see **table 5.19**); **batch B2** contains samples F-B8 to 11 (see **table 5.20**); **batch C2** contains samples F-B12NW to 14 (see **table 5.20**) and **batch D2** contains samples F-B16NW to 19 (see **table 5.21**). **NW** represents the unwashed samples.

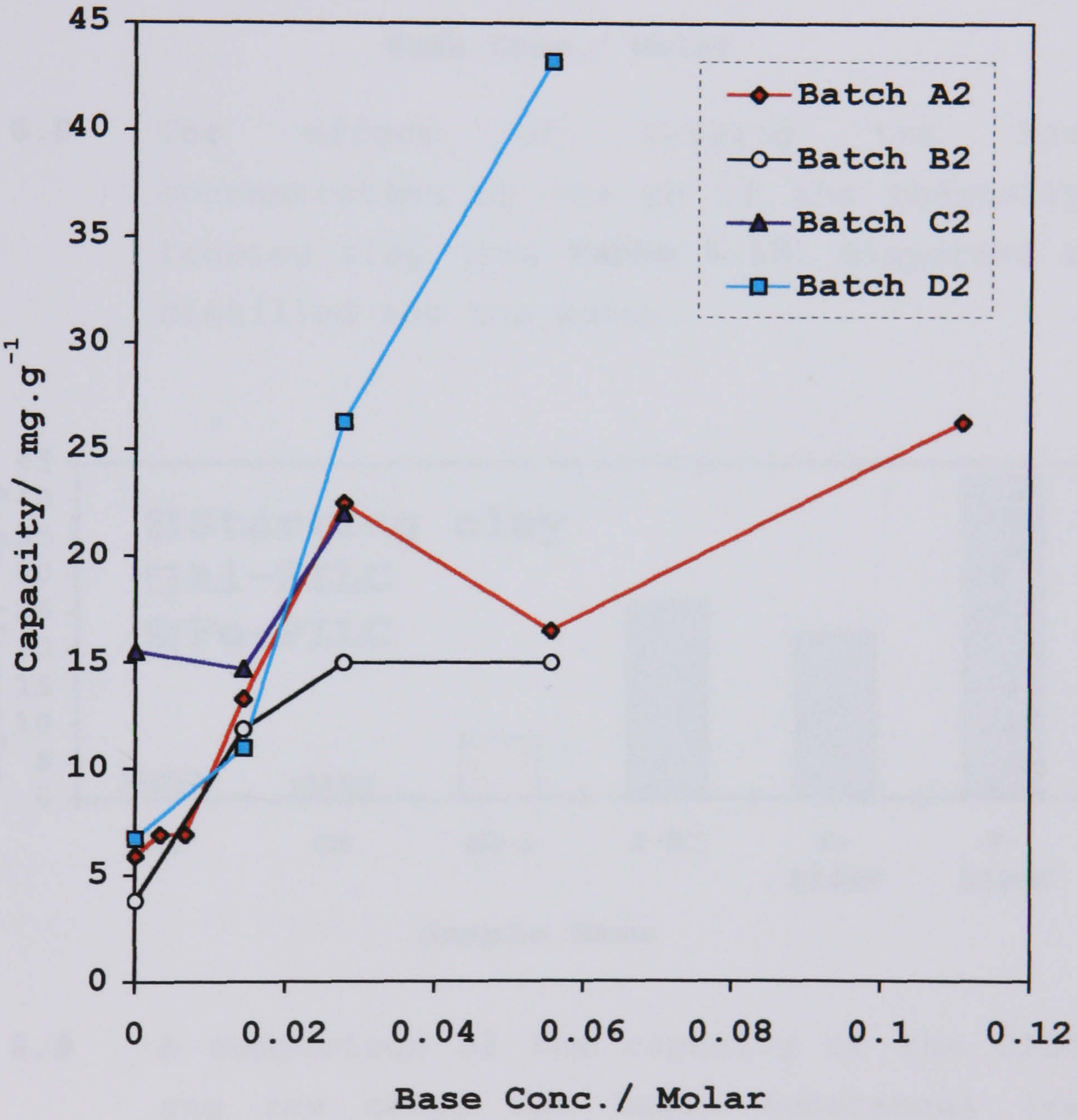


Fig. 6.7 The effect of varying the base concentration on the capacity of the clay for humic substances (see **tables 6.7** to **6.9**). For the description of the samples see **chapter 5, tables 5.19, 5.20** and **5.21.**

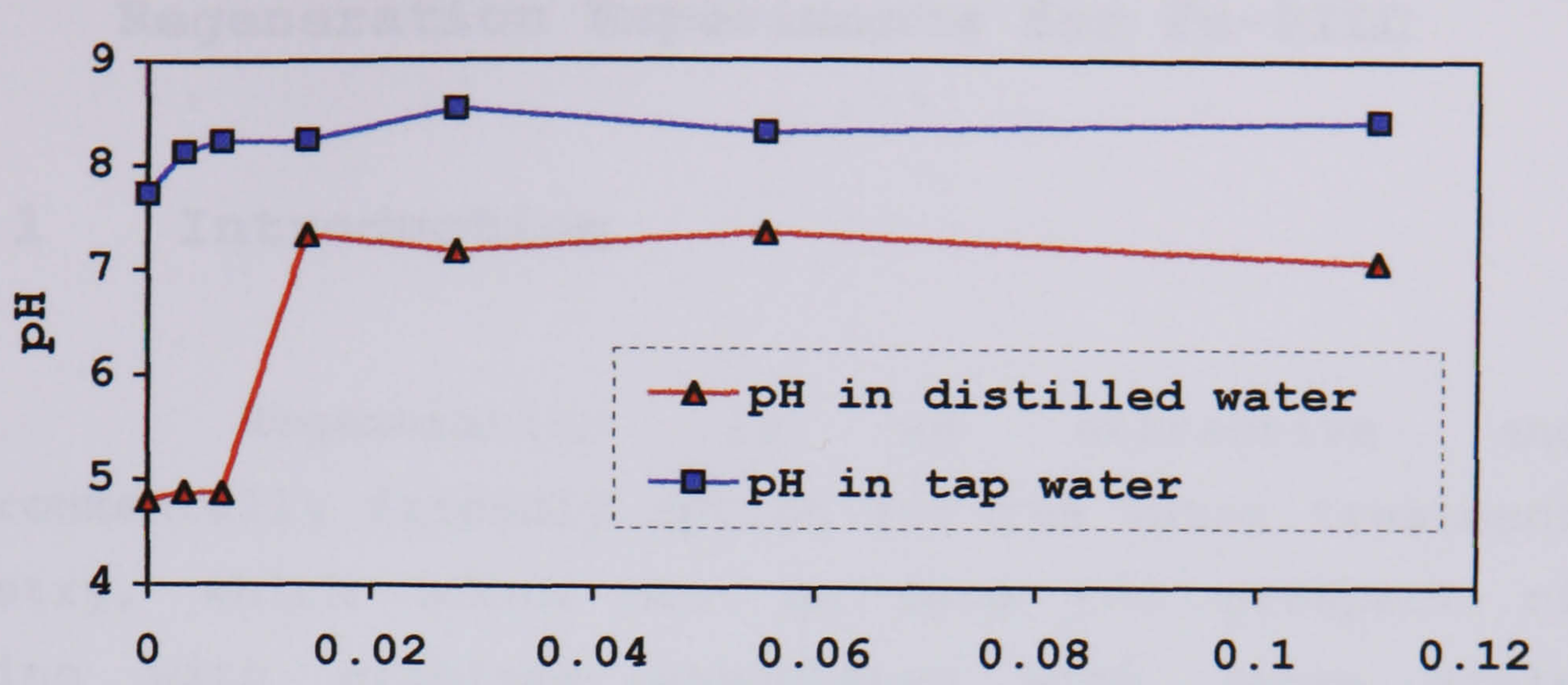


Fig. 6.8 The effect of varying the base concentration on the pH of the thermally-treated clay (see **table 5.19**) dispersed in distilled and tap water.

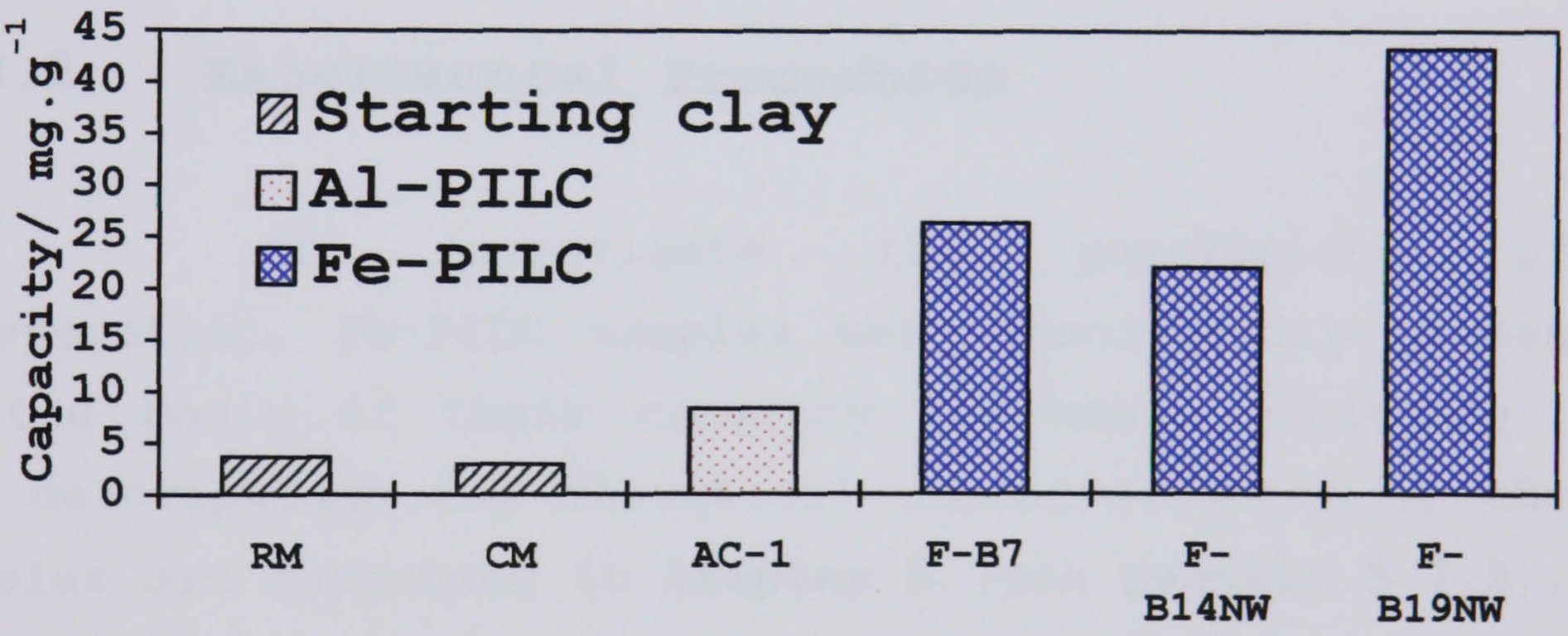


Fig. 6.9 A comparison of the capacity of the PILCs and raw clays for humic substances (see **table 6.10**). **RM** & **CM** are raw and sodium Montmorillonite respectively. For the description of the Al-PILC, AC-1, & Fe-PILC samples, F-B7, F-B14NW & F-B19NW, see **chapter 4**, **table 4.1** and **chapter 5**, **5.19**, **5.20** & **5.21** respectively. **NW** represents the unwashed sample.

6.3 Regeneration Experiments for Fe-PILC

6.3.1 Introduction

Regeneration is an attractive and environmentally friendly option for the water treatment industry, which often has to face the prospect of dealing with problems associated with large scale sludge disposal. Therefore the possibility of regenerating Fe-PILC was investigated, and a series of experiments were carried out to compare their abilities to remove humic substances from tap water before and after regeneration.

6.3.2 Experimental Procedures

To investigate the possibility of regeneration, Fe-PILC samples were specifically chosen on the basis of their capacity for humic substances. The descriptions and structural characteristics of the samples are discussed in **chapter 5** (see **section 5.7.3**). The regeneration experiments are described below.

(i) Regeneration Procedures

The used clay samples were separated from suspension using a centrifuge and they were washed with distilled water. The above procedure was repeated until the conductance was below 0.1 μS which indicated that leachable humic substances were removed from the clay. After that the clay samples were air-dried before they were heated in a furnace set at 200 °C for 10 hours to remove any humic substances from the clay

through thermal combustion. After thermal treatment the clay samples were ready for use.

(ii) After Regeneration

A series of contact tests were carried out using the regenerated clay samples. 0.1 g of clay was contacted with 50 ml of 100 ppm of humic substances in tap water while it was shaken vigorously for 18 hours until it had reached equilibrium.

6.3.3 Results and Discussion of the Regeneration Experiments

The amount of humic substances removed from the water using the Fe-PILC is represented in the percentage of removal (see **table 6.11, fig. 6.10**). The contact tests carried out demonstrate that it is possible to regenerate the used Fe-PILC. The results (see **fig. 6.10**) also show that, in the majority cases, the recycled samples of Fe-PILC have a higher capacity for humic substances than the fresh Fe-PILC samples. The increase in the percentage of removal of humic substances by the regenerated Fe-PILC may result from the introduction of new active sites into the clay. This increase in the active sites was possibly the result of thermal treatment on the organic compound in the clay. This process led to thermal decomposition of part of the organic compounds. One of the results may be due to carbonisation of the organic compounds which could occur at temperatures of approximately between 200 °C and 300 °C (Mackenzie, 1970).

In **table 6.11** and **fig. 6.10, H.S.** represents humic substances; **NW** represents the unwashed sample. For the description of the samples see **chapter 5, tables 5.19, 5.20** and **5.21.**

Table 6.11 A summary of the results of the regeneration experiments.

Sample Name	% Removal of H.S. Before Regeneration	% Removal of H.S. After Regeneration
F-B5	38.9	73.5
F-B9	53.5	77.0
F-B10	42.7	60.9
F-B13NW	51.7	76.6
F-B14NW	51.7	67.8
F-B15NW	71.3	66.5
F-B17NW	52.4	71.2
F-B18NW	24.2	72.0
F-B19NW	18.2	70.1

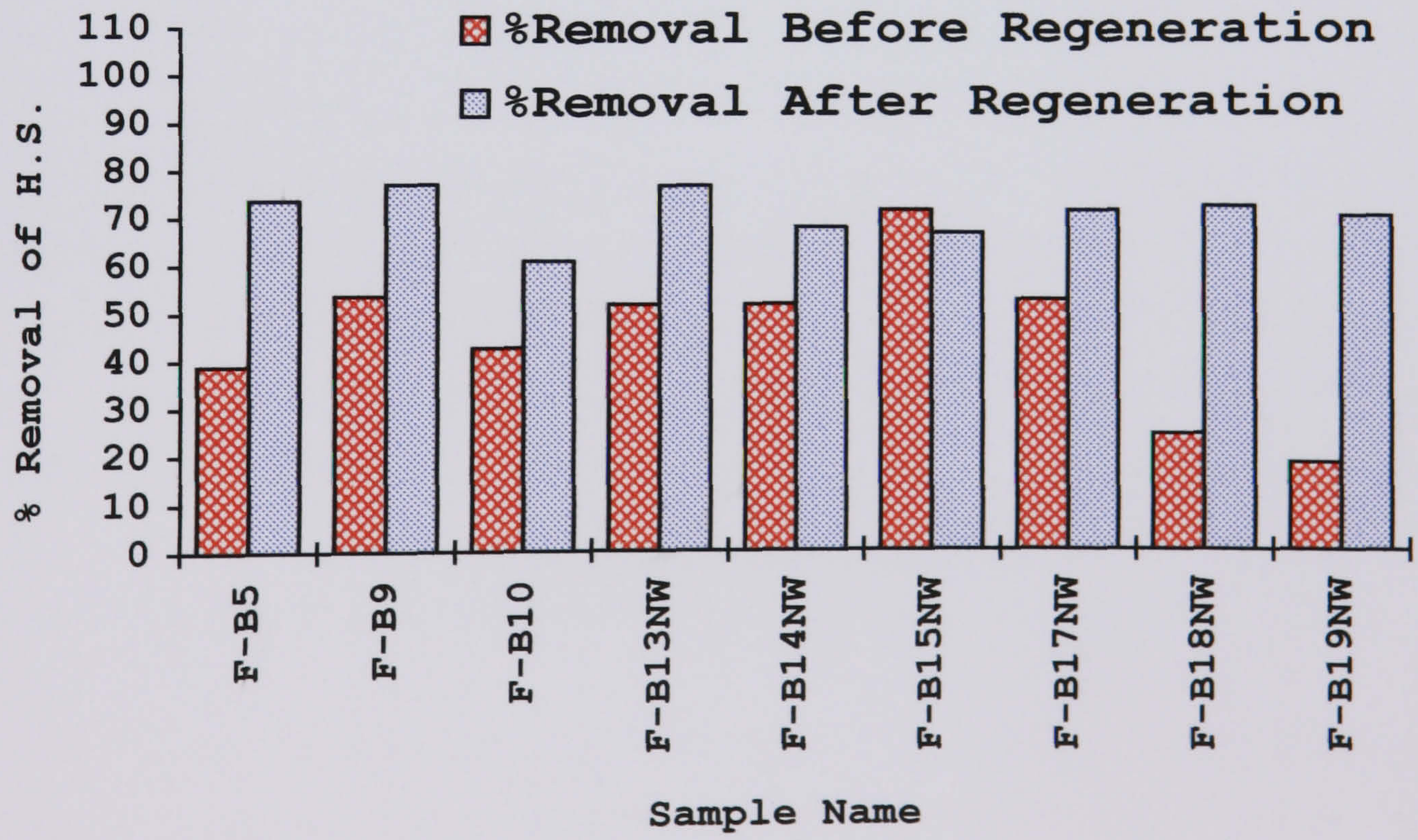


Fig. 6.10 The effect of regeneration on the capacity of the Fe-PILC for humic substances.

6.4 Conclusions

The results confirm that the modified Fe-PILC can have a dual function in the water treatment process. It can be concluded that the capacity of the Fe-PILC for the heavy metal or organic compound can be enhanced by increasing the base concentration of the Fe-PILC. Furthermore, preparing an Fe-PILC by using the optimum synthesis ratios and base concentration can result in significant improvement in the capacity of the Fe-PILC for the contaminants. The enhancement of the capacity of the Fe-PILC can result in an Fe-PILC with a capacity which is significantly higher than that of the raw Montmorillonite or the Al-PILC. The conclusion drawn from the results of the regeneration tests performed on the Fe-PILC show that the Fe-PILC can be regenerated. The process of regenerating the Fe-PILC resulted in an increase in the capacity of the Fe-PILC for humic substances.

Chapter 7 Summary of Results and Conclusions

The summary of results and conclusions of the experiments with the PILCs and the starting clays are outlined below:

X-ray diffraction analysis (XRD) has given reliable confirmation of the pillared structure in the Al-PILC and Fe-PILC. The summary of results of XRD analysis shows that the Al-PILC has typical spacing values ranging from 14.9 Å to 19 Å, whereas the Fe-PILC has much higher spacing values ranging from 11.9 Å to 26.3 Å.

The ion exchange properties of the PILCs can be studied using zeta potential analysis. The apparent zeta potential values of the PILCs are expected to remain negative over a wide range of pH (between pH 4 and 10) because the net surface charge of the structure of the starting clays is negative.

The average particle size range of the PILCs is expected to be higher than that of the raw or sodium Montmorillonite because PILCs consist of particle aggregates. The average particle size of Al-PILC and Fe-PILC ranges from greater than 118.4 μm to less than 1.9 μm, whereas that of the raw or sodium Montmorillonite ranges from 1.5 μm to 23.7 μm.

Although pillaring the clay with metal oxides results in a lower C.E.C. of the clay, there are methods which make possible the enhancement of the C.E.C. of the PILCs. In the case of Fe-PILC, a combination of factors is responsible for the increase

in the C.E.C. of the clay. It can be concluded that the most effective method of enhancing the C.E.C. of the Fe-PILC is by varying the base concentration of the clay. In general the C.E.C. of the non-modified or modified Fe-PILC is significantly higher than that of the Al-PILC. The results show that the C.E.C. of the Fe-PILC ranges from 411.5 meq/kg to 1267.9 meq/kg, whereas that of the Al-PILC ranges from 4.4 meq/kg to 102.3 meq/kg.

The capacity of the starting clays, Al-PILC, and Fe-PILC for heavy metals such as manganese can be estimated using the Langmuir adsorption model. The data obtained from the contact tests appear to correlate well with the model. In most cases the standard deviation of error (R^2) of the data is close to 1. The capacity of the Fe-PILC for heavy metals such as manganese is also affected by the synthesis parameters. The parameter which has the most influence on the capacity of the clay for manganese is again varying of the base concentration of the Fe-PILC. In general, an increase in the base concentration of the Fe-PILC leads to a rise in the capacity of the clay for the heavy metal. The overall conclusions drawn from the results of the contact tests are that an Fe-PILC with significantly higher capacity than the raw clay for the heavy metal can be prepared by modifying the clay with the addition of sodium hydrogen carbonate.

The Langmuir model can be used to estimate the capacity of the clays for organic compounds such as humic substances. The data obtained from the humic substances contact tests again correlates well with the model. The standard deviation values (R^2) of the data are close to 1. Increasing the base concentration of

the Fe-PILC will also lead to a rise in the capacity of the Fe-PILC for organic compounds such as humic substances. The results show that the capacity of the modified Fe-PILC, prepared by raising the $NaHCO_3$ concentration from 0 to 0.0566 molar, resulted in an increase in the capacity of the clay for humic substances from 6.7 mg/g to 43.2 mg/g. The modified Fe-PILC has a capacity that is significantly higher than that of the raw Montmorillonite (3.6 mg/g).

The regeneration experiments demonstrated that the Fe-PILC with adsorbed organic contaminants such as humic substances can be regenerated. The thermal treatment process of the regeneration steps can lead to a rise in the capacity of the Fe-PILC for humic substances. During the thermal treatment (at 200 °C) part of the organic compounds adsorbed into the Fe-PILC may undergo thermal decomposition. One of the forms of decomposition may be due to carbonisation of part of the organic compounds.

The above summary of results and discussion imply that a number of factors could be responsible for the observed increase in the capacity of the Fe-PILC for the various contaminants. These factors are listed below:

(a) The increase in the C.E.C. of the Fe-PILC could be due to exchange sites being created on iron oxide pillars. In the alkaline condition the hydroxyl ions reacted with the hydrous oxide to produce a cationic exchange surface (Rautiu et al., 1994). The results of zeta potential analysis are in agreement with the results of the strontium analysis. These results confirm that iron oxide

can act as a better cation exchanger than aluminium oxide in the given pH range.

(b) Precipitation of manganese on the PILC could also be responsible for the observed increase in pH of the clay. This may be another explanation for the large increase in the capacity of the clay for manganese because the cation is unstable in an alkaline condition. Manganese precipitates out of the solution when the pH of the solution is above pH 7, whereas the cation of strontium is stable at a pH of between 8 and 13 and is thus unlikely to precipitate out of the solution. Further investigation would be needed to determine the extent of precipitation of cations onto the clay.

(c) The degree of pillaring in the Fe-PILC is also responsible for the increase in the C.E.C. of the clay. The results (see **fig. 7.1**) clearly imply that the increase in the C.E.C. of the Fe-PILC for strontium is related to a rise in the degree of pillaring (R_{PI}) of the Fe-PILC. These results also show that eliminating the washing process resulted in a rise in the degree of pillaring in the clay, thus enhancing the C.E.C of the Fe-PILC.

(d) The overall results (see **fig. 7.2, 7.3, 7.4** and **7.5**) of the modified Fe-PILC, prepared by varying the base concentration of the clay, demonstrate that the degree of pillaring of the clay is not the only dominant factor which is responsible for the observed rise in the capacity of the clay for the various contaminants. These results imply that other factors such as varying the Fe/clay ratio, OH/Fe ratio and the base concentration of

the Fe-PILC are also responsible for the variation in the overall capacity of the clay. These variations in the synthesis ratios and, more importantly, the variation in the base concentration of the clay will ultimately lead to a significant change in the pH of the Fe-PILC. However the increase in the degree of pillaring in the Fe-PILC is not necessarily accompanied by an increase in the pH or base concentration of the clay (see **fig. 7.6** and **7.7**).

The above findings demonstrate that the capacity of the clay for contaminants is greatly dependant on the synthesis parameters such as synthesis ratios and the base concentration of the clay. To prepare an Fe-PILC for use as an agent in water treatment, the most suitable ranges of synthesis ratios, Fe/clay and OH/Fe ratios would be between 1.25-1.3 mmol/g and 1-2 respectively. Furthermore, the $NaHCO_3$ concentration of solution contacted with the clay should be around 0.0556 molar.

The overall conclusions drawn from the above findings confirm that the modified Fe-PILC, prepared by adding a base, can have a capacity that is significantly higher than that of the Al-PILC or the raw clay. The Fe-PILC can act as a better adsorbent than the latter two clays in removing both manganese and humic substances from the water. Regenerating the used PILC is a useful process option. Furthermore, preparing the PILC using the 'short-cut' method and eliminating the washing step would lower the production cost of the clay. Further research on the PILC should substantiate these claims.

For the definition of the estimated relative peak intensity ratio, R_{PI}, in **fig. 7.1** to **7.7**, see **chapter 5, fig. 5.4.**

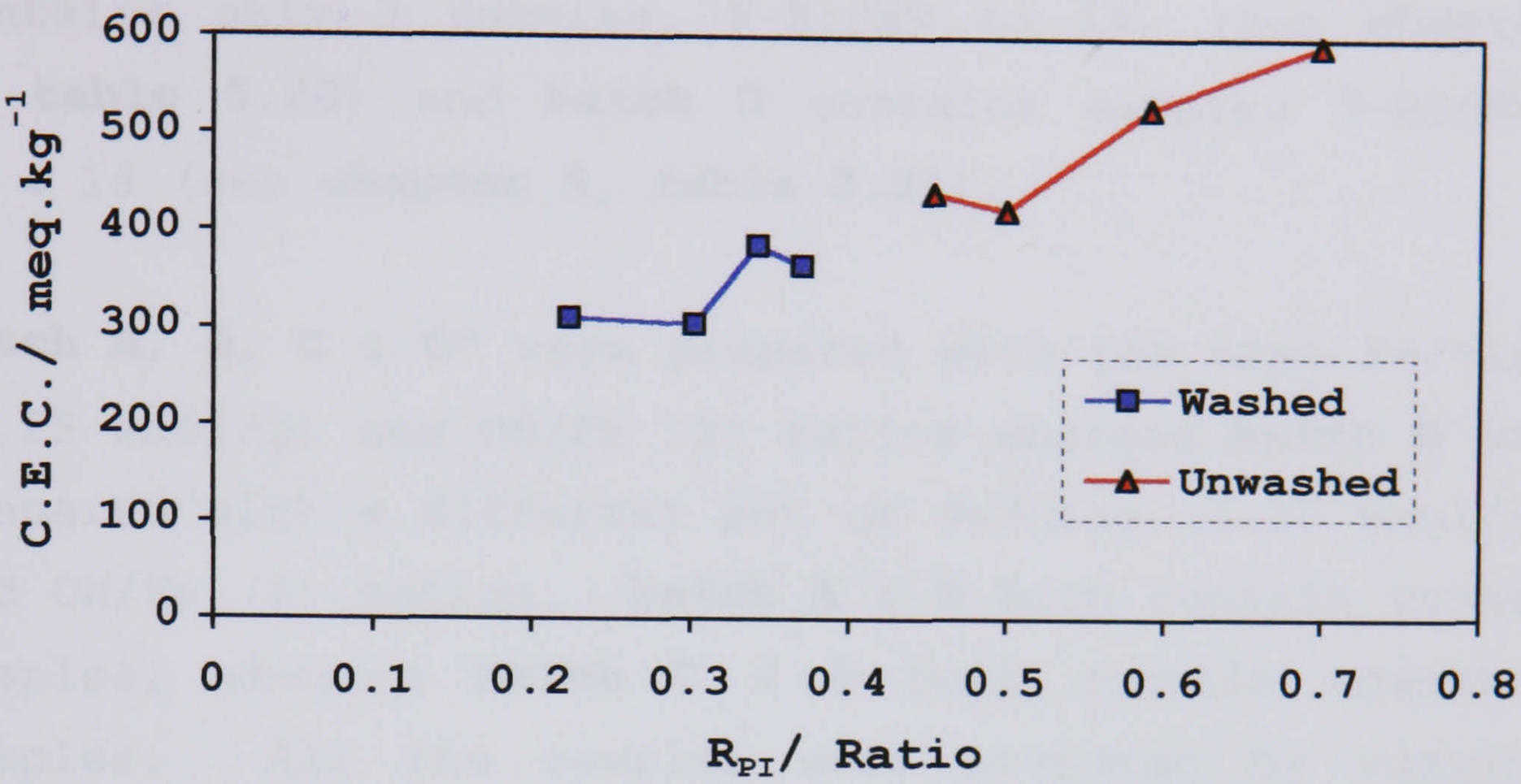


Fig. 7.1 Effect of pillaring on the C.E.C. of the clay (prepared by varying the thermal treatment temperature) for strontium (see **chapter 5, tables 5.16** and **5.18**).

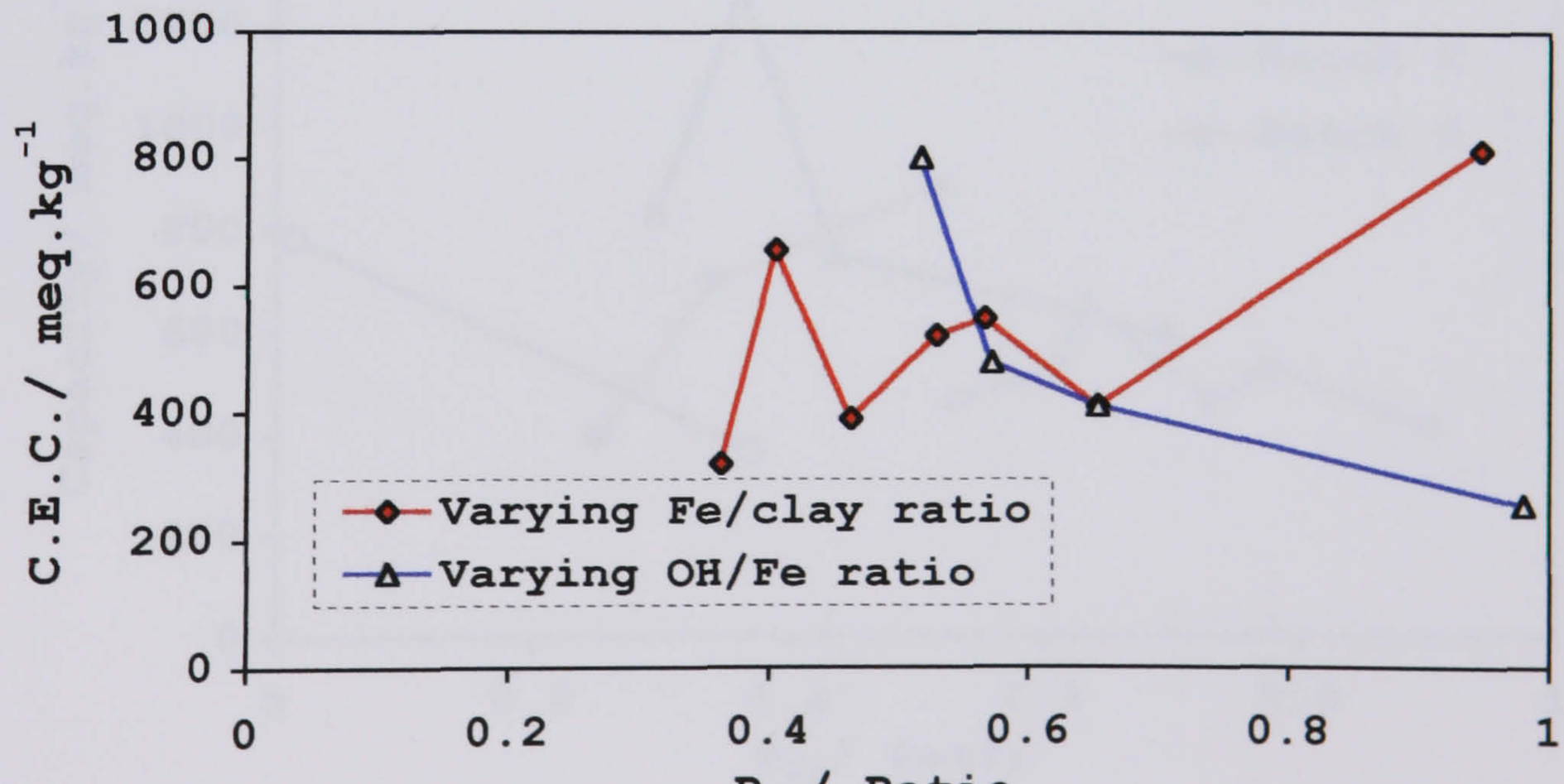


Fig. 7.2 Effect of pillaring on the C.E.C. of the clay (prepared by varying the synthesis ratios) for strontium (see **chapter 5, tables 5.7, 5.8, 5.13** and **5.14**).

In **fig. 7.3** to **7.5** & **7.7**, **batch A** contains samples F-B1 to 6 (see **chapter 5, table 5.19**); **batch B** contains samples F-B8 & 10 (see **chapter 5, table 5.20**); **batch C** contains 4 samples, F-B12NW to 15, whereas **batch C"** contains only 3 samples, F-B12NW to 14, (see **chapter 5, table 5.20**) and **batch D** contains samples F-B16NW, 18 & 19 (see **chapter 5, table 5.21**).

batch A, B, C & **C"** were prepared with the same Fe/clay (1.25 mmol/g) and OH/Fe (2) ratios whereas **batch D** was prepared with a different set of Fe/clay (1.30 mmol/g) and OH/Fe (1) ratios. **batch A** & **B** both contain washed samples, whereas **batch C** & **D** both contain unwashed samples. All the samples were prepared by varying $NaHCO_3$ concentration.

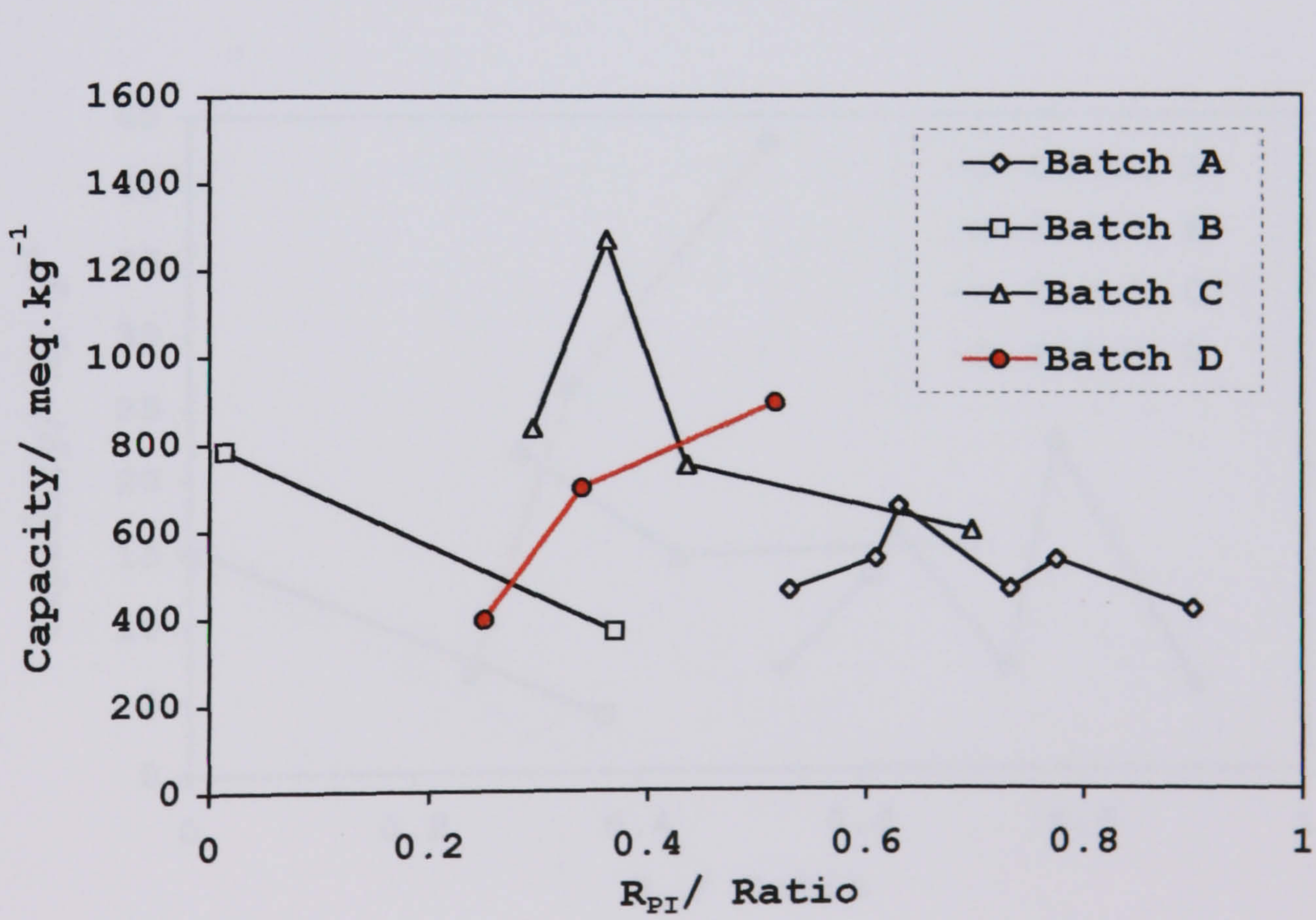


Fig. 7.3 Effect of pillaring on the capacity of the clay for strontium (see **chapter 5, tables 5.22** to **5.24** and **tables 5.28** to **5.30**).

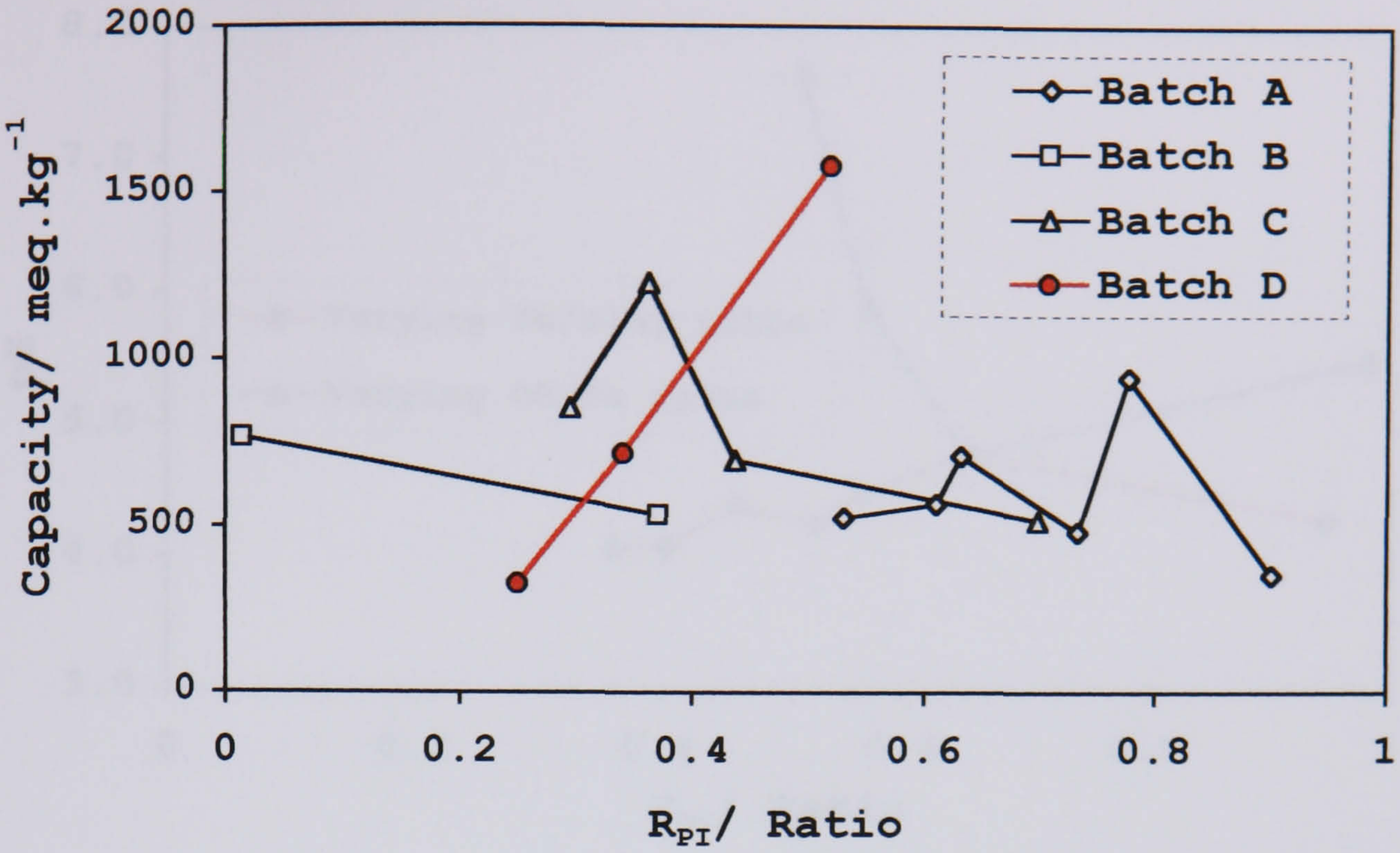


Fig. 7.4 Effect of pillaring on the capacity of the clay for manganese (see **chapter 5, tables 5.22** to **5.24** and **chapter 6, tables 6.4** to **6.6**).

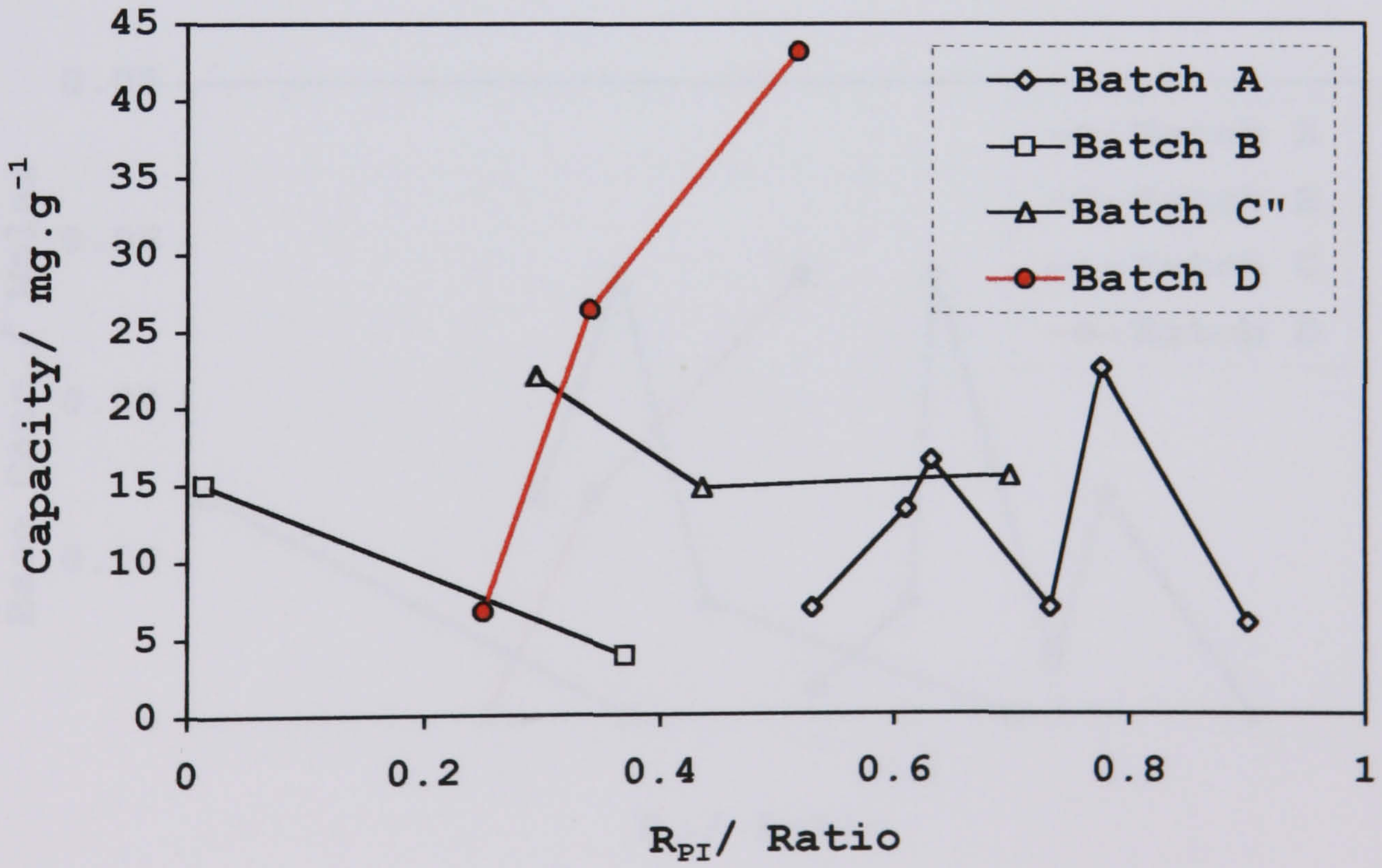


Fig. 7.5 Effect of pillaring on the capacity of the clay for humic substances (see **chapter 5, tables 5.22** to **5.24** and **chapter 6, tables 6.7** to **6.9**).

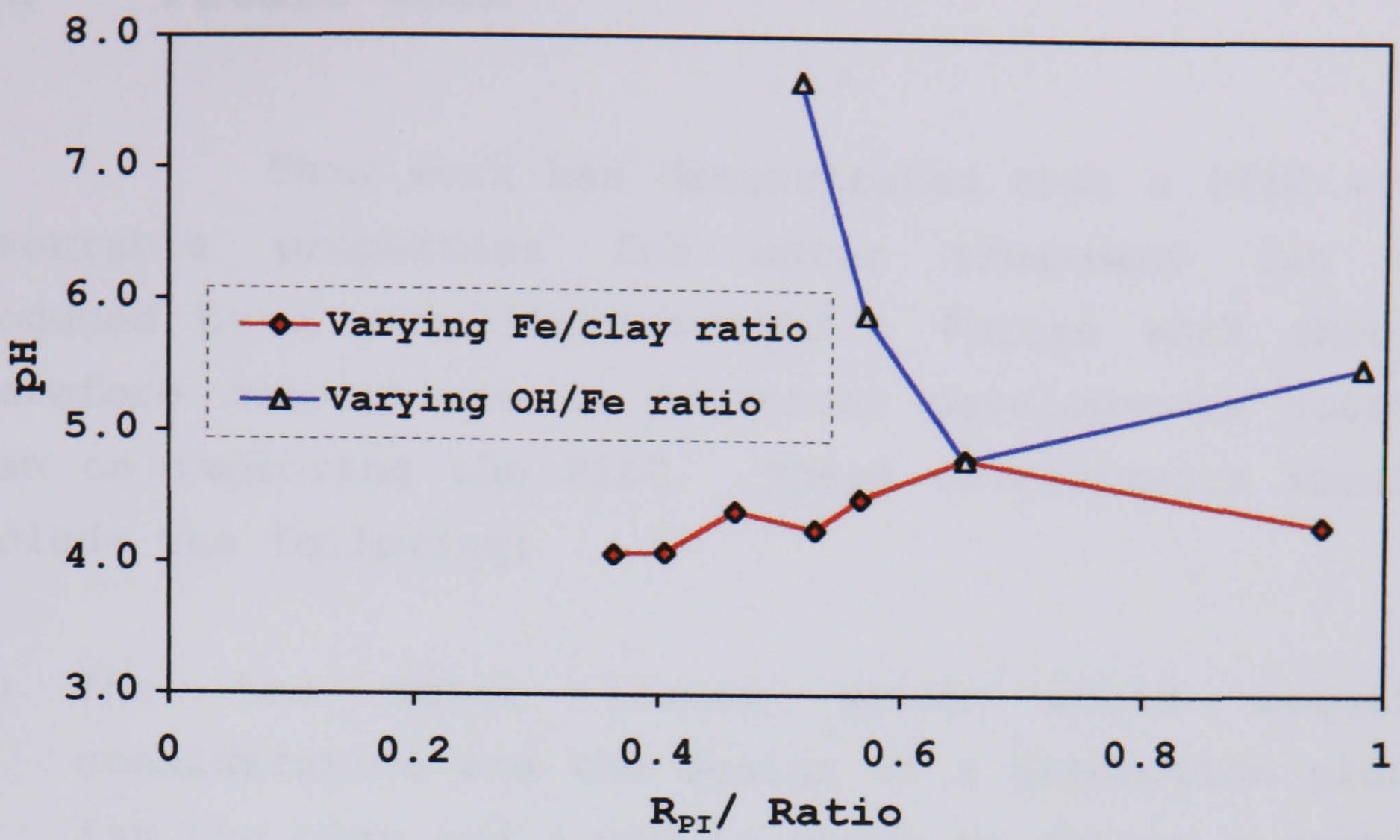


Fig. 7.6 An illustration of variations in pH of the thermally-treated clay (prepared by varying the synthesis ratios) and the degree of pillaring in the clay(see **chapter 5, tables 5.7** and **5.8**).

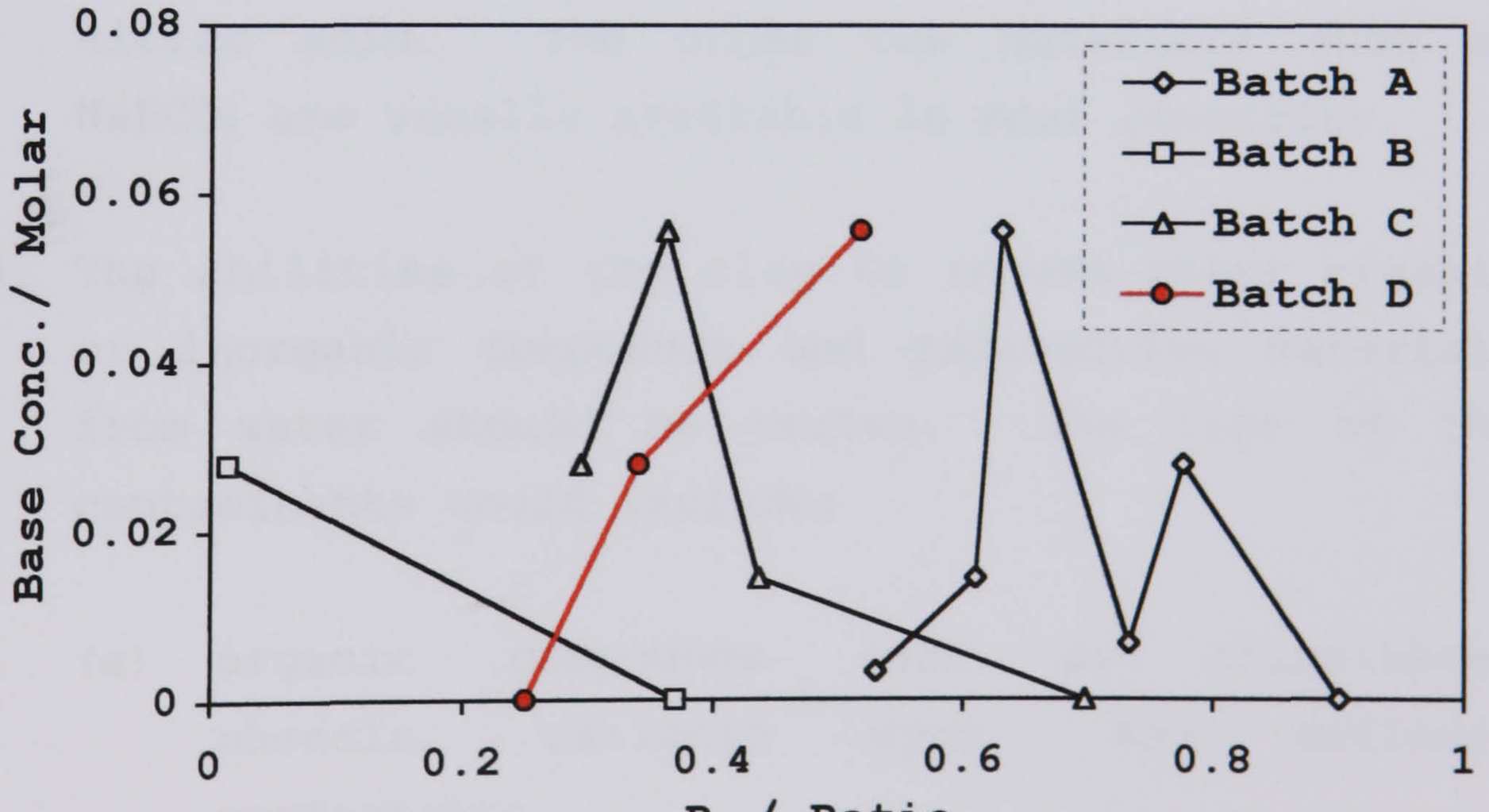


Fig. 7.7 An illustration of variations in the base concentration of the clay and the degree of pillaring in the clay (see **chapter 5, tables 5.22** to **5.24**).

7.1 Future Work

This work has demonstrated that a PILC with favourable properties for water treatment can be produced by a simplified method. Future work should therefore concentrate on practical developments rather than on improving the PILC. These developments should include the following:

(1) The two major issues which would require consideration are the design of a production plant for the clay and a way in which to obtain a supply of the raw materials. Part of the design of the plant may include the application of solar energy for the thermal treatment process of the clay. Raw materials such as the raw clay can be extracted from local quarries. Iron nitrate, on the other hand, would have to be prepared through a synthetic process, by dissolving scrap iron in nitric acid. The other raw materials such as $NaHCO_3$ are usually available in most countries.

(2) The abilities of the clay to remove other organic or inorganic compounds and radioactive materials from water should be tested. The list of the contaminants would include:

(a) organic compounds such as chlorinated phenols, cationic dyes, and cationic surfactants,

(b) inorganic cations and anions such as lead, cadmium and phosphates; and radioactive cations such as cobalt or strontium.

Furthermore the role of the clay in the process of water and sewage treatment should be considered.

(3) A number of factors in the regeneration process of the clay should be considered. One of the factors would involve determining a suitable method of separating the clay from water or sewage. Techniques such as sedimentation and filtration could be used. Other factors such as the design of a regeneration system should also be considered. Furthermore more sorption tests with regenerated clay should be performed; and the ability of the regenerated clay to remove contaminants such as manganese, and iron should be tested.

References

Papers

Altin, O., Ozbelge, H.O. and Dogu, T., 1998, Use of General Purpose Adsorption Isotherms for Heavy Metal-Clay Mineral Interactions, *J. Colloid and Interface Science*, Vol. **198**, pp. 130-140

Amal, R., Raper, J.A. and Waite, T.D., 1992, Effect of Fulvic Acid Adsorption on the Aggregation Kinetics and Structure of Hematite Particles, *J. Colloid and Interface Science*, Vol. **151**, pp. 244-257

Amin, S. and Jayson, G.G., 1996, Humic Substances Uptake by Hydrotalcites and PILCs, *Wat. Res.*, Vol. **30**, pp. 299-306

Bandosz, T.J. and Cheng, K., 1997, Changes in Acidity of Fe-Pillared/ Delaminated Smectites on Heat Treatment, *J. Colloid and Interface Science*, Vol. **191**, pp. 456-463

Corma, A., 1997, From Microporous to Mesoporous Molecular Sieve Materials and Their Use in Catalysis, *Chem. Rev.*, Vol. **97**, pp. 2373-2419

Davies, G. and Ghabbour, E.A., 1999, Understanding Life After Death, *Chemistry and Industry*, No. **11**, pp. 426-429

Diano, W., Rubino, R. and Sergio, M., 1994, Al-Pillared Montmorillonite: Preparation from Concentrated Slurries of Homoionic Ca Clay, Characterisation and Thermal Stability, *Microporous Materials*, Vol. **2**, pp. 179-184

Green-Pedersen, H., Jensen, B.T. and Pind, N., 1997, Nickel Adsorption on MnO_2, $Fe(OH)_3$, Montmorillonite, Humic Acids and Calcite: A Comparative Study, *Environmental Technology*, Vol. **18**, pp. 807-815

Ge, Z., Li, D. and Pinnavaia, T.J., 1994, Preparation of Alumina-Pillared Montmorillonites with High Thermal Stability Regular, Microporosity and Lewis/ Bronsted Acidity, *Microporous Materials*, Vol. **3**, pp. 165-175

Gil, A. and Montes, M., 1994,
Evolution of the Microporous Accessibility with the Hydrolysis Degree and the Intercalation Solution Ageing Time Conditions in Aluminium-Pillared Clays, *Microporous Materials*, Vol. **3**, pp. 319-329

Heylen, I. and Vansant, E.F., 1996,
The Stability and Porosity of Fe-PILCs in an Acidic and Basic Environment, *J. Porous Materials*, Vol. **3**, pp.41-46

Hutson, N.D., Hoekstra, M.J. and Yang, R.T., 1999,
Control of Microporosity of Al_2O_3-Pillared Clays: Effect of pH, Calcination Temperature and Clay Cation Exchange Capacity, *Microporous and Mesoporous Materials*, Vol. **28**, pp. 447-459

Jiang, J-Q. and Graham N.J.D., 1997,
Pre-Polymerised Inorganic Coagulants for Treating Water and Waste Water, *Chemistry and Industry*, pp. 388-39

Kooli, F., Bovey, J. and Jones, W., 1997,
Dependence of the Properties of Titanium-Pillared Clays on the Host Matrix: a Comparison of Montmorillonite, Saponite and Rectorite Pillared Materials, *J. Mater. Chem.*, Vol. **7**, No. 1, pp. 153-158

Lo, I.M-C. and Liljestrand, H.M., 1996,
Laboratory Sorption and Hydraulic Conductivity Tests: Evaluation of Modified-Clay Materials, *Waste Management and Research*, Vol. **14**, pp. 297-310

Li, D. and Scala, A.A., 1996,
Adsorption and Characteristics of Base-treated Pillared Clays, *Adsorption*, Vol. **2**, pp. 227-235

Maes, N. and Vansant, E.F., 1995,
Study of Fe_2O_3-Pillared Clays Synthesised Using the Trinuclear Fe(III)-Acetato Complex as Pillaring Precursor, *Microporous Materials*, Vol. **4**, pp. 43-51

Michot, L.J. and Pinnavaia, T.J., 1991,
Adsorption of Chlorinated Phenols from Aqueous Solution by Surfactant-Modified Pillared Clays, *Clays and Clay Minerals*, Vol. **39**, pp. 634-641

Michot, L.J. and Pinnavaia, T.J., 1992,
Improved Synthesis of Alumina-Pillared Montmorillonite by Surfactant Modification, *Chem. Mater.*, Vol. **4**, pp. 1433-1437

Mishael, Y.G., Rytwo, G., Nir, S., Crespin, M., Annabi-Bergaya, F. and Damme, V.H., 1999,
Interactions of Monovalent Organic Cations with Pillared Clays, *J. Colloid and Interface Science*, Vol. **209**, pp. 123-128

Mishra, T., Parida, K.M. and Rao, S.B., 1996,
Transition Metal Oxide Pillared Clay, *J. Colloid and Interface Science*, Vol. **183**, pp. 176-183

Mohan, K.K. and Fogler, H.S., 1997,
Effect of pH and Layer Charge on Formation Damage in Porous Media Containing Swelling Clays, *Langmuir*, Vol. **13**, pp. 2863-2872

Nava-Galva, G., Pacheco, G., Fetter, G., Bosch, P. and Bulbulian, S., 1996,
Sorption of Cobalt on Organic and Inorganic Intercalated Clays, *J. Radioanalytical and Nuclear Chemistry, Articles*, Vol. **207**, pp. 263-274

Occelli, M.L. and Tindwa, R.M., 1983,
Physicochemical Properties of Montmorillonite Interlayered with Cationic Oxylaluminium Pillars, *Clays and Clay Minerals*, Vol. **31**, pp. 22-28

Oades, J.M., 1984,
Interaction of Polycations of Aluminium and Iron with Clays, *Clays and Clay Minerals*, Vol. **32**, pp. 49-57

Ohtsuka, K., 1997,
Preparation and Properties of Two-Dimensional Microporous Pillared Interlayered Solids, *Chem. Mater.*, Vol. **9**, pp. 2039-2050

Parks, G.A., 1965,
The Isoelectric Points of Solid Oxides, Solid Hydroxides and Aqueous Hydroxo Complex Systems, *Chem. Rev.*, Vol. **65**, pp. 117-198

Peinemann, N. and Helmy, A.K., 1994,
Molydate Sorption by Hydroxy-Aluminium Treated Montmorillonite, *Applied Clay Science*, Vol. **8**, pp. 389-396

Rautiu, R., White, D.A., Adeleye, S.A. and Adkins, L., 1994,
The Use of Zeta Potential Measurements in Inorganic Ion Exchange Studies, *Hydrometallurgy*, Vol. **35**, pp. 361-374

Rightor, E.G., Tzou, M.S. and Pinnavaia, T.J., 1991, Iron Oxide Pillared Clay with Large Gallery Height: Synthesis and Properties as a Fischer-Tropsch Catalyst, *J. Catalysis*, Vol. **130**, pp. 29-40

Sanchez, A. and Montes, M., 1998, Influence of the Preparation Parameters (Particle Size and Aluminum Concentration) on the Textural Properties of Al-Pillared Clays for a Scale-Up Process, *Microporous and Mesoporous Materials*, Vol. **21**, pp. 117-125

Sing, K.S.W., 1989, The Use of Gas Adsorption for the Characterization of Porous Solids, *Colloids and Surfaces*, Vol. **38**, pp. 113-124

Srivastava, S.K., Tyagi, R., Pant, N. and Pal, N., 1989, Studies on the Removal of some Toxic Metal Ions. Part II (Removal of Lead and Cadmium by Montmorillonite and Kaolinite), *Environmental Technology Letters*, Vol. **10**, pp. 275-282

Storaro, L., Lenarda, M., Perissinotto, M., Lucchini, V. and Ganzerla, R., 1998, Hydroxy-Al-Pillaring of Concentrated Suspensions of Smectite Clays, *Microporous and Mesoporous Materials*, Vol. **20**, pp. 317-331

Tipping, E. and Cooke, D., 1982, The Effects of Adsorbed Humic Substances on the Surface Charge of Goethite (α-FeOOH) in Fresh Waters, *Cosmochimica Acta*, Vol. **46**, pp. 75-80

Wibulswas, R., White, D.A. and Rautiu, R., 1999, Adsorption of Phenolic Compounds from Water by Surfactant-Modified Pillared Clays, *Trans. I.Chem. E.*, Vol. **77**, pp. 88-91

Zhu, H.Y. and Vansant, E.F., 1995, Determination of Porosity in Pillared Clays by N_2 Adsorption Isotherms, *J. Porous Materials*, Vol. **2**, pp. 107-113

Bibliography

Burch, R.,
Catalysis Today, Pillared Clays, 1988, Elsevier, ISSN 0920-5861, Chapter 7 and 8

Carberry, J.B.,
Environmental Systems and Engineering, 1990, Saunders College, ISBN 0-03-029657-9, pp. 199-201

Eckenfelder, W.W.,
Industrial Water Pollution Control, 1989, McGraw-Hill, ISBN 0-07-018903-X, Chapter 8

Eslinger E. and Pevear, D.,
Clay Minerals for Petroleum Geologists and Engineers, 1988, ISBN 0-918985-73-0, Chapter 3, pp. 1-9

Faust, S.D. and Aly, O.M.,
Chemistry of Water Treatment, 1997, Ann Arbor, 1997, ISBN 1-57504-011-5, pp. 142-145

Faust, S.D. and Aly, O.M.,
Adsorption Processes for Water Treatment, 1987, Butterworths, ISBN 0-409-90000-1, pp. 16-18

Grim, R.E.,
Clay Mineralogy, 1968, McGraw-Hill, ISBN 0-317-28217-4, pp. 50

Grimshaw, R.W. and Harland, C.E.,
Ion-Exchange Introduction to Theory and Practice, 1975, Bartholomew, ISBN 0851869696, pp. 10-13

Hunter, R.J.,
Zeta Potential in Colloid Science Principle and Applications, 1988, Academic Press, ISBN 0-12-361961-0, Chapter 1

Mackenzie, R.C.,
Differential Thermal Analysis, 1970, Academic, SBN 12-464401-5, Chapter 24, pp. 673-707

Moore, D.M. and Reynolds, R.C.,
X-ray Diffraction and the Identification and Analysis of Clay Minerals, 1997, Oxford University, ISBN 0-19-508713-5, pp.61-103 and 214-220

Mitchell, I.V.,
Pillared Layered Structures Current Trends and Applications, 1990, Elsevier, ISBN 1-851-66499-8, pp. 3-12

Pinnavaia, T.J. and Thorpe, M.F.,
Access in Nanoporous Materials, 1995, Plenum, ISBN 0-306-45218-9, pp. 73-92

Schnitzer, M. and Khan, S.U.,
Humic Substances in the Environment, 1972, Marcel Dekker, pp. 253-257

Schwertmann, and Cornell, R.M.,
Iron Oxides in the Laboratory, Preparation and Characterisation, 1991, VCH, ISBN 0-89573-858-9, pp. 57

Skoog, W. H.,
Analytical Chemistry, 1996, Saunders College, ISNB 0-03-005938-0, Chapter 24 and 26

Velde, B.,
Introduction to Clay Minerals, 1992, Chapman & Hall, ISBN 0-412-37030-1, pp.34-36

Wilson, M.J.,
A Handbook of Determinative Methods in Clay Mineralogy, 1987, Chapman and Hall, ISBN 0-216-9180-4, pp. 251-262

Williams, P.A. and Hudson, M.J.,
Recent Developments in Ion Exchange 2, 1990, Elsevier, pp. 75-84